Acta Universitatis Szegediensis

Acta Biologica Szegediensis

Volume 61, Number 1, 2017

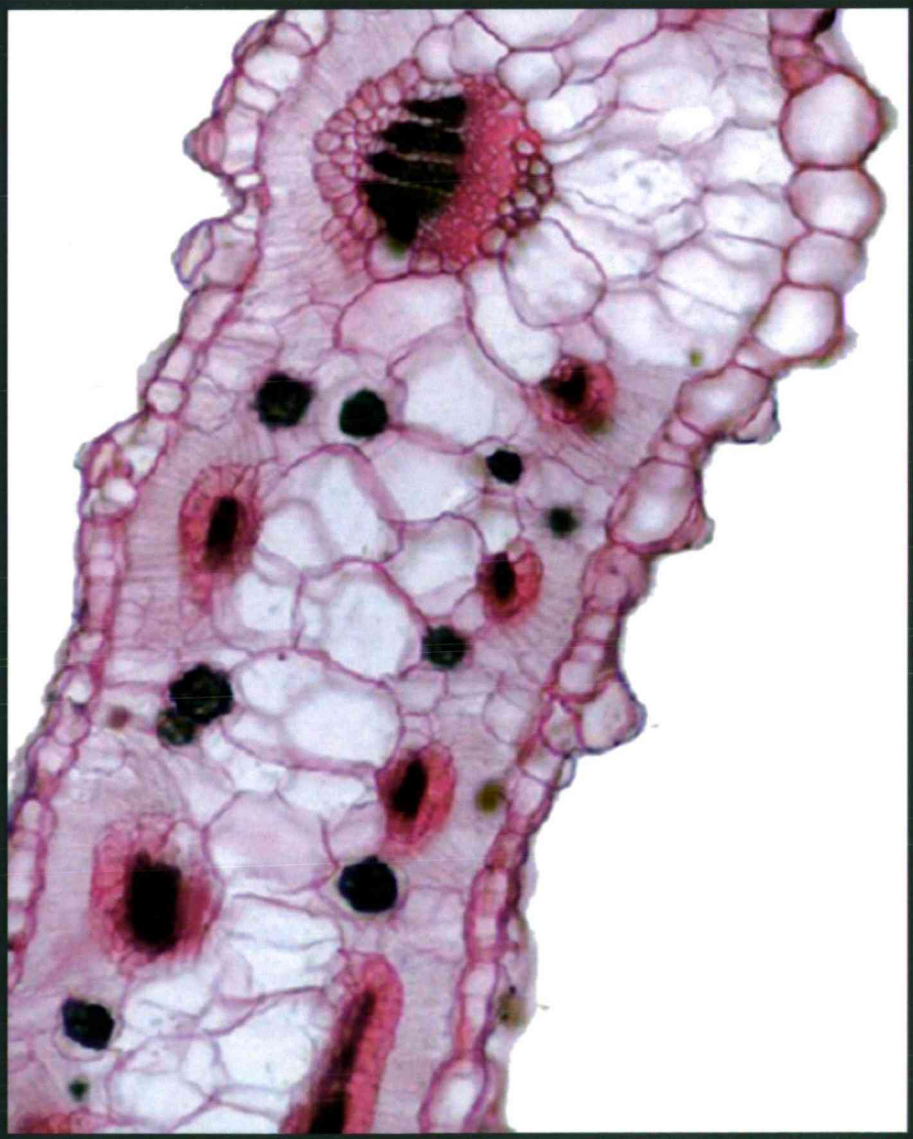

University of Szeged, Szeged, Hungary

Acta Biologica Szegediensis

Acta Biologica Szegediensis (ISSN 1588-385X print form; ISSN 1588-4082 online form) is an international peer-reviewed, open access journal published by the University of Szeged yearly, in two issues per volume.

Acta Biologica Szegediensis publishes novel findings in various fields of biology with special focus on innovative research in modern experimental life sciences. The journal publishes experimental and theoretical papers, reviews, short communications, and descriptions of new methods. Letters to the editor and conference proceedings may also be published, subject to the approval of the Editor-in-Chief.

Acta Biologica Szegediensis provides peer review by expert researchers, fast publication times, no page charge and free online accessibility. Table of contents and all issues of the journal are available at http://www2.sci.u-szeged.hu/ABS.
Acta Biologica Szegediensis is indexed in BIOSIS Database, CAB Abstracts, CABI - Review of Medical and Veterinary Mycology, EBSCO Databases, EMBASE, Excerpta Medica, Elsevier BIOBASE (Current Awareness in Biological Sciences), Enago, Google Scholar, KOBV, OCLC, Scopus, SCImago and Zoological Record.

Subscriptions

All subscriptions relate to the calendar year and must be pre-paid. The annual subscription rate is currently 100 USD and includes air mail delivery and handling.

Editor-in-Chief: Csaba Vágvölgyi
Department of Microbiology, Faculty of Science and Informatics
University of Szeged, Közép fasor 52., H-6726 Szeged, Hungary
Phone: 36 (62) 544-822, fax: 36 (62) 544-823
E-mail: csaba@bio.u-szeged.hu

Technical Editor: Tamás Mikola
Acta Biologica Szegediensis, Editorial Office
Közép fasor 52., H-6726 Szeged, Hungary
Phone: 36 (62) 544-822, fax: 36 (62) 544-823
E-mail: abs@bio.u-szeged.hu

ACTA BIOLOGICA SZEGEDIENSIS

VOLUME 61(1), 2017

Table of Contents

Articles

On the cover: Cross sections of C_4 leaf in *Bassia turkestanica* (see: Safiallah et al. in this issue).

Volume 61(1):1-11, 2017
Acta Biologica Szegediensis
http://www2.sci.u-szeged.hu/ABS

ARTICLE

In vitro endophyte-host plant interaction study to hypothetically describe endophyte survival and antifungal activities *in planta*

Hye Seung Yoo, Adeline Su Yien Ting*

School of Science, Monash University Malaysia, 47500 Bandar Sunway, Petaling Jaya, Malaysia

ABSTRACT This study is the first to adopt a hypothetical approach to establish the influence of the complex endophyte-host interaction on endophyte survival and antifungal expression. Three key interactions were evaluated; (I) influence of host-induced enzymes on endophyte growth (biomass) and colonization, (II) link between endophyte-produced cellulase, their growth and colonization, and (III) the influence of host environment on antifungal expression of endophytes. The interactions with the host were performed using plant slurry (PS) to mimic *in planta* (host) environment with analysis on interactions evaluated using Pearson correlation coefficients (*r*). Results revealed that host induced enzymes may be a limiting factor to colonization of endophytes with inverse correlations observed ($-0.046 \leq r \leq -0.7164$). These enzymes may also limit growth of endophyte although, PAL ($r = 0.536$) and TPC ($r = 0.8894$) appeared contrary. Results were also suggestive that endophytes produced cellulase to aid in colonization in host plants ($r = 0.7073$ in PS), and cellulase activities are continuously produced even when growth of endophytes are limited ($r = -0.314$ in PS). Endophytes are presumed to produce antifungal compounds *in planta* ($r = 0.2760$ in PS), and these compounds may be secondary metabolites, which are primarily produced under nutrient-depleted conditions where growth is poor (in host plant). The superior growth of endophytes in synthetic PDB media has an inverse correlation to antifungal activity ($r = -0.5129$), confirming that secondary metabolites are involved in antifungal activities. This study clearly presents that success of inoculated endophytes in colonizing, growing and expressing antifungal activities is dependent on the host plant.
Acta Biol Szeged 61(1):1-11 (2017)

KEY WORDS

antifungal activity
endophyte-host interaction
endophyte survival
Fusarium oxysporum f. sp. *cubense* tropical race 4
simulation study

Introduction

Endophytes are microorganisms that exist or spend part of their life cycle in the host plant. Their roles as biocontrol agents of various diseases are attributed to several mechanisms; direct inhibitory effect towards the pathogen (Liu et al. 2007; Ting et al. 2010a, 2011a), indirect disease suppression via plant growth improvement (Ting et al. 2008, 2009a), and induced host resistance against pathogens (Sundaramoorthy et al. 2012; Ting et al. 2009b, 2010b, 2012a). Endophytic biocontrol agents are typically isolated from an array of host species, and screened for bioactivity prior to introduction to commercially important crops. Although, the approach in using biocontrol agents is more environment-friendly, field applications seldom yield satisfactory biocontrol results (Ting et al. 2009a). For many years, poor soil conditions have been identified as the primary factor in contributing the absence of disease control in the field. The survival of introduced biocontrol agents was impeded by the intense competition with indigenous microflora in the soil, as well as physicochemical soil conditions (extreme pH, poor oxygen level/aeration, poor moisture level) (Sylvia and Neal 1990; Donnison et al. 2000). This has led to the emergence of studies in microbial bioformulations, to innovate and improve delivery and application of biocontrol agents in the field (Ting et al. 2009c; Manikandan et al. 2010; Shanmugam and Kanoujia 2011; Ting et al. 2011b).

In this study, we proposed that the complex endophyte-host plant interaction may be a contributing factor that influences endophyte survival *in planta* and their subsequent biocontrol activity towards the pathogen. This hypothesis is a refreshing perspective, which suggests that introduced endophytes are influenced by host plant factors and not solely dependent on soil factors. To establish this, an *in vitro* study was designed to determine interactions of the growth

Submitted January 3, 2017; Accepted April 10, 2017
*Corresponding author. E-mail: adeline.ting@monash.edu; adelsuyien@yahoo.com

of introduced endophytes (biomass, colonization extent, cellulase activities for colonization) with host plant factors (host defense enzymes) and their subsequent influence on the antifungal activity of endophytes against the pathogen (*Fusarium oxysporum* f. sp. *cubense* tropical race 4, FocR4). The *in vitro* study was performed using plant slurry derived from banana plantlets to mimic *in planta* conditions. The links between the factors are validated by Pearson correlation coefficients (*r*).

To the best of our knowledge, this study is the first to test several key novelties. Firstly, we explored the influence of host-induced enzymes on endophyte growth and their colonization. This is an atypical approach to link and evaluate induced host defense enzymes as a factor influencing endophyte colonization *in planta*. Secondly, we explored the influence of endophyte-produced cellulase, a cell wall-degrading enzyme (CWDE) on endophyte growth and colonization. Finally, this *in vitro* study also examined the antifungal activities of endophytes expressed under an artificial *in planta* environment (using plant slurry) to mimic host plant environment. The varying degree of inhibition suggests the possible potency of antifungal compounds produced *in planta*. Therefore, this *in vitro* study provides new insights on the endophyte-host plant interaction and its influence on endophyte survival and antifungal expression towards the pathogenic *F. oxysporum* f. sp. *cubense* tropical race 4.

Materials and Methods

Culture establishment

The fungal pathogen *F. oxysporum* f. sp. *cubense* race 4 (FocR4) (VCG 01213/16) (Bentley et al. 1998) was obtained from Prof. Dr. Sariah Meon from University Putra Malaysia as cultures on Potato Dextrose Agar (PDA, Merck). Five endophytic isolates were selected; two isolates from weeds (*Diaporthe* sp. MIF01; *Diaporthe* sp. WAA02) and three isolates from banana plants (*Penicillium citrinum* BTF08; *Cladosporium* sp. BTF21; *Trichoderma* sp. T2), and all cultures maintained on PDA (Merck) at 25 ± 2 ºC. These five endophytes have demonstrated antagonistic properties against FocR4 in plate screenings (dual culture assays) in our previous studies (Ting et al. 2009d, 2010a, 2012a).

Assays for host-induced enzymes

Tissue-cultured banana plantlets (*Pisang berangan* cv. Intan, 3-4 leaf staged) were obtained from United Plantations Pte. Ltd. To induce production of host-induced enzymes, the plantlets were inoculated by immersing (root-dipping) into 30 ml of endophyte suspension (inoculum concentration of 10^6 cfu mL^{-1}) (Ting et al. 2012a). The inoculated plantlets were maintained in sterilized soil, watered daily with sterile distilled water, and kept isolated in a growth chamber from other plants. At a daily interval (for the next 7 days), plantlets were harvested and assayed for the following enzymes; peroxidase (PO), polyphenol oxidase (PPO), phenylalanine ammonia lyase (PAL) and total phenolic content (TPC). Triplicates were prepared for each isolate at every sampling interval.

To detect PO and polyphenol oxidase PPO levels, crude extracts were first prepared by grinding 1 g (fresh weight) of the tissues in 1 mL of chilled 0.05 M Sodium Acetate Buffer (SAB) (pH 5) supplemented with 5 mg of polyvinylpyrrolidone (PVP) (British Drug Houses, BDH). The slurry was centrifuged (20 min, 4 ºC, 14 000 rpm) and the supernatant (50 µL) incubated with 0.75 mL of reaction substrate [80 mL Sodium Phosphate Buffer (SPB, pH 6), 1 mL of 30% H_2O_2 (Merck), 20 mL of guaiacol (2-methoxyphenol, Merck)] at room temperature (25 ± 2 ºC). Blanks were prepared by substituting the supernatant with distilled water. The absorbance was measured (470 nm) using a spectrophotometer (Genesys™ 20; Thermo Fisher Scientific) after 5 min of reaction. The total amount of PO was calculated using the equation as described by Ting et al. (2012a):

$$\text{Units } g^{-1} \text{ fresh weight of tissues} = \frac{(\text{absorbance at 470 nm})(\text{dilution factor})}{\text{Amount of tissue assayed, g}} \times 1000$$

For PPO, 50 µL of the supernatant was mixed with 750 µL of the reaction substrate [SPB (50 mM) with 5 x 10^{-4} M chlorogenic acid (Aldrich)] and allowed to stand at room temperature for 20 min. The absorbance was read at 410 nm and the PPO levels calculated (as for PO) and expressed as total PPO produced (units g^{-1} fresh weight of tissues). Blanks were prepared by substituting the supernatant with distilled water (Ting et al. 2012a).

For PAL assay, 1 g fresh weight of the plant tissues were ground in 5 mL of 0.1 M Sodium Borate Buffer (SBB) (pH 8.8), supplemented with 5 mM mercaptoethanol (Merck). The slurry was centrifuged (10 min, 4 ºC, 15 000 rpm) and the supernatant collected. The supernatant (1 mL) was mixed with 3 mL of 300 mM SBB amended with 30 mM L-phenylalanine (Alfa Aesar). The reaction mixture was incubated in a water bath at 40 ºC for 1 h. Spectroscopic measurement was made at 290 nm, and the PAL activity was expressed as mg of cinnamic acid produced per g fresh weight of tissues. Blanks were prepared by substituting the enzyme extract with distilled water (Podille and Laxmi 1998). Trans-cinnamic acid (Aldrich) (0 to 0.5 mg mL^{-1}) was used to construct the standard curve.

To detect TPC, 1 g (fresh weight) of plant tissues were ground in 9 mL of distilled water. The mixture was transferred to a universal bottle (wrapped in aluminum foil), and agitated at 150 rpm for 1 h. For colorimetric analysis, 100 µL of the plant extract was mixed with 0.75 mL of $1/10^{th}$ diluted Folin-Ciocalteu reagent (FS Chem), and after 5 min, 0.75 mL of

6% Na_2CO_3 (Amresco) solution and 5 mL of distilled water were added. The solution was mixed for reaction to occur at room temperature for 90 min. The absorbance was gradually read at 725 nm and TPC quantified based on standard curve plotted using gallic acid (FS Chem) of 0.01 to 0.5 mg mL^{-1} (Amin et al. 2004).

Determining colonization extent and growth of endophytes

Banana plantlets were inoculated by root-dipping into 30 mL fungal suspensions (10^6 cfu mL^{-1} of MIF01, WAA02, BTF08, BTF21, T2 or FocR4 separately). At a daily interval (for the next 7 days), the plantlets were sampled and cut into root, corm, pseudostem and leaf tissues (of approximately 1 cm^2 each), and surfaced disinfected (1 min in 5% NaOCl, 1 min in 75% ethanol, 1 min in 95% ethanol, rinsed with sterile distilled H_2O) (Schulz et al. 1993). The disinfected tissues were subsequently cut longitudinally to expose the internal tissues, which were then plated on PDA and supplemented with 50 mg L^{-1} streptomycin sulfate (Sigma) (to inhibit bacterial growth). The seeded plates (containing 3 pieces each of root, corm, pseudostem and leaf tissues per plate) were incubated at room temperature for 7 days. The extent of colonization is expressed as the percentage of colonization according to Akello et al. (2009), where the number of tissue pieces with endophyte growth detected is compared against total number of tissue pieces plated (12 pieces).

To determine the growth (proliferation) of endophytes in host tissues, endophytes were first inoculated into three different media: plant slurry (PS), a diluted Potato Dextrose Broth (PDB), and a mixture of PS + PDB. Plant slurry medium (PS) was designed to mimic conditions in the plant. It was prepared by blending fresh banana plantlets (150 g fresh weight) in 100 mL of sterile distilled water, then 3 mL of this homogenized plant material was added to 10 mL of sterile distilled H_2O. When PDB was prepared, 3 mL of sterile distilled H_2O was added to 10 mL of Potato Dextrose Broth. PS + PDB medium was prepared by mixing 3 mL of homogenized plant material with 10 mL of Potato Dextrose Broth. Two agar plugs (5 mm diameter) were then inoculated into each medium, and incubated at room temperature, with 100 rpm for 30 days. At every 10-day interval, the fungal biomass was filtered with a cheesecloth and oven-dried (60 ºC) overnight prior to weighing.

Determining cellulase activities by endophytes

Endophytes were inoculated (5 mL, 10^6 cfu mL^{-1}) into 100 mL of PS, PDB and PS + PDB. At a daily interval (for the next 7 days), 50 µL of the culture filtrate was sampled and mixed into 200 µL acetate buffer solution (125 mM, pH 5) containing 1.25% w/v carboxymethyl cellulose (CMC). The mixture was incubated at room temperature (25 ± 2 ºC) for 15 min. The reaction was terminated by adding 250 µL of reaction solution [1% DNS reagent (dinitrosalicylic acid solution: 1% DNS (Bio Basic Inc), 0.05% sodium sulphite (Bendosen), 1% sodium hydroxide (Riendemann Schmidt), 2% sodium tartrate (Riendemann Schmidt)] and boiled in water bath for 5 min. The absorbance was measured at 575 nm (Tecan Infite M200 Multi detection Microplate reader) (Ting et al. 2012b), and the cellulase activities derived from a standard curve (0-100 µmol mL^{-1} of glucose).

Antifungal activities of endophytes

Five mL of fungal inoculum (10^6 cfu mL^{-1}) was first inoculated to PS, PDB and PS + PDB. After 2 weeks, 30 mL of the culture was pipetted, centrifuged (9000 rpm, 10 min) and the supernatant filtered through sterile filter syringe (0.45 µm, MCE membrane, Biofil). The filtrate (6.5 mL) was then mixed with 6.5 mL of sterile double-strength molten PDA in Petri dishes. After the agar has solidified, mycelial plug of FocR4 was inoculated at the center of the plate and their growth was measured after 10 days. The antifungal activity is expressed as Percentage Inhibition of Diameter Growth (PIDG, %), where D1: diameter of FocR4 in control plates, D2: diameter of FocR4 in agar plates supplemented with filtrate (Zacky and Ting 2013):

$$\text{PIDG (\%)} = \frac{\text{D1-D2}}{\text{D1}} \times 100\%$$

Statistical analysis

The experiments were carried out in a Complete Randomized Design (CRD). Data was analyzed using One-way Analysis of Variance (ANOVA) at the significance level of $p<0.05$. Tukey's test ($HSD_{(0.05)}$) was used to compare the means of the triplicate. Data analysis was performed using the software SPSS (Statistical Program for Social Science) ver. 20.0 (IBM). The Pearson correlation coefficients (r) were derived and the relationships/interactions between key areas was interpreted based on the following coefficient values; where $0.5 \leq r \leq 1.0$ indicates high correlation, $0.3 \leq r \leq 0.5$ indicates moderate correlation, $0.1 \leq r \leq 0.3$ indicates weak correlation and $r \leq 0.1$ indicates no correlation.

Results

Production of host-induced enzymes elicited by endophytes

The PO, PAL and TPC levels in plantlets upon infection by various endophytes (MIF01, WAA02, BTF08, BTF21, T2)

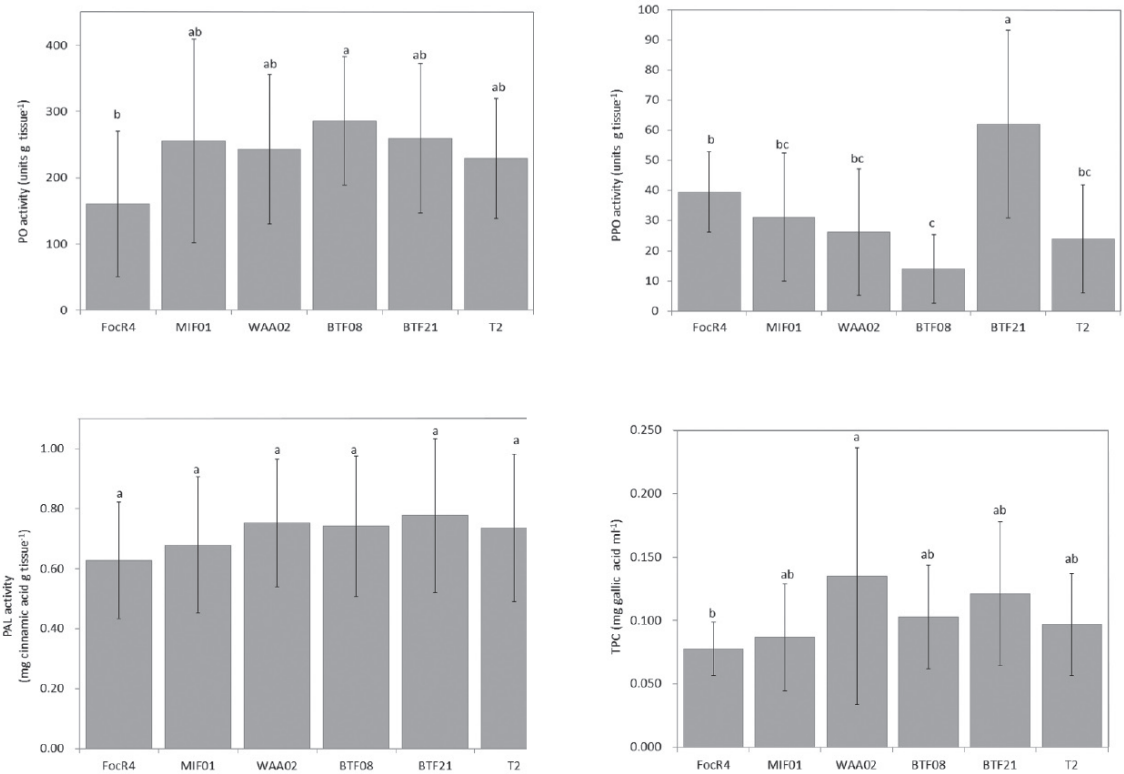

Figure 1. Plant defence response, when inoculated with various fungal isolates. (A) PO activity, (B) PPO activity, (C) PAL activity, and (D) TPC. Means with the same letters are not significantly different according to Tukey's test ($HSD_{(0.05)}$). Bars represent standard error of means.

and pathogenic FocR4 were not significantly different from one another; with PO levels of 171.54 to 285.96 units g^{-1} fresh weight of tissues, PAL levels of 0.63 to 0.78 mg cinnamic acid g^{-1} fresh weight of tissues, and TPC levels of 0.08 to 0.14 mg mL^{-1} (Fig. 1A, 1C, 1D). The PO and TPC levels were however, significantly different between isolates BTF08 and FocR4 for PO, and isolates WAA02 and FocR4 for TPC. This suggested that different species may elicit different response from the host plant. On the contrary, the PPO levels varied in plants induced by different endophytic isolates. PPO levels were the highest in plants triggered by BTF21 (62.11 units g^{-1} fresh weight of tissues), while BTF08 (14.00 units g^{-1} fresh weight of tissues) resulted in the least PPO produced. The pathogenic FocR4 was observed to elicit comparable levels of PO (171.54 units g^{-1} fresh weight of tissues), PPO (39.53 units g^{-1} fresh weight of tissues), PAL (0.63 mg cinnamic acid g^{-1} fresh weight of tissues) and TPC (0.08 mg mL^{-1}), when inoculated to plants (Fig. 1A-D).

Colonization extent and growth of endophytes

Isolate T2 had the highest percentage of tissue colonization (60.42%), followed by isolates WAA02, FocR4, BTF08, and MIF01 with 41.37, 31.85, 29.76, and 22.62%, respectively (Fig. 2). Isolate BTF21 was not detected in any of the plant tissues sampled (root, corm, pseudostem, and leaf). Isolates T2, WAA02, MIF01, BTF08 and FocR4, demonstrated better colonization in the corm tissues (65.08%), compared to pseudostem (29.56%), root (26.98%) and leaf tissues (2.38%) (data not shown). For fungal growth (proliferation), higher biomass was recovered from isolates cultured in PDB and PS + PDB compared to PS. Cultures from PDB weighed between 0.032-0.051 g, which were significantly higher than biomass collected from cultures in PS (0.003-0.110 g) (Fig. 3). An atypical growth response was demonstrated by isolate WAA02, where similar biomass was recovered from PS (0.030 g), PDB (0.047 g) and PS + PDB (0.028 g) (Fig. 3). This suggested that among the isolates tested, isolate WAA02 may have better survival potential *in planta*, while other isolates grew better in synthetic media (PDB).

Cellulase production by endophytes

Isolates inoculated in PDB produced higher cellulase levels compared to their production in the presence of PS. In PS, cellulase production is severely limited especially for isolates

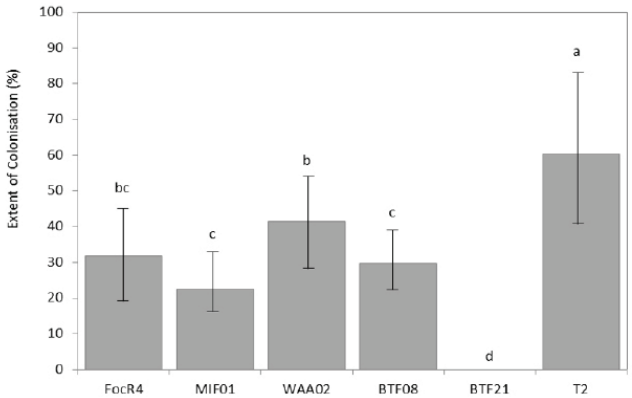

Figure 2. Overall colonisation (%) of the banana plantlets by FocR4 and the five antagonistic endophytes. Means with the same letters are not significantly different according to Tukey's test (HSD $_{(0.05)}$).

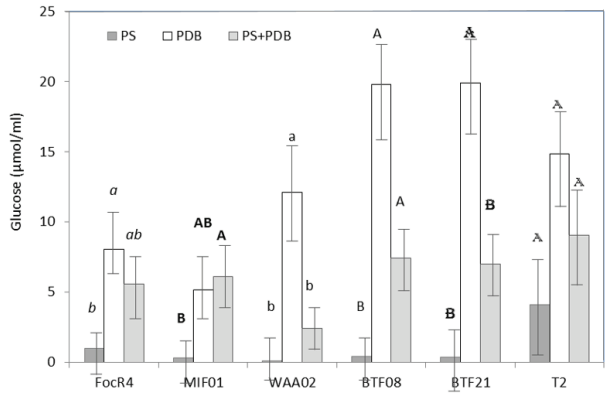

Figure 4. Cellulase activities (µmol mL^{-1}) of fungal isolates cultured in plant slurry (PS), PDB and PS + PDB. Means with the same letters are not significantly different according to Tukey's test (HSD $_{(0.05)}$). Tukey's grouping was determined for each fungal isolate among the culture media. Bars represent standard error of means.

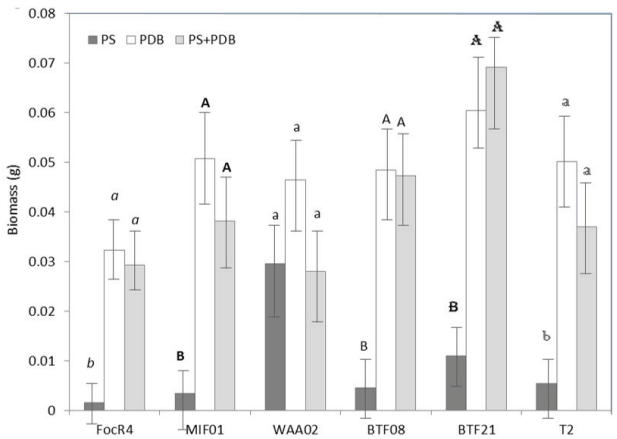

Figure 3. Mean biomass (g) of six investigated fungal isolates cultured in PS, PDB and PS + PDB. Comparison of mean dry mass was determined among the culture media for each fungal isolate. Means with the same letters are not significantly different according to Tukey's test (HSD $_{(0.05)}$). Bars represent standard error of means.

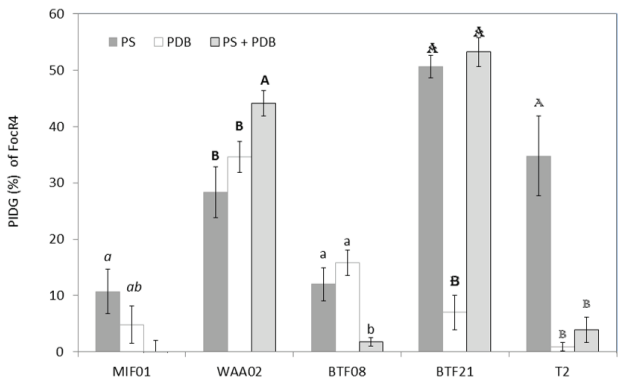

Figure 5. Percentage inhibition of diameter growth (PIDG, %) of FocR4 under the influence of cell-free extracts of respective endophytes cultured in PS, PDB and PS + PDB. Means with the same letters are not significantly different according to Tukey's test (HSD $_{(0.05)}$). Tukey's grouping was determined across the different culture media within each of the fungal isolate. Bars represent the standard error of means. PS: plant slurry; PDB: Potato Dextrose Broth; PS + PDB: plant slurry + PDB.

BTF21, BTF08 and WAA02 as the differences of cellulase levels in PS and PDB were 19.56, 19.36 and 12.04 µmol mL^{-1} cellulase, respectively. Isolates BTF21, BTF08 and WAA02 produced only 0.35, 0.41, and 0.07 µmol mL^{-1} cellulase compared to 19.90, 19.77, and 12.11 µmol mL^{-1}, respectively, when inoculated in PDB (Fig. 4). On the contrary, cellulase levels by isolate T2 were the least affected by growth conditions (PS, PDB, PS + PDB), with similar cellulase levels derived from cultures cultivated in PS (4.09 µmol mL^{-1}), PDB (14.84 µmol mL^{-1}) and PS + PDB (9.03 µmol mL^{-1}) (Fig. 4). This suggested that endophytic isolates could produce cellulase in nutrient-deprived conditions (in PS) to possibly aid in colonization, but the cellulase levels were inferior compared to nutrient-rich conditions (PDB).

Antifungal activities by endophytes

The antifungal activities by endophytes cultured in PS were relatively stronger than, if not comparable, to those derived from PDB and PS + PDB. Filtrate derived from isolates BTF21 (50.6% PIDG) and T2 (34.8%) cultured in PS showed stronger inhibitory effect compared to filtrates of the same isolates derived from PDB (7% for BTF21, 0.9% for BTF08) (Fig. 5). For isolates WAA02 (28.3%), BTF08 (12.0%), and MIF01 (10.7%), their respective filtrates from PS demonstrated similar inhibitory effect as filtrates derived from

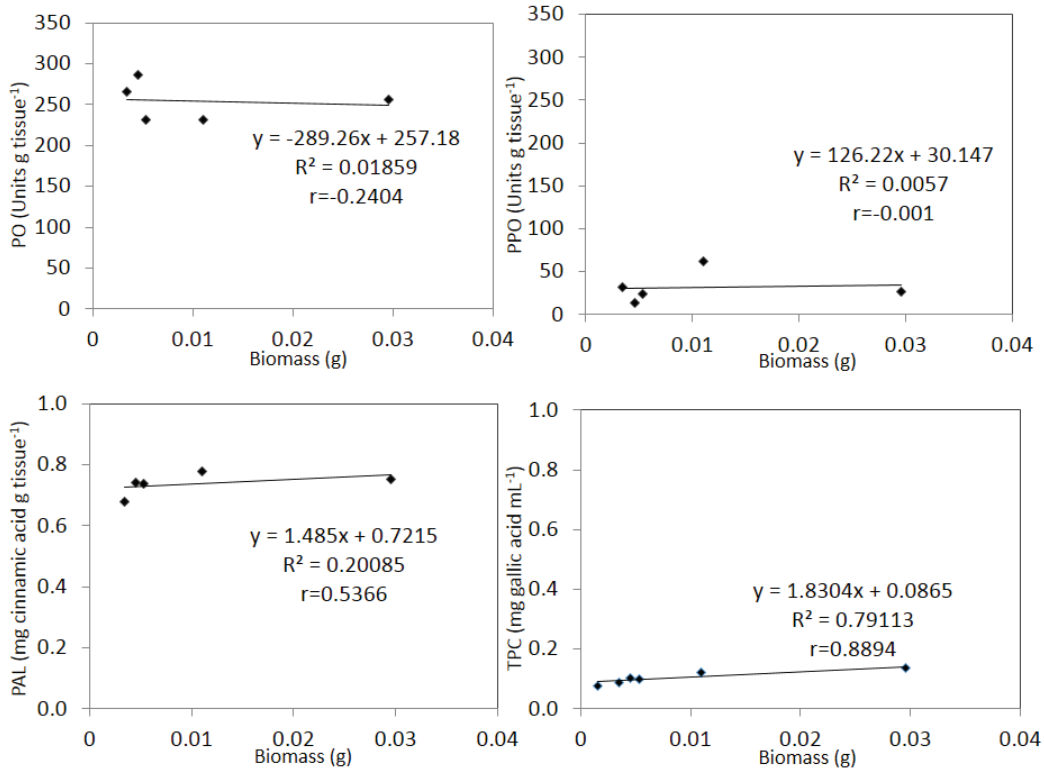

Figure 6. Correlation coefficient (r) from Pearson correlation test, for interactions between host-induced enzymes (PO, PPO, PAL, TPC) and endophyte growth (biomass).

PDB (34.7, 15.8, and 4.8%, respectively). The potential of endophytes in producing potent antifungal compounds, while cultured in PS strongly suggests that this may also occur *in planta* (host environment), which is a valuable insight on antifungal expression by endophytes in host tissues. The observations here are also suggestive that despite the nutrient-depleted host environment, endophytes are still capable of producing antifungal compounds.

Establishing endophyte-host interactions based on correlation coefficients (r)

The first endophyte-host interaction established is the possible influence of host-induced enzymes on endophyte growth and colonization. Correlation analysis using data from 3.1 and 3.2 revealed that growth (biomass) of endophytes was generally inversely correlated to host-induced enzymes (except for PAL and TPC). The inverse correlation ranges from poor/weak correlation, *i.e.* for PO (r = -0.2404) and PPO (r = -0.001) on growth, and PO (r = -0.0406), PAL (r = -0.1246) and TPC (r = -0.1392) on colonization extent; to strong/high correlation such as for PAL and colonization extent (r = -0.7164) (Fig. 6, 7). The inverse correlations are suggestive that the higher levels of enzymes, lesser the growth and colonization extent of the endophytes were detected. On the contrary, enzymes PAL and TPC have strong, positive correlations to growth of endophytes with r = 0.5366 and 0.8894, respectively (Fig. 6, 7). This indicated that host-induced enzymes triggered by endophytes, may be a limiting factor to the colonization extent (and possibly the growth to a certain degree) of endophytes in the host plant.

The second endophyte-host interaction validated is the association of endophyte growth and colonization extent to cellulase levels produced by endophytes in artificial host environment (achieved using PS). Correlation analysis was derived from data in sections 3.2 and 3.3. Endophyte growth was observed to have positive correlations to cellulase production in PDB (r = 0.5454) and PS + PDB (r = 0.53054), but an inverse correlation when cultured in PS (r = -0.3140) (Fig. 8). This suggested that growth of endophytes may potentially influence the cellulase production in nutrient-rich conditions (PDB, PS + PDB), but not in nutrient-depleted conditions (PS). The biomass and cellulase production in PS is inversely correlated, allowing the presumption that although growth may occur in PS, cellulase production is nevertheless limited and possibly vice versa. The interaction between endophyte colonization extent to cellulase levels were positively correlated for conditions in PS (r = 0.7073)

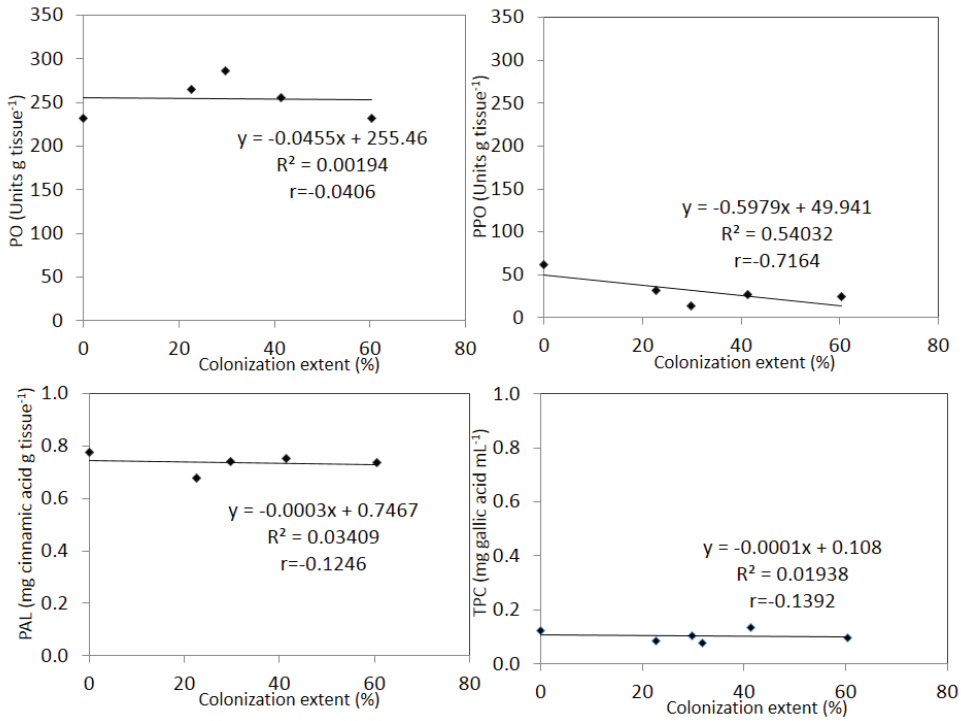

Figure 7. Correlation coefficient (r) from Pearson correlation test, for interactions between host-induced enzymes (PO, PPO, PAL, and TPC) and colonization extent for endophytes.

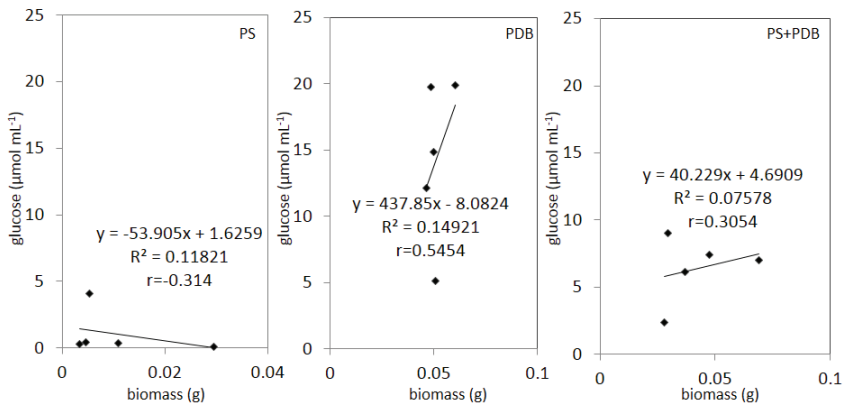

Figure 8. Correlation coefficient (r) from Pearson correlation test, for interactions between endophyte growth (biomass) and cellulase activities.

and PS + PDB ($r = 0.0778$), but inversely correlated for PDB ($r = -0.1906$) (Fig. 9). This result illustrates the importance of cellulase production in aiding colonization of endophytes as the extent of colonization is strongly correlated to cellulase activities by the endophytes. This strong correlation observed in PS, further suggests that this phenomenon is typical in host environments.

The third endophyte-host interaction studied the influence of endophyte growth on antifungal activity towards FocR4. Correlation analysis was performed using data from sections 3.2 and 3.4. Endophyte growth in PDB has an inverse correlation to antifungal activities ($r = -0.5129$), while positive correlations were obtained for growth and antifungal activities in PS ($r = 0.2760$) and PS + PDB ($r = 0.4381$) (Fig. 10). The

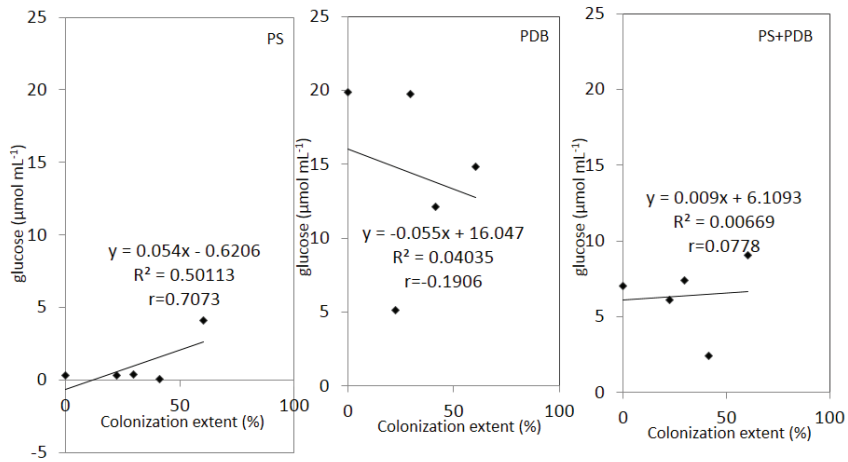

Figure 9. Correlation coefficient (r) from Pearson correlation test, for interactions between endophyte colonization with cellulase activities.

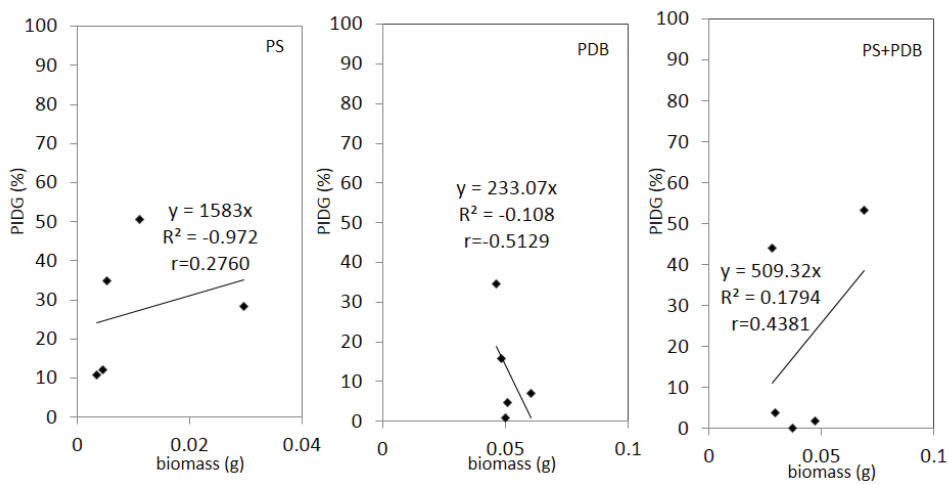

Figure 10. Correlation coefficient (r) from Pearson correlation test, for interactions between endophyte growth and antifungal activities.

inverse correlation strongly suggests that antifungal activities are compromised by the abundant growth of isolates. On the contrary, in nutrient-depleted conditions such as in host tissues (PS), the correlation is present where good fungal growth may appear to be necessary for effective production of antifungal compounds.

Discussion

We obtained several profound insights from this study. Firstly, the inverse correlation between colonization extent (and to a certain degree for growth) of endophytes and induced host enzymes provides hypothetical assumptions, that the rate and efficiency of endophyte colonization may be limited by the enzymes produced. These enzymes, produced as a natural response to presence or infection by biotic or abiotic stimulators, have conventionally been thought to be advantages as it forms mechanisms to disease resistance. These enzymes are typically studied for their roles in the production of antimicrobial compounds (quinone molecules) and the reinforcement of cell walls (lignification) to prevent spread of pathogens (Raju et al. 2008; Naveen et al. 2013). Nevertheless, here we discovered that the induction of these enzymes may also limit endophyte colonization as the enzymes are non-specific in their effect towards endophytes. The influence of induced host defense enzymes on endophytic colonization is demonstrated particularly for isolates BTF21 and T2. Although, we did not further determine the extent of

structural lignification, elevated levels of PO, PPO and PAL suggests that lignification may have occurred and restricted endophyte colonization (Ting 2014). The interaction of factors here revealed that although, BTF21 would have been a desirable biocontrol agent (high levels of induced enzymes), the endophyte is highly susceptible to induced-host enzymes where endophytic colonization is compromised. On the contrary, isolate T2, which elicited the least levels of enzymes, demonstrated better colonization. Endophytes also revealed that they are not immune to these induced enzymes, despite being natural colonizers of the host tissues.

The influence of induced host-defense enzymes on endophyte growth was tested in PS, PDB and PS + PDB. In this experiment, PS hypothetically mimics the host tissues (host environment) due to the presence of blended tissue extracts (slurry). This approach is novel and takes the lead from a study by Stevens et al. (1988). In their study, they used diced cortical tissues of apples to determine the degradation of cell wall of apple by human fecal bacteria. Similarly, the blended plant slurry used in this study mimics the possible *in planta* condition. We do not deny that this may not accurately demonstrate *in planta* conditions, especially in replicating all the major substrates present in the plant tissues; nevertheless, the use of plant slurry is deemed the closest possible approach to creating a mimicry of *in planta* environment. Blended plant slurry provided at least some of the plant metabolites, which benefited the experiment especially when it is almost impossible to replicate *in planta* conditions, definitely. The PS used in this experiment was also sterilized, therefore induction of defense enzymes in PS is not possible. As such, the growth of endophytes particularly BTF21 and WAA02 in PS, which produced relatively higher biomass compared to other isolates, clearly suggested that better growth (of BTF21 and WAA02) *in planta* (PS) was possible and achievable when independent of the presence of induced host-defense enzymes. Hence, induced enzymes not only influence colonization extent, but may also influence the growth and proliferation of endophytes *in planta*.

This study also revealed that cellulase activities have valid interactions with colonization extent and growth of endophytes. Cellulase activities are found to have a key role in influencing endophyte colonization with strong correlation detected in conditions using PS. This illustrates the colonization potential of endophytes in plants (PS), where higher cellulase levels will lead to better colonization. On the contrary, cellulase activities have an inverse correlation with endophyte growth (biomass) in PS. The production of cellulase enzymes in PS by isolate T2, corresponded with the hypothesis suggesting endophytes that colonize to great extents *in planta,* do so by producing significant amounts of cell wall degrading enzymes (CWDEs) such as cellulase to degrade plant cell wall for colonization (Deshmukh et al. 2006; Gao et al. 2010). The variations in cellulase levels produced by isolates suggest that cellulase production may be species specific, influenced by their mode of infection (penetration into cell wall) and colonization (intercellular or intracellular) (Yedidia et al. 1999; Tucker and Talbot 2001; Moy et al. 2002; Gao and Mendgen 2006; Rosenblueth and Martinez-Romero 2006; Vargas et al. 2009). For PDB, the nutrient-rich condition elicited different sets of observations. We do not rule out the possibility that high cellulase levels may be the consequence of growth. Cellulase levels are bound to or excreted by cell surface (Hurek and Reinhold-Hurek 2003), hence abundant biomass would naturally lead to higher cellulase levels.

In the final part of the study, growth/biomass of endophytes have contrasting correlation responses to antifungal activity in PS and in PDB. In PS, growth somewhat influenced antifungal activities, whereby better growth leads to stronger antifungal activities. On the contrary, an inverse correlation was detected in growth and antifungal activities in PDB. This suggested that the probable reason could be attributed to the fact that antifungal compounds are usually secondary metabolites produced under nutrient-depleted (or nutrient stress) conditions, where growth of fungi is compromised (Pavithra et al. 2012). As such, growth in PS is important to ensure the production of antifungal compounds. In PDB, where a nutrient-rich condition is present, growth is abundant and secondary metabolite production may be absent. Hence, the more growth detected in PDB, lesser the antifungal compounds were produced. Our results on the response of isolates in PS (simulation study) are of interest as they may indicate the possible antifungal activity connected to endophytes *in planta*. Although, we did not quantify the antifungal compounds produced, the results suggest that antifungal activities are expressed *in planta* and may be influenced by other factors.

In conclusion, this study has revealed some interesting insights. Firstly, we established that colonization and growth of introduced endophytes is influenced by the host plant, particularly, the role of induced defense enzymes. Low levels of plant defense enzymes led to better endophytic colonization and vice versa. The host enzymes also influenced growth of endophytes and their colonization within specific plant tissues. Therefore, host-defense enzymes, which are typically important to curb pathogen spread, have now been revealed to restrict endophyte colonization. The limitations on the growth may also lead to poorer cellulase levels that hamper its colonization activities. However, endophytes retained their antifungal activity *in planta*, despite poor growth. This indicates that endophytes can be introduced as biocontrol agents as they have ability to express antifungal activities and colonize the plant. Nevertheless, the degree of successful establishment and biocontrol expression is linked to the host plant. From this study, we do not propose a solution to managing endophyte-host plant interactions, but merely offering a better understanding on factors that may influence the

colonization of endophytes in host plants. The complexity of the endophyte-host-pathogen factors remained to be further explored. In future, investigations into the association of host-defense enzymes with endophyte colonization and their subsequent biocontrol efficacy can be performed to enhance understanding on using endophytes as BCAs.

Acknowledgements

The authors express their gratitude to the Malaysian Ministry of Higher Education (MOHE) for the Exploratory Research Grant Scheme (ERGS/1/2013/STWN03/MUSM/02/1) awarded and to Monash University Malaysia for the facilities to complete the project.

References

Akello J, Dubois T, Coyne D, Kyamanywa S (2009) The effect of *Beauveria bassiana* dose and exposure duration on colonization and growth of tissue cultured banana (*Musa* sp.) plants. Biol Contr 49:6-10.

Amin I, Norazaidah Y, Emmy-Hainida KI (2004) Antioxidant activity and phenolic content of raw and blanched *Amaranthus* species. Food Chem 94(1):47-52.

Bentley S, Pegg KG, Moore NY, Davis RD, Buddenhagen IW (1998) Genetic variation among vegetative compatibility group of *Fusarium oxysporum* f. sp. *cubense* analyzed by DNA fingerprinting. Phytopathology 88:1283-1293.

Deshmukh S, Huckelhoven R, Schaefer P, Imani J, Sharma M, Weiss M, Waller F, Kogel KH (2006) The root endophytic fungus *Piriformospora indica* requires host cell death for proliferation during mutualistic symbiosis with barley. Proc Natl Acad Sci USA 103(49):18450-18457.

Donnison LM, Griffith GS, Hedger J, Hobbs PJ, Bardgett RD (2000) Management influences on soil microbial communities and their function in botanically diverse hay meadows of northern England and Wales. Soil Biol Biochem 32:253-263.

Gao FK, Dai CC, Liu XZ (2010) Mechanisms of fungal endophytes in plant protection against pathogens. Afr J Microbiol Res 4(13):1346-1351.

Gao K, Mendgen K (2006) Seed transmitted beneficial endophytic *Stagonospora* sp. can penetrate the walls of the root epidermis, but does not proliferate in the cortex of *Phragmites australis*. Can J Bot 84:981-988.

Hurek T, Reinhold-Hurek B (2003) *Azoarcus* sp. strain BH72 as a model for nitrogen-fixing grass endophytes. J Biotechnol 106:169-178.

Liu YF, Chen ZY, Ng TB, Zhang J, Zhou MG, Song FP, Lu F, Liu YZ (2007) Bacisubin, an antifungal protein with ribonuclease and hemagglutinating activities from *Bacillus subtilis* strain B-916. Peptides 28:553-559.

Manikandan R, Saravanakumar D, Rajendran L, Raguchander T, Samiyappan R (2010) Standardization of liquid formulation of *Pseudomonas fluorescens* Pf1 for its efficacy against Fusarium wilt of tomato. Biol Contr 54:83-89.

Moy M, Li HM, Sullivan R, White Jr JF, Belanger FC (2002) Endophytic fungal β-1,6-glucanase expression in the infected host grass. Plant Physiol 130:1298-1308.

Naveen J, Hariprasad P, Chandra-Nayaka S, Niranjana SR (2013) Cerebroside mediated elicitation of defense response in chilli (*Capsicum annuum* L.) against *Colletotrichum capsici* infection. J Plant Interact 8(1):65-73.

Pavithra N, Sathish L, Ananda K (2012) Antimicrobial and enzyme activity of endophytic fungi isolated from Tulsi. J Pharm Biomed Sci 16(12):1-6.

Podille AR, Laxmi VDV (1998) Seed bacterization with *Bacillus subtilis* AF1 increases phenylalanine ammonia lyase and reduces the incidence of fusarial wilt in pigeon pea. J Phytopathol 146(5-6):255-259.

Raju S, Jayalakshmi SK, Sreeramulu K (2008) Comparative study on the induction of defense related enzymes in two different cultivars of chickpea (*Cicer arietinum* L) genotypes by salicylic acid, spermine and *Fusarium oxysporum* f. sp. *ciceri*. Aust J Crop Sci 2(3):121-140.

Rosenblueth M, Martinez-Romero E (2006) Bacterial endophytes and their interactions with hosts. Mol Plant Microbe Interact 19:827-837.

Schulz B, Wanke U, Draeger S, Aust HJ (1993) Endophytes from herbaceous plants and shrubs: effectiveness of surface sterilization methods. Mycol Res 97(12):1447-1450.

Shanmugam V, Kanoujia N (2011) Biocontrol of vascular wilt and corm rot of gladiolus caused by *Fusarium oxysporum* f. sp. *gladioli* using plant growth promoting rhizobacterial mixture. Crop Prot 30:807-813.

Stevens BJH, Selvendran RR, Bayliss CE, Turner R (1988) Degradation of cell wall material of apple and wheat bran by human faecal bacteria in vitro. J Sci Food Agric 44:151-166.

Sundaramoorthy S, Raguchander T, Ragupathi N, Samiyappan R (2012) Combinatorial effect of endophytic and plant growth promoting rhizobacteria against wilt disease of *Capsicum annuum* L. caused by *Fusarium solani*. Biol Contr 60:59-67.

Sylvia DM, Neal LH (1990) Nitrogen affects the phosphorus response of VA mycorrhiza. New Phytol 115:303-310.

Ting ASY, Meon S, Kadir J, Radu S, Singh G (2008) Endophytic microorganisms as potential growth promoters of banana. Biocontrol 53:541-553.

Ting ASY, Meon S, Kadir J, Radu S, Singh G (2009a) Field evaluation of non-pathogenic *Fusarium oxysporum* iso-

lates UPM31P1 and UPM39B3 for the control of Fusarium wilt in 'Pisang Berangan' (Musa, AAA). Acta Hortic 828:139-144.

Ting ASY, Meon S, Kadir J, Radu S, Singh G (2009b) Induced host resistance by non-pathogenic *Fusarium* endophyte as a potential defense mechanism in Fusarium wilt management of banana. Pest Technol 3(1):67-72.

Ting ASY, Fang MT, Tee CS (2009c) Assessment on the effect of formulative materials on the viability and efficacy of *Serratia marcescens* - a biocontrol agent against *Fusarium oxysporum* f. sp. *cubense* race 4. Am J Agric Biol Sci 4(4):283-288.

Ting ASY, Mah SW, Tee CS (2009d) Prevalence of endophytes antagonistic towards *Fusarium oxysporum* f. sp. *cubense* Race 4 in various plants. Am Eur J Sustain Agric 3(3):399-406.

Ting ASY, Mah SW, Tee CS (2010a) Identification of volatile metabolites from fungal endophytes with biocontrol potential towards *Fusarium oxysporum* f. sp. *cubense* race 4. Am J Agric Biol Sci 5(2):177-182.

Ting ASY, Meon S, Kadir J, Radu S, Singh G (2010b) Induction of host defense enzymes by the endophytic bacterium *Serratia marcescens* in banana plantlets. Int J Pest Manage 56:183-188.

Ting ASY, Mah SW, Tee CS (2011a) Detection of potential volatile inhibitory compounds produced by endobacteria with biocontrol properties towards *Fusarium oxysporum* f. sp. *cubense* race 4. World J Microbiol Biotechnol 27:229-235.

Ting ASY, Fang MT, Tee CS (2011b) Efficacy of clay based formulated *Serratia* in reducing inoculum of *Fusarium oxysporum* f. sp. *cubense* race 4. Acta Hortic 897:421-426.

Ting ASY, Mah SW, Tee CS (2012a) Evaluating the feasibility of induced host resistance by endophytic isolate *Penicillium citrinum* BTF08 as a control mechanism for Fusarium wilt in banana plantlets. Biol Contr 61:155-159.

Ting ASY, Tay HQ, Peh KL, Tan WS, Tee CS (2012b) Novel isolation of thermophilic *Ureibacillus terrenus* from compost of Empty Fruit Bunches (EFB) of oil palm and its enzymatic activities. Biocatal Agric Biotechnol 2(2):162-164.

Ting ASY (2014) Biosourcing endophytes as biocontrol agents of wilt diseases. In Verma VC, Gange AC (eds.), Advances in Endophytic Research. Springer, India. Pp. 283-300.

Tucker SL, Talbot NJ (2001) Surface attachment and prepenetration stage development by plant pathogenic fungi. Ann Rev Phytopathol 39:385-417.

Vargas WA, Mandawe JC, Kenerley CM (2009) Plant-derived sucrose is a key element in the symbiotic association between *Trichoderma virens* and maize plants. Plant Physiol 151:792-808.

Yedidia I, Benhamou N, Chet I (1999) Induction of defense responses in cucumber plants (*Cucumis sativus* L.) by the biocontrol agent *Trichoderma harzianum*. Appl Environ Microbiol 65:1061-1070.

Zacky FA, Ting ASY (2013) Investigating the bioactivity of cells and cell-free extracts of *Streptomyces griseus* towards *Fusarium oxysporum* f. sp. *cubense* race 4. Biol Contr 66:204-208.

Volume 61(1):13-23, 2017
Acta Biologica Szegediensis
http://www2.sci.u-szeged.hu/ABS

ARTICLE

Optimization of bioethanol production from saccharified sweet potato root flour by co-fermentation of *Saccharomyces cerevisiae* and *Pichia* sp. using OVAT and response surface methodologies

Preeti Krishna Dash[1], Sonali Mohaptra[1], Manas Ranjan Swain[2], Hrudayanath Thatoi[3]*

[1]Department of Biotechnology, College of Engineering and Technology, Biju Patnaik University of Technology, Bhubaneswar-751003, India
[2]Department of Biotechnology, Indian Institute of Technology, Madras, Chennai-600036, India
[3]Department of Biotechnology, North Orissa University, Takatpur, Baripada-757003, India

ABSTRACT In recent years with the increase in price of fossil fuels, the demand of biofuel production from tuber crops such as sweet potato has become very important to meet the future energy crisis in developing countries. In the present study, fermentation of saccharified sweet potato root flour (SPRF) was carried out using co-culture of cells of *Saccharomyces cerevisiae* and *Pichia* sp. in immobilized condition for bioethanol production. Various growth parameters like incubation time, fermentation medium pH, incubation temperature and inoculum size were initially optimized using one variable at a time (OVAT) methodology. Then, temperature, pH and incubation time were found to be the most favorable variables for the maximum ethanol production with Box-Behnken design of response surface methodology (RSM). The maximum ethanol yield of 127.2 ± 2 g/kg of SPRF was obtained at pH 5 with an incubation period of 72 h at 30 °C by OVAT methodology. RSM further enhanced the bioethanol yield to 138.6 ± 3 g/kg of SPRF with an overall increase of 8.22% as compared to the OVAT method.

Acta Biol Szeged 61(1):13-23 (2017)

KEY WORDS

bioethanol
OVAT
Pichia
RSM
Saccharomyces cerevisiae
sweet potato

Introduction

The bioconversion of biomass resources in large-scale, especially starchy materials to ethanol, was expected to find its application in the production of biofuel (Shigechi et al. 2004). In the recent years, increase in the price of the fossil fuel is one of the major reasons for search of renewable fuels to meet the future energy demand (Liimatainen et al. 2004). The major constraint for industrial bioethanol production includes the collection of the raw material and its processing costs (Vucurovic et al. 2009). Hence, studies were focused to search for raw materials with high carbohydrate content and efficiently developed transformation processes for enhanced bioethanol production to meet the fuel crisis (Dias et al. 2012; Soccol et al. 2010). Bioethanol produced from tuber crops like sweet potato, cassava, potato, etc., is a promising option since it contains sufficient amount of starch (15-37%) that could be hydrolyzed to sugars and then fermented to ethanol (Lin et al. 2010). Among the tuber crops, sweet potato (*Ipomoea batatas* L.) represents an important biomass resource for fuel ethanol production due to high density of starch compared to other forms of biomass (Roukas 1994). It contains starch (178 g/kg), total sugars (26 g/kg) and protein (3.2 g/kg) on fresh weight basis (Tian et al. 1991).

Generally, the starchy substrates require a reaction of starch with water and enzymes (hydrolysis) to break down the starch into fermentable sugars by a process known as saccharification. The hydrolysis process involves the mixing of starch with water to form slurry, which is subjected to heat treatment for the cell wall to rupture. Enzymes, like α-amylase and glucoamylase, which are responsible for the breakdown of the chemical bonds in the starch, are applied at various times during the heat treatment (Badger 2002). The α-amylase randomly hydrolyzes internal α-1,4-glycosidic bonds in starch, and liberates soluble dextrin and oligosaccharides that are more suitable for efficient conversion to glucose. This process is the dextrinization. It is followed by saccharification, in which glucoamylase hydrolyzes 1,4 and 1,6-alpha linkages in liquefied starch and thereby converting

Submitted October 10, 2016; Accepted March 27, 2017
*Corresponding author. E-mail: hnthatoi123@gmail.com

the starch to sugar (Van der Maarel et al. 2002). The microorganisms utilized in fermentation for ethanol production should have attributes like high ethanol yield, high productivity and have the capacity to withstand high concentrations of ethanol (Von Sivers and Zacchi 1996). The *Saccharomyces cerevisiae* is the most preferred organism for utilizing part of hexose sugar present in the substrate during fermentation of ethanol; however, a substantial amount of the sugar remains unutilized. Thus, use of another strain as co-culture can be preferred over a single strain (Pornkamol and Friedrich 2010). Recently, *Pichia stipitis* has seen to be a promising microorganism for industrial application as it gives high ethanol yield (Du Preez and Prior 1985), and able to ferment a wider range of sugars (Du Preez et al. 1986).

In the fermentation, the microorganisms are immobilized with suitable matrix, in order to use the strain in perpetual basis for an economical bioethanol production. Use of the immobilized strains for fermentation of ethanol have several advantages over freely suspended cells as the immobilized cells can be easily separated and recycled further (Giordano et al. 2008; Zhou et al. 2008). Co-immobilization of different kinds of microorganisms within the same porous matrix is a simple technique, which reduces the energy input and increases the efficiency of substrate utilization and the rate of production (Lee et al. 2012).

The response surface methodology (RSM) is extensively used in bioethanol production as this model predicts experimental modifications like changes in operational conditions, various processing steps, which ultimately help in designing an experimental setup with minimum requirements and maximum yields (Uncu and Cekmecelioglu 2011). RSM comprises of a group of mathematical and statistical procedure that can be used to study the optimization of culture conditions and it has already been successfully applied for optimization of media and culture conditions in many fermentation processes for production of ethanol, enzymes and amino acids (Kar et al. 2009). The aim of this work was to develop a simultaneous single-step system for bioethanol fermentation from saccharified sweet potato root flour, using co-immobilized cells of yeast *S. cerevisiae* and *Pichia* sp. at submerged fermentation condition. Further optimization of the major fermentation parameters was carried out by applying OVAT and response surface methodology (RSM) for enhanced bioethanol production.

Materials and Methods

Microorganisms

Saccharomyces cerevisiae used for alcoholic fermentation in factories and *Pichia* sp. isolated from toddy samples in our laboratory (strain CET) were adopted as the experimental strains. Both strains were maintained on potato dextrose agar medium (PDA; g/l: potato, 200; dextrose, 20; agar, 15; pH 7) and stored at 4 °C for further use.

Immobilization and co-fermentation

S. cerevisiae (3 x 10^9 CFU/ml) was mixed with 2.5% (w/v) Na-alginate solution and was added drop wise into 0.2 N $CaCl_2$ solution using a 50-ml syringe and beads of calcium alginate with entrapped cells, and were formed with a diameter of 3-4 mm. Then the beads were allowed to harden in 0.2 N $CaCl_2$ for overnight at 4 °C. Similarly, preparation of immobilized *Pichia* sp. cells was carried out by using this method. For co-fermentation, the immobilized beads of *S. cerevisiae* and *Pichia* sp. that were prepared separately, were mixed together in equal proportions and used for further studies.

Multiplication of immobilized yeast cells

In order to obtain a high yeast cell density, the cells were allowed to grow on the beads for 24 h before used in the fermentation. The gel beads, containing the immobilized yeast cells, were immersed in yeast extract peptone dextrose (YEPD) agar medium, [(g/l): yeast extract, 5; peptone, 5; glucose, 20; agar, 15; pH 5.5]. The immobilized cells of *S. cerevisiae* (5.3 x 10^9 CFU/ml) and *Pichia* sp. (5.3 x 10^9 CFU/ml) were grown separately in 250 ml Erlenmeyer flasks, containing 100 ml sterilized YEPD broth at 30 ºC for 24 h, and were used for further ethanol production experiments.

Substrate

Sweet potato (*Ipomoea batatas* L.) was purchased from the local market of Bhubaneswar, Odisha, India during the month of February, 2013. The tubers were washed thoroughly, to remove the dust and other debris, peeled off and chopped into small pieces. These sieves were then placed in oven at 70 °C for 24 h, still the moisture content reduced to 11-12% and were grinded into flour using a mixture grinder (Bajaj Pvt. Ltd, India) at 250 rpm. The flour was sieved through a steel mesh to get 2-3 mm diameter size and stored in airtight container for further use.

Enzymatic saccharification of SPRF

The sweet potato root flour (SPRF) slurry was prepared in 250 ml Erlenmeyer flasks with a working volume of 100 ml by adding tap water in a ratio of 1:10 (sweet potato root flour:water) for experiment. In the first step the slurry was dextrinized by addition of 32 µl Palkolase-HT (Maps Enzymes, Ahmadabad, India) at pH 5.5 and 90 °C for 2 h, and then it was cooled down to room temperature. In the second

step, 329.7 µl of Palkodex (Maps Enzymes, Ahmadabad, India) was added to the cooled dextrinized slurry, and it was incubated at pH 4.5 and 60 °C for 24 h for saccharification.

Ethanol fermentation from saccharified SPRF

Ethanol fermentation was conducted by co-culture of cells of *S. cerevisiae* and *Pichia* sp. under anaerobic conditions in an Erlenmeyer flask (250 ml) sealed with rubber stopper equipped with opening for CO_2 venting. The saccharified SPRF (100 ml) was inoculated with freshly harvested co-fermentation cells of *S. cerevisiae* and *Pichia* sp. (10% w/v, 5.3 x 10^9 CFU/ml) aseptically. Flasks (n = 3) were incubated in an incubator-cum shaker at 30 ± 2 °C for 120 h with a constant shaking of 100 rpm. The fermented broth was distilled to recover ethanol using alcohol distillation apparatus (Borosil Glass Works, Mumbai, India).

Study of fermentation parameter

The saccharified SPRF slurry was inoculated with co-immobilized cells of *S. cerevisiae* and *Pichia* sp. and incubated at different incubation times (24-120 h). The fermentation medium (saccharified 10% SPRF slurry) with pH 3-5.5 at 0.5 interval was inoculated with immobilized cells of *Saccharomyces cerevisiae* and *Pichia* sp. separately and incubated at 30 °C for 72 h.

The saccharified 10% SPRF slurry at pH 5 was inoculated with co-immobilized cells and incubated for 72 h at different temperatures (20-40 °C). The fermentation medium with pH 5.0 was incubated at 30 °C for 72 h by 10% inoculums of *S. cerevisiae* and *Pichia* sp. comprising with different proportions (2:1, 1:1, and 1:2).

Analytical techniques

The ethanol concentration of the fermentation medium was determined based on the density of the alcohol distillates obtained from the fermentation broth. The density of the distilled alcohol sample was calculated as following: ρ (g/kg) = (W_{sample}-W)/(W_{water}-W), where W_{sample} is the mass of pycnometer, containing distilled ethanol from the sample, *i.e.* filtrated mash (50 ml) and then filled up with distilled water up to the marker level. W is the mass of clean and dry pycnometer (50 ml); W_{water} is the mass of the pycnometer filled up with distilled water. Ethanol concentration of the fermentation liquid was determined by measuring the specific gravity of the distillate according to the procedure described by Amerine and Ough (1984).The pH was measured using a pH meter (Systronics, Ahmadabad, India) fitted with a glass electrode.

Calculations

The maximum theoretical ethanol yield from sugar was calculated according to the stoichiometric relation represented by Equation 1. Accordingly, 100 g of hexose produces 51.1 g of ethanol and 48.9 g of CO_2. The fermentation efficiency (Y_1) and average ethanol productivity rate (Y_2) were calculated according to Equation 2 and 3.:

Eq. 1.

$$C_2H_{12}O_6 \rightarrow 2CH_3CH_2OH + 2CO_2$$

Eq. 2.

Y_1 = Ethanol produced in fermentation (g/kg starch) x 100/
Ethanol produced in theoretical (g/kg starch)

Eq. 3.

Y_2 = Final ethanol concentration/Fermentation time

RSM experimental design and optimization

The effect of different factors responsible for the ethanol production from SPRF was optimized using response surface methodology. The statistical model was studied by using Central Composite Design (CCD) experiments. Incubation time (A), pH (B) and temperature (C) were taken as independent variables as shown in Table 4. These three parameters were chosen as they were seen to influence the ethanol productivity to a more extent. Ethanol concentration was chosen as the dependent variable. The twenty experiments based on CCD were carried out with different combinations of variables and the results were presented in Table 2. The response was measured in terms of ethanol production, which was taken as the dependent variable.

Statistical analysis

The data obtained from RSM on total ethanol production were subjected to the analysis of variance (ANOVA). The results of RSM were used to fit a second order polynomial equation (4) as it represents the behavior of such a system more appropriately.

Eq. 4.

$$y = \beta_0 + \sum_{i=1}^{3} \beta_i X_i + \sum_{i=1}^{3} \beta_{ii} X_i^2 + \sum_{i=1}^{3} \times \sum_{j=i+1}^{3} \beta_{ij} X_i X_j$$

The Y is response variable, β_0 is intercept, β_1, β_2, and β_3 are linear coefficients, $\beta_{1,1}$, $\beta_{2,2}$ and $\beta_{3,3}$ are squared coefficient, $\beta_{1,2}$, $\beta_{1,3}$ and $\beta_{2,3}$ are interaction coefficient and A, B, C, A^2,

Table 1. Effect of incubation period on bioethanol production.

Time interval (h)	Ethanol production (g/kg)	Total sugar (g/kg)
0	0	224.8 ± 0.4
24	27.8 ± 0.9	194.8 ±0.3
48	74.6 ± 1	173.2 ± 0.5
72	127.2 ± 2	120.7 ± 0.6
96	127.9 ± 1.1	114.4 ± 0.4
120	127.6 ± 0.8	110.4 ± 0.8

Table 2. Effect of fermentation medium pH on bioethanol production.

pH	Ethanol production (g/kg)	Total sugar (g/kg)
3	11.8 ± 0.9	218.8 ± 0.3
3.5	28.6 ± 0.1	199.2 ± 0.3
4	57.2 ± 0.6	170.7 ± 0.9
4.5	91.9 ± 1.1	151.4 ± 0.9
5	129.4 ± 5	110.9 ± 0.1
5.5	130.1 ± 0.1	100.2 ± 0.2

Table 3. Effect of temperature on bioethanol production.

Temperature (°C)	Ethanol production (g/kg)	Total sugar (g/kg)
20	47.6 ± 0.6	182.7 ± 1.2
25	81.9 ± 1.9	143.5 ± 1.5
30	131.6 ± 3	107.6 ± 3
35	131.8 ± 0.9	104.3 ± 0.2
40	131.9 ± 0.1	94.3 ± 0.6
45	132.1 ± 2	75.3 ± 1.2

B^2, C^2, AB, AC and BC are level of independent variables. Statistical significance of the model equation was determined by Fisher's test value, and the production of variance explained by the model was given by the multiple coefficient of determination, R squared (R^2) value. Design Expert® Software was used in this investigation. Three-dimensional plots were obtained to study the interaction of one parameter with other. The optimum ethanol production was identified in the three-dimensional plot.

Results and Discussion

Optimization of SSF parameters following OVAT methodology

In the present study, different process parameters influencing the ethanol production of single immobilized *S. cerevisiae* and *Pichia* sp. were studied in conical flasks using enzymatic saccharified SPRF as substrate. Then, use of immobilized cells of *S. cerevisiae* and *Pichia* sp. was studied for ethanol production in laboratory scale. Optimization of the various parameters of saccharified SPRF was carried out using OVAT and RSM technologies. Four process parameters (incubation time, temperature, pH, and inoculum size) were considered, as these parameters mostly influence the growth of both yeast strains. All the experiments for OVAT were carried out in triplicate and data in Table 1, 2 and 3 are presented as mean ± SE (standard error).

Table 4. Coded levels of the independent variables for the design of the experiment.

Independent variables	Symbols	Coded levels		
		-1	0	+1
Incubation period (h)	A	48	84	120
pH	B	4	5	6
Temperature (°C)	C	25	30	35

Comparison of single immobilization and co-fermentation for bioethanol production

The ethanol production from enzymatic saccharified SPRF was studied using immobilized *S. cerevisiae* and *Pichia* sp., separately in conical flasks. Ethanol production of 75.1 ± 2 g/kg and 62.6 ± 2 g/kg was obtained from single immobilized *S. cerevisiae* and *Pichia* sp., respectively, whereas, the co-immobilized cells of *S. cerevisiae* and *Pichia* sp. produced 120.5 ± 2 g/kg of ethanol. Since the co-immobilized cells demonstrated higher ethanol yield than single cultures, further process optimization was carried out with co-immobilized cells of *S. cerevisiae* and *Pichia* sp.

Effect of incubation period on ethanol production

The effect of incubation period on ethanol production from SPRF by co-immobilized strains of *S. cerevisiae* and *Pichia* sp. was studied. Ethanol production increased sharply up to 72 h and then a steady state was obtained, which was decrease in the glucose uptake capacity of the immobilized yeast cells. The sharp increase in the ethanol concentration may be due to the rapid utilization of the glucose by the two separately immobilized yeast strains. The maximum ethanol of 127.2 ± 2 g/kg of SPRF was obtained at 72 h of incubation with total sugar consumption up to 53.7% (Table 1). This may be due to rapid increase in biomass and ethanol concentration (Swain et al. 2007). In a study by Mohanty et al. (2009), maximum ethanol concentration was obtained after 72 h of incubation

from mahula (*Madhuca latifolia* L.) flowers. McGhee et al. (1996) studied the bioethanol production from molasses by separately immobilized cells of *S. cerevisiae*, *S. uvarum* and *Zymomonas mobilis* in calcium alginate. The immobilized *S. cerevisiae* was found to be the best alcohol producer yielding 4.7 g ethanol/100 g 10% glucose solution within 72 h. Improved ethanol production from sweet sorghum was achieved to 29.7 g ethanol/100 g dry sorghum stalks by using *Fusarium oxysporum* mixed culture with *Z. mobilis* (Swain et al. 2013). These studies also suggest that immobilized yeast cells with 72 h incubation time generally present high ethanol yield, which is in good agreement with our current study.

Effect of pH on ethanol production

The pH value of the fermentation medium is a very important factor for bioethanol production (Pirselova et al. 1993). The effect of pH on ethanol production yield of co-fermenting yeasts from saccharified sweet potato root flour was studied by conducting batch experiments at different pH ranging from pH 3 to 5.5 (Table 2). Ethanol concentration increased drastically with the increase in pH up to 5 and decreased beyond this value. The maximum ethanol concentration of 129.4 ± 5 g/kg of SPRF was obtained at pH 5 with a decrease in the total and reducing sugar. In another study by Lee et al. (2012), ethanol production of 3.05% (v/v) was achieved at an initial pH 4 followed by 2.65% (v/v) at pH 5, from sweet potato by the co-immobilization of *A. oryzae* and *S. cerevisiae*. In a study by Neelakandan and Usharani (2009), increasing the pH from 4 to 6 resulted increased ethanol production with highest production yield at pH 6 from cashew apple juice by immobilized *S. cerevisiae.* According to Narendranath and Power (2005), yeasts having pH optimum between 4 and 6 can grow under pH range conditions of 2.5 to 8.5. It was also shown that no ethanol production exists lower than pH 4 (Graves et al. 2006). The effect of pH on ethanol production was studied by Pitt (1993) using mixed cultures of *Zymomonas mobilis* and *Paenibacillus* sp. on raw starchy material from sweet potato. In a similar study, ethanol production from wheat bran flour was investigated by co-culturing of *Aspergillus niger* and *Kluyveromyces marxianus* and the optimum pH was found to be 5.5 (Manikandan and Viruthagiri 2010). According to Clarence et al. (2010), the pH of the fermentation medium significantly affects the growth of the microorganisms and ethanol production.

Effect of temperature on ethanol production

The amount of bioethanol production depends on the optimal temperature, because it influences sugar utilization by yeast cells (Manikandan and Viruthagiri 2010). In the present study, increase in the fermentation temperature from 20 to 45 °C significantly affected the ethanol concentration, ethanol productivity and fermentation efficiency and sugar concentration (Table 3). Both low (20 °C) and high (45 °C) temperature had negative effect on ethanol production. The maximum ethanol concentration (131.6 ± 3 g/kg SPRF) was obtained at 30 °C (pH 5) with an incubation period of 72 h. The total and reducing sugars decreased with the increase in the ethanol concentration. This was probably due to the decrease in viable cell number above 30 °C, because at higher temperatures the yeast cells degrade (Periyasamy et al. 2009). According to Hashem and Darwish (2011), high temperature affects the growth of some yeast strains, which inhibit the ethanol fermentation. Temperature range of 25 to 30 °C is found to be optimum for ethanol production of mesophilic *S. cerevisiae* strains in SSF of sweet sorghum (Mamma et al. 1996). The effect of temperature on ethanol production from glucose was studied using calcium alginate-immobilized *Candida tropicalis* and *S. cerevisiae* (Jamai et al. 2007). It was observed that the fermentation capacity and the ethanol production reduced by 25% at 40 °C. In another study, Shuler and Kargi (2002) achieved high ethanol production at temperature range between 30-35 °C from glucose.

Effect of inoculum size on ethanol production

The size of inoculum in ethanol fermentation has a great importance for completion of the fermentation process. Maximum ethanol concentration of 131.4 ± 4 g/kg of SPRF was achieved at 10% (1:1 = *S. cerevisiae*:*Pichia* sp.) inoculum concentration by utilizing (73.4% by *S. cerevisiae* and 75.1% by *Pichia* sp) of total sugars. A study of Swain et al. (2013), concluded that the maximum ethanol was obtained with a concentration of 10% (1:4 = *Trichoderma* sp.: *S. cerevisiae)* in sweet potato flour by co-culture of *Trichoderma* sp.: *S. cerevisiae.* In another study by Guo et al. (2008) co-immobilized mixed cultures of *Kluyveromyces marxianus* and *S. cerevisiae* were used for bioethanol production from cheese whey powder and the results revealed that maximum ethanol was produced using equal volume cells of *K. marxianus* and *S. cerevisiae*. In general, 3-10% (v/v) inoculum of *S. cerevisiae* has been reported for maximum bioethanol concentration from various substrates such as mahula (Maiti et al. 2011) and cashew apple (Tahir et al. 2010).

Cycles of the co-fermentation for ethanol production

In this study, to investigate the fermentation efficiency of immobilized cell recycling, repeated-batch fermentations were carried out and the results revealed that the immobilized cells were successfully recycled for three more times without much affecting the final ethanol concentration. There was a 3% decrease in ethanol production in the fourth cycle, which indicated a decrease in the efficiency of the immobilized yeast

Table 5. Growth and fermentation kinetics of immobilized microbial (*S. cerevisiae* and *Pichia* sp.) cells.

Growth and fermentation kinetics	Immobilized cells
Final ethanol (P, g/l)	22.7
Final biomass concentration (X, g/l)	5.23
Specific growth rate (μ, h)	0.098[a]
Cell yield (Yx/s, g/g)	0.013
Ethanol yield (Yp/s, g/g)	0.579
Volumetric substrate uptake (Qs, g/l/h)	0.431
Volumetric product productivity (Qp, g/l/h)	0.643
Conversion rate (%) into ethanol	82.8

Yp/s = Mass of ethanol formed/Mass of glucose consumed; Yx/s = Mass of yeast cell formed/Mass of glucose consumed; Qs = Substrate (glucose) uptake (g) per litre of hydrolysate per hour; Qp = Product formed (g) per litre of hydrolysate per hour; [a]μ (h^{-1}) = Standardized value (0.098) for specific growth rate of micro organism (yeast) under specific substrate (glucose) consumption

Table 6. Ethanol production by Box-Behnken factorial design.

Run	Time (h)	pH	Temp. (°C)	Ethanol (g/kg)
2	48.00	4.00	25.00	84.3
14	120.00	4.00	25.00	43.75
1	48.00	6.00	25.00	56.72
5	120.00	6.00	25.00	36.
6	48.00	4.00	35.00	31.4
12	120.00	4.00	35.00	18.3
19	48.00	6.00	35.00	64.
4	120.00	6.00	35.00	29.7
7	23.46	5.00	30.00	124.3
11	144.54	5.00	30.00	21.2
16	84.00	3.32	30.00	93.1
20	84.00	6.68	30.00	91.5
10	84.00	5.00	21.59	102.3
17	84.00	5.00	38.41	106.2
15	84.00	5.00	30.00	138.7
18	84.00	5.00	30.00	138.7

cells for ethanol production and hence no further cycles were repeated. The cells not only survived, but also were active physiologically yielding almost equal volume of bioethanol up to three cycles (131.3 ± 2, 128.7 ± 2, and 128.2 ± 2 g/kg of SPRF) without hampering the ethanol productivity. In recent years, many workers have used immobilized cell systems to ferment a wide variety of carbohydrates to ethanol. A similar study using co-immobilized yeast cells by Ghorbani et al. (2011) was reported, in which the immobilized cells were active up to four cycles of fermentation. However, there are some more reports where the immobilized cells were active for still longer period as evidenced from more number of cycles.

In a study by Amutha and Paramasamy (2001), the co-immobilized gel beads of *Saccharomyces diastaticus* and *Z. mobilis* on liquefied cassava starch were stable up to seven successive batches for ethanol production. The advantage of using co-immobilized cells was that the used cells survived and were active on the support used for immobilization for four cycles of fermentation, which could save considerable time and energy (Amutha and Paramasamy 2001).

The growth and fermentation kinetics of immobilized (Ca alginate) cells of *S. cerevisiae* and *Pichia* sp. were studied (Table 5). The ethanol concentration (P) obtained by co-immobilized cells was 22.7 g/l, and the volumetric substrate uptake was found to be 0.431 g/l/h. The ethanol yield and volumetric product productivity (Q_p) and (Qs) were found to be 0.643 g/l and 0.431 g/l/h, respectively, for the co-immobilized cells. The final sugar to ethanol conversion rate was found to be 82.8%. However, the final biomass concentration (X) was 5.23 after a successful fermentation and maximum ethanol fermentation. The above parametric optimization study from co-immobilized *S. cerevisiae* and *Pichia* sp. indicates co-fermentation is an efficient technique for ethanol production from saccharified SPRF. Similar study carried out by Behera et al. (2010), showed that, the ethanol concentration (P) obtained with immobilized cells using agar-agar and calcium alginate were 25.2 and 25.75 g/l, respectively, whereas, the volumetric substrate uptake (Qs) were found to be 0.552 and 0.554 g/l/h, respectively.

Statistical optimization and model validation

For further enhancement of ethanol production, a Box-Behnken factorial design was performed as given in Table 6. Since, the most important physical factors affecting the final ethanol yield were the temperature, pH and incubation time, these parameters were considered for the RSM methodology. In the present experiment, the inoculum size seemed to be less important in ethanol production and therefore it was not included in the RSM plots. It was observed that the predicted values that were obtained for ethanol production was in good agreement with RSM plots. The effects of the fermentation variables and their possible interactions were studied by ANOVA. Coefficients of a full model were evaluated by regression analysis and tested for their significance. Suitable levels for these parameters were determined using a statistical 2^3 full factorial design. Twenty experiments were performed for evaluation of ethanol production parameters by using co-immobilized *S. cerevisiae* and *Pichia* sp. The highest ethanol concentration 138.6 ± 3 g/kg substrate was obtained at 30 °C for 84 h, corresponding to an ethanol volumetric production rate of 0.48 g ethanol/l/h. However, the Q_p value was lower at 84 h. ANOVA performed on this models demonstrates that the models are statistically valid with *p*-values lower than 0.0001. ANOVA for model terms and its significance (*p*-values lower than 0.05 indicated that model terms were significant) showed linear effect of temperature, pH and incubation time on ethanol production (Table 7). The absence of interactions

Table 7. ANOVA for Response Surface Quadratic Model Analysis of Variance table (Partial sum of squares-Type III).

Source	Sum of squares	Df	Mean square	F-value	P-value
Model	284100	9	31570.12	21.61	<0.0001
A (Incubation period)	97814.39	1	97814.39	66.94	<0.0001
B (pH)	9860.29	1	9860.29	6.75	0.0266
C (Temperature)	4273.00	1	4273.00	2.92	0.1180
AB	330.89	1	330.89	0.23	0.6444
AC	1531.53	1	1531.53	1.05	0.3301
BC	42.55	1	42.55	0.029	0.8679
A^2	73318.17	1	73318.17	50.18	<0.0001
B^2	86656.81	1	86656.81	59.31	<0.0001
C^2	42760.24	1	42760.24	29.26	0.0003
Residual	14611.57	10	1461.16		
Lack of Fit	14611.57	10	1461.16	14611.57	10
Pure Error	0.000	5	0.000		
Cor Total	298700	19			
R-Squared	0.9511				
Adj R-Squared	0.9071				

between factors (p>0.05) may lead to the assumption that factors have an additive effect on the response. The relationship between the response and variables was visualized by the response surface or contour plot to see the influence of the parameters. The quadratic polynomial equations to experimental data (from Eq. 4) can be described by the response surface plots for ethanol production. The proportion of total variation attributed to each fit can be evaluated by the value of *R*-squared (a value of *R*-square>0.75 indicate the aptness of the model) (Haaland 1989). The regression equation obtained after ANOVA indicated an *R*-squared value of 0.951 that was in good agreement with the adjusted *R*-squared of 0.907. This ensured a satisfactory adjustment of the theoretical values to the experimental data by this model. The lack of fit is significant; however, *R*-squared value is high indicating that the models are well adapted to the responses. Therefore, the model is suitable to predict optimum ethanol production from the sweet potato flour by using co-immobilized *S. cerevisiae* and *Pichia* sp. The optimum values of the selected variables for ethanol production were obtained by solving the regression equation.

The highest R^2 value that was obtained in response can be explained by the second order polynomial equation giving the ethanol (406.7 g/kg) as a function of time (A), pH (B) and temperature (C). Using the results of the experiments, the following second order polynomial equation was obtained:

$$R1 = 405.43 + 84.63 \times A + 26.87 \times B + 17.69 \times C - 6.43 \times A \times B + 13.84 \times A \times C - 2.31 \times B \times C - 71.33 \times A^2 - 77.54 \times B^2 - 54.47 \times C^2$$

$$R1 = -4270.94961 + 10.18413 \times \text{Incubation period} + 831.15691 \times \text{pH} + 130.11842 \times \text{Temperature} - 0.17865 \times \text{Incubation period} \times \text{pH} + 0.076868 \times \text{Incubation period} \times \text{Temperature} - 0.46125 \times \text{pH} \times \text{Temperature} - 0.055036 \times \text{Incubation period}^2 - 77.54430 \times \text{pH}^2 - 2.17886 \times \text{Temperature}^2$$

A satisfactory correlation can be seen between the observed values and the predicted values in the parity plot (Fig. 1).

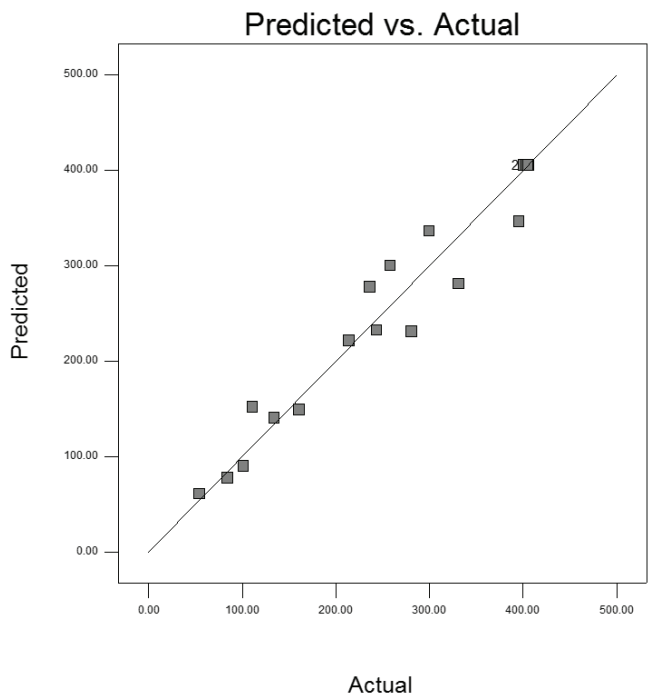

Figure 1. Parity graph showing the distribution of actual vs. predicted values of ethanol yield.

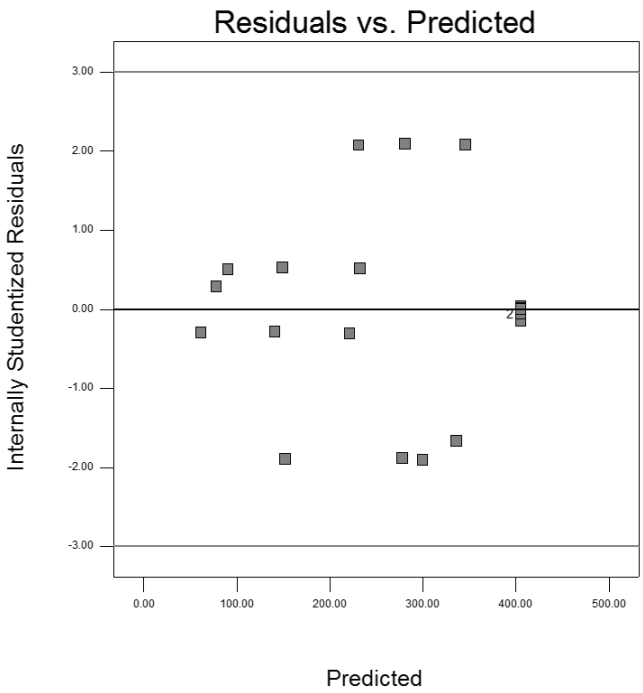

Figure 2. Parity graph showing the distribution of residual vs. predicted values of ethanol yield.

Additionally, the Parity graph showing the distribution of residual and predicted values of ethanol yield (Fig. 2). The clustered points around the diagonal line indicate good fit of the model since there is less deviation between the observed and predicted values. Figure 3 depicts the effects of the factors (incubation time, pH, and temperature) on ethanol production. The lines in the perturbation graph represent the influence and sensitivity of respective factors for ethanol production.

Interactions among the factors

Response surface was generated by plotting the response (bio-ethanol production) on the y-axis against any two independent variables on the x-axis, while keeping the other independent variables at zero level. Therefore, three response surfaces were obtained by considering the possible combinations. Figure 4 (a, b, c) represents the three-dimensional surface plots for the optimization conditions. The plot illustrates the main and the interactive effects of the independent variables on the dependent ones. The response surface plots were generated by plotting the response on the y-axis. Figure 4 (a) shows the effect of temperature and pH on ethanol production keeping the other variable (incubation period) at zero level. Ethanol production increased with the increase in temperature and pH, but it was observed that a further increase in these two variables reversed the trend. In the case of medium pH, ethanol production was increased up to pH 5 and then declined.

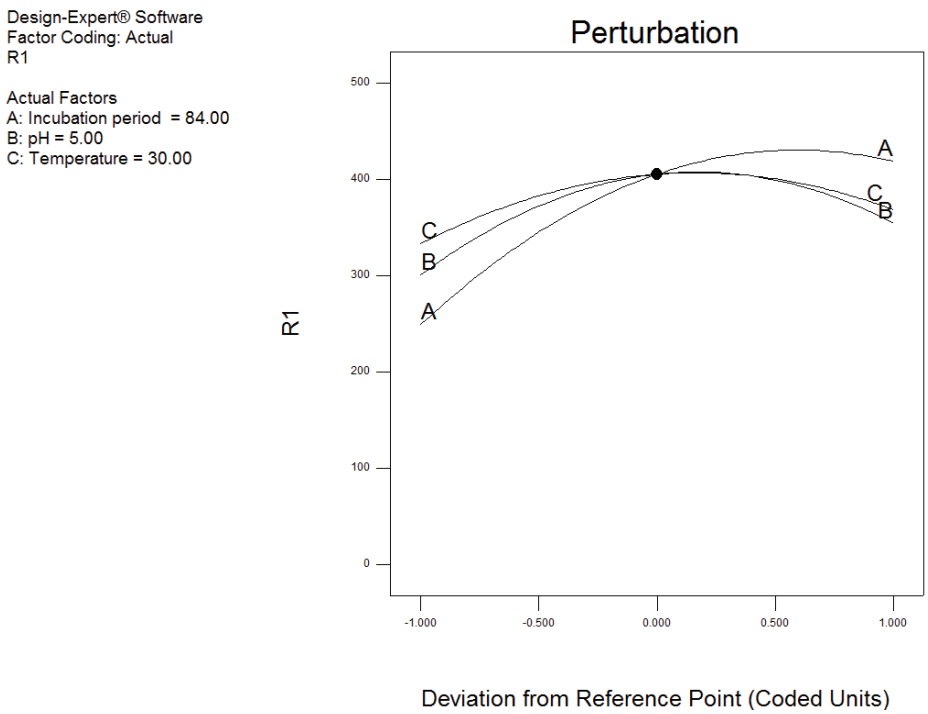

Figure 3. Perturbation graph representing the influence and sensitivity of respective factors for ethanol production.

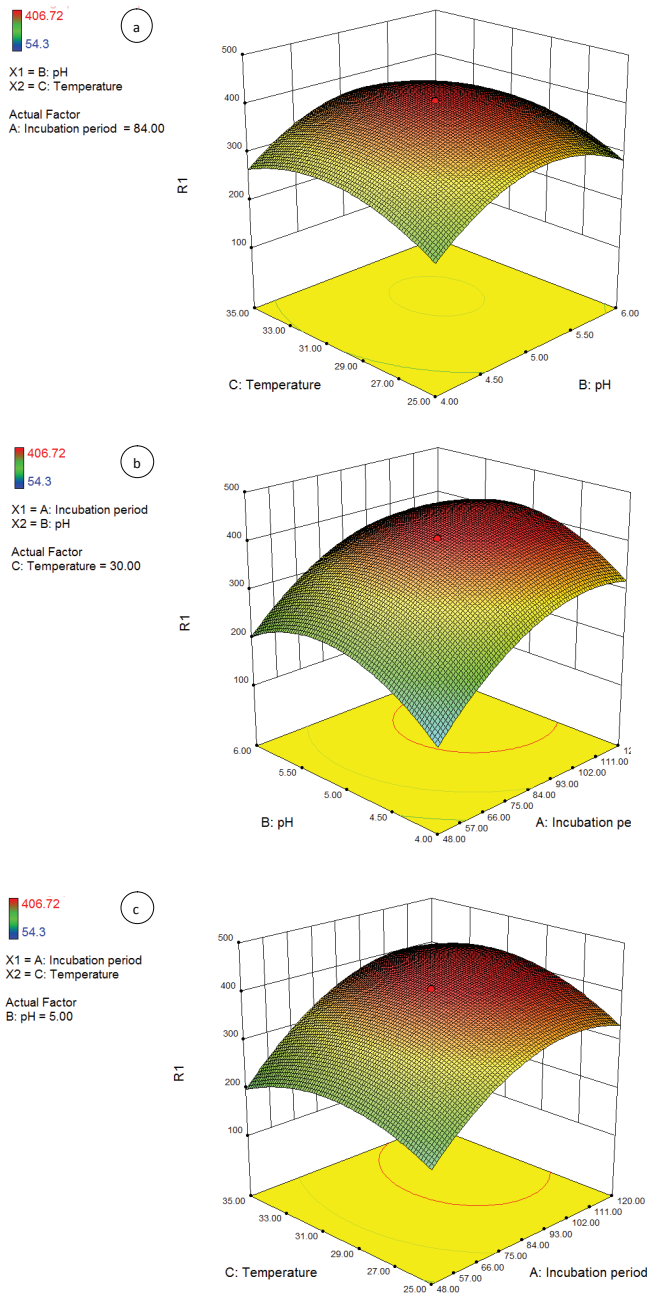

Figure 4. (a). Response surface plot of temperature vs. pH on ethanol production (time was kept constant at 72 h). (b). Response surface plot of pH vs. incubation period on ethanol production. (c). Response surface plot of temperature vs. incubation period on ethanol production.

When the level of incubation period was increased, a linear increase in ethanol production was recorded up to 84 h (Fig. 4b). The response between incubation period and temperature indicated that temperature at 30 °C was optimum with 84 h incubation period for bioethanol production (Fig. 4c).

The Model F-value of 21.61 implies the model is significant. Therefore, the model can be used to navigate the design space. The optimum values of temperature at 30 °C incubation time for 84 h, and at a medium pH of 5 were determined by the point prediction tool of the software with 98.93% validity. The results of the variables, temperature and pH agreed with the OVAT results, but a slight variation was observed for incubation time. For OVAT the incubation time was observed to be 72 h, whereas, for RSM it was predicted to be 84 h. Further, this variation did not hold any significant effect on ethanol production, with ethanol yields of 131.6 ± 2 and 138.7 ± 2 g/kg of substrate by OVAT and RSM, respectively. The present research shows that ethanol concentration can be increased in SPRF when fermented by co-immobilized cultures of *S. cerevisiae* and *Pichia* sp. under optimized medium and process parameters as developed by the response surface methodology. The result showed a similarity with the OVAT methodology results; hence, it could be inferred that the RSM model is useful to predict the optimization of the experimental conditions.

Conclusion

Sweet potato flour is plentily available in the Asia-Pacific regions, including Odisha (India). Being a cheap source of fermentable carbohydrate bio-resource, it could be employed to produce fuel ethanol. In the present investigation, maximum ethanol production from saccharified sweet potato flour in submerged fermentation was obtained at incubation period, 72 h; pH, 5; temperature, 30 °C; inoculums concentration [10% (1:1)] by using co-immobilized culture of *S. cerevisiae* and *Pichia* sp., which are active for three cycles. The present results revealed that co-immobilization is found to be a promising technique for bioethanol production from saccharified sweet potato flour as compared to pure culture and co-culture technique and it reduces the energy input and increases the efficiency of substrate utilization. Further, the ethanol concentration can be increased in SPRF, when fermented by co-immobilized cultures of *S. cerevisiae* and *Pichia.* sp. under optimized medium and process parameters as developed by the response surface methodology.

Acknowledgments

The Department of Science and Technology, Government of Odisha is gratefully acknowledged for the financial support to carry out this research work at CET (Project no.3897/ST, dated 07/08/10). The authors are thankful to the Maps Enzymes Ltd, Ahmedabad, India for providing the enzymes. We thank the Principal, College of Engineering and Technology for providing necessary facilities for this research work.

References

Amerine MA, Ough CS (1984) Wine and must analysis. New York, USA, Wiley.

Amutha R. Paramasamy G (2001) Production of ethanol from liquefied cassava starch using co-immobilized cells of *Zymmomonas mobilis* and *Saccharomyces diastaticus*. J Biosci Bioengi 92:560-564.

Badger PC (2002) Ethanol from cellulose: a general review. In Janick J, Whipkey A (eds), Trends in New Crops and New Uses. ASHS Press, Alexandria, VA.

Behera S, Kar S, Mohanty RC, Ray RC (2010) Comparative study of bio-ethanol production from mahula (*Madhuca latifolia* L.) flowers by *Saccharomyces cerevisiae* cells immobilized in agar agar and Ca-alginate matrices. Appl Energ 87:96-100.

Clarence SY, Sunny EI, Emmanuel IU (2010) Temperature optimization for bioethanol production from corn cobs using mixed yeast strains. J Biol Sci 10:103-108.

Dias M, Junqueira T, Cavalett O, Cunha MP (2012) Integrated versus stand-alone second generation ethanol production from sugarcane bagasse and trash. Bioresour Technol 103:152-161.

Du Preez JC, Prior BA (1985) A quantitative screening of some xylose fermenting yeast isolates. Biotechnol Lett 7:241-246.

Du Preez JC, Bosch M, Prior BA (1986) The fermentation of hexose and pentose sugars by *Candida shehatae* and *Pichia stipites*. Appl Microbiol Biotechnol 23:228-233.

Giordano RL, Trovati J, Schmidell W (2008) Continuous production of ethanol from starch using glucoamylase and yeast co-immobilized in pectin gel. Appl Biochem Biotechnol 147:47-61.

Ghorbani F, Younesi H, Sari AE (2011) Cane molasses fermentation for continuous ethanol production in an immobilized cells reactor by *Saccharomyces cerevisiae*. Renew Energ 36:503-509.

Graves T, Narendranath NV, Dawson K (2006) Effect of pH and lactic or acetic acid on ethanol productivity by *Saccharomyces cerevisiae* in corn mash. J Ind Microbiol Biotechnol 33:469-474.

Haaland PD (1989) Experimental Design in Biotechnology. Marcel Dekker, New York.

Hashem M, Darwish S (2011) Production of bioethanol and associated by-products from potato starch residue stream by *Saccharomyces cerevisiae.* Biomass Bioenerg 34:901-909.

Jamai L, Ettayebi K, Yamani JE (2007) Production of ethanol from starch by free and immobilized *Candida tropicalis* in the presence of amylase. Bioresour Technol 98:2765-2777.

Kar S, Swain MR, Ray RC (2009) Statistical optimization of alpha amylase production with immobilized cells of *Streptomyces erumpens* MTCC 7317 in *Luffa cylindrica* L. sponge discs. Appl Biochem Biotechnol 152:177-188.

Lee WS, Chen IC, Chang CH (2012) Bioethanol production from sweet potato by co-immobilization of saccharolytic molds and *Saccharomyces cerevisiae*. Renew Energ 39:216-222.

Liimatainen H, Kuokkanen T, Kaariainen J (2004) Development of bioethanol production from waste potatoes. In Pongracz E, ed., Proceedings of the Waste Minimization and Resources Use Optimization Conference, June 10th 2004, University of Oulu, Finland. Oulu University Press, Oulu, pp. 123-129.

Lin CW, Tran DT, Lai CY (2010) Response surface optimization for ethanol production from *Pennisetum alopecoider* by *Klebsiella oxytoca* THLC0409. Biomass Bioenerg 34:1922-1929.

Maiti B, Rathore A, Srivastava S (2011) Optimization of process parameters for ethanol production from sugar cane molasses by *Zymomonasmobilis* using response surface methodology and genetic algorithm. Appl Microbiol Biotechnol 90:385-395.

Mamma D, Koullas D, Fountoukidis G (1996) Bioethanol from sweet sorghum: simultaneous saccharification and fermentation of carbohydrates by a mixed microbial culture. Process Biochem 31:1359-5113.

Manikandan K, Viruthagiri T (2010) Optimization of C/N ratio of the medium and fermentation conditions of ethanol production from tapioca starch using co-culture of *Aspergillus niger* and *Saccharomyces cerevisiae*. Int J Chem Technol Res 2:947-955.

McGee DC, Olanya OM, Hoyos GM (1996) Populations of *Aspergillus flavus* in the Iowa cornfield ecosystem in years not favorable for aflatoxin contamination of corn grain. Plant Dis 80:742-746.

Mohanty SK, Behera S, Swain MR (2009) Bioethanol production from mahula (*Madhuca latifolia* L.) flowers by solid-state fermentation. Appl Energ 86:640-644.

Narendranath NV, Power R (2005) Relationship between pH and medium dissolved solids in terms of growth and metabolism of *Lactobacilli* and *Saccharomyces cerevisiae* during ethanol production. Appl Environ Microbiol 71:2239-2243.

Neelakandan N, Usharani N (2009) Optimization and production of bioethanol from cashew apple juice using immobilized yeast cells by *Saccharomyces cerevisiae*. AEJSR 4(2):85-88.

Periyasamy S, Venkatachalam S, Ramasamy S (2009) Production of bio-ethanol from sugar molasses using *Saccharomyces cerevisiae*. Modern Appl Sci 3(8):32-37.

Pirselova K, Smogrovicova D, Balaz S (1993) Fermentation of starch to ethanol by a co-culture of *Saccharomycopsis fibuligera* and *Saccharomyces cerevisiae.* World J Micro-

biol Biotechnol 9:338-341.

Pitt RE (1993) A descriptive model of mold growth and aflatoxin formation as affected by environmental conditions. J Food Protect 56(2):139-146.

Pornkamol U, Friedrich S (2010) Continuous production of ethanol from hexoses and pentoses using immobilized mixed cultures of *Escherichia coli* strains. J Biotechnol 150:215-223.

Roukas T (1994) Solid-state fermentation of carob pods for ethanol production. Appl Microbiol Biotechnol 41:296-301.

Shigechi H, Koh J, Fujita Y, Matsumoto T (2004) Direct production of ethanol from raw corn starch via fermentation by use of a novel surface-engineered yeast strain co-displaying glucoamylase and alpha amylase. Appl Environ Microbiol 70:5037-5040.

Soccol CR, Vandenberghe LPS, Medeiros ABP (2010) Bioethanol from lignocelluloses: status and perspectives in Brazil. Bioresour Technol 101:4820-4825.

Shuler ML, Kargi F (2002) Bioprocess Engineering-Basic Concepts. Prentice Hall of India, New Delhi, India.

Swain MR, Kar S, Sahoo AK (2007) Ethanol fermentation of mahula (*Madhuca latifolia L.)* flowers using free and immobilized yeast *Saccharomyces cerevisiae.* Microbiol Res 162:93-98.

Swain MR, Mishra J, Thatoi HN (2013) Bioethanol production from sweet potato (*Ipomoea batatas* L.) flour using co-culture of *Trichoderma* sp. and *Saccharomyces cerevisiae* in solid-state fermentation. Braz Arch Biol Technol 56:171-179.

Tahir A, Aftab M, Farasat T (2010) Effect of cultural conditions on ethanol production by locally isolated *Saccharomyces cerevisiae* BIO-07. J Appl Pharma Sci 3:72-78.

Tian SJ, Rickard JE, Blanshard JMV (1991) Physicochemical properties of sweet potato starch. J Sci Food Agric 57(4):459-491.

Van der Maarel MJEC, Van der Veen B, Uitdehaag JCM (2002) Properties and applications of starch-converting enzymes of the α-amylase family. J Biotechnol 94:137-155.

Von Sivers M, Zacchi G (1996) Ethanol from lignocellulosics: A review of the economy. Bioresour Technol 56:3-14.

Vucurovic VM, Razmovski RN, Popov SD (2009) Ethanol production using *Saccharomyces cerevisiae* cells immobilized on corn stem ground tissue. Proc Nat Sci, Matica Srpska Novi Sad 116:315-322.

Uncu ON, Cekmecelioglu D (2011) Cost-effective approach to ethanol production and optimization by response surface methodology. Waste Manag 31:636-643.

Zhou MH, Han FF, Li J (2008) Isolation and identification of a novel alginate-degrading bacterium *Ochrobactrum* sp. J Sci Technol 30(2):135-140.

Volume 61(1):25-33, 2017
Acta Biologica Szegediensis
http://www2.sci.u-szeged.hu/ABS

ARTICLE

Statistical optimization of laccase production by *Aspergillus flavus* PUF5 through submerged fermentation using agro-waste as cheap substrate

Priyanka Ghosh, Uma Ghosh*

Department of Food Technology & Biochemical Engineering, Jadavpur University, Kolkata-700032, West Bengal, India

ABSTRACT The plan of this work was to valorize agro-wastes following statistical approach to the production of laccase enzyme by *Aspergillus flavus* PUF5 through submerged fermentation process (SmF). The process parameters influencing the enzyme production and initially identified using "one variable at a time (OVAT)" design. Among the variables screened, fermentation temperature, pH of the medium, concentration of yeast extract, and NaCl were found most considerable when waste ribbed gourd peel was used as substrate. The most favorable levels of these significant parameters were determined employing the central composite design (CCD). The goodness of fit of the model was checked by the determination coefficient (R^2). The contour plots revealed that the optimal values of the process conditions lie within the range; temperature: 25 °C, pH: 4, yeast extract concentration: 0.3% and NaCl: 0.07%. By using the optimal fermentation medium, the improved laccase production was found to be 15.96 U/ml; this was about 4.6-fold higher than the unoptimized media. **Acta Biol Szeged 61(1):25-33 (2017)**

KEY WORDS

agro-waste
laccase
response surface methodology
ribbed gourd
valorization

Introduction

Laccases (EC 1.10.3.2, benzenediol:oxygen oxidoreductase) are multicopper polyphenol oxidases, which mediate the oxidation of a wide range of phenolic compounds and aromatic amines with the concomitant four-electron reduction of O_2 to H_2O. The laccases are widely distributed in plants, fungi, bacteria and insects (Qiu et al. 2014). Among all these sources, laccases from fungi are of special interest, because of their aptitude to degrade lignocellulosic biomass by elaborating extracellular laccase enzyme (Ding et al. 2014). Laccase plays a major role in lignin degradation and their industrial and food application are increasing day by day (Osma et al. 2007). Laccases have broad substrate specificity, which makes them excellent candidates for biotechnological applications and provide green route in various biochemical processing such as oxidation of a wide variety of substrates like phenols, diphenols, polyphenols, substituted phenols, diamines, aromatic amines, and various non-phenolic compounds, delignification in paper pulping and pulp bleaching, degradation of textile dyes, bioremediation of herbicides, pesticides and xenobiotics generated by industrial processes, development of biosensors and biofuel cells, conversion of lignocellulosic for biofuel production and organic synthesis, juice and wine clarification (Sweeney and Xu 2012; Woolridge et al. 2014). From the industrial aspects, higher product yield and lower production cost are preferable during optimization of fermentation processes. The traditional optimization studies varying one parameter, while keeping the others at constant level (OVAT process), is simple, but it often fails to seek the optimum region, because the combinational effects of factors are not considered. In order to overcome this problem, optimization studies are done using response surface methodology (RSM). It is a collection of mathematical and statistical techniques for designing experiments, building models, evaluating the effects of factors (Roriz et al. 2009), which extracts the maximal information with the minimal number of runs. This technique has been widely used to determine the effects of several variables and to optimize different biotechnological processes such as optimization of media, process conditions, catalyzed reaction conditions, oxidation, production of different enzymes like amylases, lipases, proteases, cellulases, chitinases etc., (Beg et al. 2003; Das et al. 2013). Considering the importance of laccase enzyme, this study was carried out to optimize its production using a potent fungal strain *A. flavus* PUF 5 by the traditional OVAT process followed by statistical optimization of the fermentation process by response surface methodology based on central composite design (CCD) utilizing agricultural wastes as substrate.

Submitted January 1, 2017; Accepted March 27, 2017
*Corresponding author. E-mail: ughoshftbe@yahoo.co.in

Materials and Methods

Microorganism and inoculum preparation

A potent laccase producing fungal strain *Aspergillus flavus* PUF5 prescreened from the soil was used in this study. This strain was identified by cultural, microscopic and molecular characterization (data not shown). The strain was grown on potato dextrose agar slants at 30 °C for 5 days (until good sporulation occurred) and stored at 4 °C until use. Inoculum was prepared by adding 5 ml of sterile distilled water to a fully sporulated culture slant. The spores were dislodged by gentle pipetting under aseptic conditions. The concentration of the prepared spore suspension was adjusted to about 5×10^9 spores/ml.

Optimization of submerged fermentation for laccase production by OVAT process

All the fermentation experiments were carried out in 250 ml Erlenmeyer flasks. Laccase production by *A. flavus* PUF5 was first optimized by 'one variable at a time' (OVAT) approach to find out the most important factors affecting the fermentation process. The mold was grown in Olga medium (Desai et al. 2011) with various agro-wastes (2%, w/v) to find the most suitable carbon source for laccase production. The effects of fermentation time and temperature on laccase production were investigated by incubating the flasks for up to 9 days at varying temperatures (25-40 °C); whereas the effect of pH was assessed by adjusting the pH (2-7) of the medium (before autoclaving) using 1 M HCl or NaOH. Screening of supplementary carbon source (1% w/v) and its concentration (0.2-1.4%) was studied by addition of different commercial carbohydrates in the culture flasks, while the effect of additional nitrogen sources was assessed by supplementation the fermentation media with different commercial nitrogen sources (0.5% w/v). The effect of metal salts on laccase production was studied using different metal salts like $MgSO_4$, $MnSO_4$, $FeSO_4$, $CuSO_4$, NaCl, etc., with a final concentration of 0.05% in the fermentation medium.

Fermentation kinetics

The specific rate of enzyme production (q_p) was determined as the maximum enzyme activity/g of fungal biomass/h. The growth of fungus was determined on the basis of dry biomass (mg/ml), which was also used to calculate the value of specific growth rate as

$$\mu\ (h^{-1}) = \ln (m_t / m_o)/T$$

Where, m_t is fungal biomass at a given time T (h), m_o is the baseline spore biomass at the start of the fermentation (Sterner and Elser 2002).

Statistical experimental design and data analysis

Four major factors that significantly affected the laccase production through OVAT process were further optimized using the response surface methodology (RSM). The central composite design (CCD) of response surface method was used to obtain data that fits a full second order polynomial model. The CCD with three factors and five levels including six replicates at the center point was used to fit the response surface. The proportion of variance explained by the polynomial models obtained was given by multiple coefficient of determination, R^2. The fitted polynomial equation was expressed as three-dimensional response surface plots to find the concentration of each factor for maximum laccase production. These diagram shows relationship between the responses and the experimental levels of each factor used in the design. To optimize level of each factor for maximum response 'Numerical optimization' process was employed. The combination of different optimized parameters, which gave maximum laccase yield, was tested experimentally to validate the model.

Statistical analysis was performed using the statistical software Design-Expert Version 6.0.10, Stat-Ease, Minneapolis, USA.

Assay of enzyme and fungal biomass

Laccase activity was measured by the method adopted by Desai et al. (2011). The laccase activity in U/ml is calculated using the guaiacol at 450 nm. The specific laccase activity was determined as U/mg of protein, where amount of soluble protein was determined by Lowry method (Lowry et al. 1951). Fungal biomass estimation was carried out by determining the amount of N-acetyl glucosamine released by the acid hydrolysis of the chitin, present in the cell wall of the fungi, following the process of Ramachandran et al. (2005).

Results and Discussion

Screening of different agro-wastes for maximum laccase production

Biotechnological applications require large amounts of low-cost enzymes. Therefore, one of the appropriate approaches for this purpose is to utilize the potential lignocellulosic waste residues, which may contain significant concentrations of soluble carbohydrates and inducers of enzyme synthesis ensuring efficient production of laccase enzymes. In the current study, different lignocellulosic wastes (2%) (like wheat bran, rice bran, orange peel, tea waste, potato peel, ribbed

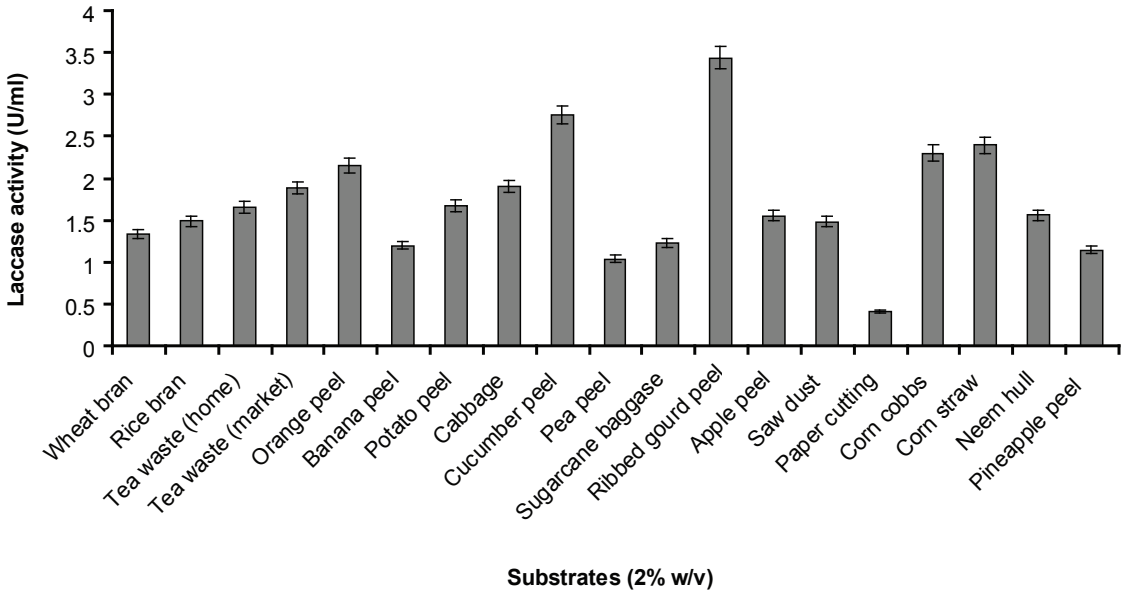

Figure 1. Effect of different lignocellulosic wastes/residues on production of laccase by *A. flavus* PUF5 through submerged fermentation.

gourd peel, sawdust, corn straw, corn cobbs, etc) were used instead of glucose in the media for laccase production. The pH of media was adjusted at 5. Results (Fig. 1) showed that the maximum laccase activity of 3.44 U/ml was recorded with ribbed gourd peel followed by cucumber peel (2.76 U/ml) and corn straw (2.40 U/ml). In recent times, agricultural waste products like chestnut shell were often used for laccase production (Dong et al. 2014). Thus, the value added to agronomic waste residue will not only reduce the disposal problem, but the chances of the environmental pollution will also be reduced.

Time course for laccase production

The growth kinetics and production of laccase from ribbed gourd peel in shake flask batch culture was examined by growing the fungi in Olga medium as described in Materials and Methods. The flasks were incubated for 9 days and laccase activity was measured at 24 h intervals. The results (Fig. 2) suggested that under normal condition laccase secretion started on the 3rd day of incubation and the maximum activity (5.74 U/ml) was achieved on the 7th day suggesting its constitutive production, which was also reported by Scheel et al. (2000). Besides laccase production, fungal biomass was also gradually increased and reached maximum (9.2 mg/ml) with specific growth rate (μ) of 26.91/h on the 7th day of fermentation, suggesting that laccase production was growth associated. It was found that the amount of soluble protein (138.3 μg/ml, after 7 days of fermentation) was also increased in accordance with the fungal growth and laccase production. The result revealed that the laccase production was growth associated, and the enzyme secretion was dependent on the fungal biomass and the specific growth rate of *A. flavus* PUF5.

Earlier reports on *Trametes hirusta* indicated maximum laccase enzyme activity (7.614 U/ml) after an incubation period of 20 days using wheat bran (Bakkiyaraj et al. 2013). In another study, *Ganoderma lucidum* was reported to obtain maximum laccase activity of 2.7 U/ml after 14th days of incubation with wheat bran (Songulashvili et al. 2007).

Optimization of fermentation temperature and initial medium pH

Among the different fermentation parameters for production of enzymes, incubation temperature and the pH of substrate play a vital role in the metabolic activity of microbial cell. During optimization of culture condition for laccase from *A. flavus* PUF5, the maximum laccase activity was detected at a temperature of 30 °C (Fig. 3A). Further increase in temperature resulted decrease in laccase activity, which is incongruence with a report on *Agaricus* sp. where the maximum laccase is produced at 30 °C (Yang et al. 2011). In general, fermentation temperature between 25 °C and 30 °C is optimal for fungal laccase production (Kunamneni et al. 2007). It was found that at elevated temperatures the activity of ligninolytic enzymes was diminished (Viswanath et al. 2014).

The pH of the medium is another vital parameter affecting the production of enzymes as well as growth of microorganisms. The effect of initial culture pH on growth

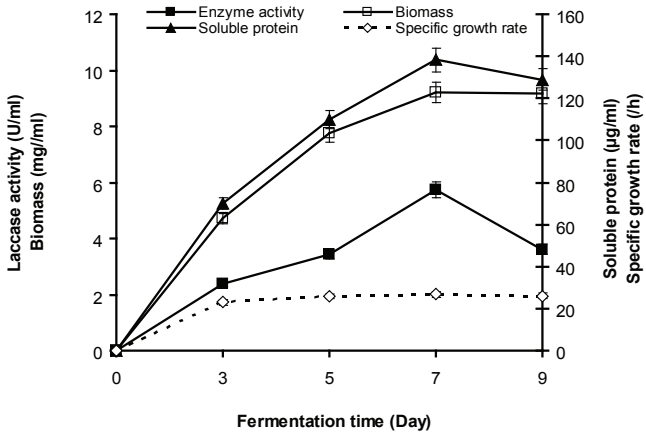

Figure 2. Optimization of fermentation time for maximum laccase production by *A. flavus* PUF5 through submerged fermentation.

of *A. flavus* PUF 5 and laccase production are summarized in Figure 3B. The results clearly indicated that maximum laccase production (5.93 U/ml) took place at pH 5 and its formation occurred over a broad range of pH values. With the increase in fermentation pH, both the fungal biomass and the amount soluble protein were also gradually decreased. Being proteins, enzymes contain different ionizable groups and their structures and functions are highly affected by the pH of the culture medium. Thus, development of an optimal pH control strategy is helpful in obtaining higher enzyme production by efficient fungal strains. It has been reported that at medium pH of 5, excess laccase production was observed in *A. bisporus* (Yang et al. 2011). Fungal laccases are reported to be generally active at low pH values (pH 3-5) (More et al. 2011). This observation is also in accordance with the optimum pH of 5 for laccase production by *T. versicolor* (Minussi et al. 2007).

Effect of substrate concentration on laccase production

Substrate concentration is another important parameter for suitable microbial growth and production of primary metabolites like enzymes. For optimization of substrate concentration, varied amount of ribbed gourd peel was subjected to fermentation and the result indicated that 4% substrate concentration was optimum for maximum laccase production (5.81 U/ml). The amount of fungal biomass and soluble protein also gradually increased (Fig. 4).

Effect of supplementary carbon and nitrogen sources on laccase production

Comparison of fermentation kinetics related to enzyme production and growth of the organism were studied in presence of different types of carbohydrate like glucose, sucrose, maltose, carboxymethyl cellulose (CMC), and soluble starch (1.0%, w/v) in the culture media in attempt to study the effect of supplementary carbon source, as well as inducer for biosynthesis of laccase enzymes by *A. flavus* PUF 5. Table 1 shows that easily utilizable carbohydrate like glucose supported highest specific fungal growth (µ: 29.70) and produced maximum soluble proteins (239 µg/ml), but the specific rate of enzyme production (q_p) was significantly reduced. Laccase production was maximum (9.21 U/ml) in presence of soluble starch (1%) followed by carboxymethyl cellulose. During further optimization of starch concentration, it was found that laccase production was gradually increased with the increase of starch concentration up to a certain level (1%) above, which enzyme production was markedly decreased (Fig. 5A). This can be attributed to the high viscosity of culture broth, which can interfere with the O_2 transfer rate leading to the limitation of dissolved oxygen required for the growth of

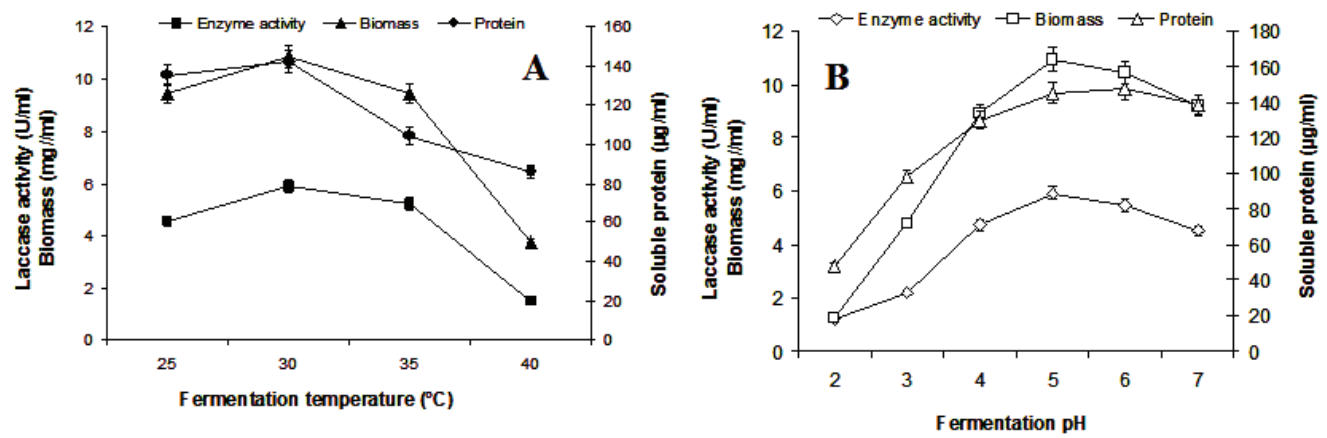

Figure 3. Effect of fermentation temperature (A) and pH (B) on laccase production by *A. flavus* PUF5 through submerged fermentation.

organism (Das et al. 2013).

Nitrogen is involved in amino acid synthesis, which makes up proteins and other value added substances. In the present study, different inorganic and organic nitrogen sources (0.5%, w/v) *viz.* urea, sodium nitrate, ammonium sulfate, yeast extract, peptone etc., was supplemented in broth and it was found that laccase production was greatly varied with the type of nitrogen source used. Among the tested nitrogen sources after 7 days of fermentation maximum enzyme production (9.77 U/ml) was achieved with yeast extract as compared to control (Fig. 5B), which may be due to higher growth of the organism (Anwer et al. 2012). Generally, a high carbon to nitrogen ratio is required for laccase production. Vahidi et al. (2004) reported that when yeast extract was used as nitrogen source it increased laccase production. Casein also has been reported to significantly increase laccase activity (7.08 U/ml) after 13 days of fermentation by *Pleurotus sajor-caju* PS-2001 (Bettin et al. 2009). *Pleurotus ostreatus* fungi showed the highest laccase activity with ammonium chloride (Stajic et al. 2006).

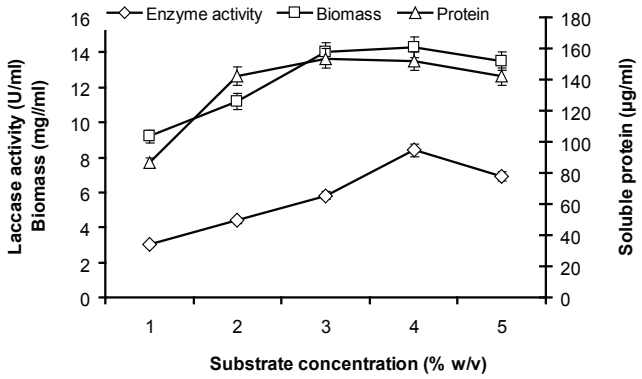

Figure 4. Optimization of substrate concentration for maximum laccase production by *A. flavus* PUF5 through submerged fermentation.

Effect of metal salt on laccase production

In this study, different metal salts like $MgSO_4$, $MnSO_4$, $FeSO_4$, $CuSO_4$, NaCl, etc., with a final concentration of 0.05% were added in the fermentation medium. Among them, NaCl supported the maximum laccase production followed by $CuSO_4$ and $MgSO_4$ (Fig. 6). The phenomenon of increased laccase production with addition of different metal ions has already been established in different reports. Laccase production by *Ganoderma applanatum* and *Peniophora* sp. was stimulated 49.2-fold and 19.7-fold, respectively, by adding copper (Fonseca et al. 2010). The stimulating effect of copper was attributed to the regulation of laccase gene transcription (Collins and Dobson 1997). Potassium at 1.0 mM also yielded the highest production of laccase in *Schizophyllum commune* (Irshad and Asgher 2011).

Optimization of laccase production through response surface methodology

From OVAT process, four most influencing parameters like fermentation temperature (ºC), fermentation pH, concentration of yeast extract, and concentration of NaCl were chosen and subjected to further optimization through response sur-

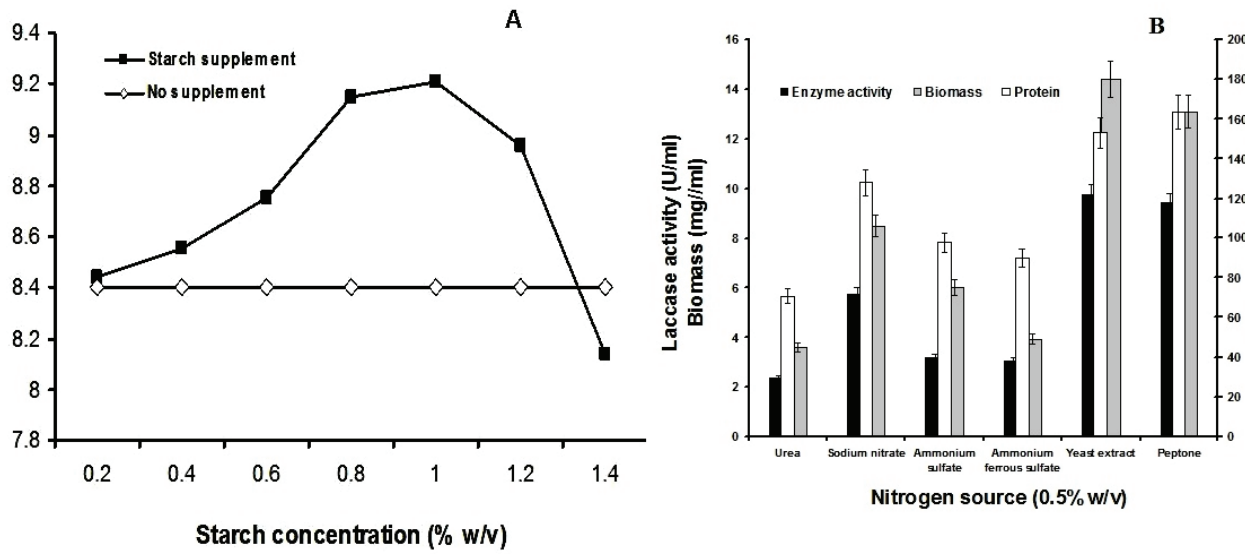

Figure 5. Optimization of supplementary starch (A) and nitrogen (B) sources for maximum laccase production by *A. flavus* PUF5 through submerged fermentation.

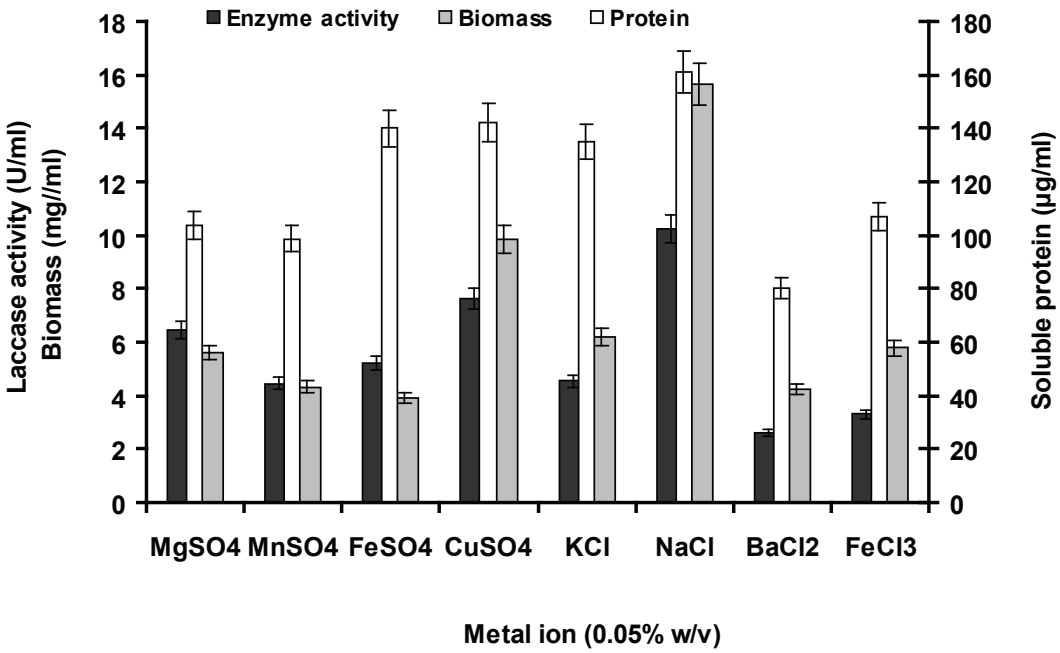

Figure 6. Optimization metal salts for maximum laccase production by *A. flavus* PUF5 through submerged fermentation.

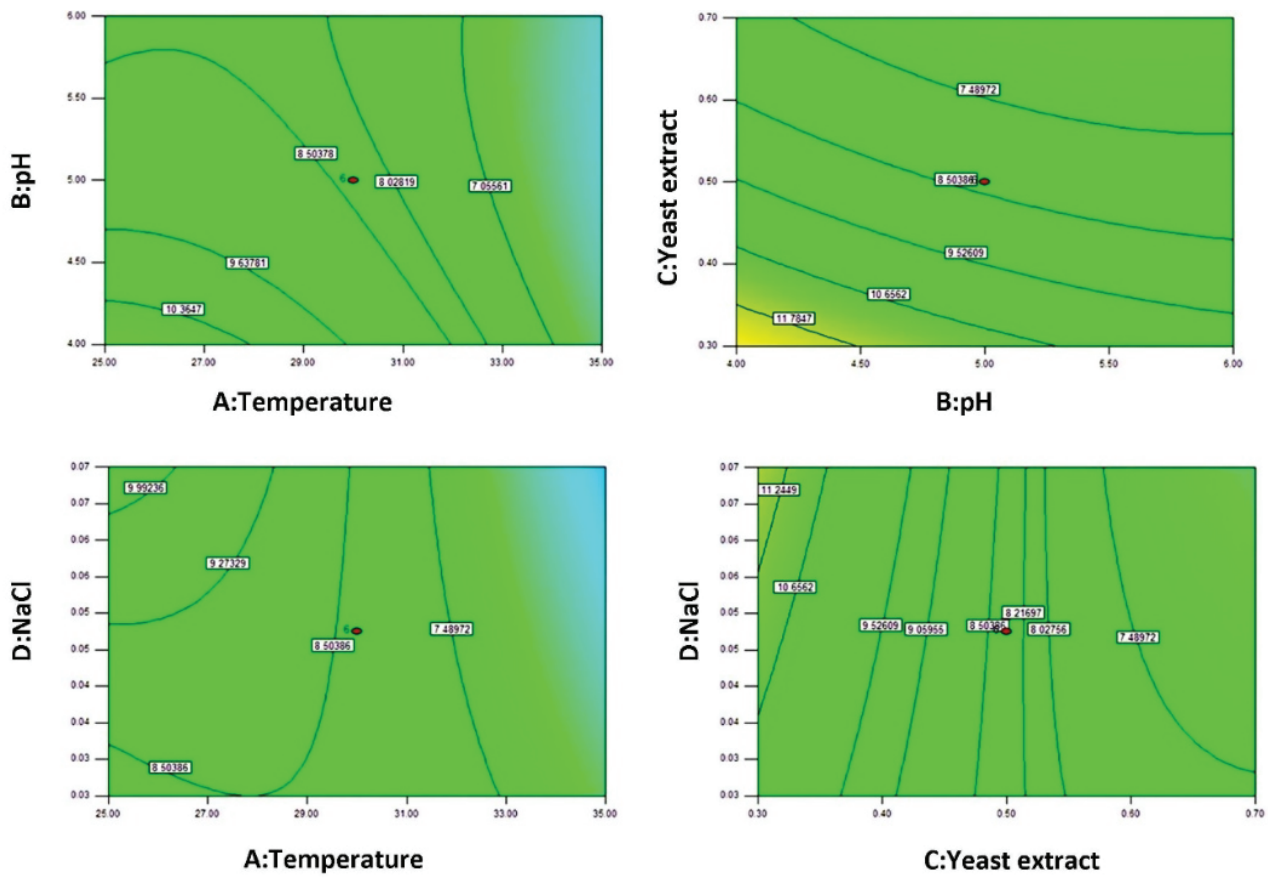

Figure 7. Contour plots showing the effects of different factors on laccase production.

Table 1. Effect of different carbon sources on laccase production by *A. flavus* PUF5.

Carbon source (1%)	Laccase activity (U/ml)	Protein (µg/ml)	Biomass (mg/ml)	Specific growth rate (µ)	Specific rate of enzyme production (q_p)
glucose	5.16	239	14.7	29.70	0.06
fructose	2.2	170	10.59	27.75	0.036
sucrose	3.6	131	7.32	25.55	0.086
maltose	2.27	86	5.41	23.75	0.076
carboxymethyl cellulose	8.47	133.8	12.8	28.88	0.111
soluble starch	9.21	142.7	13.6	29.24	0.113

Table 2. Central composite experiments design matrix with experimental and predicted values for laccase production from *A. flavus* PUF5.

Run	Selected factor (level with coded value)					
	Temperature (°C)	pH	Yeast extract (%)	NaCl (%)	Observed response	Predicted response
1	35 (+1)	4 (-1)	0.70 (+1)	0.03 (-1)	5.8	6.14
2	25 (-1)	6 (+1)	0.30 (-1)	0.07 (+1)	12.4	12.34
3	35 (+1)	4 (-1)	0.30 (-1)	0.03 (-1)	9.1	9.11
4	25 (-1)	6 (+1)	0.70 (+1)	0.03 (-1)	6.9	6.88
5	35 (+1)	6 (+1)	0.70 (+1)	0.03 (-1)	6.6	6.76
6	30 (0)	5 (0)	0.50 (0)	0.09 (+2)	8.9	8.52
7	35 (+1)	6 (+1)	0.30 (-1)	0.03 (-1)	7.7	7.82
8	20 (-2)	5 (0)	0.50 (0)	0.05 (0)	7.6	8.08
9	35 (+1)	4 (-1)	0.70 (+1)	0.07 (+1)	2.9	3.44
10	30 (0)	5 (0)	0.50 (0)	0.05 (0)	8.5	8.35
11	25 (-1)	4 (-1)	0.70 (+1)	0.07 (+1)	9.2	9.36
12	30 (0)	5 (0)	0.50 (0)	0.05 (0)	8.1	8.35
13	35 (+1)	6 (+1)	0.70 (+1)	0.07 (+1)	6.3	6.68
14	30 (0)	3 (-2)	0.50 (0)	0.05 (0)	12	11.55
15	30 (0)	5 (0)	0.10 (-2)	0.05 (0)	15	14.93
16	30 (0)	5 (0)	0.50 (0)	0.05 (0)	8.7	8.35
17	40 (+2)	5 (0)	0.50 (0)	0.05 (0)	1.3	0.55
18	30 (0)	5 (0)	0.50 (0)	0.05 (0)	8.2	8.35
19	30 (0)	7 (+2)	0.50 (0)	0.05 (0)	8	8.18
20	30 (0)	5 (0)	0.50 (0)	0.01 (-2)	8.2	8.32
21	25 (-1)	6 (+1)	0.30 (-1)	0.03 (-1)	10	9.44
22	25 (-1)	6 (+1)	0.70 (+1)	0.07 (+1)	7.3	7.27
23	25 (-1)	4 (-1)	0.30 (-1)	0.07 (+1)	16.5	16.32
24	25 (-1)	4 (-1)	0.70 (+1)	0.03 (-1)	8.4	8.01
25	35 (+1)	6 (+1)	0.70 (+1)	0.07 (+1)	3.2	3.11
26	30 (0)	5 (0)	0.50 (0)	0.05 (0)	8.6	8.35
27	30 (0)	5 (0)	0.90 (+2)	0.05 (0)	7.1	6.90
28	35 (+1)	4 (-1)	0.30 (-1)	0.07 (+1)	8.6	8.91
29	30 (0)	5 (0)	0.50 (0)	0.05 (0)	8.1	8.35
30	25 (-1)	4 (-1)	0.30 (-1)	0.03 (-1)	12.1	12.48

face methodology. Experiments were performed, according to the CCD experimental design given in Table 2 in order to search for the optimum combination of process parameters for the maximum laccase production. The experimental data showed a good fit with the second order polynomial equations, which were statistically acceptable at $P<0.05$ level. ANOVA for laccase production indicated 'F-value' of 100.19, which implied that the model was appropriate. Model terms having 'Prob>F' values less than 0.05 are considered to be significant. In this case, fermentation temperature, pH and concentration of yeast extract were significant model terms. A similar result was observed by Sun et al. (2013), where fermentation temperature and pH were found to be significant factors for laccase production by *Coriolus hirsutus*. Youshuang et al. (2011) also found yeast extract to be a significant nitrogen source for laccase production by *Trametes versicolor* sdu-4 during optimization process through CCD under submerged fermentation. The goodness of fit of the model was

Table 3. Analysis of variance (ANOVA) for laccase production in second-order polynomial model.

Source	Sum of squares	DF	F-value	Prob>F
Model	281.79	14	100.19	<0.0001
Temperature	85.13	1	423.75	<0.0001
pH	17.00	1	84.63	<0.0001
Yeast extract	96.80	1	481.87	<0.0001
NaCl	0.060	1	0.30	0.5828
AB	3.06	1	15.24	0.0014
AC	2.25	1	11.20	0.0044
AD	16.40	1	81.65	<0.0001
BC	3.61	1	17.97	0.0007
BD	0.90	1	4.49	0.0511
CD	6.25	1	31.11	<0.0001
A^2	27.89	1	138.82	<0.0001
B^2	3.94	1	19.63	0.0005
C^2	11.29	1	56.22	<0.0001
D^2	7.619E-003	1	0.038	0.8482
Residual	3.01	15		
Cor Total	284.80	29		

R^2 - 0.9894, Adj R^2 - 0.9795, Pred R^2 - 0.9454. Adequate precision - 49.744

checked by the determination coefficient (R^2). According to Table 3, the R^2 value of 0.9894 was in good agreement with the adjusted R^2 value of 0.9795. The coefficient value of variation (CV) was also low as 5.35 indicate that the deviations between experimental and predicted values are low. The 'adequate precision' value of 49.744 indicated an adequate signal and suggested that the model can be used to navigate the design space (Table 1). The contour plots were plotted to study the interaction among various physicochemical factors used and to find out the optimum concentration of each factor for maximum laccase production from *A. flavus* PUF5. The contour plots for laccase production are shown in Figure 7. It shows that increase in fermentation temperature and pH of the medium, leads to decrease in laccase production, whether increased NaCl concentration supported laccase yield. Result also indicated that a lower concentration of yeast extract supported maximum laccase production. The studies of the contour plot also reveal the best optimal values of the process conditions lies within the range; temperature: 25 °C, pH: 4, yeast extract concentration: 0.3% and NaCl: 0.07%. Under these conditions, confirmation experiments were conducted in three replicates. The observed mean laccase activity was 15.96 U/ml. This value was largely consistent with the predicted value of 16.325 U/ml.

Conclusion

The results of this work disclosed the potential of *Aspergillus flavus* PUF5 to produce laccases in a liquid medium when waste ribbed gourd peel was used as substrate. Among the different additional sources of nitrogen tested, yeast extract was the most appropriate for laccase production, especially at a concentration of 0.3% (w/v) in the culture medium, under the conditions of the present assays. The addition of NaCl 0.07% (w/v) to the medium increased not only the laccase production, but also soluble protein and fungal biomass in the medium. In addition, it was observed that soluble starch, a relatively cheap carbohydrate, also induced laccase production, particularly when added to the medium at a concentration of 1% (w/v). The most significant parameters and their favorable levels were further optimized employing the central composite design and the results revealed that the optimal values of the process conditions lie within the range; temperature: 25 °C, pH: 4, yeast extract concentration: 0.3% and NaCl: 0.07%. The improved laccase production was found to be 15.96 U/ml, which was about 4.6-fold higher than the unoptimized media. The results show a good alternate of valorization of agro-waste in to value added product and preventing environmental pollution.

Acknowledgments

The authors are thankful to the University Grant Commission [Sanction no: F/2016-17/NFO201517OBCWES 32372/(SAIII/Website)], Government of India for the financial assistant in this study.

References

Anwer R, Khursheed S, Fatma T (2012) Detection of immune active insulin in *Spirulina*. J Appl Phycol 24:583-591.

Bakkiyaraj S, Aravindan R, Arrivukkarasan S, Viruthagiri T (2013) Enhanced laccase production by *Trametes hirusta* using wheat bran under submerged fermentation. Int J Chem Tech Res 5:1224-1238.

Beg QK, Sahai V, Gupta R (2003) Statistical media optimization and alkaline protease production from *Bacillus mojavensis* in a bioreactor. Proc Biochem 39:203-209.

Bettin F, Montanari Q, Calloni R, Gaio TA, Silveira MM, Dillon AJP (2009) Production of laccases in submerged process by *Pleurotus sajor-caju* PS-2001 in relation to carbon and organic nitrogen sources, antifoams and Tween 80. J Ind Microbiol Biotechnol 36:1-9.

Collins PJ, Dobson A (1997) Regulation of laccase gene transcription in *Trametes versicolor*. Appl Environ Microbiol 63:3444-3450.

Das A, Paul T, Halder SK, Jana A, Maity C, Das Mohapatra PK, Pati BR, Mondal KC (2013) Production of cellulolytic

enzymes by *Aspergillus fumigatus* ABK9 in wheat bran-rice straw mixed substrate and use of cocktail enzymes for deinking of waste office paper pulp. Bioresour Technol 128:290-296.

Das A, Paul T, Halder SK, Maity C, Das Mohapatra PK, Pati BR, Mondal KC (2013) Study on regulation of growth and biosynthesis of cellulolytic enzymes from newly isolated *Aspergillus fumigatus* ABK9. Polish J Microbiol 62(1):31-43.

Desai SS, Tennali GB, Nityanand Channur N, Anup AC, Deshpande G, Murtuza BPA (2011) Isolation of laccase producing fungi and partial characterization of laccase. Biotechnol Bioinf Bioeng 1(4):543-549.

Ding Z, Chen Y, Xu Z, Peng L, Xu G, Gu Z, Zhang L, Shi G, Zhang K (2014) Production and characterization of laccase from *Pleurotus ferulae* in submerged fermentation. Ann Microbiol 64:121-129.

Dong YC, Dai YN, Xu TY, Cai J, Chen QH (2014) Biodegradation of chestnut shell and lignin-modifying enzymes production by the white-rot fungi *Dichomitus squalens*, *Phlebia radiate*. Bioprocess Biosyst Eng 37:755-764.

Fonseca MI, Shimizu E, Zapata PD, Villalba LL (2010) Copper inducing effect on laccase production of white rot fungi native from Misiones (Argentina). Enzyme Microb Technol 46:534-539.

Irshad M, Asgher M (2011) Production and optimization of ligninolytic enzymes by white rot fungus *Schizophyllum commune* IBL-06 in solid state medium banana stalks. Afr J Biotechnol 10:18234-18242.

Lowry OH, Rosebrough NJ, Farr A L, Randall RJ (1951) Protein measurement with Folin phenol reagent. J Biol Chem 193:265-275.

Minussi RC, Miranda MA, Silva JA, Ferreira CV, Aoyama H, Marangoni S, Rotilio D, Pastore GM, Durán N (2007) Purification, characterization and application of laccase from *Trametes versicolor* for colour and phenolic removal of olive mill waste water in the presence of 1-hydroxy benzotriazole. Afr J Biotechnol 6:1248-1254.

More SS, Renuka PS, Pruthvi K, Swetha M, Malini S, Veena SM (2011) Isolation, purification, and characterization of fungal laccase from *Pleurotus* sp. Enzym Res, ID 248735.

Osma JF, Toca-Herrera JL, Rodrıguez Couto S (2007) Banana skin: a novel waste for laccase production by *Trametes pubescens* under solid-state conditions. Application to synthetic dye decolouration. Dyes Pigm 75:32-37.

Qiu W, Zhang W, Chen H (2014) Flavonoid-rich plants used as sole substrate to induce the solid-state fermentation of laccase. Appl Biochem Biotechnol 172:3583-3592.

Ramachandran S, Roopesh K, Nampoothiri KM, Szakacs G, Pandey A (2005) Mixed substrate fermentation for the production of phytase by *Rhizopus* spp. using oilcakes as substrates. Proc Biochem 40:1749-1754.

Roriz MS, Osma JF, Teixeira JA, Couto SR (2009) Application of response surface methodological approach to optimize Reactive Black 5 decolouration by crude laccase from *Trametes pubescens*. J Hazard Material 169:691-696.

Scheel T, Hofe M, Ludwig S, Holker U (2000) Differential expression of manganese peroxidase and laccase in white-rot fungi in the presence of manganese or aromatic compounds. Appl Microbiol Biotechnol 54:686-691.

Songulashvili G, Elisashvili V, Wasser SP, Nevo E, Hadar Y (2007) Basidiomycetes laccase and manganese peroxidase activity in submerged fermentation of food industry wastes. Enzym Microb Technol 41:57-61.

Stajić M, Persky L, Friesem D, Hadar Y, Wasser SP, Nevo E, Vukojević J (2006) Effect of different carbon and nitrogen sources on laccase and peroxidases production by selected *Pleurotus* species. Enzyme Microb Technol 38:65-73.

Sterner RW, Elser JJ (2002) Ecological Stoichiometry: The Biology of Elements from Molecules to the Biosphere. Princeton University Press Princeton NJ, 584.

Sun W, Xu M, Xia C, Li A, Sun G (2013) Enhanced production of laccase by *Coriolus hirsutus* using molasses distillery wastewater. Front Environ Sci Eng 7(2):200-210.

Sweeney MD, Xu F (2012) Biomass converting enzymes as industrial biocatalysts for fuels and chemicals: Recent developments. Catalysts 2:244-263.

Vahidi H, Kobarfard F, Namjoyan F (2004) Effect of cultivation conditions on growth and antifungal activity of *Mycena leptocephala*. Afr J Biotechnol 3(11):606-609.

Viswanath B, Rajesh B, Janardhan A, Kumar AP, Narasimha G (2014) Fungal laccases and their applications in bioremediation. Enzym Res, ID 163242.

Woolridge EM (2014) Mixed enzyme systems for delignification of lignocellulosic biomass. Catalysts 4:1-35.

YangY, Ma F, Yu H, Fan F, Wan X, Zhang X, Jiang M (2011) Characterization of a laccase gene from the white-rot fungi *Trametes* sp. 5930 isolated from Shennongjia Nature Reserve in China and studying on the capability of decolorization of different synthetic dyes. Biochem Eng J 57:13-22.

Youshuang Z, Haibo Z, Mingle C, Zhenzhen W, Feng H, Peiji G (2011) Production of a thermostable metal-tolerant laccase from *Trametes versicolor* and its application in dye decolorization. Biotechnol Bioprocess Eng 16:1027-1035.

Volume 61(1):35-44, 2017
Acta Biologica Szegediensis
http://www2.sci.u-szeged.hu/ABS

ARTICLE

Effect of a three-component bacterial consortium in white shrimp farming for growth, survival and water quality management

Prasenjit Barman[1], Sangeeta Raut[2], Sudip Kumar Sen[3], Umar Shaikh[3], Partha Bandyopadhyay[4], Pradeep Kumar Das Mohapatra[1]*

[1]Department of Microbiology, Vidyasagar University, Midnapore, West Bengal, India
[2]Gandhi Institute of Engineering and Technology, Gunupur, Rayagada, Odisha, India
[3]In Gene Research Lab, Biostadt India Ltd., Waluj, Aurangabad, Maharashtra, India
[4]Biostadt India Ltd., Worli, Mumbai, Maharashtra, India

ABSTRACT The effect of a bacterial consortium containing *Rhodopseudomonas palustris* SUP-2, *Bacillus subtilis* SUP-3, and *Bacillus firmus* SUP-1 strains for white shrimp (*Penaeus vannamei*) farming were investigated. Shrimp growth, water quality, survival rate and enzymatic activities were followed at different stages of farming. Consortium developed using equal proportion of each bacterium was added to shrimp ponds at different concentrations. Dosages were adjusted in three different stages, first 40 days (10 l/ha), second 40 days (15 l/ha) and then continued up to harvest (20 l/ha). Consortium was used in the experiment ponds and no consortium was used in the control ponds. The mean survival rates were significantly lower, 65.1 ± 1.4% and 67.8 ± 2.2% in control ponds BPC-1 and BPC-2 ($P<0.001$), respectively. The statistical analysis showed significant differences ($P<0.05$) in the weight of the animals between the treatment (34.98 ± 0.1 in BTP 1 and 35.26 ± 0.1 g in BTP 2) and control (29.23 ± 0.1 in BCP 1 and 30.41 ± 0.1 in BCP 2) groups.

Acta Biol Szeged 61(1):35-44 (2017)

KEY WORDS

amylase
bacterial consortium
pathogen
shrimp

Introduction

Aquaculture and particularly shrimp culture has become a pivotal economic activity in many countries. An intensive culture system is commonly used for shrimp cultivation, because it produces higher yields than other systems (Shang et al. 1998). Since intensive shrimp culture needs high volume of pelleted feed and other additives, inadequate management may cause degradation of pond water environmental parameters including accumulation of black and glutinous sediment, called as organic sludge, in pond bottom soil (Shang et al. 1998; Rosenberry 1993). The bio-remediating agents used in shrimp aquaculture are predominantly photosynthetic bacteria (PSB) having antagonistic activity against shrimp pathogen at the same time improving water quality (Vine et al. 2006; Kesarcodi-Watson et al. 2008). Recently, an approach of using combined probiotics (microbial consortium) is gaining popularity worldwide (Wang and Wang 2008). It is proposed that application of beneficial microorganisms to the pond soil can accelerate decomposition of undesirable organic matters and other waste products through bioremediation and perhaps even increase ambient levels of oxygen (Wang and Han 2007; Sonnenholzner and Boyd 2000a).

The antibiotic resistance and its epidemiological magnitudes led to the investigation of several alternate approaches for disease management in aquaculture systems. Amongst them the most scientific, eco-friendly and cost-effective approach is the use of probiotics as prophylactics. The microbiota in the gastrointestinal tract (GIT) of shrimps can be modified by ingestion of other microorganisms; therefore, microbial manipulation establishes a practical tool to reduce or eliminate the prevalence of opportunistic pathogens (Balcazar et al. 2006). Natural production of some substances (Dinh et al. 2010; Iyapparaj et al. 2013) by bacteria in flocculating condition has been reported to prevent growth of co-habiting pathogenic species such as *Vibrio harveyi* (Defoirdt et al. 2007; Halet et al. 2007). Species in the genus *Vibrio* constitute the major bacterial pathogens in cultivated shrimp worldwide (Lightner 1993), and also *Aeromonas* that have been considered as foremost pathogens in aquaculture systems (Sindermann 1990).

The potential benefits of addition of bacterial consortium

Submitted September 12, 2016; Accepted May 22, 2017
*Corresponding author. E-mail: pkdmvu@gmail.com

in shrimp ponds include upgrading of water quality, enhancement of nutrition of host species through the production of auxiliary digestive enzymes, lower incidence of diseases and greater survival, and improved immune protection system (Verschuere et al. 2000). In the year 2003, Gamboa-delgado and co-workers reported that amylase activity increased the shrimp body weight. Maugle and co-workers (1983b) reported incremental increases in growth with increasing amylase supplements.

The aim of this study was to determine the effect of bioremediating isolates derived from brackish water on water quality parameters and the spectrum of antagonism against *Vibrio* and *Aeromonas* shrimp pathogens. This study was also involved digestive enzyme parameter assays and characterization, where protease and amylase were used as indicators.

Materials and Methods

Chemicals, media and reagents

All chemicals, media and reagents used in this study were of analytical grade and procured from Rankem and Hi-Media (India).

Sampling site and sampling procedure

Water samples were collected from the center of the Junput (21.68°N and 87.55°E) at Purba Midnapore district (West Bengal, India). Water depth (measured from the bottom of morphological structures) ranged from approximately 5 to 20 cm, depending on low wave. Water at the collection sites had temperature between 27 to 33 °C, salinity 14 ppt and pH 7.8. Each water sample (100 µl) was spread directly onto agar plates (containing tryptone 1%, yeast extract 0.5%, NaCl 0.5% and agar 1.5%, pH 7) at the study site. Water samples were also carried to the laboratory in sterile plastic containers within an hour at ambient temperature for further analysis. One ml of water sample had been serially diluted in sterile distilled water to get a concentration range between 10^{-1} to 10^{-6} dilution.

The bacterial isolates had been further sub-cultured on the respective media, in order to obtain pure culture and among them three isolates (SUP-1, SUP-2 and SUP-3) were selected based on their prevalence and antagonistic activity against shrimp pathogen.

Identification of the isolates

The preliminary morphological characteristics were determined by bright field microscopy (Zeiss Axiostar Plus, Zeiss, Germany). All isolates were also evaluated by conventional biochemical tests (Bergey's Mannual 2014). Scanning electron microscopy was conducted for selected isolates. The bacterial culture was smeared on cover slip, fixed with *p*-glutaraldehyde (4% v/v) and dehydrated (ethanol gradient: 30, 50, 70, 90 and 100% v/v for 15 min on absolute ethanol). Then it was coated with gold spattering and examined under SEM (Carl Zeiss SMT AG, Germany). Molecular identification of microbial isolates was performed by sequence comparison of amplified 16S rDNA region using primers and conditions as reported earlier (Ray Chaudhuri and Thakur 2006).

Screening of potent amylase producer

To find out potent amylase producing bacterial strains using modified medium containing (g/l) starch 10, peptone 10, yeast extract 20, KH_2PO_4 0.50, CaCl2.2H2O 0.50, agar 10, pH 8 at 32 °C temperature for 24 h. After incubation, 1% iodine solution (freshly prepared) was flooded on the starch agar plate. Presence of blue color around the growth indicates negative result and a clear zone of hydrolysis surrounded the growth, indicates positive result. Based on the highest clear zone to colony size ratio (cz/cs), bacterial colony was selected and designated as SUP-2. The isolate was preserved at 4 °C (in plate, stab and liquid form) and sub cultured at a regular interval for further use.

Media composition and fermentation condition

Amylase production by the isolate (SUP-2) was carried out in Erlenmeyer flasks (250 ml) contained 100 ml fresh liquid medium (modified medium containing (g/l) starch 10, peptone 10, yeast extract 20, KH_2PO_4 0.50, $CaCl_2.2H_2O$ 0.50). The physicochemical and cultural conditions were optimized by studying one variable at a time (OVAT) approach, where one factor is varied keeping others constant. The effect of physical parameters like, *e.g.,* incubation period (6-24 h), temperature (20-60 °C), pH (5.0-9.0) and chemical parameters like carbon sources (glucose, galactose, lactose, maltose, mannose, starch, sucrose) nitrogen sources (yeast extract, urea, peptone, beef extract, NH_4Cl, NH_4NO_3, KNO_3 and $NaNO_3$) and phosphate sources (KH_2PO_4, K_2HPO_4, Na_2HPO_4, NaH_2PO_4 and (NH_4) H_2PO_4) were evaluated for amylase production. The whole optimization process was carried out using freshly grown SUP-2 strain (A620~1.63). The fermented medium was centrifuged at 5000 rpm for 5 min and the amylase activity in the supernatant was measured through dinitrosalicylic acid method according to the protocol of Maity et al. (2011).

Antimicrobial sensitivity test

Different pathogenic strains from Tryptone Soy Agar (TSA) slants were inoculated into Tryptone Soy Broth (TSB) and incubated at 30 ºC for 24 h to prepare young cultures. The cul-

tures of pathogenic strains, *Vibrio parahaemolyticus* (MTCC 451), *Vibrio harveyi* (MTCC 1639) and *Aeromonas veronii* (MTCC 3249) were diluted 10^{-3} times using sterile Normal Saline Solution (0.9% NaCl) to reach the concentration of 10^{-6} cfu ml^{-1}. Antimicrobial sensitivity test was performed using agar-well diffusion method. After preparation of Tryptone Soy Agar plate the test organisms were swabbed on the Petri plates and left for 10 min. Next to that the wells were made on the plate and the crude centrifuged (5000 rpm) fermented medium was aspirated and loaded into the wells with the capacity of 100 µl each. The Petri plates were incubated overnight without inverting at optimum temperature of 32 °C.

Experimental design

The study was conducted from March 21, 2015 to August 13, 2015 at Contai shrimp ponds, located in the East Coast of the Bay of Bengal Sea. Four shrimp ponds were selected with two treatments (BPT-1 and BPT-2) and two controls (BPC-1 and BPC-2). The formulated (ECO-PRO) consortium (SUP-1, SUP-2 and SUP-3 strains in equal concentration) was added into the treatment ponds and not into the control ponds. The maximum depth was 120 to 130 cm with similar morphometric and size features (0.34-0.36 ha). The ponds had been used for four culture cycles and therefore, were considered aged ponds. The management and husbandry process was slightly modified, described by Corre et al. (2000). The pond bottom sun dried, desilted and was sanitized using lime stone power with soil conditioner (WitaMin, Biostadt India, Mumbai, India) prior to stocking. All the ponds were filled with cloth-filtered seawater (80, 100, and 120 meshes) having 15 ppt salinity after 10 days solarization. Each pond was stocked with *Penaeus vannamei* PL 12 (Vaishaki Biomarine, Vishakapatnam, India) at a density of 50 pcs/m^2. Shrimps were fed with commercial pellets (CP, India) twice a day for the first 30 days at a rate of 5-10% of the shrimp body weight and after that Automatic Feeder (Aron, Thailand) was used up to harvest. Paddle wheel aerators were used 3-4 h for 1st 30 days, 6-8 h for 30-90 days and 10-12 h up to harvest and adjusted the numbers/HP with 400 kg biomass after 30 days.

The probiotics was formulated in liquid form packed in airtight HDPE bottles. The product had bacterial cell densities of $1x10^9$ CFU (colony-forming units) ml^{-1} and contained consortium with equal mixture of SUP-1, SUP-2 and SUP-3. The rate and frequency of application of the formulated consortium probiotics in shrimp treatment ponds was 10 l/ha for first 40 days, 15 l/ha for second 40 days and then 20 l/ha continue up to harvest. Dosage was given in every 10 days and adjusted as per the above schedule.

Water quality sampling

Water pH, temperature and salinity were monitored daily at 06:00-07:00 h and 17:00-18:00 h using KIT (Allvet-Thailand), digital water thermometer (Hicks-Japan) and refractometer (Atago-India), respectively. Other water parameters were analyzed weekly. Unionized ammonia and particulate organic matter (POM) were analyzed following the procedures prescribed by Strickland and Parsons (1972). Cu, B, Zn and Mn were analyzed through Atomic Absorption Spectroscopy (Shimazdu AA7000, Japan). Quantitative analysis of phytoplankton was done using a hemocytometer and a compound microscope following the procedure of Martinez et al. (1975). Presumptive *Vibrio* counts were determined by a spread plate technique on thiosulfate-citrate-bile salt sucrose (TCBS) agar by employing the method of Reilly (1982). The agar plates were incubated for 18-24 h in ambient temperature. Yellow and green colonies were counted after 24 h and were assumed to be *Vibrio*. Luminescent colonies were counted on TCBS plates in a darkened room.

Table 1. Characterization of three different bacterial isolates isolated from sample site (Junput).

Strains	SUP-1	SUP-2	SUP-3
Physiological characterization			
Temperature tolerance range	10-65 °C	15-60 °C	15-55 °C
Optimum temperature	30 °C	30 °C	32 °C
pH tolerance range	3-11	4-11	3-12
Optimum pH	8.0	8.5	8.0
Biochemical characterization			
Amylase	Positive	Positive	Positive
Catalase	Positive	Positive	Positive
Protease	Positive	Negative	Positive
Urease	Negative	Positive	Positive
Methyl red	Negative	Positive	Negative
Voges-Proskauer test	Negative	Negative	Negative
Indole	Negative	Negative	Negative
Citrate	Negative	Positive	Negative
Maximum identity with organism			
	B. firmus	*R. palustris*	*B. subtilis*

Statistical analysis

Statistical differences among treatments were analyzed using the analysis of variance (ANOVA) and Duncan's multiple range test (DMRT) with the SigmaStat software V.10.0 (SPSS, 1999) at 5% level of significance.

Results and Discussion

Bacterial isolation and identification

Based on their abundance and antagonistic activity against

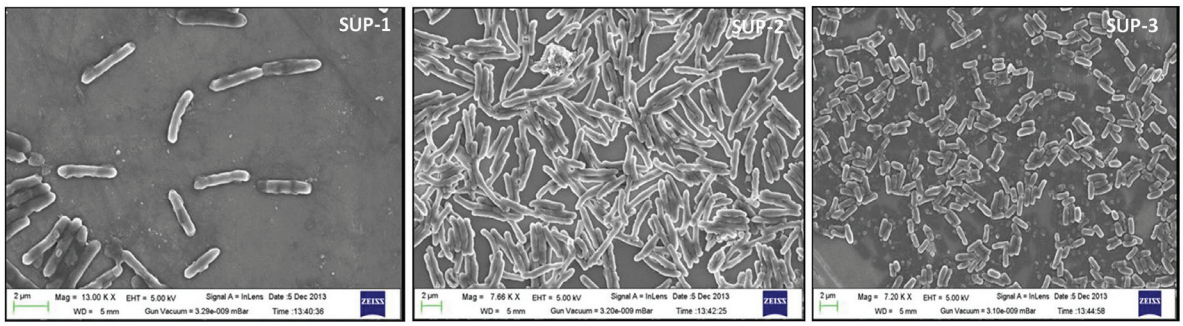

Figure 1. Scanning Electron Microscopic photograph of SUP-1, SUP-2 and SUP-3.

pathogen, molecular characterization was performed, which indicated that SUP-1 and SUP-3 as *Bacillus* sp., where the similarity is greater than 98% (data not shown) and SUP-2 showed 99% similarity with *Rhodopseudomonas* sp. The Gen-Bank Accession Number of the isolates was KT875347, KT875348 and KT875349, respectively. The details of the morphological, biochemical and physiological characterization are presented in Table 1. Scanning electron micrograph of selected strains are depicted in Figure 1 and the neighbor joining phylogenetic tree from analysis of 16S rDNA gene sequence of bacterial isolates is presented in Figure 2.

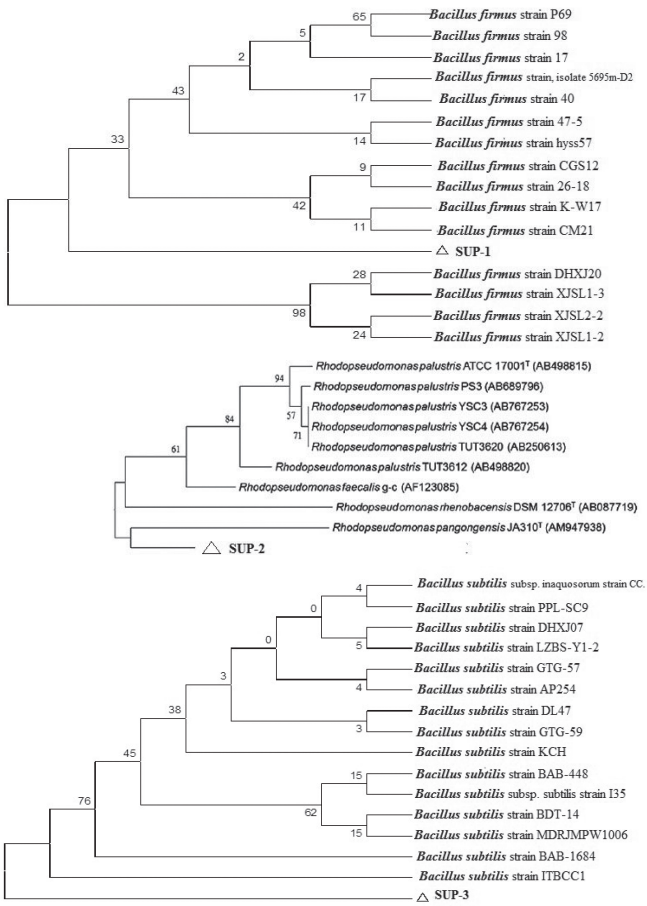

Figure 2. Phylogenetic tree of SUP-1, SUP-2 and SUP-3 strains.

Optimization of α-amylase production

Optimization of α-amylase production in submerged fermentation was performed by using quasi-optimum (OVAT) protocol. Among the different carbon sources used (glucose, galactose, lactose, maltose, mannose, starch, sucrose) α-amylase production was higher with starch as sole carbon source at 1.0% level (Fig. 3a). From the present findings, it is observed that the activation of α-amylase needs substrates having α-1, 4 glycosidic bond, including starch and maltose, but glucose represses its production. The biosynthesis of α-amylase in most species is repressed by readily metabolizable substrates, particularly glucose, by a mechanism of catabolite repression, facilitated by the protein encoded CreA gene (Kato et al. 1996). *Rhodopseudomonas palustris* SUP-2 produced a substantial amount of α-amylase in presence of all the tested nitrogen sources, while highest enzyme biosynthesis of 375.6 U/ml occurred in presence of 0.5% (w/v) beef extract (Fig. 3b). Basic nitrogen is essential component for growth of microbes and production of secondary metabolites. Among these, studied phosphate source (Fig. 3c). $(NH_4)\ H_2PO_4$ with 0.5% (w/v) concentration maximized amylase production (292 U/ml). During OVAT optimization, *R. palustris* SUP-2 was found to produce the highest amount of amylase (363.4 U/ml) after 18 h of fermentation (Fig. 3d). Figure 4e depicted

Table 2. Antimicrobial assay of isolated strains against test organisms (inhibition zone in mm).

Isolated strains	*V. parahaemolyticus*	*V. harveyi*	*Aeromonas veronii*
SUP-1	4.3	1.4	0.4
SUP-2	1.8	2.3	2.1
SUP-3	NIL	0.9	3.2

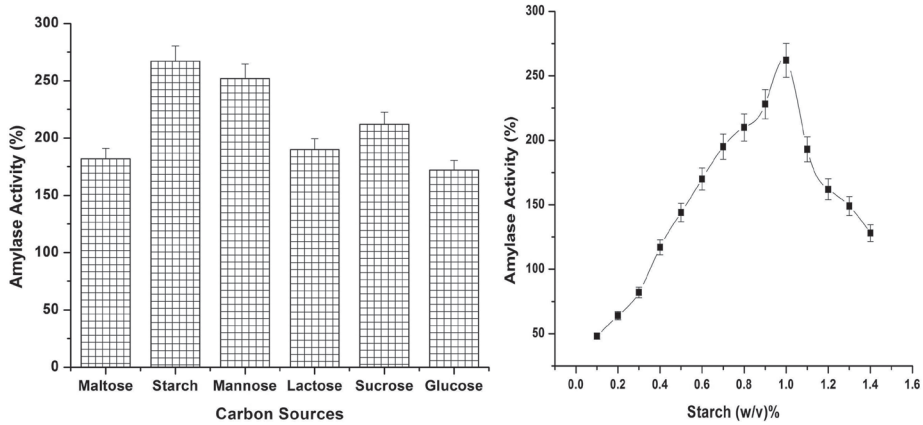

Figure 3a. Effect of different carbon sources and starch concentration (%) on α-amylase production.

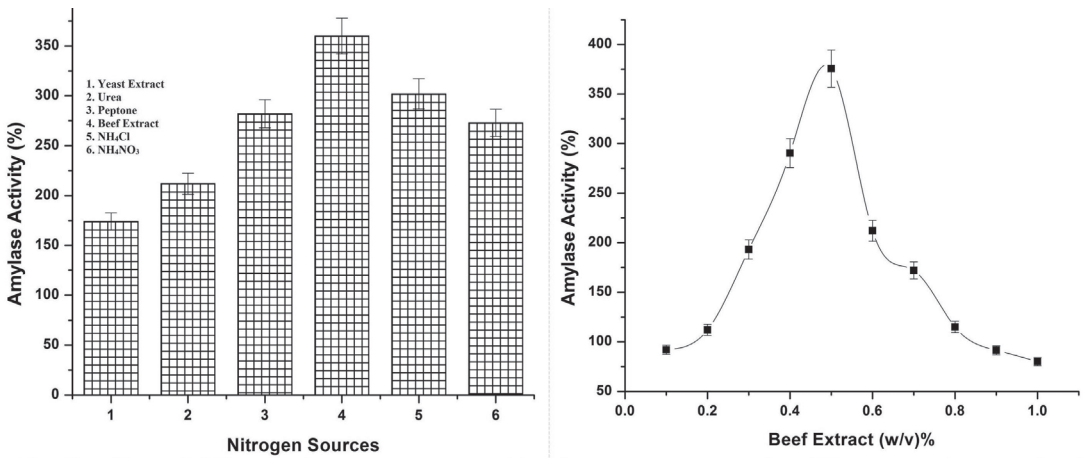

Figure 3b. Effect of different nitrogen sources and beef extract concentration (%) on α-amylase production.

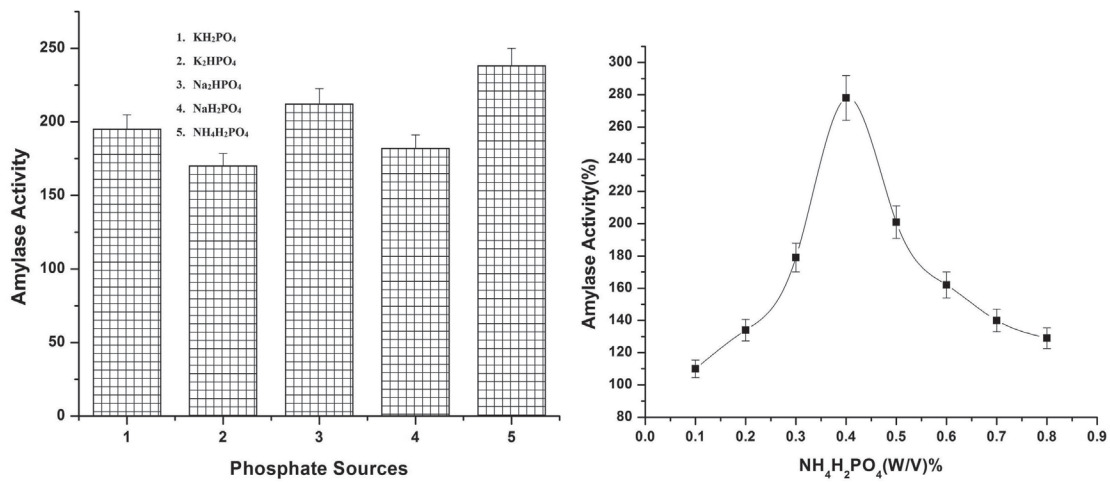

Figure 3c. Effect of different phosphate sources and $(NH_4)H_2PO_4$ concentration (%) on α-amylase production.

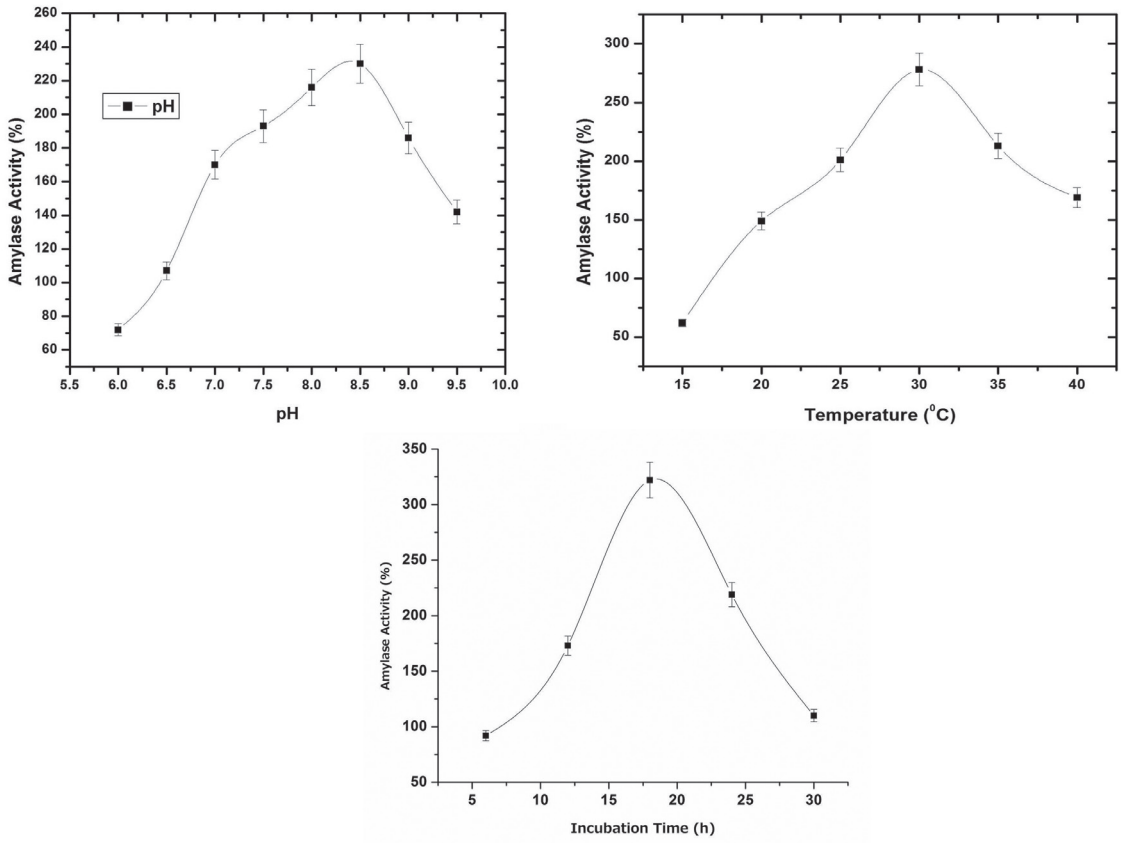

Figure 3d. Effect of pH, temperature (°C) and time (h) on α-amylase production.

the effect of different pH, incubation time and temperature on α-amylase production.

Determination of antimicrobial activity

Antimicrobial activity of the extracellular supernatants against the pathogenic bacteria was determined with the plate diffusion method (Fig. 4) and zone of inhibition represented in Table 2. Antimicrobial activities against test bacteria were observed in plates with pH non-adjusted SUP-1 and SUP-3 cultures. In contrast, slight inhibition was observed in pH-adjusted cultures. In pH-adjusted and pH non-adjusted SUP-2 cultures, strong antimicrobial activities were evident toward all target bacteria. Previous studies reported antimicrobial

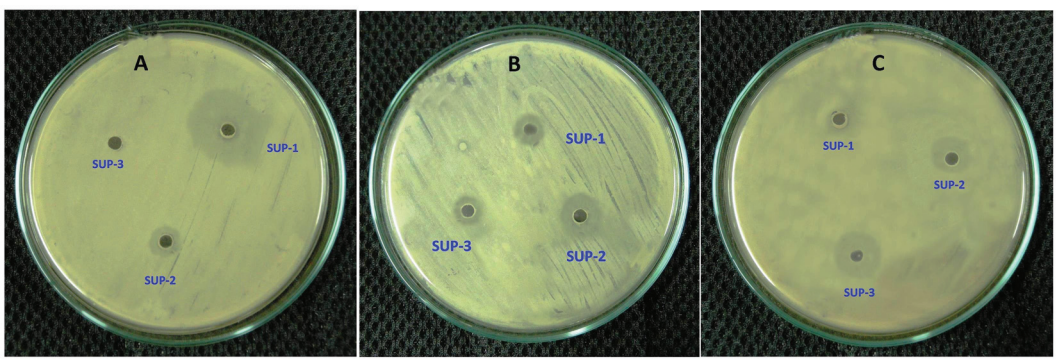

Figure 4. Inhibition by SUP-1, SUP-2 and SUP-3 culture supernatant as measure with the plate diffusion assay. Supernatant were placed on to lawns of (A) *V. parahaemolyticus*, (B) *V. harveyi* and (C) *A. veronii*.

Table 3. Zootechnical results and significant differences in BPC-1 and BPC-2 (control) and BPT-1 and BPT-2 (treatment) ponds.

	BPC-1	BPC-2	BPT-1	BPT-2	Significance
Survival (%)	61.1 ± 1.4	63.8 ± 2.2	69.04 ± 1.4	77.9 ± 2.2	P<0.001
FCR	1.65 ± 0.4	1.69 ± 0.4	1.41 ± 0.4	1.49 ± 0.4	P<0.05
Final body weight (g)	29.23 ± 0.1	30.41 ± 0.1	34.98 ± 0.1	35.26 ± 0.1	Not Significant

effects due to the production of antibiotics, siderophores, bacteriocins, proteases, hydrogen peroxide and lysozyme; changes in pH; and the production of organic acids and ammonia (Nissen-Meyer and Nes 1997; Le Marrec et al. 2000; Verschuere et al. 2000). In spite of boiling the SUP-1 and SUP-3 culture, antimicrobial activity remained same. Reddy (2000) recommended that the pH range of 7.5 to 8.5 was the best for shrimp culture. For this reason the antimicrobial activity of three organisms were tested at pH 8. It was found that SUP-2 showed the antimicrobial activity against all the tested pathogens but SUP-1 and SUP-3 did not showed such antimicrobial activities at pH 8. These results suggested that among the three organisms, SUP-2 was showed the best antimicrobial activity against pathogens. The characterization of inhibitory substance derived from SUP-2 cultures will be resolved in future studies.

Zootechnical results

Table 3. presents the zootechnical results of shrimps reared in both controlled and treated ponds. The mean survival rates were respectively 65.1 ± 1.4% and 67.8 ± 2.2% for BPC-1 and BPC-2 pond (P<0.001). Probiotic treatment was found to significantly improves the survival rate (P<0.001) and the food conversion ratio (P<0.05) (Table 3.). In BPT-1 and BPT-2, survival was higher by 13% and 21% and FCR lower by 15% and 12% compared to control pond BPC-1 and BPC-2, respectively. The treated pond showed that average mean shrimp weights after 117 days were 34.98 ± 0.1 and 35.26 ± 0.1 g and control pond 29.23 ± 0.1 and 30.41 ± 0.1, respectively. The statistical analysis depicted significant differences (P<0.05) in the weight between the treatment and control groups.

Previous studies have suggested that some bacteria may also help in the process of digestion of shrimp by producing extracellular enzymes like, proteases, lipases and carbohydrolases, as well as providing necessary growth factors for controlling the physicochemical parameters of soil and water in the culture ponds (Arellano and Olmos 2002; Ochoa and Olmos 2006; Bandyopadhyay et al. 2015).

Consortium of microorganisms (SUP-1, SUP-2 and SUP-3) induced the best growth performance and antagonistic activity against shrimp pathogens. Similar result was reported by Ghosh et al. (2003) and Wang and Xu (2006).

Environmental parameters of pond

Particulate organic matter (POM) and unionized ammonia were significantly different (P<0.05) in all treatments as compared to control ponds (Fig. 5a-b). The status of unionized ammonia ranged from, 0.001 mg/L to 0.750 mg/L and 0.003 mg/L to 0.160 mg/L, while the POM obtained were 12.56 mg/L and 2.10 mg/L in control and treatment ponds, respectively. POM and unionized ammonia was found to be

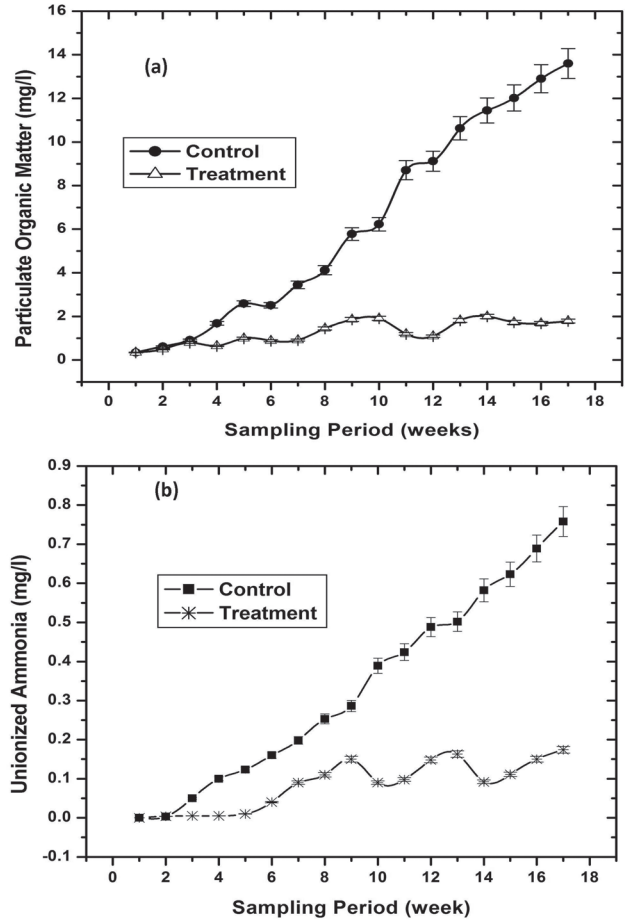

Figure 5. Weekly particulate organic matter level (mg/l) and unionized ammonia level (mg/l) of the pond (control and treated). Each mark represents mean and standard error of three replicates.

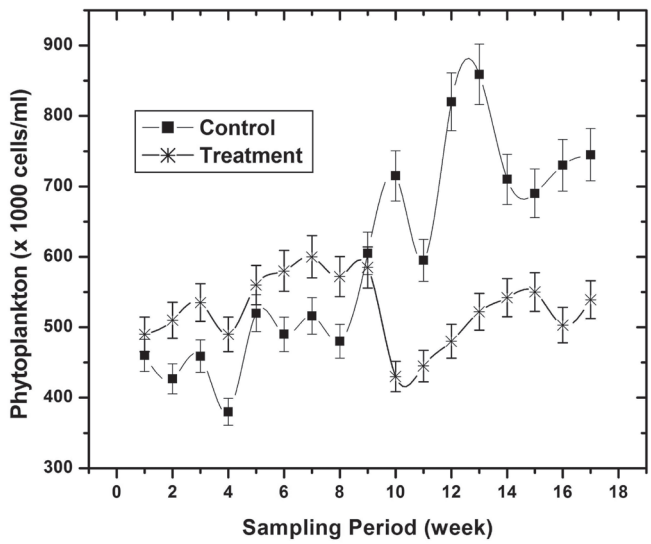

Figure 6. Weekly phytoplankton count (cells/ml) of the control and treated ponds. Each mark represents mean and standard error of three replicates.

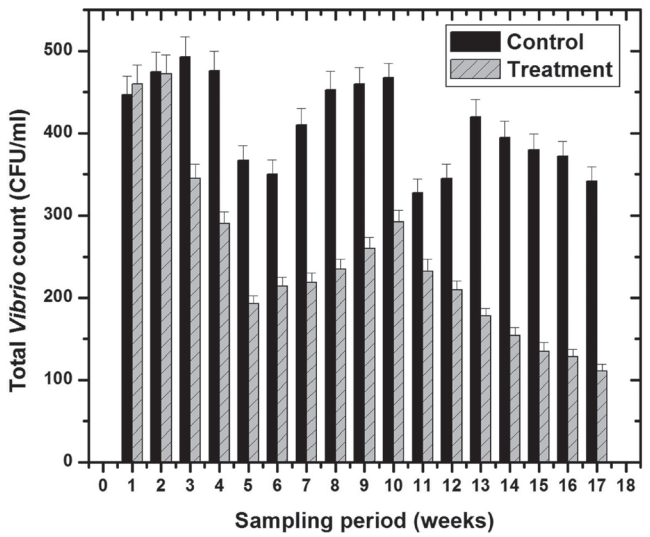

Figure 7. Weekly total reasonable *Vibrio* bacterial counts (cfu/ml) of the pond water. Each mark represents mean and standard error of three replicates.

significantly low and stable in ponds throughout the culture period. Mean phytoplankton count was mostly same among the treated ponds, but significantly higher in the control ponds. However, a relatively stable phytoplankton count was noticed in treated ponds compared to control ponds (Fig. 6). Over population of plankton creates detrimental effect of plankton crash in the pond. It mainly happened due to eutrophication. Simultaneously, *R. palustris* helps sulfur reduction in pond water and stabilize the plankton bloom. The reason behind that bacteria convert ammonium to nitrite and then to nitrate (NH_3, NO_2^-, NO_3^-). The aerobic ammonia-oxidizing bacteria (AOB) oxidize ammonia to nitrite through hydroxylamine and then the nitrite-oxidizing bacteria (NOB) oxidize nitrite to nitrate. Denitrifying bacteria possess several clusters of genes involved in denitrification (Philippot 2002). These genes encoded by four metalloenzymes like nitrate reductase, nitrite reductase, nitric oxide reductase and nitrous oxide reductase, which chronologically reduce nitrate to N_2 (NO_3^-, NO_2^-, NO^-, N_2O, N_2). The phytoplankton density in probiotic treatments was dominated by the beneficial plankton, *i.e.* the diatoms and green algae (*Chlorella*), which comprised about 80-85% of the total plankton. The blue-green algae (*Microcystis*) dominated the phytoplankton in control ponds. Close to end of the culture period, more microcystis and dinoflagellates (*Chattonella*) population was observed. Metals ions were found in negligible amount after end of the culture (data not shown).

The reasonable *Vibrio* counts on TCBS plates were significantly lower ($P<0.05$) in treated ponds (111 ± 10 cfu/mL) when compared with the control ponds (346 ± 15 cfu/mL) (Fig. 7).

The luminous *Vibrio* species present in pond water were ruled out when a specific *Bacillus* species were added (Moriarty 1998). Most bacterial cells are passing in the gut with continuous intrusion of microbes coming from the water and food (Gatesoupe 1999). The routine practice of probiotics enhanced digestion by enhancing the population of beneficial microorganisms, microbial enzyme activity and improved feed consumption (Bomba et al. 2002). Rengpipat et al. (1998) reported that appropriate probiotics applications were shown to better intestinal microbial balance, thus leading to improved food absorption.

Conclusion

White shrimp culture ponds treated with bio remediating consortium had better growth, survival, lower FCR, better soil and water quality parameters than control ponds. It has also been critically observed that bacterial strains SUP-2 (*R. palustris*) had much better effect than other two strains. SUP-2 also showed better inhibitory effect against *V. parahaemolyticus,* which became a big threat for Early Mortality Syndrome (EMS) in white shrimp farming in several South East Asian countries and Mexico. Further research is going on for standardization of dosage and other enzymatic activities for bioremediation.

References

Arellano CF, Olmos SJ (2002) Thermostable α-1,4- and α-1,6-glucosidase enzymes from *Bacillus* sp. isolated from a marine environment. World J Microbiol Biotechnol 18:791-795.

Balcazar JL, Blas Id, Ruiz-Zarzuela I, Cunningham D, Vendrell D, Muzquiz JL (2006) The role of probiotics in aquaculture. Vet Microbiol 114:173-186.

Bandyopadhyay P, Sarkar B, Mahanty A, Rathore RM, Patra BC (2015) Dietary administered *Bacillus* sp. PP9 enhances growth, nutrition and immunity in *Cirrhinus mrigala* (Hamilton). Proc Natl Acad Sci India, Sect B, Biol Sci. DOI10.1007/s40011-015-0561-6.

Bomba A, Nemcoa R, Gancarcikova S, Herich R, Guba P, Mudronova D (2002) Improvement of the probiotic effect of microorganisms by their combination with maltodextrins, fructo-oligosaccharides and polyunsaturated fatty acids. Br J Nutr 88 (Suppl. 1):95-99.

Corre Jr VL, Janeo RL, Caipang CMA, Calpe AT (2000) Use of probiotics and reservoir with "green water" and other tips for a successful shrimp culture. Aquac Asia V, 34-38.

Defoirdt T, Halet D, Vervaeren H, Boon N, Van de Wiele T, Sorgeloos P, Bossier P, Verstraete W (2007) The bacterial storage compound poly-β-hydroxybutyrate protects Artemia franciscana from pathogenic *Vibrio campbelli*. Environment Microbiol 9:445-452.

Dinh TN, Wille M, De Schryver P, Defoirdt T, Bossier P, Sorgeloos P (2010) The effect of poly-β-hydroxybutyrate on larviculture of the giant freshwater prawn (*Macrobrachium rosenbergii*). Aquaculture 302:76-81.

Gamboa-delgado J, Molina-poveda C, Cahu C (2003) Digestive enzyme activity and food ingesta in juvenile shrimp Litopenaeus vannamei (Boone, 1931) as a function of body weight. Aquacult Res 34(15):1403-1411.

Gatesoupe FJ (1999) The use of probiotics in aquaculture. Aquaculture 180:147-165.

Ghosh K, Sen SK, Ray AK (2003) Supplementation of an isolated fish gut bacterium, *Bacillus circulans*, in formulated diets for rohu, *Labeo rohita*, fingerlings. Isr J Aquac Bamidgeh 55:13-21.

Halet D, Defoirdt T, Van Damme P, Vervaeren H, Forrez I, Van de Wiele T, Boon N, Sorgeloos P, Bossier P, Verstraete W (2007) Poly-β-hydroxybutyrate-accumulating bacteria protect gnobiotic *Artemia franciscana* from pathogenic *Vibrio campbelli*. FEMS Microbiol Ecol 60:363-369.

Iyapparaj P, Maruthiah T, Ramasubburayan R, Prakash S, Kumar C, Immanuel G, Palavesam A (2013) Optimization of bacteriocin production by *Lactobacillus* sp. MSU3IR against shrimp bacterial pathogens. Aquatic Biosystems 9:1-12.

Kato M, Sekine K, Tsukagoshi N (1996) Sequence-specific binding sites in the Taka-amylase A G2 promoter for the CreA repressor mediating carbon catabolite repression. Biosci Biotechnol Biochem 60:1776-1779.

Kesarcodi-Watson A, Kaspar H, Lategan MJ, Gibson L (2008) Probiotics in aquaculture: the need, principles and mechanisms of action and screening processes. Aquaculture 274:1-14.

Lightner DV (1993) Diseases of cultured penaeid shrimps, In: Mc Vey, J.P. (Ed.), CRC Handbook of Mariculture, 2nd ed. CRC Press, Boca Raton, USA, pp. 393-486.

Le Marrec C, Hyronimus B, Bressollier P, Verneuil B, Urdaci MC (2000) Biochemical and genetic characterization of coagulin, a new antilisterial bacteriocin in the pediocin family of bacteriocins, produced by *Bacillus coagulans*. Appl Environ Microb 66:5213-5220.

Maity C, Samanta S, Halder SK, Das Mohapatra PK, Pati BR, Jana M, Mondal KC (2011) Isozymes of α-amylases from newly isolated *Bacillus thuringiensis* CKB19: production from immobilized cells. Biotechnol Bioprocess Eng 16:312-319.

Martinez MR, Chakroff RP, Pantastico JB (1975) Direct phytoplankton counting technique using the haemocytometer. Phil Agric 55:43-50.

Moriarty DJW (1998) Control of luminous *Vibrio* species in penaeid aquaculture ponds. Aquaculture 164:351-358.

Maugle PD, Deshimaru O, Katayama T, Simpson K (1983b) The use of amylase supplements in shrimp diets. J World Maricult Society 14:25-37.

Nissen-Meyer J, Nes IF (1997) Ribosomally synthesized antimicrobial peptides: Their function, structure, biogenesis and mechanism of action. Arch Microbiol 167:67-77.

Ochoa SJL, Olmos SJ (2006) The functional property of *Bacillus* for shrimp feeds. Food Microbiol 23:519-525.

Philippot L (2002) Denitrifying genes in bacterial and Archaeal genomes. Biochim Biophys Acta 1577:355-376

Reddy R (2000) Culture of the tiger shrimp *Penaeus monodon* (Fabricius) in low saline waters. Master's Thesis, Annamalai University, India.

Reilly A (1982) Laboratory Course in Fish Microbiology. Diliman, QC: GTZ-DFPT-CFUPV, p. 98.

Rengpipat S, Phianphak W, Piyatiratitivorakul S, Menasveta P (1998) Effects of a probiotic bacterium on black tiger shrimp *Penaeus monodon* survival and growth. Aquaculture 167:301-313.

Rosenberry B (1993) World Shrimp Farming. Aquaculture Digest, San Diego. California, USA, pp. 1-19.

Shang YC, Leung P, Ling BH (1998) Comparative economics of shrimp farming in Asia. Aquaculture 164:183-200.

Ray Chaudhuri S, Pattanayak AK, Thakur AR (2006) Microbial DNA extraction from sample of varied origin. Curr Sci 12:1697-1700.

Sindermann CJ (1990) Principal Diseases of Marine Fish

and Shellfish 2nd ed., vol. 2. Academic Press, New York. 516 pp.
Strickland JD, Parsons TR (1972) A Practical Handbook of Seawater Analysis, 2nd ed. Fisheries Research Board of Canada, Ottawa, Canada, p. 310.
Sonnenholzner S, Boyd CE (2000a) Managing the accumulation of organic matter deposited on the bottom of shrimp ponds. Do chemical and biological probiotics really work? World Aquac 31:24-28.
Verschuere L, Rombaut G, Sorgeloos P, Verstraete W (2000) Probiotic bacteria as biological control agents in aquaculture. Microbiol Mol Biol Rev 64:655-671.
Vine NG, Leukes WD, Kaiser H (2006) Probiotics in marine larviculture. FEMS Microbiol Rev 30:404-427.
Wang YM, Wang YG (2008) Advance in the mechanisms and application of microecologics in aquaculture. Prog Vet Med 29:72-75 (in Chinese).
Wang YB, Han JZ (2007) The role of probiotic cell wall hydrophobicity in bioremediation of aquaculture. Aquaculture 269:349-354.
Wang YB, Xu ZR (2006) Effect of probiotics for common carp (*Cyprinus carpio*) based on growth performance and digestive enzyme activities. Anim Feed Sci Technol 127:283-292.

Volume 61(1):45-50, 2017
Acta Biologica Szegediensis
http://www2.sci.u-szeged.hu/ABS

ARTICLE

A comparative study on optimisation of protein extraction methods for *Saccharomonospora azurea*

István Fodor[1], Andrea Valasek[2], Péter Urbán[2], Márk Kovács[2], Csaba Fekete[2], Ildikó Kerepesi[1]*

[1]Department of Genetics and Molecular Biology, Institute of Biology, Faculty of Sciences, University of Pécs, Hungary
[2]Department of General and Environmental Microbiology, Institute of Biology, Faculty of Sciences, University of Pécs, Hungary

ABSTRACT To establish the optimal cell disruption and protein extraction protocol for achieving the most efficient whole-cell protein extraction of *Saccharomonospora azurea*, four commonly used methods (X-Press, bead-vortexing, freezing-throwing and TCA/acetone/phenol extraction) were compared. Total protein content, as well as 1D and 2D SDS-PAGE protein patterns were assayed in the extracts to study the efficacy of these methods. Accordingly, of the four methods the X-Press proved the most effective for all initial weight (maximum 21.523 ± 0.23 mg/ml protein) followed by TCA/acetone/phenol method (maximum 13.682 ± 0.15 mg/ml protein), while the effectiveness of the two other methods were substantially inferior (maximum 3.188 ± 0.03 mg/ml protein). The analysis of protein gels proved that the X-Press method revealed a protein pattern characterised by the presence of the highest number of protein bands (on average of 52 and 385, on 1D and 2D gels, respectively). The TCA/acetone/phenol extraction provided similar effectiveness for only 100-300 mg initial bacteria mass, whereas bead-vortexing produced maximum 35 and 227 separated protein bands, on 1D and 2D gels, respectively. It can be stated that of the four methods the X-Press was the most effective one for all initial weight of bacteria, while the TCA/acetone/phenol method provides interpretable results for the 100-300 mg weight-range of bacteria. **Acta Biol Szeged 61(1):45-50 (2017)**

KEY WORDS
bead-vortexing
freezing-throwing
protein extraction
Saccharomonospora azurea
SDS PAGE
X-Press

Introduction

The spread of multi-resistant bacteria inspires researchers to search for new effective antibiotics. The primycin complex first described by Vály-Nagy et al. (1954) produced by *Saccharomonospora* sp. seems promising in tackling this problem. Re-investigated of the efficacy of this antibiotic, Feiszt et al. (2014) clearly demonstrated that primycin possesses high activity against the most frequent Gram-positive pathogens including some multi-resistant strains, without the development of remarkable resistance. Due to its great properties, a wider range of medical applications would be possible upon our better understanding of the regulation of synthetic processes of this "new-old" antibiotic. As first step, to get deeper insight into the bioactive natural products metabolism of *Saccharomonospora azurea* SZMC 14600, whole-genome sequencing was performed (Csepregi et al. 2012). Since proteomics represents a dynamic view of expressed genes, the proteomic approach combined with genetic studies provides a more comprehensive insight into the regulation of secondary metabolism to identify proteins associated with primycin production. In this context, the reliable knowledge of protein distribution is essential.

Efficient protein extraction highly depends on the quality of cell disruption. There is a great diversity of techniques including physical (bead-mill, French press, ultrasonic vibration) and chemical (detergents, lysozyme, osmotic shock) methods as well as the combination of them available for protein extraction of different types of samples and for various purposes (Wilson and Walker 2000; Islam et al. 2004; Singh 2013; Alam and Ghosh 2014; Malafaia et al. 2015; Tiong et al. 2015), therefore, it is a challenge to find a technique that can produce high yields and the greatest possible number of proteins in the sample analysed. Presently, we know of no comparative studies about the total protein distribution of *S. azurea*, consequently no currently available the most effective methods can be associated with this bacterium.

Therefore, in this study we compare four different commonly used total protein extraction methods including X-Press, bead-vortexing, freezing-throwing and the TCA/acetone/phenol technique to achieve a highly efficient isolation of total proteins for protein profiling of *S. azurea* SZMC

Submitted February 13, 2017; Accepted May 15, 2017
*Corresponding author. E-mail: ilda@gamma.ttk.pte.hu

14600. The effectiveness of the studied methods was evaluated by total protein content, 1D and 2D SDS-PAGE.

Materials and Methods

Bacterial cultures were maintained according to the industrial primycin fermentation processes (Juhász et al. 2011). *S. azurea* SZMC 14600 freeze-dried stock cultures maintained at -80 °C were used to directly inoculate 50 ml of pre-fermentation medium (PF) containing (w/v): 3% soy flour, 4.2% water soluble starch, 0.36% NaCl, 0.6% $CaCO_3$ and 0.5% (v/v) sunflower oil (pH 8). PF culture was grown for 2 days at 37 °C in an orbital shaker at 200 rpm. Thereafter, 1 ml suspension of bacterial cells was used to inoculate 35 ml of main fermentation medium (MF) containing (w/v): 4% soy flour, 4% water soluble starch, 0.3% NaCl, 0.5% $CaCO_3$, 0.6% sunflower oil, 0.3% stearic acid and 0.1% KH_2PO_4 (pH 9.5). The MF cultures were incubated at 28 °C for 5 days. The cultures were harvested by centrifugation (9000 g, 4 ºC, 15 min). Soluble proteins were extracted from 100, 200, 300, 500, and 1000 mg fresh weight of bacterial mats.

TCA/acetone/phenol method

The whole-cell protein was extracted according to the method described by Wang et al. (2006).

X-Press method

The frozen (-20 °C) bacterial mats in 5 ml phosphate buffer (PBS: 0.1 M, pH 7.4, 10 mM PMFS) were forced through an orifice and subjected to very high hydraulic pressures in X-Press Disintegrator Type X25 (Ab Biox; Göteborg, Sweden) appliance.

Bead-vortexing method

The modified method of Sánchez et al. (2003) consisted of adding 250 mg of glass beads (diameter 425-500 µm) to the bacteria mats suspended in 5 ml SDS treatment buffer (0.0625 M Tris, pH 7.4, 2% (w/v) SDS, 10% (v/v) glycerol, 10 mM PMFS) and vortexing (Tissue Lyzer, Quiagen) for 4 min (30 s vortexing/30 s in ice) at the maximum setting. After cooling on ice and centrifuging (13600g, 15 min, 4 °C), supernatants were used for further experiments.

Freezing-throwing method

The cells were destroyed by freezing and thawing five times, using liquid nitrogen (Kajiwara et al. 2003). Proteins were extracted by 5 ml lysis buffer (7 M urea, 1 mM-os PMFS, 4 % (w/v) CHAPS, 2% (v/v) Triton X-100, 5 % (v/v) 2-mercaptoethanol, 0.5 M EDTA). After centrifugation, (13600 g, 15 min, 4 °C), supernatants were used for further experiments.

The purified proteins were stored at -20 °C. For further studies protein extracts from different methods and initial mass of bacteria (100 mg, 200 mg, 300 mg, 500 mg, and 1000 mg) were diluted to the same volume. Protein concentration was measured by the Bradford method (Bradford 1976).

Each extraction was performed in triplicate. A statistical analysis was performed using one-way analyses of ANOVA. Values are reported as mean ± SD (standard deviation). The level of significance was adopted at $p<0.05$.

SDS-PAGE

The gel electrophoresis of whole cell protein extracts was performed according to Laemmli (1970) on vertical slab gels (8.6 x 6.7 x 0.1 cm) in a Mini Protean Tetra Cell gel electrophoresis apparatus (Bio-Rad Laboratories) using 12% separating gel (pH 8.8) and 5% stacking gel (pH 6.8). The running buffer contained 25 mM Tris, 192 mM glycine, 0.1% (w/v) SDS (pH 8.35), 5 µl and 10 µl of samples and 10 µl of protein molecular weight standard (Precision Plus Protein Unstained standard, Bio-Rad) were applied. Electrophoresis was performed at a constant current of 120 V for two hours. At the end of electrophoresis, the gels were visualized by staining with Coomassie Brilliant Blue (10% (v/v) acetic acid, 45% (v/v) methanol, 0.25% (w/v) Coomassie Brilliant Blue R-250) with constant shaking followed by decolorization with a solution of 10% (v/v) methanol and 10% (v/v) acetic acid.

2D electrophoresis

Isoelectric focusing of rehydrated protein samples (250 µg) were performed on 7 cm IPG Strips (pH 3-10, Bio-Rad) at 250 V for 15 min (rapid voltage ramping), at 4000 V for 1 h (linear voltage ramping), at 4000 V (rapid voltage ramping) up to 15 000 Vh . The IPG strips were equilibrated in 2% (w/v) DTT containing buffer (6 M urea, 20% (v/v) glycerol, 2% (w/v) SDS, 0.05 M Tris-HCl, pH 8.8), for 20 min. 2D electrophoresis were performed on 12.5% (w/v) SDS-PAGE gels, using the Bio-Rad Mini-PROTEAN Tetra Cell vertical electrophoresis system. Runs were carried out at room temperature for 10 min at 50 V and successively for 1 h at 200 V. Gels were stained with Coomassie Brilliant Blue (Sigma-Aldrich) as described above.

Gel images were captured by AlphaImager high performance gel documentation system (Protein Simple, Alpha Innotech, San Leandro, CA) and analysed using Prodigy 1D and SameSpots 2D Software package (Nonlinear Dynamics) according to the instructions of manufacturers.

Table 1. Protein recovery from *S. azurea* (SZMC 14600) cells using different extracting protocols. Values (mg/ml protein) are reported as means ± SD of three independent experiment (n = 3).

Mass of bacteria	X-Press	TCA/acetone/phenol	Bead-vortexing	Freezing-throwing
100 mg	3.284 ± 0.36	12.693 ± 0.	1.531 ± 0.02	0.572 ± 0.04
200 mg	7.010 ± 0.06	13.682 ± 0.15	2.153 ± 0.03	0.547 ± 0.06
300 mg	8.062 ± 0.07	12.997 ± 0.14	2.764 ± 0.03	1.863 ± 0.21
500 mg	12.368 ± 0.16	2.325 ± 0.03	3.188 ± 0.03	1.634 ± 0.18
1000 mg	21.523 ± 0.23	2.146 ± 0.03	3.034 ± 0.04	1.561 ± 0.21

Table 2. Number of protein bands on SDS-PAGE gels obtained from *S. azurea* (SZMC 14600) applying different extraction methods and initial weight of bacteria for extraction. Values are reported as means ± SD of three independent experiment (n = 3).

Number of protein bands					
Initial weight of bacteria	100 mg	200 mg	300 mg	500 mg	1000 mg
X-Press	27 ± 4	48 ± 6	53 ± 6	52 ± 6	52 ± 5
TCA/acetone/phenol	42 ± 6	51 ± 5	53 ± 5	12 ± 3	11 ± 3
Bead-vortexing	16 ± 4	25 ± 4	35 ± 4	37 ± 5	35 ± 5

Results

In order, to monitor the optimal cell disruption and protein extraction protocol for achieving the maximal release of total protein from *S. azurea* SZMC 14600 four methods were compared. As shown in Table 1, the protein recovery strongly depended both on one hand methods used and the initial mass of bacteria. Accordingly, of the four methods the X-Press was effective for all initial weights of bacteria, while TCA/acetone/phenol method did not provide usable results for the higher mass (500 mg, 1000 mg). The effectiveness of two other methods was significantly lower, to the extent that the freezing/throwing technique proved to be completely inadequate, therefore, the results of this protocol was no longer estimated.

The changes in protein pattern obtained from *S. azurea* SZMC 14600 by different extraction protocols were evaluated by SDS-PAGE. Figure 1 shows representative Coomassie Brilliant Blue staining gels of the whole-cell protein extractions. The SDS-PAGE analysis revealed that the extractions presented good quality proteins, with well-defined bands

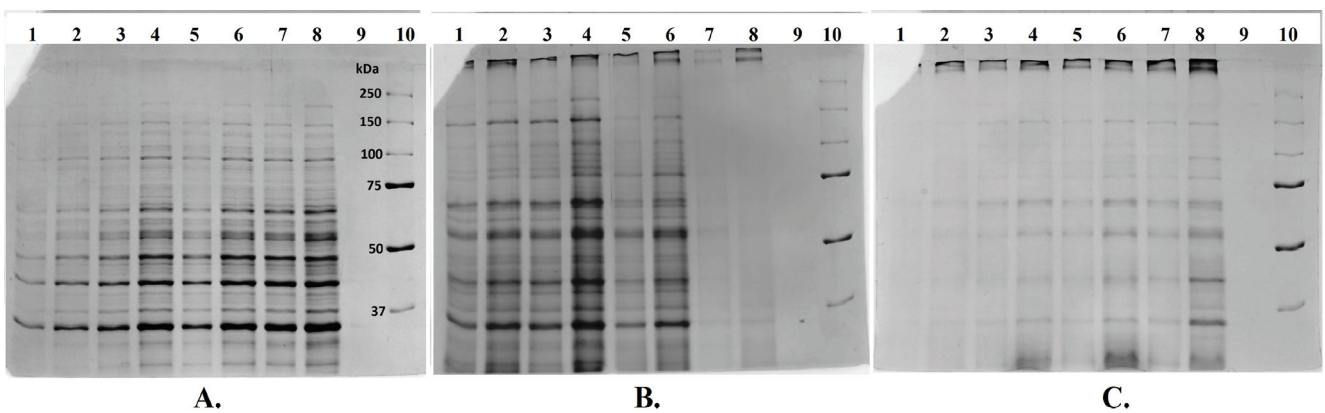

Figure 1. Whole cell protein patterns obtained by SDS-PAGE for *S. azurea* SZMC 14600 by using different homogenisation and protein extraction protocols. Lane 1 and 2: 100 mg initial mass of bacteria (5 µl and 10 µl, respectively). Lane 3 and 4: 200 mg initial mass (5 µl and 10 µl, respectively). Lane 5 and 6: 300 mg initial mass of bacteria (5 µl and 10 µl, respectively). Lane 7: 500 mg initial mass of bacteria (5 µl). Lane 8: 1000 mg initial mass of bacteria (5 µl). Lane 10: molecular weight standard (Precision Plus Protein Unstained, 5 µl; Bio-Rad). A: X-Press; B: Bead-vortexing; C: TCA/acetone/phenol.

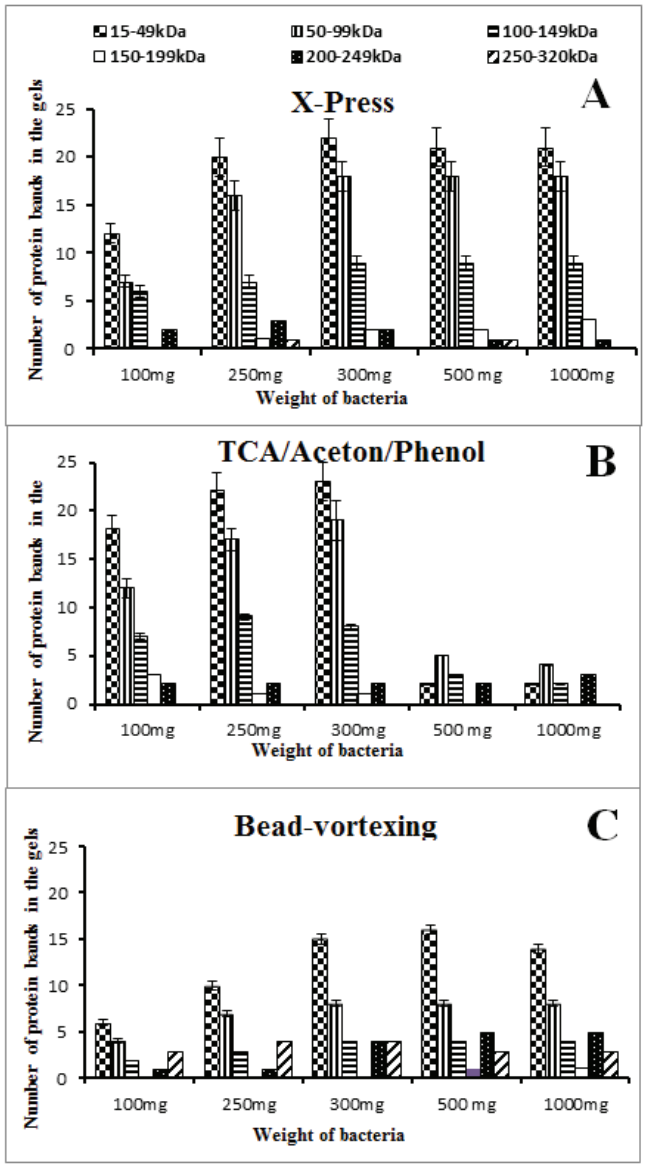

Figure 2. Distribution of separated proteins on the basis of molecular weight in different protein extraction methods applied. Values are reported as means ± SD of three independent experiments (where there was difference in the number of protein bands).

without signs of degradation. Nevertheless, the band intensity of one-dimensional gel electrophoresis, in spite of the same volume of samples provides only limited options for image analyses, it can clearly be seen that the density of bands was in accordance with the protein content of data presented in Table 1.

Beyond the quantitative differences, well-characterised variation in the number of detected bands could be observed amongst the methods (Table 2). The data of qualitative analysis of SDS-PAGE protein pattern clearly demonstrated that the X-Press method gave the bacterial mass-dependent results characterised by the presence of 27-53 protein bands, whereas the TCA/acetone/phenol extraction method allowed for the similar effectiveness for only 100-300 mg bacterial mass, while the bead-vortexing method produced maximum 37 separated protein bands.

Distribution of proteins, based on Mw was also different in the methods compared. Regarding molecular weight, six different groups were created ranging from 15 to 320 kDa (Fig. 2). Of them the proteins of 15-49 kDa proved the highest amount of whole-cell proteins (50%) followed by the 50-99 kDa set (40%) obtained by the X-Press method at all initial bacteria mass (Fig. 2A), and by the TCA/acetone/phenol method using 100-350 mg bacteria (Fig. 2B). The bead-vortexing technique provided conspicuously different molecular weight distribution with a higher rate of the high molecular weight proteins (Fig. 2C).

Moreover, to investigate the effectiveness of the selected protein extraction methods, total protein extracts was separated on the 2D gel covering pH 3-10 and molecular masses of 14 to 116 kDa ranges. Building on the 1D SDS-PAGE results samples from the 300 mg, initial weight of bacteria was compared. As shown in Figure 3, the X-Press and TCA/acetone/phenol methods were obtained a similar, high resolution 2D protein separation, revealing approximately 372 ± 36 and 331 ± 28 spots, respectively, while the bead-vortexing technique provided only 227 ± 25 spots. Most proteins were separated in the molecular mass range of 10-90 kDa. The pH range where the most of protein appeared was pH 4-7, but in this aspect minor differences were observed among the methods used.

Discussion

Appropriate cell disruption and protein extraction method is crucial for proteomic strategy, including the protein yield or outcome of gel electrophoresis. There are numerous methodical studies on optimal release of proteins from bacteria, which concluded for example that the effectiveness of freezing-thawing is strongly dependent on the density of suspensions and on the number of cycles (Benov and Al-Ibraheem 2002), or that the major factor that influenced cell disruption by vortexing is the ratio of beads and the duration of treatment (Velapatiño et al. 2013), as well as the number of passes in French press (Jaschke et al. 2009) and the list goes on. The conclusion of these and other studies suggest that every single experiment needs careful consideration for the selection and adaptation of the appropriate method optimised for the actual organism and the aim of the study (Malafaia et al. 2015). There is no single method for efficient isolation of all kinds of proteins of interest. This statement may

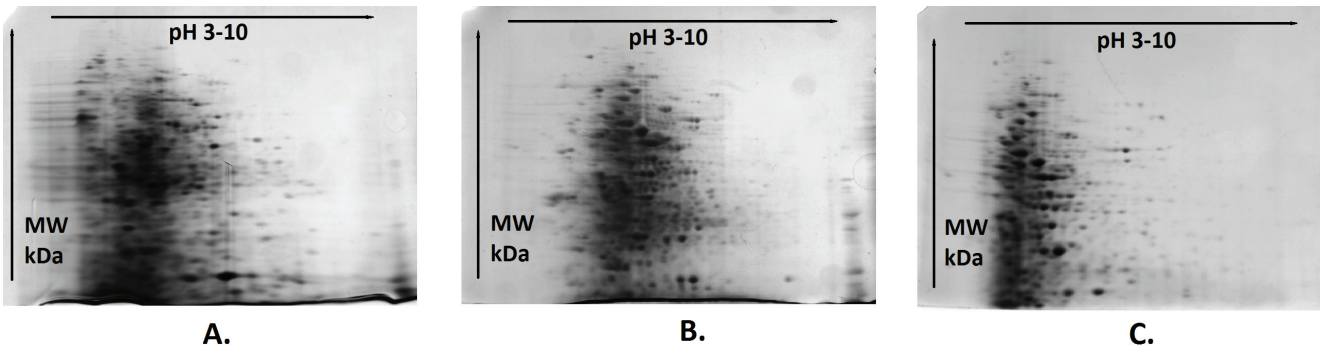

Figure 3. Representative 2D whole cell protein profile of *S. azurea* SZMC 14600 using, A: X-Press; B: TCA/acetone/phenol; C: Bead-vortexing cell disruption and extraction method.

be based on the different chemical composition of cells. In any case, during sample preparation the cell envelope as the main barrier needs to be disrupted to recover the intracellular materials. For Gram-positive bacteria, the main barrier is a thick cell wall, which is mainly composed of peptidoglycan, teichoic acid and polysaccharides. In Gram-negative bacteria, the peptidoglycan cell wall is significantly thinner than in Gram-positive bacteria, which itself is surrounded by an external layer composed of lipopolysaccharides and proteins. Another difference is the presence of the periplasmic layers, which many times thicker than is found in the Gram-positive ones. The composition of cell wall or periplasmic layer may fundamentally determine the cell disruption method (Tan et al. 2011; Cafaro et al. 2014).

In this study four commonly used protein extraction methods were compared to achieve efficient whole-cell protein extraction from *S. azurea* SZMC 14600. To answer the question, in the light of protein content and 1D SDS-PAGE gel results, it can be stated that of methods applied X-Press produced the most reliable productivity independent of the initial weight of bacteria. The bead-vortexing and freezing-throwing techniques proved to be unusable in this respect, while the efficacy of TCA/acetone/phenol method was commeasurable with X-Press, but only for 100-300 mg initial bacteria mass (Fig. 1, Table 1, 2). Furthermore, it can be concluded that the X-Press and TCA/acetone/phenol methods provided similar results with respect to the protein patterns, while the bead-vortexing offered different distribution in molecular mass (Fig. 2). Thus, the latter method is considered inadequate to produce usable images. The results of 2D protein separations showed a good coincidence with these statements. The number of protein spots and the pH region of the greatest protein expression was similar that found in other bacterial species (Wongtrakoongate et al. 2007; Yang et al. 2014). Noticeable, but slight difference among the methods on pH distribution of 2D electrophoresis separated protein spots (Fig. 3) can be attributed to the different concentration of salt or amphoteric components in the extracting solutions which could affect the IEF (isoelectric focusing), the first properties of 2D separation.

In summary, for *S. azurea* SZMC 14600, as a Gram-positive bacterium, the X-Press or TCA/acetone/phenol method proved to be suitable for whole-cell protein extraction, therefore they are recommended for use in proteomic studies. Our results provide a good starting point for further 2D electrophoresis studies combined with MALDI-TOF peptide mass mapping to get more accurate proteomic information on the molecular mechanism responsible for primycin metabolism.

Acknowledgements

The present scientific contribution is dedicated to the 650th anniversary of the foundation of the University of Pécs, Hungary

References

Alam M, Ghosh W (2014) Optimization of a phenol extraction-based preparation method amenable to downstream 2DE and Maldi-MS-based analysis of bacterial proteomes. Proteomics 14:216-221.

Benov L, Al-Ibraheem J (2002) Disrupting *Escherichia coli*: A comparison of methods. J Biochem Mol Biol 35:428-431.

Bradford M (1976) A rapid and sensitive method for the quantitation of microgram quantities of protein utilizing the principle of protein-dye binding. Anal Biochem 72:248-254.

Cafaro C, Bonomo MG, Rossano R, Larocca M, Salzano

G (2014) Efficient recovery of whole-cell proteins in *Oenococcus oeni* - a comparison of different extraction protocols for high-throughput malonic starter applications. Folia Microbiol 59:399-408.

Csepregi K, Valasek A, Pénzes Á, Tóth Zs, Kiss ÉI, Kerepesi I, Horváth B, Nagy I, Fekete Cs (2012) Draft genome sequence of an efficient antibiotic-producing industrial strain of *Saccharomonospora azurea*, SZMC 14600. J Bacteriol 194:1263.

Feiszt P, Mestyán G, Kerényi M, Dobay O, Szabó J, Dombrádi Z, Urbán E, Emődy L (2014) Re-evaluation of *in vitro* activity of primycin against prevalent multi-resistent bacteria. Int J Med Microbiol 304:1077-1085.

Islam N, Lonsdale M, Upadhyaya NM, Higgins TJ, Hirano H, Akhurst R (2004) Protein extraction from mature rice leaves for two-dimensional gel electrophoresis and its application in proteome analysis. Proteomics 4:1903-1908.

Jaschke PR, Drake I, Beatty JT (2009) Modification of French pressure cell to improve microbial cell disruption. Photosynth Res 102:95-97.

Juhász Á, Pénzes Á, Péteri AZS, Pallos PJ, Seffer D, Feiszt P, Pesti M, Fekete Cs, Vágvölgyi Cs, Gazdag Z, Papp G (2011) Process for producing primycin, primycin component(s), precursors and metabolites thereof via fermentation by the use of bacterial species *Saccharomonospora azurea.* 5 May 2011, WIPO patent application WO/2011/051741.

Islam N, Lonsdale M, Upadhyaya NM, Higgins TJ, Hirano H, Akhurst R (2004) Protein extraction from mature rice leaves for two-dimensional gel electrophoresis and its application in proteome analysis. Proteomics 4: 1903-1908.

Kajiwara H, Kaneko T, Ishizaka M, Tajima S, Kouchi H (2003) Protein profile of symbiotic bacteria *Mesorhizobium loti* MAFF303099 in mid-grown phase. Biosci Biotechnol Biochem 67:2668-2673.

Laemmli UK (1970) Cleavage of structural proteins during the assembly of the head of bacteriophage T4. Nature 227:680-685.

Malafaia CB, Guerra ML, Silva TD, Paiva PMG, Souza EB, Correia MTS, Silva MV (2015) Selection of a protein solubilization method suitable for phytopathogenic bacteria: a proteomics approach. Proteome Sci 13:5.

Sánchez I, Seseña S, Palop L (2003) Identification of lactic acid bacteria from spontaneous fermentation of 'Almagro' eggplants by SDS-PAGE whole cell protein fingerprinting. Int J Food Mirobiol 82:181-189.

Singh RS (2013) A comparative study on cell disruption methods for release of aspartase from *E. coli* K-12. Indian J Exp Biol 51:997-1003.

Tan AA, Azman SN, Abdul-Rani NR, Kua BC, Sasidharan S, Kiew LV, Otman N, Noordin R, Chen Y (2011) Optimal protein extraction methods from diverse sample types for protein profiling by using Two-Dimensional Electrophoresis (2DE). Trop Biomed 28:620-629.

Tiong HK, Hartson S, Muriana PM (2015) Comparison of five methods for direct extracton of surface proteins from *Listeria monocytogenes* for proteomic analysis by orbitrap mass spectrometry. J Microbiol Meth 110:54-60.

Yang Q, Ding, Liu X, Liu S, Sun J, Yu Z, HU S, Rang J, He H, He L, Xia L (2014) Differential proteomic profiling reveals regulatory proteins and novel links between primary metabolism and spinosad production in *Saccharopolyspora spinosa.* Microb Cell Fact 13:27.

Vályi-Nagy T, Úri J, Szilágyi I (1954) Primycin, a new antibiotic. Nature 174:1105-1106.

Velapatiño B, Zlosnik J EA, Hird TJ, Speert DP (2013) Total protein extraction and 2D gel electrophoresis methods for *Burkholderia* species. J Vis Exp 80:50730.

Wang W, Vignani R, Scali M, Cresti M (2006) A universal and rapid protocol for protein extraction from recalcitrant plant tissues for proteomic analysis. Electrophoresis 27:2782-2786.

Wilson K, Walker J (2000) Principles and Techniques of Practical Biochemistry. 5th Ed., Cambridge University Press.

Wongtrakoongate P, Mongkoldhumrongkul N, Kamchonwongpaisan SK, Tungpradabkul S (2007) Comparative proteomic profiles and potential markers between *Bulkholderia pseudomallei* and *Bulkholderia thailandensis.* Mol Cell Probes 21:81-91.

Volume 61(1):51-58, 2017
Acta Biologica Szegediensis
http://www2.sci.u-szeged.hu/ABS

ARTICLE

Screening of health beneficial microbes with potential probiotic characteristics from the traditional rice-based alcoholic beverage, *haria*

Mousumi Ray[1], Papan Kumar Hor[1], Som Nath Singh[2], Keshab Chandra Mondal[1]*

[1]Department of Microbiology, Vidyasagar University, Midnapore-721102, West Bengal, India
[2]Division of Nutrition, Defence Institute of Physiology and Allied Sciences, Delhi-110054, India

ABSTRACT Fermented foods are natural habitats of various food-grade microorganisms which not only fortify the food material with bioactive molecules, but they could directly exert health beneficial effect to the consumers. The present study aimed to screen the microbial consortium of *haria* (a traditional alcoholic rice beverage), for therapeutic potentiality. Twenty-nine fermented beverage samples were collected from different areas of Bankura District (West Bengal, India). Initially, 45 dominant bacterial isolates were purified from the collected samples. From these, 3 microorganisms were screened out based on growth and acidification kinetics: these proved to be *Bifidobacterium* sp. (MKK4), *Pediococcus lolli* (MKK21), and *Lactobacillus* sp. (MKK37) isolates. Finally, based on a cumulative probiotic score, MKK4 (*Bifidobacterium* sp.) was selected for further studies. The ubiquitous presence of this strain in the collected samples was confirmed through PCR-DGGE fingerprinting. This strain was considerably stable in simulated acid and bile solutions; it also exhibited strong auto-aggregation and cell surface hydrophobicity of 82% and 53%, respectively. Under conditions of nutrient depletion, the isolate was capable to form biofilm (66.3%). The selected bacterium showed strong antimicrobial activities against *Shigella dysenteriae* MB14, *Salmonella typhi* E 1590, *Micrococcus luteus* ATCC 9341, *Staphyloccus aureus* MB13, *Vibrio cholerae* K510, and *Escherichia coli* ATCC 25922 isolates. These results suggest that the food-borne *Bifidobacterium* sp. MKK4 can be used as potent probiotic agent.
Acta Biol Szeged 61(1):51-58 (2017)

KEY WORDS
Bifidobacterium
fermented food
haria
probiotic
rice-based beverage

Introduction

Fermented foods are the products of artisanal food culture which is prevailed even today among the native people. These foods are prepared particularly by the rural women by using simple utensils and locally available plant/animal raw materials. From the very beginning, food fermentation has applied for preservation of locally available excess raw food during harvesting (Ray et al. 2016). Nowadays, scientific exploration established that these foods are nutritive as well as exert medicinal value compared to the raw food. The complex consort of microorganisms and their metabolic interplay result the changes in flavour, aroma, texture, nutritional quality as well as the self-life of the raw foods (Mondal et al. 2016). The acceptance of these fermented foods is increasing but their scientific as well as technological upgradation till now in nascent stage to commercially exploit these advantages, particularly in developing countries. These indigenous fermented foods are now subjected to global attention to explore their hidden resources (nutrient and therapeutic components) as these are experienced by the native people from generation to generation as safe and effective to different ailments (Ghosh 2016).

The prevalent microorganisms in these foods are mainly lactic acid-producing bacteria and yeasts which either come from the environment or from a starter culture. In both cases, microbes participate in food fermentation either singly or as part of a complex microbial population. They remain biochemically active in the intestine and these are historically referred as "healthy microorganisms", and now considered as probiotic microorganisms (Ray et al. 2016). According to the World Health Organization (WHO 2002), probiotics are defined as live microorganisms that when administered in adequate amounts, confer health benefits on the host. Food-originated probiotic bacteria are becoming popular because these are generally regarded as safe (GRAS), biochemically active, secrets different bioactive molecules, do not show pathogenicity and survive from the environmental stresses

Submitted January 31, 2017; Accepted April 6, 2017
*Corresponding author. E-mail: mondalkc@gmail.com

in respect to faecal originated probiotics. Considering the multifaceted health benefits of probiotics, their global market was $27.9 billion in 2011 and it will reach $44.9 billion in 2018 (Starling 2013). Indian probiotic market is valued at $12 million in 2011, is expected to witness a CAGR (Compound Annual Growth Rate) of 11% by 2016 (Sharma et al. 2013). The stability and growth of organism in intestinal lumen are the prerequisite for any probiotic organisms and that can be assessed by many *in vitro* tests like tolerance to the harsh environment (gastric juices or bile), the ability to adhere to the intestinal surface, production of antimicrobial substances, biofilm formation, and the ability to modulate the immune response in the host.

Rice-based fermented foods and beverages are part of the cultural heritage, particularly in Asia. In general, it is believed that the fermented rice is nutritionally more enriched than the raw rice and confers more health benefits over dairy-based products (Ray et al. 2017). Ghosh and co-workers (2014) reported *haria*, an ethnic rice beverage, very popular in East-Central India, has ethnomedicinal importance in certain degenerative and infectious diseases and many gastrointestinal ailments, particularly dysentery, diarrhoea, amoebiasis, acidity, and vomiting. Earlier, a group of food-grade microbes like *Lactobacillus* spp., *Bifidobacterium* spp., *Lactococcus* spp., *Bacillus* spp., and *Saccharomyces* spp. were reported from *haria* (Ghosh et al. 2015a). One isolate from this beverage, *Lactobacillus fermentum* KKL1, has been characterised as a potent probiotic organism (Ghosh et al. 2015b). The role of other dominant microbes in this beverage, as well as their health beneficial impacts is now determining to establish this as a national ethnic drink. The exploitation and consumption of bifidobacteria from this beverage was postulated as safe by the long historical consumption of this fermented product and the growing knowledge about bifidobacterial taxonomy, physiology and health beneficial impacts (Schell et al. 2002). Considering the indigenous microbes from traditional fermented food as natural biological resource for health beneficial impacts, this study aimed to explore some potent food-grade probiotic that can be helpful for the formulation of probiotic food preparation as well as proprietary probiotic medicine.

Materials and Methods

Sample collection and microbiological exploration

Fresh fermented rice beverage (*haria*) samples (n = 29) were collected from different villages of Bankura District, West Bengal, India (23.1645°N, 87.0624°E) in sterile conical flasks with cotton plugs. They were immediately transported into the laboratory under chilled condition. Samples were serially diluted in peptone water and inoculated into sterile selective MRS agar (HiMedia, India) and incubated under slightly anaerobic conditions (78.18% N_2, 19.85% O_2, 0.85% Ar, and 5.04% CO_2) at 37 °C for at least 48 h. Microbial colonies developed into the matrix of the poured solid medium were enumerated on the basis of colony forming units per gram of wet solid substrate (cfu/gwss), and some of them selected according to their larger colony size. These colonies were purified until homogeneity by repeated sub-culturing. The isogenic microbial isolates were preserved in glycerol stock (20% v/v) at -20 °C for further analysis.

Screening and selection of potent isolate

Forty-five different dominant colonies were selected from the collected samples. In a two-step screening procedure, ten and finally three isolates were selected out from these. In the first round, 10 isolates were selected based on growth rate and colony size, and from these, 3 isolates were screened out based on their growth at different temperature and pH, acidic conditions, catalase, microscopic appearance and gram reaction. Finally, one potent isolate was selected based on different probiotic properties, like the growth at simulated salivary, gastric, intestinal fluid, bile salt tolerance capacity, synthesis of α-amylase and glucoamylase, acidification capability. The composition of all the tested fluids and procedure for tolerance study were done according to the description and methodology of Vizoso Pinto et al. (2006). The activity of α-amylase and glucoamylase were measured as per the method of Ghosh et al. (2015a).

Calculation of probiotic potential

The cumulative probiotic potential of the MKK4 isolate was calculated by using standard score card. Cumulative probiotic potential is the sum of score of growth at acidic condition and physiological temperature, production of hydrolytic enzymes, tolerance to saliva, gastric, intestinal, bile, antibacterial and antibiotic resistance profile. Probiotic potential was calculated as observed score divided by maximum score and multiplied by hundred.

$$\text{Probiotic potential} = (\text{Observed score}/\text{Maximum score}) \times 100$$

Genomic DNA isolation and PCR-DGGE fingerprinting

The probiotic isolate MKK4 was selected and identified previously (Ray et al. 2017) based on 16S rRNA sequencing and its occurrence within the collected sample diversity was checked through PCR-DGGE fingerprinting. Initially total genomic DNA was isolated from representative food

samples of four different zones (East, West, North and South zones of Bankura District, West Bengal) by using Hipura Bacterial Genomic DNA purification Kit (HiMedia, India). The extracted genomic DNA was used as a template for PCR amplification by specific GC clamp primer sets, GC clamp was added in the 5' end of the reverse sequence (Bif164-f, 5'-GGGTGGTAATGCCGGATG-3' and Bif662-GC-r, 5'-CGCCCGCCGCGCGCGGCGGGCGGGGCG-GGGGCACGGGGGGCCACCGTTACACCGGGAA-3'). The PCR mixture for 25 µl reaction volume was prepared by using 2X PCR master mix for required number of reactions. In brief, each reaction mixture containing 12.5 µl of PCR master mix, 1 µl of each primer (20 pmol), 1 µl of DNA template (50 ng/µl) and 9.5 µl of sterile Milli-Q water. Samples were amplified in a thermocycler using the following protocol: initial denaturation at 95 °C for 5 min, 10 cycles of denaturation at 94 °C for 30 sec, annealing at 66-56 °C for 30 sec, extension at 72 °C for 30 sec, another 20 cycles of denaturation at 94° C for 20 sec, annealing at 56 °C for 30 sec, final extension at 72 °C for 30 sec, final extension at 72 °C for 7 min, and store at 4 °C). The PCR product of samples was subjected to DGGE analysis following the method of Satokari et al. (2001). DGGE was performed with a DCode electrophoresis system (Bio-Rad) and gels measuring 16 cm × 16 cm × 1 mm. PCR products were loaded onto a 45 to 55% gradient of urea and formamide in a polyacrylamide gel (8%) and electrophoresed at a constant temperature of 60 °C and a constant voltage of 85 V for 16 h. A 100% denaturant corresponds to 7 M urea and 40% (v/v) formamide. Gels were stained with ethidium bromide (0.5 mg/l) in TAE buffer for 20 min, destained in sterile deionized water for 10 min and viewed by UV transillumination.

In vitro probiotic characteristics

Autoaggregation and hydrophobicity assay

The autoaggregation pattern of the isolate MKK4 was measured according to the method of Rahman et al. (2008). For that, cells of target bacterium were inoculated and incubated for 24 h, the selected young cells were mixed vigorously by vortexing for 15 s and allowed to stand at 37 °C. Changes in absorbance were monitored at 660 nm after 4 h. Autoaggregation ability was expressed as relative percentage of autoaggregation (AAg%) and calculated using

Relative percentage of autoaggregation (%) =

$$(A_0 - A/A) \times 100$$

Where, A_0 and A are the absorbance of cultured media at 0 h and after 4 h of intervals, respectively. From the relative percentage of autoaggregation (%) value, organisms are classified into three major groups, *viz*., high autoaggregation (>70%), medium autoaggregation (20-70%) and low autoaggregation (<20%) able strains.

The cell surface hydrophobicity of the isolate MKK4 was determined following the method described by Thapa et al. (2004). Briefly, overnight cell pellet was suspended in 10 ml of Ringer solution (6% NaCl, 0.0075% KCl, 0.01% $CaCl_2$, and 0.01% $NaHCO_3$) and initial absorbance was taken at 600 nm (A^i_{600}). Next, equal volume of n-hexadecane was added to the cell suspension and mixed thoroughly by vortexing for 2 min. The two immiscible phases were separated by 30 min of standby, and absorbance of the lower phase was recorded at the same wavelength (A^f_{600}). The percentage of hydrophobicity of the strain adhering to hexadecane was calculated using the equation:

Hydrophobicity (%) = $(A^i_{600} - A^f_{600}) / A^i_{600} \times 100$

Antibacterial activity

Supernatant of the *Bifidobacterium* sp. MKK4 culture was used to determine the antibacterial activity against enteric pathogens (Badji et al. 2007). The test isolates were *Shigella dysenteriae* MB14, *Salmonella typhi* E 1590, *Micrococcus luteus* ATCC 9341, *Staphyloccus aureus* MB13, *Vibrio cholerae* K510, and *Escherichia coli* ATCC 25922. The antibacterial activity was evaluated by agar well diffusion method. Samples of clear (filtered) culture supernatant (50 µl) were transferred into the wells in the agar plates previously inoculated with the test microorganisms. Ciprofloxacin (20 µg/disc) was used as positive control. The diameters of inhibition zones were measured after an incubation at 37 °C for 24 h.

Biofilm formation and confocal microscopy

To evaluate biofilm formation by the isolate MKK4, young cells were washed with phosphate buffer saline (PBS) and inoculated (1×10^7 cells/ml) in the microtiter plate wells (12 well) containing 2 ml of minimal MRS broth (1/2 strength), and incubated for 90 min at 37 °C (adherence phase). Non-adherent cells were removed by gentle washing with 4 ml PBS (pH 7.0). Next, the well was again filled by fresh minimal MRS broth and incubated anaerobically (5% CO_2) for 48 h at 37 °C. Biofilms were quantified using a slightly modified crystal violate assay procedure as described previously by Stepanović et al. (2000). After staining, the adsorbed crystal violate was eluted using 1 ml of 70% v/v ethanol. The amount of dye solubilised was measured colorimetrically at 590 nm and expressed as directly proportional to biofilm size. The fresh and washed MKK4 biofilm were stained with acridine orange for imaging by confocal microscopy (Olympus BX51, Japan).

Statistical analysis

Collected data were presented as the arithmetic mean of three

Table 1. Primary screening among different dominant isolates present in the rice-based fermented beverage, *Haria*.

Isolate ID	Gram reaction	Morphology	Catalase	Growth at different pH			Growth at different temperature			Length/ diameter (µm)	Acidification capacity (ml)
				pH 3.0	pH 5.0	pH 7.0	10 °C	25 °C	40 °C		
MKK2	+	Rod shaped	–	<0.1	1.0-2.0	1.0-2.0	<0.1	1.0-2.0	>2.0	2.83 ± 0.02/ 1.36 ± 0.03	9.81 ± 0.68
MKK4	+	Slightly irregular rods	–	1.0-2.0	>2.0	>2.0	<0.1	>2.0	>2.0	3.01 ± 0.07/ 1.33 ± 0.04	18.26 ± 0.52
MKK12	+	Slightly irregular rods	–	1.0-2.0	>2.0	>2.0	<0.1	1.0-2.0	>2.0	1.79 ± 0.03/ 0.98 ± 0.02	8.69 ± 0.70
MKK14	+	Irregular rods	–	>2.0	>2.0	>2.0	<0.1	1.0-2.0	1.0-2.0	1.66 ± 0.03/ 1.02 ± 0.01	11.43 ± 0.57
MKK19	+	Slightly irregular rods	–	0.1-1.0	1.0-2.0	1.0-2.0	<0.1	1.0-2.0	1.0-2.0	0.83 ± 0.01/ 0.69 ± 0.02	9.82 ± 0.48
MKK21	+	Coccus	–	1.0-2.0	>2.0	>2.0	0.1-1.0	>2.0	>2.0	1.21 ± 0.04/ 1.18 ± 0.03	15.25 ± 0.73
MKK26	+	Rod shaped	–	<0.1	<0.1	1.0-2.0	<0.1	1.0-2.0	1.0-2.0	2.71 ± 0.04/ 0.76 ± 0.03	10.23 ± 0.82
MKK28	+	Rod shaped	+	1.0-2.0	>2.0	>2.0	1.0-2.0	1.0-2.0	>2.0	0.97 ± 0.04/ 0.63 ± 0.00	13.27 ± 1.04
MKK33	+	Rod shaped	+	<0.1	<0.1	1.0-2.0	1.0-2.0	1.0-2.0	1.0-2.0	2.97 ± 0.05/ 0.71 ± 0.03	15.18 ± 0.29
MKK37	+	Rod shaped	–	1.0-2.0	>2.0	>2.0	<0.1	1.0-2.0	>2.0	1.47 ± 0.02/ 0.82 ± 0.02	16.03 ± 0.91

The screening included the main characteristics like growth at different pH and temperature, acidification value (ml) is the average increase of titratable acidity equivalent to production of lactic acid over the control sample (uninoculated sample), Microbial growth was measured after 48 h as the absorbance of the culture at 600 nm. The growth ability (GA) was categorized on the basis of OD value as - GA < 0.1: no growth ability; 0.1 < GA < 1.0: weak growth ability; 1.0 < GA < 2.0: moderate growth ability, and GA > 2.0: Strong growth ability.

Table 2. Secondary screening of three potent dominant isolates, *viz*., MKK4, MKK21 and MKK37 selected from primary level screening.

	Enzyme production (U/ml)		Tolerance to simulated juices*				Acidification capacity (ml)
	α-Amylase	Glucoamylase	Saliva	Gastric	Intestinal	Bile	
MKK4	23.49 ± 0.62	11.24 ± 0.93	+++++	++++	++++	+++	16.62 ± 0.94
MKK21	14.03 ± 0.58	5.91 ± 0.69	+++++	+++	++++	+++	11.79 ± 0.72
MKK37	27.16 ± 0.91	2.62 ± 0.11	+++++	+++	+++	++++	14.31 ± 0.77

*+++++ = heavy growth (OD>2.00); ++++ = moderate growth (OD 1.5-2.0); +++ = less growth (OD 1.0-1.5)

replicates (mean ± SD). Significant variation was accepted at the level of 5% (*i.e.* $p<0.05$) was measured by student *t*-test using Sigmastat 11.0 (USA) statistical software.

Results and Discussion

Sample collection

Twenty-nine *haria* samples were collected from various parts of Bankura District of West Bengal, India. The principal constituent of this traditional drink is only rice (*Oryza sativa* L., *Poaceae*), that fermented by a group of indigenous microbes originated from the plant based starter. This is healthy drink consumed by the tribal people of rural West Bengal and contains numerous food-grade microorganisms as described by Ghosh et al. (2014).

Screening for some dominant organisms

Forty-five diverse types of colonies were isolated from the 29 *haria* samples using MRS broth medium (HiMedia, India). Among them, 10 isolate (Table 1) were selected primarily according to their larger colony size (>3 mm) after 2 days of growth. Out of these 10 isolates, 3 isolates (Table 2) were selected according to the growth at wide range of temperature and pH values, catalase, and acidification test. These 3

Table 3. Calculation of cumulative probiotic effect of MKK4, MKK21, and MKK37.

Test parameters	Score limits	MKK4	MKK21	MKK37
Growth at acidic condition (pH 3.0)	Heavy growth (>2.0) = 2 Moderate growth (1.0-2.0) = 1 No/less growth (<1.0) = 0	1	1	1
Growth at temperature (25 °C)	Heavy growth (>2.0) = 2 Moderate growth (1.0-2.0) = 1 No/less growth (<1.0) = 0	2	2	1
Acidification value	≥15.0 ml = 1 <14.0 ml = 0	1	0	1
α-Amylase	≥25 U/ml = 2 24-20 U/ml = 1 ≤19 U/ml = 0	1	0	1
Glucoamylase	≥10 U/ml = 2 9-5 U/ml = 1 ≤4 U/ml = 0	2	1	0
Saliva juice tolerance	≥+++++ = 2 ++++-+++ = 1 ≤++ = 0	2	2	2
Gastric	≥+++++ = 2 ++++-+++ = 1 ≤++ = 0	1	1	1
Intestinal	≥+++++ = 2 ++++-+++ = 1 ≤++ = 0	1	1	1
Bile	≥+++++ = 2 ++++-+++ = 1 ≤++ = 0	1	1	1
Sensitivity to tetracycline	≥23 = 3 15-22 = 2 ≤14 = 1	3	3	2
Sensitivity to amoxicillin	≥23 = 3 15-22 = 2 ≤14 = 1	3	3	3
Sensitivity to methicillin	≥23 = 3 15-22 = 2 ≤14 = 1	3	3	3
Antimicrobial against *S. typhi* B3274	≥10 = 3 6-9 = 2 ≤5 = 1	3	3	3
Antimicrobial against *S. faecalis*	≥10 = 3 6-9 = 2 ≤5 = 1	3	3	3
Observed score		27	24	23
Percent of maximum possible score (= 32)		84.37	75.0	71.87

isolates were further characterised according to their tolerance to saliva, gastric and intestinal juice, tolerance to bile salt, α-amylase and glucoamylase production, as well as their acidification capability. The selected three strains were identified on the basis of 16S rDNA sequence as *Pediococcus lolli* MKK21, *Lactobacillus* sp. MKK37, and *Bifidobacterium* sp. MKK4 (Ray et al. 2017). Among them, one potent strain (MKK4) was finally selected based on these enzymatic, probiotic characteristics and acidification capability.

Cumulative Probiotic Score of strain MKK4

The probiotic potential of any bacterial strain is based upon the cumulative probiotic score. Probiotic potential of the selected isolate MKK4 was calculated in the present study and the probiotic potential for MKK4 was 81.82%. Thus, MKK4 qualify the score to be recommended as commercial probiotics (Table 3). The commercially available probiotic preparations have probiotic score in a range of 75-85% (Gautam and Sharma 2015). The present study revealed that MKK4 follows the criteria of FAO/WHO.

PCR-DGGE profiling

Isolation of specific group of organisms by using selective media can almost excluded many members of the microbial

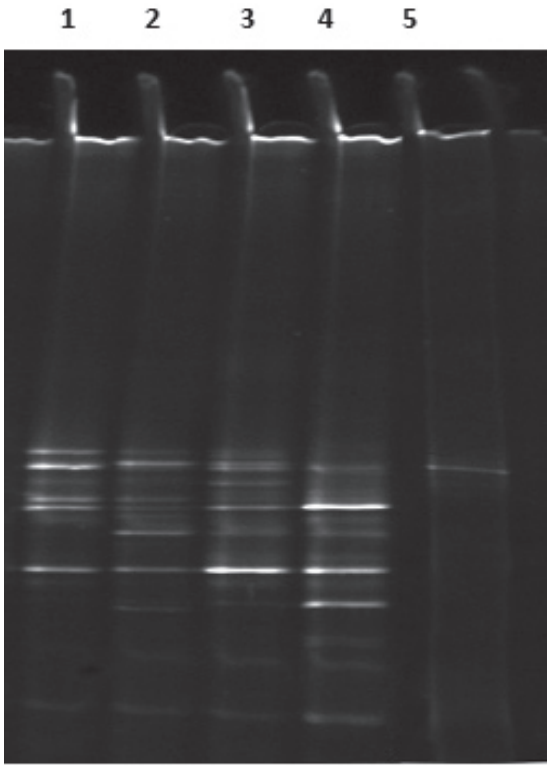

Figure 1. DGGE profiling of fermented beverages (lane 1-4) and isolated strain MKK4 (lane 5).

community (Chen et al. 2008) as, most of the microbes are till now uncultivable. PCR-DGGE based method is a preferred tool for rapid analysis of specific group of cultivable as well as uncultivable microbial community in an ecological niche. To determine the diversity of bifidobacterial strains and occurrence of our isolate in the collected samples, a PCR-DGGE profiling was made using bifidobacterial species specific primers. The DGGE profile showed the isolated organism (MKK4) ubiquitously present in all the collected samples (Fig. 1).

In vitro evaluation of probiotic characteristics

After initial selection and identification, some important properties of the selected strain *Bifidobacterium* sp. MKK4 was assessed *in vitro* for evaluation of its effective probiotic characteristics.

Hydrophobicity and autoaggregation

The relative auto-aggregation of *Bifidobacterium sp.* MKK4 was found to be 82% with the relative cell surface hydrophobicity of 53% with hexadecane. Autoaggregation and hydrophobicity of strain are the two independent but both traits are related with the adhesion of the cell to the intestinal wall (Rahman et al. 2008). These two manners could be used for the preliminary screening to identify potentially adher-

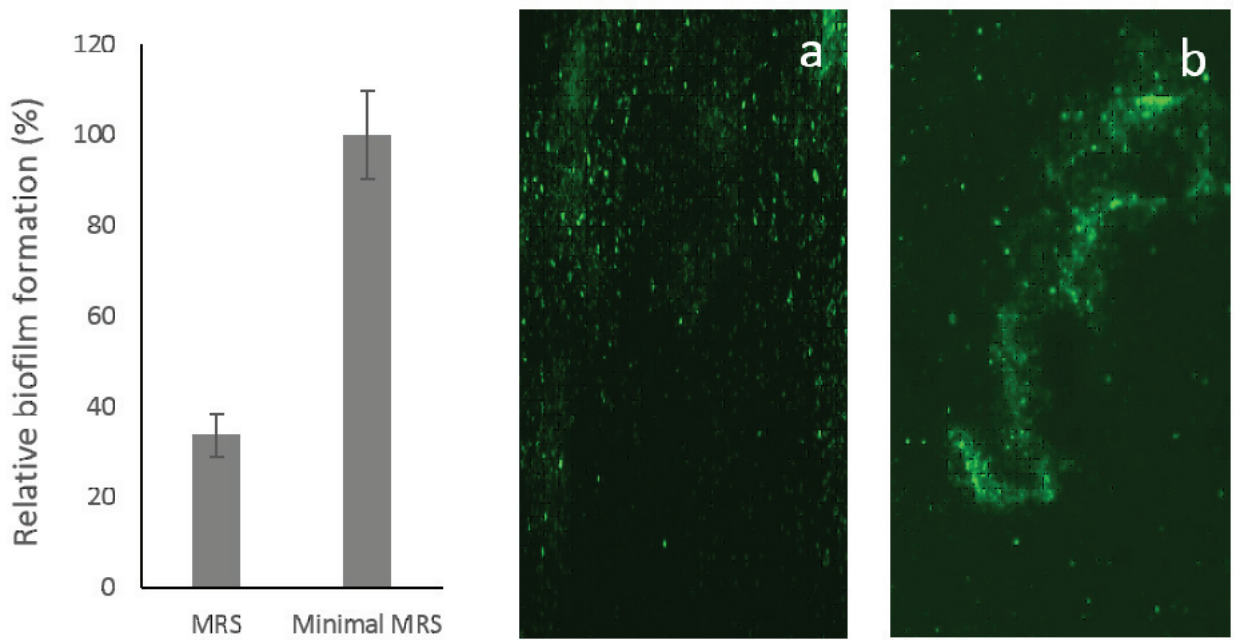

Figure 2. The biofilm formation ability of *Bifidobacterium* sp. MKK4 under minimal nutritional condition (minimal MRS broth) and the planktonic appearance (a) of the isolate compared to the sessile appearance (b) under minimal nutrition (details described in the Materials and Methods section).

Table 4. Antimicrobial activities of *Bifidobacterium* sp. MKK4 against several human pathogens (type strains and indigenous isolates).

Pathogenic bacteria	Zone of inhibition (mm)
Shigella dysenteriae MB14	3.68
Salmonella typhi E 1590	8.21
Micrococcus luteus ATCC 9341	4.51
Staphyloccus aureus MB13	3.94
Vibrio cholerae K510	4.26
Escherichia coli ATCC 25922	5.84

ent isolates (Del Re et al. 2000). Cellular aggregation is an important feature for probiotics as it is related to inter and intra-species microbial interaction as well as interaction with host epithelial cells. Probiotic bacterial autoaggregation can also prevent the pathogen colonization along the intestinal epithelial surfaces. The higher auto-aggregation of the isolate MKK4 led the organisms to form biofilm. Cell surface hydrophobicity of the organism measures the bacterial adhesion to a certain substratum not measure the intrinsic microbial cell surface hydrophobicity (Busscher and Van der Mei 1995).

Biofilm formation

The relative biofilm formation of *Bifidobacterium* sp. MKK4 was tested and found to be induced by 66.3% under nutrient depletion. Microbial biofilm formation seems to be a major mechanism for pathogen exclusion and it is possibly dependent upon the probiotic ability to reduce the environmental pH (Chapman et al. 2014). The relative biofilm formation ability of *Bifidobacterium* sp. MKK4 was comparable with the normal MRS medium and nutrient depletion medium by visualizing microscopic appearance of the cells. The planktonic cells were observed more in MRS broth, whereas, sessile growth was observed in the nutrient depleted condition with the visibly appeared exopolysaccharide (EPS) network (Fig. 2). The phenotypic expression of biofilm is an essential and functional probiotic characteristic generally adapted in unfavourable microenvironment and effective to adhere on mucosal layer.

Antibacterial activity

Lactic acid producing bacteria have inherent ability to fight against enteral pathogens by exerting a group of inhibitory metabolic substances like organic acids, free fatty acids, ammonia, diacetyl, hydrogen peroxide, and bacteriocins. The selected *Bifidobacterium* sp. MKK4 showed the strong antimicrobial activities against *Shigella dysenteriae* MB14, *Salmonella typhi* E 1590, *Micrococcus luteus* ATCC 9341, *Staphyloccus aureus* MB13, *Vibrio cholerae* K510, *Escherichia coli* ATCC 25922 (Table 4).

Conclusion

Ethnic fermented foods are wealth resources of health beneficial microbes and their metabolites. As these foods are consumed from ancient times and generation to generation, their microbial consortia can be generally considered as safe. Present days the probiotic concept derived considering this safety issues and health benefits of the food-grade microorganisms. This study demonstrated that microorganisms isolated from *haria* have variable probiotic activities and among them *Bifidobacterium* sp. MKK4 have been identified as a potential probiotic organism. This study for the first time highlighted the occurrence of probiotic *Bifidobacterium* and *Lactobacillus* in this type of rice-based alcoholic beverage and there is enough scope to exploit their bio-therapeutic potential in the future.

Acknowledgments

Authors are thankful to the SEED Division, Department of Science and Technology, New Delhi, India [Reference Number SEED/TSP/CODER/005/2012 (G), dt-07/07/2015] for fellowships and funding. However, funder had no role in experimental designing or in manuscript preparation.

References

Badji B, Mostefaoui A, Sabaou N, Lebrihi A, Mathieu F, Seguin E, Tillequin F (2007) Isolation and partial characterization of antimicrobial compounds from a new strain *Nonomuraea* sp. NM94. J Ind Microbiol Biotechnol 34:403-412.

Busscher HJ, van der Mei HC (1995) Use of flow chamber devices and image analysis methods to study microbial adhesion. Method Enzymol 253:55-477.

Chapman CM, Gibson GR, Roeland I (2014) Effects of single- and multi-strain probiotics on biofilm formation and in vitro adhesion to bladder cells by urinary tract pathogens. Anaerobe 27:71-76.

Chen H-C, Wang S-Y, Chen M-J (2008) Microbiological study of lactic acid bacteria in kefir grains by culture-dependent and culture-independent methods. Food Microbiol 25:492-501.

Del Re B, Sgorbati B, Miglioli M, Palenzona D (2000) Adhesion, autoaggregation and hydrophobicity of 13 strains of *Bifidobacterium longum*. Lett Appl Microbiol 31:438-442.

Gautam N, Sharma N (2015) Evaluation of probiotic potential

of new bacterial strain, *Lactobacillus spicheri* G2 isolated from Gundruk. Proc Natl Acad Sci India, Sect B Biol Sci 85:979-986.

Ghosh K (2016) Profiling of nutrients and lactic acid bacteria in a rice-based fermented beverage. Ph.D. Thesis, Vidyasagar University, Midnapore, India.

Ghosh K, Maity C, Adak A, Halder SK, Jana A, Das A, Parua S, Das Mohapatra PK, Pati BR, Mondal KC (2014) Ethnic preparation of Haria, a rice-based fermented beverage, in the province of lateritic West Bengal, India. Ethnobot Res App 12:39-49.

Ghosh K, Ray M, Adak A, Dey P, Halder SK, Das A, Jana A, Parua (Mondal) S, Das Mohapatra PK, Pati BR, Mondal KC (2015a) Microbial, saccharifying and antioxidant properties of an Indian rice based fermented beverage. Food Chem 168:196-202.

Ghosh K, Ray M, Adak A, Halder SK, Das A, Jana A, Parua (Mondal) S, Vágvölgyi C, Das Mohapatra PK, Pati BR, Mondal KC (2015b) Role of probiotic *Lactobacillus fermentum* KKL1 in the preparation of a rice based fermented beverage. Biores Technol 188:161-168.

Mondal KC, Ghosh K, Mitra B, Parua S, Das Mohapatra PK (2016) Rice-based Fermented Foods and Beverages: Functional and Nutraceutical properties. In Ray RC, Montet D, Eds., Fermented Foods, Part II: Technological Intervention. CRC Press, New York, pp. 150-176.

Rahman MM, Kim WS, Kumura H, Shimazaki K.-i (2008) Autoaggregation and surface hydrophobicity of bifidobacteria. World J Microbiol Biotechnol 24:1593-1598.

Ray RC, Montet D (eds) Fermented Foods. Part II: Technological Intervention. CRC Press, New York, pp. 150-176.

Ray M, Ghosh K, Har PK, Singh SN, Mondal KC (2017) Fortification of rice gruel into functional beverage and establishment as a carrier of newly isolated *Bifidobacterium* sp. MKK4. Res J Microbiol 12:102-117.

Ray M, Ghosh K, Singh SN, Mondal KC (2016) Folk to functional: An explorative overview of rice-based fermented foods and beverages in India. J Ethn Food 3:5-18.

Satokari RM, Vaughan EE, Akkermans AD, Saarela M, de Vos WW (2001) Bifidobacterial diversity in human feces detected by genus-specific PCR and denaturing gradient gel electrophoresis. Appl Environ Microbiol 67:504-513.

Schell MA, Karmirantzou M, Snel B, Vilanova D, Berger B, Pessi G, Zwahlen MC, Desiere F, Bork P, Delley M, Pridmore RD, Arigoni F (2002) The genome sequence of *Bifidobacterium longum* reflects its adaptation to the human gastrointestinal tract. Proc Natl Acad Sci USA 99(22):14422-14427.

Sharma S, Arora M, Baldi A (2013) Probiotics in India: current status and future prospects. PharmAspire 1:1-11.

Starling S (2013) Global probiotics market to grow 6.8% annually until 2018. http://www.nutraingredients.com/Markets-and-Trends.

Stepanović S, Vuković D, Dakić I, Savić B, Švabić-Vlahović M (2000) A modified microtiter-plate test for quantification of staphylococcal biofilm formation. J Microbiol Methods 40:175-179.

Thapa N, Pal J, Tamang JP (2004) Microbial diversity in Ngari, Hentak and Tungtap, fermented fish products of North-East India. World J Microbiol Biotechnol 20:599-607.

Vizoso Pinto MG, Franz CMAP, Schillinger U, Holzapfel WH (2006) *Lactobacillus* spp. with in vitro probiotic properties from human faeces and traditional fermented products. Int J Food Microbiol 109:205-214.

Volume 61(1):59-68, 2017
Acta Biologica Szegediensis
http://www2.sci.u-szeged.hu/ABS

ARTICLE

Efficiency of partial 16S rRNA gene sequencing as molecular marker for phylogenetic study of cyanobacteria, with emphasis on some complex taxa

Zeinab Shariatmadari[1]*, Farideh Moharrek[2], Hossein Riahi[1], Fatemeh Heidari[1], Elaheh Aslani[1]

[1]Faculty of Life Sciences and Biotechnology, Shahid Beheshti University, G.C. Tehran, Iran
[2]Department of Plant Biology, Faculty of Biological Sciences, Tarbiat Modares University, Tehran, Iran

ABSTRACT At present, the analysis of 16S rRNA gene sequences is the most commonly used molecular marker for phylogenetic studies of cyanobacteria. However, in many studies partial sequences is used. To evaluate the performance of this molecular marker, phylogenetic relationship of several taxa from this phylum, especially some intermixed taxa, was studied. We analyzed a data set consisting of three categories of cyanobacterial strains, traditionally classified in three orders, by morphological and phylogenetic analyses. The phylogenetic analyses were performed with an emphasis on partial 16S rRNA gene sequences (600 bp) and the phylogenetic relationships were assessed using Maximum Parsimony, Maximum Likelihood and Bayesian Inference. In morphometric study, numerical taxonomy was performed on several morphospecies, and cluster analysis was performed using SPSS software. Based on the findings of this study, unlike the morphological analysis which was useful in several taxonomic ranks, this molecular marker is recommended for use only in high taxonomic levels such as order and family, because, contrary to our expectations, using partial 16S rRNA gene sequencing in the lower taxonomic levels, even in the genus level, was not necessarily successful. Inefficiency of this molecular marker in taxonomy of some genera, especially intermixed taxa, was another finding of the present study, which represents the genetic similarity of these taxa. **Acta Biol Szeged 61(1):59-68 (2017)**

KEY WORDS

cyanobacteria
intermixed taxa
molecular phylogeny
taxonomy
16S rRNA gene

Introduction

Most widespread reports about the use of 16S rRNA gene sequencing in taxonomy of cyanobacteria (cyanoprokaryotes) indicate the importance of this molecular marker as a new mean to classifying this group. Although numerous studies have shown the efficiency of the sequence analysis of genes encoding small-subunit ribosomal RNA (16S rRNA) in taxonomy of cyanobacteria (Nübel et al. 1997; Komàrek 2005), not much attention has been paid to the performance of partial 16S rRNA gene sequencing for phylogenetic studies. Furthermore, not much attention has been paid to the performance of this marker in separating complex taxa. Complex cyanobacteria are defined as microorganisms that are not well-defined yet, and further investigations and research for new characters are needed which would clearly define these taxa (Palinska et al. 2011).

Submitted November 13, 2016; Accepted ?March 26, 2017
*Corresponding author. E-mail:z_shariat@sbu.ac.ir

Several reasons can be cited for this complexity. Morphological flexibility of these microorganisms is certainly one of these reasons. Many studies indicate the instability of morphological, biochemical and physiological characteristics of cyanobacteria in several habitats (Moisander et al. 2002; Bittencourt-Oliveira et al. 2012; Soares et al. 2013; Iranshahi et al. 2014). These diverse environmental responses create complexity in this group of prokaryotic microorganisms. The shape of colony, the presence or absence of gelatinous envelope, the width of envelope, and even traits such as the shape and size of cells are characters which are quite influenced by the environmental factors (Yamamoto and Nakahara 2009). However, many of these characters are the bases for classification and separation of several taxa. For example, the genus *Anabaena* is one of the nostocacean cyanobacteria with a special taxonomical history. This genus, which belongs to a group with diverse characteristics, can show phenotypic diversity in several habitats. The genera *Wollea* and *Trichormus* are other taxa placed in Nostocaceae family and are very similar to *Anabaena* species. It should be noted that some taxa of the latter genera were recently separated from Genus *Anabaena*. Therefore, despite all the differences,

similarities between the mentioned genera are striking. It is expected that using molecular markers such as 16S rRNA gene sequencing can be useful in the classification of these similar genera. However, can this molecular marker define the precise boundary of these taxa?

In response to this question it should be noted that, although numerous studies have introduced the efficiency of the 16S rRNA in all taxonomic levels above species, not much attention has been paid to the efficiency of this molecular marker in separating taxa with high complexity. The aim of this study was to investigate the efficiency of 16S rRNA gene sequences (partial 16S rRNA gene sequences) on separation and classification of cyanobacteria as well as its accuracy in several taxonomic ranks. In addition, in the present study this molecular marker was used for separating taxa with high complexity such as *Anabaena* and other intermixed taxa.

Materials and Methods

Isolation and purification of cyanobacterial strains

For isolating cyanobacterial strains, soil and water samples were collected from several terrestrial and aquatic ecosystems of Iran (Table 1). The samples were collected over three consecutive years (from 2008 until 2010) and in accordance with the methodologies of Rangaswamy (1966) as well as Hötzel and Croome (1999).

The isolation and purification of cyanobacterial strains were performed according to Stanier et al. (1971). Purified cultures of taxa were grown in BG11 medium (with and without nitrate). Incubation of cultures was performed in a culture chamber at 25 ± 2 °C for two weeks under artificial light illumination (74 µmol photons m^{-2} s^{-1}) with a 12/12 h light-dark cycle.

Morphological observation and morphometric studies

It is necessary to mention that morphometric study was performed only based on taxa isolated from several ecosystems of Iran (aquatic and terrestrial). Morphological observations were made on liquid as well as solid media. For taxonomic determinations, semi-permanent slides of colonies were prepared and the morphometric study was performed by light microscopy (Model BH-2, Olympus) according to previous studies (Desikachary 1959; Prescott 1970; Wehr et al. 2002; John et al. 2002; Komárek 2005; Komárek and Zapomělová 2008).

Characters were selected based on those reported by Nayak and Prasanna (2007) and our own field observations. The main morphological characteristics which separate several genera are listed in Table 2. Morphometric studies were done with emphasis on the population of several taxa from three orders of cyanobacteria. Ten filaments from each population were used for this purpose. In total, 19 quantitative and qualitative morphological characters were studied (Table 2).

Statistical analysis

In order to determine the taxa interrelationships, cluster analysis and principal component analysis (PCA) were performed. For multivariate analyses the mean of quantitative characters were used, while qualitative characters were coded as binary/multistate characters. Standardized variables (mean = 0, variance = 1) were used for multivariate statistical analyses. The Euclidean distance was used as dissimilarity coefficient in cluster analysis of morphological data (Podani 2000). In this study, SPSS software was used for statistical analysis.

DNA isolation, PCR amplification and sequencing

Genomic DNA was extracted from the fresh mass of 29 strains of cyanobacteria by Genomic DNA Extraction Kit (AccuPrep®, Bioneer). PCR amplification was performed as described in the literature (Ezhilarasi and Anand 2009). The 16S rRNA gene was amplified using primers A2 (AGAGTTTGATCCTGGCTCAG) and S8 (TCTACGCATTTCACCGCTAC). The PCR mixture contained 10 µl Taq commercial buffer, 10 µl purified DNA, 150 µM of each dNTP, 500 ng of each primer and 2.5 U Taq polymerase. The PCR reactions were carried out with a denaturation step of 4 min at 95 °C, followed by 35 cycles of 1 min denaturation at 95 °C, 1 min annealing at 59 °C, and 2 min extension at 72 °C, followed by a final extension step of 8 min at 72 °C. The PCR products were migrated on 1% (w/v) agarose gel and were visualized by ethidium bromide. Selected PCR products of 16S rRNA were sequenced by Avicenna Research Institute (Tehran, Iran).

Sequence alignment

Sequences were edited using BioEdit ver. 7.0.9.0 (Hall 1999) and aligned with MUSCLE under default parameters (Edgar 2004), followed by manual adjustment. Positions of indels were treated as missing data for all datasets. Pairwise genetic distances between sequences were calculated using the maximum composite likelihood model with pairwise deletions and gamma-distributed among-site rate variation, as implemented in MEGA version 1.5 (Tamura et al. 2011).

Table 1. Voucher information and GenBank accession number for 56 species and related taxa.

Taxon designation	Strain code	Origin	GenBank Accession Number
Wolleava ginicola	ISB26	Iran, Lorestan, Visan / paddy field soil	KM017086
Wollea vaginicola	ISB22	Iran, Lorestan, Visan / paddy field soil	KM017090
Wollea vaginicola	ISB24	Iran, Fars, Kamfiroz / paddy field soil	KM017088
Wollea vaginicola	ISB21	Iran, Esfahan, Jojil / paddy field soil	KM017091
Wollea saccata	-	Russia, Yenissei River / river basin	GU434226
Wollea ambigua	ISB17	Iran, Esfahan, Jojil / paddy field soil	KM035410
Anabaena iyengarii	-	India / paddy field soil	GQ466548
Anabaena torulosa	ISB20	Iran, KhorasanRazavi / paddy field soil	KM017092
Anabaena torulosa	ISB19	Iran, Mazandaran, Savadkoh / paddy field soil	KM017093
Anabaena sphaerica	ISB23	Iran, Esfahan, Falavarjan / paddy field soil	KM017089
Anabaena sphaerica	-	India / -	EF375612
Anabaena sphaerica f. *conoidea*	-	Italy, Umbria / -	FM177480
Anabaena sphaerica	-	- / -	DQ439647
Anabaena cylindrica	-	India / -	EF375611
Anabaena verrucosa	-	India / -	EF375614
Anabaena oscillarioides	-	India / paddy field soil	GQ466544
Trichormus variabilis	ISB27	Iran, Gilan, Rahimabad / paddy field soil	KM017085
Anabaena variabilis	-	- / -	EF488831
Anabaena aphanizomenoides	-	- / -	FJ830569
Wollea ambigua	-	India / paddy field soil	KP792338
Anabaena sp.	ISB54	Iran, Khorasan Razavi / paddy field soil	KT254261
Anabaena sp.	ISB 55	Iran, Khorasan Razavi / paddy field soil	KT254262
Trichormus variabilis	-	- / -	DQ234832
Trichormus variabilis	-	- / -	DQ234833
Trichormus variabilis	-	- / -	DQ234829
Trichormus azollae	-	- / -	AJ630454
Nostoc spongiaeforme	ISB50	Iran, Fars, Firozabad / paddy field soil	KT254257
Nostoc sp.	ISB49	Iran, Fars, Ebrahimabad / paddy field soil	KT254256
Nostoc muscorum	-	Brazil / -	AY218828
Cylindrospermum minutissimum	ISB48	Iran, Esfahan, Zarrinshahr / paddy field soil	KT254255
Cylindrospermum muscicola	ISB46	Iran, KhorasanRazavi / paddy field soil	KT254251
Cylindrospermum michailovscoense	ISB47	Iran, Mazandaran, Tazehabad / paddy field soil	KT254253
Cylindrospermum sp.	ISB57	Iran, Fars, Esmaeelabad / paddy field soil	KT254254
Cylindrospermum sp.	ISB53	Iran, KhorasanRazavi / paddy field soil	KT254260
Cylindrospermum sp.	ISB56	Iran, KhorasanRazavi / paddy field soil	KT254266
Cylindrospermum alatosporum	-	France / Soil	GQ287650
Cylindrospermum stagnale	-	- / -	AF132789
Cylindrospermum catenatum	-	Slovakia / -	KF052615
Calothrix sp.	ISB52	Iran, KhorasanRazavi / paddy field soil	KT254259
Calothrix elenkinii	-	India / -	GU292083
Calothrix sp.	-	- / -	HF678491.1
Tolypothrix sp.	-	Spain / running water	HM751850.1
Tolypothrix sp.	-	Spain / running water	AM230668.1
Oscillatoria minima	ISB29	Iran, Ramsar / hot spring water	KJ534024
Oscillatoria subbrevis	ISB30	Iran, Khamir / hot spring water	KJ534025
Oscillatoria subbrevis	ISB37	Iran, Geno / hot spring water	KJ546666
Oscillatoria angusta	ISB40	Iran, Chah Ahmad / hot spring water	KJ543481
Oscillatoria angusta	ISB38	Iran, Ramsar / hot spring water	KJ546665
Oscillatoria angusta	ISB35	Iran, Khamir / hot spring water	KJ546668
Oscillatoria sp.	-	- / -	EF150796.1
Synechocystis aquatilis	ISB33	Iran, Chah Ahmad / hot spring water	KJ546670
Synechocystis aquatilis	ISB32	Iran, Geno / hot spring water	KJ546671
Synechocystis sp.	-	- / -	HQ900668.1
Synechocystis sp.	-	- / -	AB039001.1
Synechococcus elongates	ISB34	Iran, Khamir / Hot spring water	KJ546669
Synechococcus elongatus	-	Iran, Ramsar / Hot spring water	JQ771323.1
Synechococcus sp.	-	- / -	AF448077
Bacillus subtilis	-	- / -	HQ232422
Bacillus amyloliquefaciens	-	- / -	HM016080

ISB: Shahid Beheshti University Algal Collection, Tehran, Iran

Table 2. Morphological characters and their character states in studied taxa.

Characters	Character state
Vegetative cell shape	0) Discoid; 1) Sub-quadrate; 2) Barrel shape; 3) Oblong; 4) Cylindrical
Apical cell shape	0) Rounded; 1) Conical with rounded apex
Heterocyst	0) Present; 1) Absent
Heterocyst shape	0) Sub-spherical; 1) Spherical; 2) Oblong with rounded apex; 3) Cylindrical; 4) Barrel shape
Heterocyst position	0) Only intercalary; 1) Only terminal; 2) Terminal & Intercalary
Akinet	0) Present; 1) Absent
Akinet position	0) At heterocyst; 1) Distant from heterocyst
Akinet shape	0) Oblong; 1) Long cylindrical with rounded ends; 2) Ellipsoidal; 3) Widely oval; 4) Sub-spherical
Akinet number	0) Single or two; 1) Several
Gelatinous sheath	0) Present; 1) Absent
Number of trichome in sheath	0) Single; 1) Several
Trichome colour	0) Blue-green; 1) Dark blue-green; 2) Yellowish brown
Colonial form	0) Mucilaginous; 1) Not mucilaginous
Colonial mass shape	0) Spreading; 1) Scattering; 2) Globose
Filaments structure	0) Entangled; 1) Not entangled
Thallus form	0) Filamentous; 1) Colony
Symmetry of filament	0) Symmetric; 1) Asymmetric
Trichome structure	0) Apoheterocytic; 1) Paraheterocytic
Division form	0) Binary division; 1) Hormogonium; 2) Akinet

Phylogenetic analyses

Fifty-seven taxa of cyanobacteria were used in phylogenetic analyses. It is necessary to mention that some sequences were obtained from GenBank (Table 1). Phylogenetic relationships were assessed using Maximum Parsimony (MP), Maximum Likelihood (ML) and Bayesian Inference (BI). MP was conducted using PAUP* version 4.0b 10 (Swofford 2002). The heuristic search option was employed for the dataset, using tree bisection-reconnection (TBR) branch swapping, with 100 replications of random addition sequence and an automatic increase in the maximum number of trees. Branch supports were assessed by 1000 bootstrap replicates (yielding bootstrap percentages, BP; Felsenstein 1985) with the same settings as for the heuristic searches.

The substitution model was obtained using the program MrModeltest version 2.3 (Nylander 2004) based on the Akaike information criterion (AIC) (Posada and Buckley 2004). GTR + G + I (six substitution types with rate variation across sites were modelled using a gamma distribution, with a proportion of invariant sites) was identified as the best model for the dataset.

ML analysis was performed for the dataset in raxmlGUI ver. 1.3. (Silvestro and Michalak 2012). The model of evolution employed for the dataset was the same as that of BI. Bootstrap values for maximum likelihood (ML BS) was calculated in raxmlGUI based on 1000 replicates in a single run.

The program MrBayes version 3.2 (Ronquist and Huelsenbeck 2003) was used for the Bayesian reconstruction. Two simultaneous analyses with eight Metropolis-coupled Markov chain Monte Carlo (MCMCMC) chains with incremental heating of 0.2 were run for 10 million generations and sampled every 100 generations. TRACER v.1.5 was used to evaluate mixing of chains and to determine burn-in. The first 25% of trees were discarded as the burn-in. The remaining trees were then used to build a 50% majority rule consensus tree, accompanied with posterior probability (PP) values. Tree visualisation was carried out using TreeView version 1.6.6 (Page 2001).

Results

Morphological study

In morphometric study, the morphological diversity of cyanobacteria was investigated among several species and genera from several families. A list of cyanobacteria, identified and used in this study, is given in Table 1. Six morphotypes corresponding to the genera *Anabaena*, *Trichormus*, *Wollea*, *Nostoc*, *Cylindrospermum* and *Calothrix* from Nostocales, as well as several taxa from Oscillatoriales (filamentous cyanobacteria without heterocytes and akinetes) and Synechococcales (coccoid and colonial cyanobacteria with binary fission of cells) were presented among the studied strains. The most important characteristics of studied genera is summarized in Table 2. This study was conducted with an emphasis on similar genera from nostocacean cyanobacteria such as *Anabaena*, *Trichormus* and *Wollea.*

In the cluster analysis based on all morphological char-

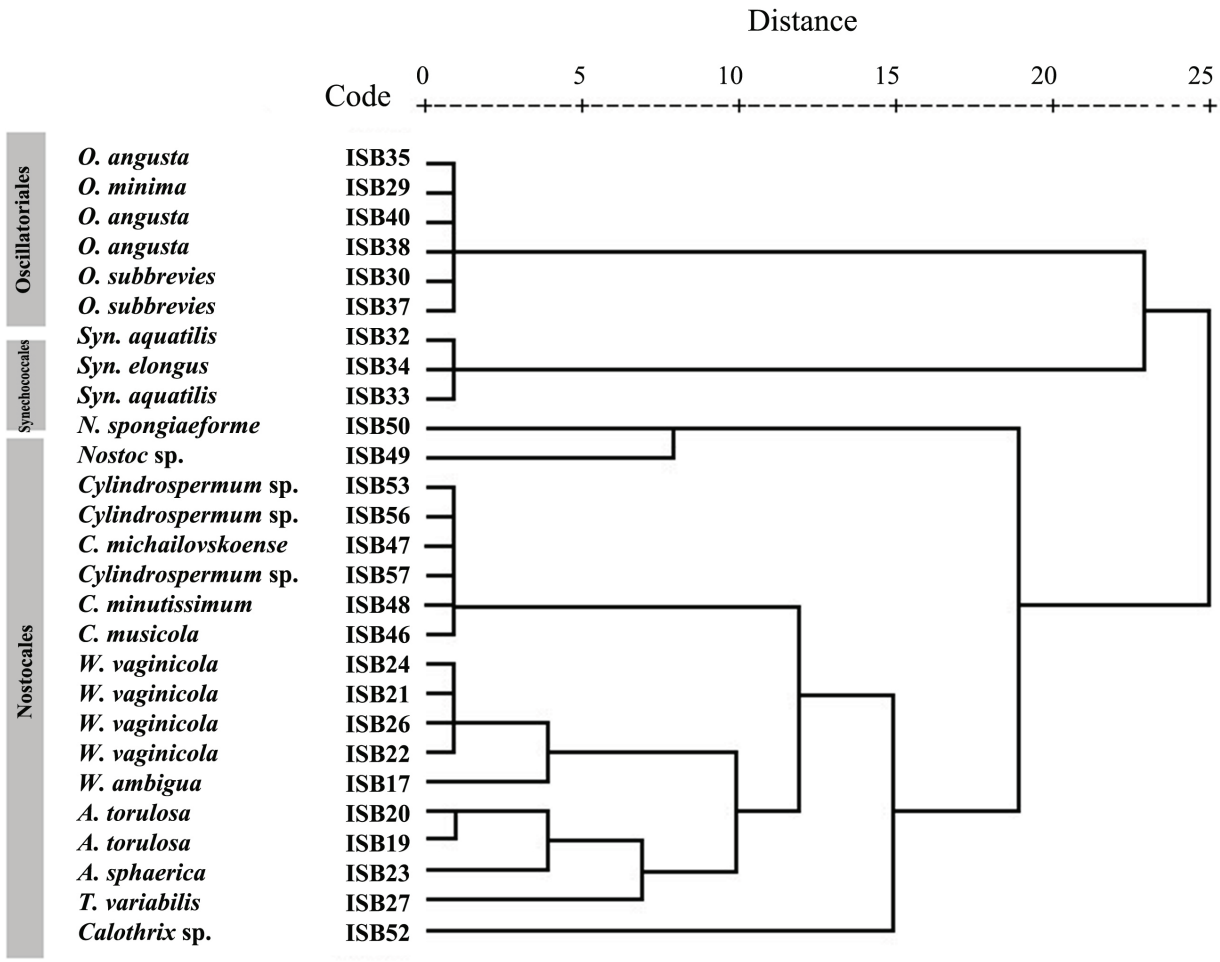

Figure 1. Hierarchical cluster analysis dendrogram of cyanobacterial taxa based on morphological characters using UPGMA method.

acters, two major clusters were found. The first major cluster separated nostocacean taxa from Oscillatoriales and Synechococcales. In other words, primary clustering clearly separated heterocystous taxa from the others (Fig. 1). Two sub-clusters or two groups can be seen in the cluster which belongs to Nostocales. In the first group, apoheterocytic cyanobacteria except *Trichormus ellipsosporus*, and in the second one paraheterocytic taxa are presented. Among taxa presented in this cluster, *Anabaena* species such as *A. variabilis* var. *ellipsospora* and *A. ambigua* are currently considered as synonyms of *Trichormus ellipsosporus* and *Wollea ambigua*. The results of morphometric analysis indicate a high morphological similarity between *Anabaena* species and these taxa (Fig. 1). Therefore, these genera were placed in the same sub-cluster with *Anabaena* species.

In order to determine the most variable morphological characters which separated studied taxa, PCA analysis was performed. The analysis revealed that the first four factors comprise about 95% of total variance. In the first factor with about 48% of total variance, characters such as apoheterocytic or paraheterocytic form of filaments, heterocyst and akinet shape, akinet number in filament, position of akinet with regard to heterocyst and the form of thallus possessed the highest positive correlation. In the second factor with about 22% of total variance, characters like vegetative cells shape, filament structure (entangled or not) and symmetry of filament possessed the highest positive correlation. Therefore, these are the most variable morphological characters among the studied taxa, especially nostocacean cyanobacteria.

Phylogenetic study

Sequence analyses

Sequences characteristics, tree statistics and model choice of data set are summarized in Table 3.

Phylogenetic analyses

Maximum Parsimony, Likelihood analyses, and Bayesian inference gave very similar results. However, support and resolution were improved using the latter approach. Hence, we here show the BI tree along with PP, ML BS and BP (Fig. 2). In all gained trees, Nostocales and Synechococcales were each recovered as monophyletic (PP = 0.88, ML BS = 78, BP = 77 and PP = 0.90, ML BS = 82, BP = 89, respectively), and sister relationship among them was supported (PP = 0.84, ML BS = 80, BP = 86). Species of *Oscillatoria* were recovered as the paraphyletic taxa in the base of the trees.

The inferred phylogenies indicated that the resolution within the Nostocales clade was rather poor, but some small groups with low to high supports were found across this clade. This lack of resolution is a reflection of the low sequence divergence values across the Nostocales clade, less than 0.1 (0.02-0.059) substitutions per site for pairs of taxa. Many species, represented by multiple accessions, were poorly resolved. The genus *Anabaena* was found to be paraphyletic by the nested inclusion of *Wollea* and *Trichormus*. *Anabaena oscillarioides* and *A. iyengarii* made a separate subclade which is close to the *Cylindrospermum* species.

Most specimens of the genus *Cylindrospermum* were grouped in a separate subclade which also included *Trichormus azollae*. But, two taxa, *C. michailovskoense* and *C. catenatum,* were separated from others. Species of the genus *Nostoc* were found to be monophyletic with a high nodal support (PP = 0.98, ML BS = 90, BP = 92). *Tolypothrix* and *Calothrix* grouped together with a low nodal support (PP = 0.78, ML BS = 72, BP = 73), but adjusent to other para-heterocytic taxa.

Discussion

The purpose of the study was to investigate the efficiency of partial 16S rRNA gene sequencing, as a common molecular marker, in several taxonomic ranks. In phylogenetic study, a data set, consisting of cyanobacterial strains from three orders, Nostocales, Oscillatoriales and Synechococcales, were analyzed. In all analyses (BI, ML and MP), Nostocales taxa formed a monophyletic group. According to Komàrek et al. (2014), Nostocales represents a large and monophyletic cluster of filamentous cyanobacteria with special cells such as heterocysts and akinetes. Other studies also emphasize on monophyly of this order (Wanigatunge et al. 2014; Valério et al. 2009; Ishida et al. 2001). This order contains several families with a range of diversity from isopolar to heteropolar structures. From the isopolar families, *Nostocaceae* family and from heteropolar of them *Rivulariaceae* and *Tolypothrichaceae* can be noted.

Table 3. DNA sequence characteristics and phylogenetic statistics of data partition.

Number of sequences	59
Number of characters	600
GC contents (%)	53.1
Number of variable characters	257
Number of PI characters	212
ASD, all sequences (%)	0.118
ASD, between *Anabaena* spp. and *Wollea* spp. (%)	0.059
ASD, between *Anabaena* spp. and *Cylindrospermum* spp. (%)	0.065
ASD, between *Anabaena* spp. and *Trichormus* spp. (%)	0.061
ASD, between *Anabaena* spp. and *Tolypothrix* spp. (%)	0.062
ASD, between *Anabaena* spp. and *Calothrix* spp. (%)	0.062
ASD, between *Anabaena* spp. and *Nostoc* spp. (%)	0.063
ASD, between *Tolypothrix* spp. and *Calothrix* spp. (%)	0.028
ASD, between the Nostocales species	0.064
ASD, between *Synechocystis* spp. and *Synechococcus* spp. (%)	0.061
Number of MPTs	806
Length of MPTs	382
C.I. of MPT	0.474
R.I. of MPT	0.784
Evolutionary model selected (under AIC)	GTR+I+G

*ASD: Average sequence divergence

The Nostocaceae is an important family which consists of unbranched heterocystous cyanobacteria with isopolar or heteropolar filaments (Komàrek et al. 2014). In our study, most of the genera from this family were separated relatively by partial 16S rRNA gene sequencing, but it seemed ineffective in some cases. For example, taxa such as *Wollea vaginicola* (= *Anabaena vaginicola*) showed a close relationship with *Anabaena torulosa*; also, *Anabaena sphaerica* and *Wollea saccata* were placed in one group. *Trichormus variabilis* (= *Anabaena varibilis*) is another taxon of this family which was placed adjacent to *Anabaena* species such as *A. verrucosa* and *A. cylindrica* (PP = 0.97, ML BS = 90, BP = 90).

Recent studies indicate that several nostocacean cyanobacteria such as genera *Anabaena, Trichormus* and *Wollea* are polyphyletic and can be noted as intermixed taxa (Rajaniemi et al. 2005; Kozhevnikov and Kozhevnikova 2011). Inefficiency of this molecular marker in taxonomy of these taxa may be due to simillarity of genes encoding small-subunit ribosomal RNA in these genera. Previous studies also confirm the presence of this similarity. For example, the results of the present study are in agreement with those of Kozlíková-Zapomělová et al. (2016). According to this study, separation of these genera (*Anabaena*, *Wollea* and *Trichormus*) is not well suported by the partial 16S rRNA gene analysis. Kozhevnikov and Kozhevnikova study (2011) also confirm the phylogenetic similarity of these genera, especially genera *Wollea* and *Anabaena*.

By traditional classification, the genus *Wollea* were placed

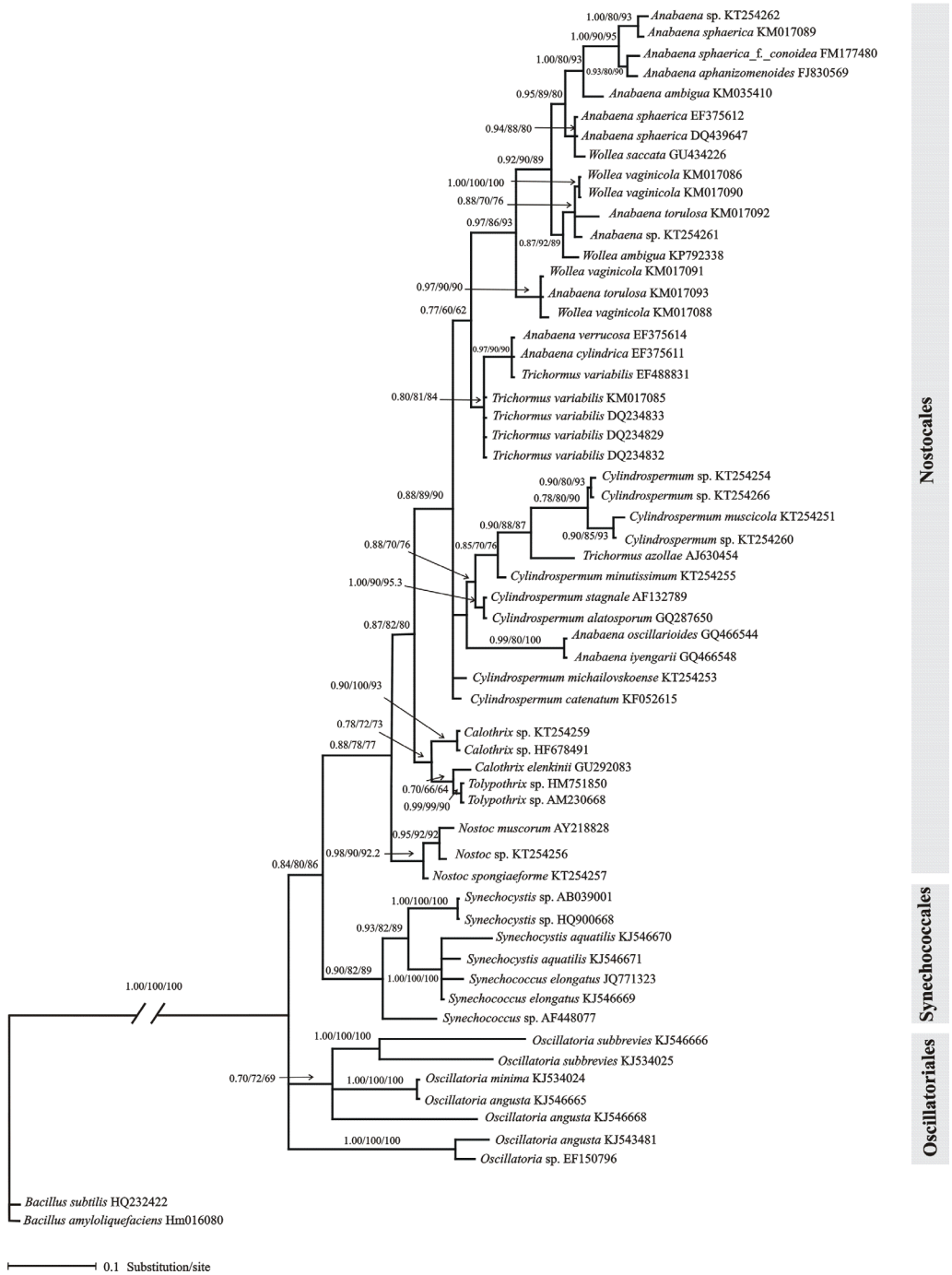

Figure 2. Fifty percent majority rule consensus tree resulting from Bayesian analysis of the 16S rRNA dataset. Numbers above branches are posterior probability and likelihood as well as parsimony bootstrap values, respectively. Values <50% were not shown.

in Nostocaceae family (Nostocales) and some of its taxa were recently separated from genus *Anabaena*. The similarity of these two genera is much more than we expected. For example, the *Wollea ambigua* is very similar to *Anabaena* species such as *Anabaena sphaerica*; also *Wollea vaginicola* is very similar to *Anabaena torulosa*. This similarity was clearly shown in our phylogenetic analyses (Fig. 2).

It is necessary to mention that *Wollea* specimens were separated from *Anabaena* species with characters such as macroscopic gelatinous colonies (which sometimes appear

tube-like), trichomes which are irregularly (or more or less) parallel and densely arranged in common and diffluent mucilage, and the absence of sheaths around trichomes (Kozhevnikov and Kozhevnikova 2011). But, according to several authors, these characters are not sufficient for the taxonomical separation of these two genera (Komàrek 1975; Shariatmadari et al. 2014).

Trichormus variabilis is another nostocacean cyanobacteria which was recently separated from the traditional genus *Anabaena* based on akinete development or apoheterocytic form of trichomes (Rajaniemi et al. 2005). The similarity of these two genera is also very much, especially before akinetes formation. Our results support this similarity, in both morphological and phylogenetic analyses (Fig. 1 and 2).

In addition to the *Nostocaceae* family, the taxa of heteropolar families such as *Rivulariaceae* and *Tolypothrichaceae* were analyzed. The *Rivulariaceae* is characterized by tapered trichomes, a part from short phases of hormogonium formation, and mostly has a terminal heterocyst in the maturity (Berrendero 2008). The *Tolypothrichaceae* is also characterized as a heteropolar cyanobacteria with non-attenuated, false branching trichomes (Komàrek et al. 2014).

The results of the present study indicate the close affinity of these two families. In all analyses (BI, ML and MP), heteropolar taxa, *Calothrix* and *Tolypothrix*, were placed in a separated clade. Heteropolarity is one of the most important properties of taxa which are placed in this clade and the taxonomic complexity is one of the dificulties seen in this group. For example, several families have been proposed for some taxa of this heteropolar group such as *Tolypothrix*. The *Rivulariaceae*, *Microchaetaceae* and *Tolypotrichaceae* are from these proposed families (Hauer et al. 2014; Sihvonen et al. 2007; Rippka et al. 1979; Desikachary 1959). Althought *Tolypothrix,* according to the Botanical code, was classified in family *Rivulariaceae*, nowadays this genus is separated from *Calothrix* and is placed in *Tolypotrichaceae* family (Hauer et al. 2014). In the present study and according to partial 16S rRNA gene sequencing, these two genera (*Calothrix* and *Tolypothrix*) showed a close relationship and placed as the sister taxa**.** Thus, although this molecular marker could separate heteropolar taxa such as *Calothrix* and *Tolypothrix* from the others, it does not seem appropriate for separation of *Rivulariaceae* and *Tolypothrichaceae* taxa.

The results of the present study also showed that Synechococcales, similar to Nostocales, was monophyletic and several taxa of this order were placed in one group with high support (PP = 0.90, ML = 82, MP = 89) (Fig. 2). In other words, the Synechococcales taxa such as genera *Synechocystis* and *Synechococcus* are well separated from the filamentous taxa (Nostocales and Oscillatoriales taxa) based on the information given by the partial 16S rRNA gene sequencing. It should be noted that some algologists placed this genera in Chroococcales. The Chroococcales was known as an order of the cyanobacteria with unicellular or colonial taxa, sometimes forming a pseudofilamentous colony and never differentiated into base and apex. Polyphyly of this order was reported in previous studies (Wanigatunge et al. 2014). Unlike Chroococcales, the order Synechococcales is introduced as a monophyletic family. According to Thomazeau et al. (2010), Synechococcales is also a large and monophyletic group of cyanobacteria with both unicellular (plus colonial) and filamentous structure. In addition to studies that show monophyly of this order, some studies emphasize the polyphyly of Synechococcales (Komárek et al. 2014). Even some genera of this order have been reported as a polyphyletic taxa. For example, according to Dvořák et al. (2014), the genus *Synechococcus* Nägeli from Synechococcales represents an enigmatic group of cyanobacteria with polyphyletic evolutionary origin. The studies conducted by Haverkamp et al. (2009) also represent the polyphyly of this genus according to several molecular markers. The polyphyletic origin of *Synechococcus* was also confirmed in the present study (Fig. 2). In this study it was observed that this molecular marker could not separate morphologicaly similar genera such as *Synechocystis* and *Synechococcus*. It should be noted that the genetic similarities of these genera are supported with morphological similarities.

Polyphyly of Oscillatoriales is another result that can be derived from the results of the present study. This order includes filamentous taxa with more complicated cytology (Komárek et al. 2014). In previous classifications, Oscillatoriales taxa were placed in Nostocales. But, later studies transferred these taxa to several families of Oscillatoriales. The uniseriate filaments as well as non-heteterocystous structure of them are among the important characteristics of this order.

In the present study, using partial 16S rRNA gene sequencing could not separate the boundry of Oscillatoriales taxa completely. In other words, all samples belonging to this order were not observed in a single clade of phylogenetic tree. Our results confirmed the results of the previous studies which emphasized the polyphyly of Oscillatoriales (Ishida et al. 2001; Lokmer 2007; Valério et al. 2009).

In conclusion, our results revealed the efficiency of partial 16S rRNA gene sequencing as a molecular marker, specially in high taxonomic levels such as order and family. In contrast, our results did not support the efficiency of this molecular marker in the taxonomy of lower taxonomic ranks such as genera. This inefficiency, particularly in the complex taxa such as *Anabaena*, *Wollea* and *Trichormus,* was considerable. It seems that the genetic similarity of these taxa prevents their separation by the described molecular marker. This genetic similarity, which is also supported by the morphological similarity, indicates that the taxonomic status of intermixed taxa such as *Anabaena*, *Wollea* and *Trichormus* needs to be revised further.

Acknowledgment

The authors wish to thank University of Shahid Beheshti for funding this project. Thanks are also due to Dr. Somayeh Keypour for her kind assistance during the research and help in editing and reviewing this paper.

References

Berrendero E, Perona E, Mateo P (2008) Genetic and morphological characterization of *Rivularia* and *Calothrix* (Nostocales, Cyanobacteria) from running water. Int J Syst Evol Microbiol 58:447-460.

Bittencourt-Oliveira MC, Buch B, Hereman TC, Arruda-Neto JDT, Moura AN, Zocchi SSJ (2012) Effects of light intensity and temperature on *Cylindrospermopsis raciborskii* (Cyanobacteria) with straight and coiled trichomes: growth rate and morphology. Braz J Biol 72(2):343-51.

Desikachary TV (1959) Cyanophyta. Indian Council of Agricultural Research, New Delhi, India.

Dvořák P, Hindák F, Hašler P, Hindáková A, Poulicková A (2014) Morphological and molecular studies of *Neosynechococcus sphagnicola*, gen. et sp. nov. (Cyanobacteria, Synechococcales). Phytotaxa 170(1):24-34.

Edgar RC (2004) Muscle: multiple sequence alignment with high accuracy and high throughput. Nucl Acids Res 32:1792-1797.

Ezhilarasi A, Anand N (2009) Phylogenetic analysis of *Anabaena* spp. (Cyanobacteria) using sequences of 16S rRNA gene. Aust J Basic Appl Sci 3(4):4026-4031.

Felsenstein J (1985) Confidence limits on phylogenies: an approach using the bootstrap. Evolution 38:783-791.

Hall TA (1999) BioEdit: a user friendly biological sequence alignment editor and analysis program for Windows 95/98/NT. Nucl Acids Symp Ser 41:95-98.

Hauer T, Bohunickà M, Johansen JR, Mareš J, Berrendero-Gomez E (2014) Reassessment of the cyanobacterial family *Microchaetaceae* and establishment of new families *Tolypothrichaceae* and *Godleyaceae*. J Phycol 50:1089-1100.

Haverkamp TH, Schouten D, Doeleman M, Wollenzien U, Huisman J, Stal LJ (2009) Colorful microdiversity of *Synechococcus* strains (picocyanobacteria) isolated from Baltic Sea. ISME J 3:397-408.

Hötzel G, Croome R (1999) A Phytoplankton Methods Manual for Australian Freshwaters. Land and Water Resources Research and Development Corporation, Canberra, Australia.

Iranshahi S, Nejadsattari T, Soltani N, Shokravi S, Dezfulian M (2014) The effect of salinity on morphological and molecular characters and physiological responces of *Nostoc* sp. ISC 101. Iran J Fish Sci 13(4):907-917.

Ishida T, Watanabe MM, Sugiyama J, Yokota A (2001) Evidence for polyphyletic origin of the members of the orders of Oscillatoriales and Pleurocapsales as determined by 16S rDNA analysis. FEMS Microbiol Lett 201:79-82.

John DM, Whitton BA, Brook A (2002) The Freshwater Algal Flora of the British Isles: An Identification Guide to Freshwater and Terrestrial Algae. Cambridge University Press, London, UK.

Komárek J, Kastovsky J, Mares J, Johansen JR (2014) Taxonomic classification of cyanoprokaryotes (cyanobacterial genera) using a polyphasic approach. Preslia 86(4):295-335.

Komárek J, Zapomělová E (2008) Planktic morphospecies of the cyanobacterial genus *Anabaena* = subg. Dolichospermum-2. Part: Straight types. Fottea 8(1):1-14.

Komárek J (2005) Studies on the cyanophytes (Cyanobacteria, Cyanoprokaryota) of Cuba 11. Freshwater *Anabaena* species. Preslia 77:211-234.

Komárek J (2003) Planktic oscillatorialean cyanoprokaryotes (short review according to combined phenotype and molecular aspects). Hydrobiologia 502:367-382.

Komàrek J (1975) Blaualgen aus dem Naturschutzgebiet "Řežabinec" bei Ražice. Nova Hedwig 26:601-643.

Kozhevnikov IV, Kozhevnikova NA (2011) Phylogenetic and morphological evaluation of *Wollea saccata* (Nostocales, Cyanobacteria) isolated from the Yenissei River basin (Eastern Siberia, Russia). Fottea 11(1):99-106.

Kozlíková-Zapomělová E, Chatchawan T, Kaštovský J, Komárek J (2016) Phylogenetic and taxonomic position of the genus *Wollea* with the description of *Wollea salina* sp. nov. (Cyanobacteria, Nostocales). Fottea 16(1):43-55.

Lokmer A (2007) Polyphasic approach to the taxonomy of the selected oscillatorian strains (Cyanobacteria). Master Thesis, Faculty of Biological Sciences, University of South Bohemia, České Budějovice.

Moisander PH, McClinton IIIE, Paerl HW (2002) Salinity effects on growth, photosynthetic parameters, and nitrogenase activity in estuarine planktonic cyanobacteria. Microb Ecol 43:432-442.

Moreira C, Vasconcelos V, Antunes A (2013) Phylogeny and biogeography of Cyanobacteria and their produced toxins. Mar Drugs 11:4350-4369.

Nayak S, Prasanna R (2007) Analysing diversity among Indian isolates of *Anabaena* (Nostocales, Cyanophyta) using morphological, physiological and biochemical characters. World J Microbiol Biotechnol 23:1575-1584.

Nübel U, Garcia-Pichel F, Muyzer G (1997) PCR primers to amplify 16S rRNA genes from cyanobacteria. Appl Environ Microbiol 63(8):3327-3332.

Nylander JAA (2004) MrModeltest v2. Program distributed by the author. Evolutionary Biology Centre, Uppsala

University, Uppsala, Sweden.
Page DM (2001) Treeview (Win32) version 1.6.6. Available: http:// taxonomy.zoology.gla.ac.uk/rod/treeview.html.
Palinska KA, Deventer B, Hariri K, Lotocka M (2011) A taxonomic study on Phormidium-group (cyanobacteria) based on morphology, pigments, RAPD molecular markers and RFLP analysis of the 16S rRNA gene fragment. Fottea 11(1):41-55.
Podani J (2000) Introduction to the Exploration of Multivariate Biological Data. English translation. Backhuys Publishers, Leiden.
Posada D, Buckley TR (2004) Model selection and model averaging in phylogenetics: advantages of akaike information criterion and Bayesian approaches over likelihood ratio tests. Syst Biol 53:793-808.
Prescott GW (1970) Algae of the Western Great Lakes Area. W. C. Brown Co., Dubuque, Iowa, USA.
Rajaniemi P, Hrouzek P, Kaštovskà K, Willame R, Rantala A, Hoffmann L, Komàrek J, Sivonen K (2005) Phylogenetic and morphological evaluation of the genera *Anabaena*, *Aphanizomenon*, *Trichormus* and *Nostoc* (Nostocales, Cyanobacteria). Int J Syst Evol Microbiol 55:11-26.
Rangaswamy G (1966) Agricultural Microbiology. Asia Publishing House, Bombay, India.
Rippka R, Deruelles J, Waterbury JB, Herdman M, Stanier RY (1979) Generic assignments, strain histories and properties of pure cultures of cyanobacteria. J Gen Microbiol 111:1-61.
Ronquist F, Huelsenbeck JP (2003) MrBayes 3: Bayesian phylogenetic inference under mixed models. Bioinformatics 19:1-210.
Shariatmadari Z, Riahi H, Sonboli A (2014) Morphometric and phylogenetic analyses of *Anabaena* strains (Cyanoprokaryota) from terrestrial habitats of Iran. Iran J Bot 20(1):119-129.
Sihvonen LM, Lyra C, Fewer DP, Rajaniemi-Wasklin P, Lehtimäki JM, Wahlsten M, Sivonen K (2007) Strains of the cyanobacterial genera *Calothrix* and *Rivularia* isolated from the Baltic Sea display cryptic diversity and are distantly related to *Gloeotrichia* and *Tolypothrix*. FEMS Microbial Ecol 61:74-84.
Silvestro D, Michalak I (2012) raxmlGUI: a graphical front-end for RAxML. Org Divers Evol 12:335-337.
Soares MCS, Lurling M, Huszar VLM (2013) Growth and temperature-related phenotypic plasticity in the cyanobacterium *Cylindrospermopsis raciborskii*. Phycol Res 61:61-67.
Stanier RY, Kunisawa R, Mandal M, Cohen-Bazire G (1971) Purification and properties of unicellular blue-green algae (order Chroococcales). Bacteriol Rev 35:171-305.
Swofford DL (2002) PAUP*: Phylogenetic Analysis Using Parsimony (*and other methods), Version 4.0b10. Sinauer Associates, Sunderland.
Tamura K, Peterson D, Peterson N, Stecher G, Nei M, Kumar S (2011) MEGA5: molecular evolutionary genetics analysis using maximum likelihood, evolutionary distance, and maximum parsimony methods. Mol Biol Evol 28:2731-273.
Thomazeau S, Houdan-Fourmont A, Couté A, Duval C (2010) The contribution of sub-saharan African strains to the phylogeny of Cyanobacteria: focusing on the Nostocaceae (Nostocales, Cyanobacteria). J Phycol 46:564-579.
Valério E, Chambel L, Paulino S, Faria N, Pereira P, Tenreiro R (2009) Molecular identification, typing and traceability of cyanobacteria from freshwater reservoirs. Microbiology 155:642-656.
Wanigatunge RP, Magana-Arachchi DN, Chandrasekharan NV, Kulasooriya SA (2014) Genetic diversity and molecular phylogeny of cyanobacteria from Sri Lanka based on 16S rRNA gene. Environ Eng Res 19(4):317-329.
Wehr JD, Sheath RG, Thorp JH (2002) Freshwater Algae of North America: Ecology and Classification. Aquatic Ecology Press, California, USA.
Yamamoto Y, Nakahara H (2009) Seasonal variations in the morphology of bloom-forming cyanobacteria in a eutrophic pond. Limnology 10:185-193.

Volume 61(1):69-75, 2017
Acta Biologica Szegediensis
http://www2.sci.u-szeged.hu/ABS

ARTICLE

Dioxin analysis in pine honey from Turkey

Aslı Özkök[1]*, Kadriye Sorkun[1, 2], Gül Çelik Çakıroğulları[3], Hatice Gür Yağlı[3], İbrahim Alsan[3], Berkay Bektaş[3], Devrim Kılıç[3]

[1]Hacettepe University, Bee and Bee Products Applied and Research Center (HARUM), 06800-Beytepe, Ankara, Turkey
[2]Hacettepe University, Faculty of Sciences, Department of Biology, 06800-Beytepe, Ankara, Turkey
[3]Republic of Turkey Ministry of Food, Agriculture and Livestock, National Food Reference Laboratory, Yenimahalle, Ankara, Turkey

ABSTRACT The aim of the study is to determine concentrations of polychlorinated dibenzo-p-dioxins (PCDDs), polychlorinated dibenzofurans (PCDFs), dioxin-like polychlorinated biphenyls (dl-PCBs) and indicator PCBs (ind-PCBs) in pine (honeydew) honey, which is endemic and popular in Turkey. *Marchalina hellenica*, which lives on *Pinus brutia*, is the main source of honeydew, and *Apis mellifera* L. collects the honeydew for making the pine honey. Pine honey is a very important bee product due to the export all over the world. In this study, honey samples were collected from Muğla and were researched via microscope. The quality of honey samples was determined by correlating NHE (Number of Honeydew Elements) to NTP (Number of Total Pollen) ratio and the honey, which has NHE to NTP ratio higher than 4.5 was accepted as a high density-superior quality pine honey. According to identifications, which have been made via microscope, pooled high quality pine honey sample was selected and analysed for dioxin. All the dioxin results were found lower than the European Union regulatory limits.
Acta Biol Szeged 61(1):69-75 (2017)

KEY WORDS

Apis mellifera
dioxin analysis
Marchallina hellenica
pine (Honeydew) honey
Pinus brutia

Introduction

The term "dioxin" generally refers to the polychlorinated dibenzo-p-dioxins (PCDDs), polychlorinated dibenzofurans (PCDFs) and dioxin-like polychlorinated biphenyls (dl-PCBs) with similar biological and toxicological properties, which are lipophilic contaminants and accumulate in lipids of biological systems (Fries 1995; Olanca et al. 2014).

The dioxin contamination incidents involving food and feedstuffs happened in recent years and the re-evaluation of the Tolerable Daily Intake (TDI) of dioxins (Van Leeuwen et al. 2000) have prompted wide-ranging efforts and the tightening of regulations to reduce dioxin release into the environment (Commission Regulation 2000). In 2006, the World Health Organization (WHO) re-evaluated the toxicity equivalent factors (TEFs) assigned to dioxins and dioxin-like PCBs (DL-PCBs) for the calculation of the toxic equivalent quantities (TEQs) (Van Den Berg et al. 2006) and the European Commission has recently established maximum permissible levels of dioxins and DL-PCBs in foods (Commission Regulation 2011).

Submitted February 11, 2017; Accepted April 10, 2017
*Corresponding author. E-mail: asozkok@gmail.com

The International Agency for Research on Cancer (IARC) classified 2,3,7,8-TCDD, the most toxic of the dibenzo-p-dioxins, as a Group 1 carcinogen, meaning a "known human carcinogen". PCDD/Fs and PCBs cause a variety of health problems in organisms (Kodavanti et al. 1998; WHO 2016). Exposure of human populations to dioxins and PCBs occurs via the food chain (Hays and Aylward 2003).

Honey is a natural product that honeybees (*Apis mellifera L.*) make from the nectar of blossoms or from secretions coming from living parts of plants. The bees collect, transform and combine this material with specific substances of their own (enzymes), store and leave to ripen in the honeycombs of beehive (Council Directive 2001). Pine (Honeydew) honey is prepared from secretions of living parts of plants or excretions of plant-sucking insects on the living part of plants (Sanz et al. 2005). Honeydew is the origin of pine honey, which is a class of honeys. It refers to honey produced by honeybees collecting sweet substances, which are exuded from other insects such as aphids or scale insects (Zander and Koch 1994). Insects take essential nutrients from concentrated sugar solution in the floem and exude the remains. Honeybees take these remains and bring to the hive and convert into honey. This honey is called honeydew honey (Zander and Koch 1994).

Honeydew honey is generally characterized by honeydew elements composed of microscopic algae, fungus spores.

If a honey with the ratio "number of honeydew elements (NHE)"/"number of total pollens (NTP)" is greater than 3, is considered as honeydew honey (Louveaux et al. 1978; Soria et al. 2004).

Marchalina hellenica (syn. *Monophlebus hellenicus*) (Coccidea: Homoptera), which lives on *Pinus brutia*, is the main source of honeydew in Turkey. The habitats of this insect are only Turkey and Greece (Santas 1979). *Marchalina hellenica* is mainly found in Southern Marmara, the Aegean and West Mediterranean regions of Turkey (Gürkan 1989). Muğla is one of the best places for pine honey, which has been produced by *Marchalina hellenica*. About 30% of honey yield of Turkey is produced in the region of Muğla. Muğla, having nearly 60 000 hectares of *Pinus brutia* forest, is a very important site for the production of pine honey (Şahin 2000). From 25 to 30 tons of pine honeys are produced each year and majority of them are exported all over the world (Maybir 2015).

Nowadays, bee products are being produced in an environment polluted by different sources of contamination, which can be transported by honey bees to the hive and incorporated into the honey (Tomasini et al. 2012). It is difficult to protect food and animal feed from the sources of toxic chemicals ubiquitous in the environment (Kim et al. 2013) particularly in the case of honey, since honeybees travel long distances and come close to many plants (Mohr et al. 2014a).

Residues of some Persistent Organic Pollutants (POPs) have been found in honey samples, such as organochlorine pesticides (Erdogrul 2007; Wang et al. 2010) and non-dioxin-like polychlorinated biphenyls (NDL-PCBs) (Herrera et al. 2005). There are very limited studies regarding PCDDs, PCDFs, and DL-PCBs' levels in honey (Mohr et al. 2014a; Wang et al. 2012).

In this study, we have determined amount of dioxin in pine honey, which is an important food and beekeeping product in Turkey. This paper presents the first results of analysis of honey samples for PCDDs, PCDFs, dioxin-like and indicator PCBs in Turkey. Therefore, the values obtained from this study are compared with the results reported in a few studies (Mohr et al. 2014a; Wang et al. 2012) and the EU standards.

As indicated by Devillers and Pharm-Delegue (2002) and Mohr et al. (2014b) during the process of gathering nectar, water, and pollen from flowers by the honeybee workers, various chemical particles, which are suspended in the air, are intercepted by these workers and retained in the hair of their body surface, or inhaled and attached to their trachea. Honey can be contaminated in an indirect way by industrial chemicals (Kujawski and Namieśnik 2008) and has been used as an environmental bioindicator in some studies (Kujawski et al. 2012; Wang et al. 2010; Rissato et al. 2007; Blasco et al. 2004; Blasco et al. 2011).

Materials and Methods

Microscopic analysis of honey samples

Honey samples were collected from 10 different hives in Muğla region in September to October 2014, pooled together, and then transferred to the laboratory. Upon collection, sample was given a unique laboratory reference number, and the sample details were logged into a database.

Preparates, to identify NTP and NHE in 10 grams of honey, were obtained as follows (Moar 1985; Sorkun 2008). Five-hundred grams of stock honey was well stirred with a sterile glass stick and 10 g of it was separated. Then 20 ml distilled water was added and the mixture was placed in a tube together with a tablet as positive control containing 12542 *Lycopodium* spores. To melt down the tablet, tubes were left in a water bath at 45 °C for 10-15 min. After the tablet fully melted, few drops of basic fuchsin were added for colouring pollens and spores and then the material was centrifuged in 3500 rpm for 45 min. Water was removed from the tubes and they were left upside down on a drying mat for full drainage. Homogenous mixing was ensured by adding 1 ml of 50% glycerine to each tube. From this mixture, 0.01 ml was taken and plated on a lam. The material was covered by a lamella of size 18 x 18 mm and two separate preparates were obtained for microscopic analysis.

Examination of the Number of Total Pollens (NTP)

Pollen and spore preparates were examined and counted under a Nikon Eclipse E400 light microscope. Objectives of 20x and 40x were used for counting pollens. During the counting process, the specimen was examined starting from the top left corner and by fully scanning the area of size 18 x 18 mm. The numbers of all pollens and *Lycopodium* spores in this area were taken separately. Counts of two separate samples were taken and the average was applied to the formula given below. The resulting figure is the total number of pollens in 10 g of honey.

NTP/10 gr = Number of pollens counted x 12542 / Number of *Lycopodium* spores counted

Examination of the Number of Honeydew Elements (NHE)

In the same preparates, in which NTP was counted, the number of honeydew elements (NHE) was also determined. During this process, starting from the top left corner and by fully scanning the area of size 18 x 18 mm the numbers of all spores, hyphae and, if there are any algae were taken. The

Table 1. Classification of honey samples by NHE/NTP ratio.

NHE/NTP	Identification	Honey type
0-1,5	Low density	Floral honey
1,5-3,0	Medium density	Pine + floral honey
3,0-4,5	Dense	Pine honey
>4,5	High dense	Superior quality pine honey

NHE content in 10 g of honey was calculated by using the following formula:

NHE/10 g = Number of spores + hyphae + algae counted x 12542 / Number of *Lycopodium* spores counted

NHE/NTP ratio

According to the obtained results, by using NHE/NTP ratio, a pine honey can be classified as High Density-Superior Quality Pine Honey, Dense Pine Honey, Floral Honey Added Pine Honey and Low Density Floral Honey (Louveaux et al. 1978; Şahin 2000; Sawyer 1988). Table 1 displays honey types and classes based on NHE/NTP ratio values.

The microscopic view of a High Dense-Superior Quality Pine Honey sample (Fig. 1) exhibits the presence of honeydew elements (spores and hyphae) and few pollens. Following microscopic examinations, honey sample was determined as high density-superior quality pine honey sample and prepared for dioxin analysis.

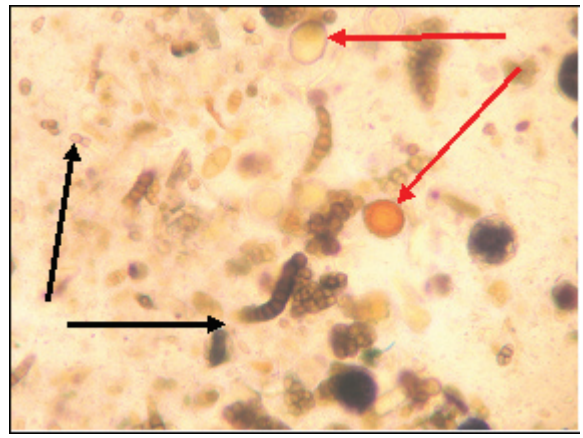

Figure 1. Microscopic view of high density-superior quality pine honey. Spores and hyphae: Black arrows. Pollens: red arrows.

Analytical procedure

Standards

All standards were bought from Cambridge Isotope Laboratories (Tewksbury, MA). A seven-point calibration curve was plotted for dioxins with a concentration range of 0.02-20 pg μl^{-1} and an eight-point calibration curve was used for PCBs, with a concentration range of 0.10-50 pg μl^{-1}. ^{13}C-labelled standards were also added to calibration standards. Laboratory has participated in every proficiency tests coordinated by EURL Dioxin Laboratory since 2011.

Extraction and clean-up

A 50-51 g of homogenised pooled pine honey sample was taken and spiked with ^{13}C-labelled internal standards. After that, extraction was performed with Smedes and Thomasen method (1996). Extracted honey sample was dissolved in hexane before clean-up step. After that, ^{13}C-labelled clean-up standard was added. In Power-PrepTM system, all samples were treated with the silica, alumina and carbon columns (Focant et al. 2005). For elution of the columns, hexane, hexane/dichloromethane, ethyl acetate/toluene and toluene were used (Traag et al. 2008). Two fractions were collected, one containing all mono-ortho and indicator PCBs, and the other containing the non-ortho PCB and dioxin congeners. The solvents were then evaporated in a TurboVap system. Hexane was added to the TurboVap tubes and then pipetted to smaller tubes. These tubes were concentrated to dryness under a gentle nitrogen stream in a heating mantle. For the PCDD/Fs 10 µl and PCB congeners 200 µl, labelled recovery standards were added to the tubes, after vortexing, and were pipetted into the vials to be injected into the HRMS system (USEPA 1994; USEPA 1999; Traag et al. 2003).

Instrumental analysis

PCDD/Fs and PCBs' determination was carried out via GC-HRMS (EI + mode) equipped with a DB-5MS column. The source temperature and detector voltage were 260 °C and 350 V, respectively. Perfluorokerosen was used as the mass reference. Inlet temperature of the GC method used in the determination of the dioxin and non-ortho PCB congeners was 280 °C. For determination of the congeners; the injection volume is 2 µl, and the temperature ramps of the oven programme was started with 110 °C, in increments of 20 °C min^{-1} up to 200 °C, 4 °C min^{-1} up to 280 °C, holding time 20 min, 5 °C min^{-1} up to 300 °C and holding time 8 min (USEPA 1994; USEPA 1999). Carrier and make-up gas was helium with a flow of 1.2 ml min^{-1}. Compounds were acquired by selected ion monitoring with the resolution being maintained at 10.000 (10%).

Table 2. Concentrations of PCDD/F, dl-PCB (Upper boundary WHO-TEQ$_{(2005)}$ pg g^{-1} fresh weight and also pg g^{-1} fresh weight) and indicator PCB congeners (pg g^{-1} fresh weight) in honey sample. Source: Mu la-Turkey. Sample weight: 50.12 g. Collection time: September-October 2014. NHE: 47363. NTP: 6855. NHE/NTP: 6.91. Fat: 0.35 g. Fat (%): 0.698.

Congener IUPAC no.	Concentration (pg/g fresh weight)	pg WHO-TEQ/g fresh weight (u.b.)	LOQ (pg/g fresh weight)	Recovery (%)
2,3,7,8-TCDF	0.0040	0.0004	0.004	72.9
1,2,3,7,8-PeCDF	0.0060	0.0002	0.006	56.3
2,3,4,7,8-PeCDF	0.0040	**0.0012**	0.004	77.7
1,2,3,4,7,8-HxCDF	0.0030	0.0003	0.003	79.9
1,2,3,6,7,8-HxCDF	0.0030	0.0003	0.003	78.2
2,3,4,6,7,8-HxCDF	0.0030	0.0003	0.003	91.6
1,2,3,7,8,9-HxCDF	0.0030	0.0003	0.003	88
1,2,3,4,6,7,8-HpCDF	**0.0036**	0.0000	0.002	86.7
1,2,3,4,7,8,9-HpCDF	0.0030	0.0000	0.003	89.3
OCDF	0.0060	0.0000	0.006	88.8
2,3,7,8-TCDD	0.0050	**0.0050**	0.005	78.8
1,2,3,7,8-PeCDD	0.0050	**0.0050**	0.005	74.6
1,2,3,4,7,8-HxCDD	0.0030	0.0003	0.003	83.4
1,2,3,6,7,8-HxCDD	0.0030	0.0003	0.003	88.2
1,2,3,7,8,9-HxCDD	0.0030	0.0003	0.003	103.9
1,2,3,4,6,7,8-HpCDD	0.0040	0.0000	0.004	84.4
OCDD	**0.0101**	0.0000	0.005	88.8
PCB81	0.0100	0.0000	0.01	28
PCB77	**0.0447**	0.0000	0.007	36.7
PCB126	**0.0090**	**0.0009**	0.006	76.4
PCB169	**0.0054**	0.0002	0.004	91.8
PCB 123	0.0920	0.0000	0.092	80.4
PCB 118	**0.3712**	0.0000	0.097	78.4
PCB 114	0.0960	0.0000	0.096	80.5
PCB 105	**0.1210**	0.0000	0.097	79.1
PCB 167	0.0940	0.0000	0.094	69.6
PCB 156	0.0840	0.0000	0.084	75.8
PCB 157	0.0960	0.0000	0.096	71.3
PCB 189	0.0680	0.0000	0.068	75.5
PCB 028	**1.6419**	**1.6419**	0.196	27.5
PCB 052	**0.7975**	0.7975	0.094	44.3
PCB 101	**0.6873**	0.6873	0.111	89.3
PCB 153	**0.8361**	0.8361	0.086	87.9
PCB 138	**0.5092**	0.5092	0.09	84.9
PCB 180	**0.3784**	0.3784	0.064	86.8
Σ WHO-PCDD/Fs-TEQ (2005)	**0.014**			
Σ WHO-Non-ortho PCBs-TEQ (2005)	**0.001**			
Σ WHO-Mono-ortho PCBs-TEQ (2005)	**0.000**			
Σ Indicator PCBs	**4.850**			
Σ WHO-DL-PCBs-TEQ (2005)	**0.001**			
Σ WHO-PCDD/F-PCB-TEQ (2005)	**0.015**			
Dioxin-Furan/dL-PCB ratio	**12.72**			

Results

Concentrations were determined with isotope dilution and the results were expressed in pg TEQ g^{-1} fresh weight calculated with appropriate WHO-TEFs (Van Den Berg et al. 2006). Table 2 shows that the concentrations of PCDD/F, dl-PCB (Upper boundary WHO-TEQ$_{(2005)}$ pg g^{-1} fresh weight and pg g^{-1} fresh weight) and indicator PCB congeners (pg g^{-1} fresh weight) in honey sample. The results are obtained with comparison according to calibration table. These results are in mass/volume concentration. By multiplying with user divisor, dilution factor, these results are converted into mass/mass concentration.

Discussion

The percentage of fat was determined according to Smedes and Thomasen (1996). The result for each congener was multiplied by the appropriate WHO toxic equivalent factor

(WHO-TEF) (Van Den Berg et al. 2006) and summed (TEQ) for all PCDDs/PCDFs and DL-PCBs congeners. TEQ results of the honey samples for the PCDDs/PCDFs and dl-PCBs calculated according to upper bound principle, in which LOQ levels were used in calculation when the concentration of a congener is below LOQ, are shown in Table 2. All the results are given in fresh weight basis. Dry weight of honey is not taken into account. Thus, on dry weight basis the results may differ slightly.

The summed concentration of indicator PCBs is the sum of the concentrations of the congeners measured. All indicator PCBs analysed for were detected above the LOQs. The concentration of fat in the sample was 0.698%. Most of the concentrations of PCDDs/PCDFs and dioxin-like PCBs in honey sample were at LOQs level except 1,2,3,4,6,7,8-HpCDF, OCDD, PCB 77,126,169,118 and 105.

Among the dioxin and furan congeners detected and quantified, highest concentrations (TEQ_{2005}, Upper-bound calculation) were found for 2,3,4,7,8-PeCDF, 2,3,7,8-TCDD, and 1,2,3,7,8-PeCDD. The highest dioxin concentrations detected in the sample were 2,3,7,8-TCDD and 1,2,3,7,8-PeCDD with the concentration of 0.0050 WHO-$TEQ_{(2005)}$ pg/g fresh weight. The main dioxin-like and indicator PCBs detected were PCB 126 and 28. The highest dioxin-like PCB concentration detected in the samples was PCB 126 with a concentration of 0.0009 WHO-$TEQ_{(2005)}$ pg/g fresh weight. The highest indicator PCB concentration detected in all samples was PCB 28 with a concentration of 1.6419 pg/g fresh weight. Although, there is no limit for honey indicated in the EU regulation, all the results were significantly lower than the EU regulation limits for all types of food (Commission Regulation 2011). There is no data on contamination level of the region where this honey was collected, and as mentioned before, these results are the first results of analysis of honey samples for PCDDs, PCDFs, and dioxin-like and indicator PCBs in Turkey. In order to compare the results of this study, a few studies could be found in the literature (Mohr et al. 2014a; Wang et al. 2012). In terms of PCDDs/PCDFs and dioxin-like PCBs concentration, the values found in this study are lower than those found in honey samples from Brazil and Spain (Mohr et al. 2014a). The most remarkable findings found in Mohr et al. (2014a) study were the large contribution of the highly chlorinated PCDD/Fs, and PCBs 105 and 118 to the total PCDD/Fs and DL-PCBs in the honey samples were similar with this study. Very low contamination levels in honey sample show, in terms of PCDDs/PCDFs and dioxin-like PCBs concentration, the values are like those found by Wang et al. (2012) in honey from Taiwan and Mainland China.

According to the results of this study, it can be mentioned that honey sample from Muğla-Turkey is safe for the consumers. Beside these studies, further studies are essential for evaluating relationship between dioxin and honey or other bee products (*e.g.*, pollen, propolis)

Acknowledgements

We would like to thank Muğla Beekeepers' Association (MAYBİR) and local people, who helped us provide samples during our fieldwork.

References

Blasco C, Lino CM, Picó Y, Pena A, Font G, Silveira MIN (2004) Determination of organochlorine pesticide residues in honey from the central zone of Portugal and the Valencian community of Spain. J Chromatogr A 1049:155-160.

Blasco C, Vasquez-Roig P, Onghena M, Masia A, Picó Y (2011) Analysis of insecticides in honey by liquid chromatography-ion-trap-mass spectrometry: comparison of different extraction procedures. J Chromatogr A 1218:4892-4901.

Commission Regulation (2000) (EC) No 76/2000/EC setting maximum levels for dioxins in emissions of municipal waste incinerators. OJEC L 321:91-100.

Commission Regulation (2011) (EU) No 1259/2011 of 2 December amending regulation (EC) No 1881/2006 as regards maximum levels for dioxins, dioxin-like PCBs and non dioxin-like PCBs in foodstuffs. (text with EEA relevance) OJEU L 320/18, 03.12.2011, 18-23.

Council Directive (2001) /110/EC of 20 December 2001 relating to honey. Official Journal of the European Communities (OJEC) L 221/10, 12.1.2002, 47-52.

Devillers J, Pharm-Delegue MH (2002) Honey Bees: Estimating the Environmental Impact of Chemicals. CRC Press, London, UK.

Erdoğrul Ö (2007) Levels of selected pesticides in honey samples from Kahramanmaraş, Turkey. Food Control 18:866-871.

Focant JF, Pirard C, Massart A-C, Scholl G, Eppe G, De Pauw E (2005) Integrated PLE-multi step automated cleanup and fractionation for the measurement of dioxins and PCBs in food and feed. Organohalogen Compd 67:261-264.

Fries GF (1995) A review of the significance of animal food products as potential pathways of human exposure to dioxins. J Anim Sci 73:1639-1650.

Gürkan B (1989) Çam pamuklu koşnili Marchalina hellenica (Genadius)'nın Biyo-Ekolojisi ve Populasyon Dinamiği. Doktora Tezi, Ankara.

Hays SM, Aylward LL (2003) Dioxin risks in perspective: past, present, and future. Regul Toxicol Pharmacol 37:202-217.

Herrera A, Pérez-Arquillué C, Conchello P, Bayarri S (2005)

Determination of pesticides and PCBs in honey by solid-phase extraction cleanup followed by gas chromatography with electron-capture and nitrogen-phosphorus detection. Anal Bioanal Chem 381:695-701.

Kim M, Kim D, Bong Y H, Jang J, Son S (2013) Concentrations of PCDD/Fs, dioxin-like PCBs, PBDEs, and hexachlorobenzene in fat samples from cattle of different ages and gender in Korea. Food Chem 138:1786-1791.

Kodavanti PR, Ward TR, Derr-Yellin EC, Mundy WR, Casey AC, Bush B, Tilson HA (1998) Congener-specific distribution of polychlorinated biphenyls in brain regions, blood, liver, and fat of adult rats following repeated exposure to Aroclor 1254. Toxicol Appl Pharmacol 153:199-210.

Kujawski MW, Namieśnik J (2008) Challenges in preparing honey samples for chromatographic determination of contaminants and trace residues. Trends Anal Chem 27:9.

Kujawski MW, Pinteaux E, Namieśnik J (2012) Application of dispersive liquid-liquid microextraction for the determination of selected organochlorine pesticides in honey by gas chromatography-mass spectrometry. Eur Food Res Technol 234:223-230.

Louveaux J, Maurizio A, Vorwohl G (1978) International Commission for Bee Botany of IUBS. Methods of Melissopalynology. Bee World 59:139-157.

Maybir (2015) Muğla İli Arı Yetiştiricileri Birliği: http://www.maybir.org.tr/.

Moar NT (1985) Pollen analysis of New Zealand honey. New Zeal J Agric Res 28:38-70.

Mohr S, García-Bermejo A, Herrero L, Gómara B, Costabeber IH, González MJ (2014a) Determination of Polychlorinated Dibenzo-P-Dioxins (PCDDs), Dibenzofurans (PCDFs) and Dioxin-Like Polychlorinated Biphenyls (Dl-PCBs) in commercial honeys from Brazil and Spain. Organohalogen Compd 76:530-533.

Mohr S, García-Bermejo Á, Herrero L, Gómara B, Costabeber IH, González MJ (2014b) Levels of brominated flame retardants (BFRs) in honey samples from different geographic regions. Sci Total Environ 472:741-745.

Olanca B, Çakıroglulları CG, Ucar Y, Kırısık D, Kılıç D (2014) Polychlorinated dioxins, furans (PCDD/Fs), dioxin-like polychlorinated biphenyls (dl-PCBs) and indicator PCBs (ind-PCBs) in egg and egg products in Turkey. Chemosphere 94:13-19.

Rissato SR, Galhiane MS, Almeida MV, Generutti M, Apon BM (2007) Multiresidue determination of pesticides in honey samples by gas chromatography-mass spectrometry and application in environmental contamination. Food Chem 101:1719-1726.

Şahin A (2000) Marmaris-Muğla Yöresinde Üretilen Çam Ballarının Mikroskobik Analizi ve Organoleptik Özelliklerinin Saptanması. Yüksek Lisans Tezi, Ankara.

Santas LA (1979) Marchalina hellenica An Important Insect for Apiculture of Greece. The 27th International Congress of Apiculture of Apimondia, Athens 419-422.

Sanz ML, Gonzalez M, Lorenzo C, Sanz J, Martinez-Castro I (2005) A contribution to the differentiation between nectar honey and honeydew honey, Food Chem 91:313-317.

Sawyer R (1988) Honey Identification, Cardiff Academic Press, UK, 109 p.

Smedes F, Thomasen TK (1996) Evaluation of the bligh and dyer lipid determination method. Mar Pollut Bull 32:681-688.

Soria AC, Gonzalez M, Lorenzo C, Martinez-Castro I, Sanz J (2004) Characterization of artisanal honeys from Madrid (Central Spain) on the basis of their melissopalynological, physicochemical and volatile composition data. Food Chem 85:121-130.

Sorkun K (2008) Türkiye'nin Nektarlı Bitkileri, Polenleri ve Balları, Palme Yayıncılık, 341s.

Tomasini D, Sampaio M RF, Caldas SS, Buffon JG, Duarte FA, Primel EG (2012) Simultaneous determination of pesticides and 5-hydroxymethylfurfural in honey by the modified QuEChERS method and liquid chromatography coupled to tandem mass spectrometry. Talanta 99:380-386.

Traag WA, Immerzeel J, Onstek C, Kraats C, Lee M K, Van der Weg G, Mol H, Hoogenboom LAP (2008) Automation of chemical analysis of PCDD/Fs, dl-PCBs, indicator PCBs and polybrominated diphenyl ethers in food and feed. Organohalogen Compd 70:54-57.

Traag WA, Kan CA, Zeilmaker MA, Hoogenboom LAP (2003) Carry-over of dioxins and PCBs at low levels from feed to egg. Organohalogen Compd 61:381-384.

USEPA (United States Environmental Protection Agency) (1994) Method 1613, Tetra- through octa- chlorinated dioxins and furans by isotope dilution HRGC/HRMS. United States of America: United States Environmental Protection Agency. Office of Water (4303).

USEPA (United States Environmental Protection Agency) (1999) Method 1668, Revision A: Chlorinated biphenyl congeners in water, soil, sediment and tissue by HRGC/HRMS. United States of America: United States Environmental Protection Agency, Office of Water (4303). EPA No. EPA-821-R-00-002.

Van den Berg M, Birnbaum L, Denison M, De Vito M, Farland W, Feeley M, Fiedler H, Hakansson H, Hanberg, A, Haws L, Rose M, Safe S, Schrenk D, Tohyama C, Tritscher A, Tuomisto J, Tysklind M, Walker N, Peterson RE (2006) The 2005 World Health Organization Reevaluation of Human and Mammalian Toxic Equivalency Factors for Dioxins and Dioxin-Like Compounds. Toxicol Sci 93:223-241.

Van Leeuwen FXR, Feeley M, Schrenk D, Larsen JC, Farland W, Younes M (2000) Dioxins: WHO's tolerable daily intake revisited. Chemosphere 40:1095-1101.

Wang J, Klil MM, Jun S, Li QX (2010) Residues of organo-

chlorine pesticides in honeys from different geographic regions. Food Res Int 43:2329-2334.

Wang YH, Xu DM, Hung CH, Cheng SR., Yu JY, Lee MS, Yu PP, Chang-Chien GP (2012) Investigation of PCDD/Fs, dioxin-like PCBs and metal element in honey from Taiwan and Mainland China. Adv Mat Res 356-360:908-913.

WHO (World Health Organization) (2016) Dioxins and their effects on Human Health. Fact Sheet No. 225.

Zander E, Koch A (1994) Der Honig. Eugen Ulmer Verlag, Stuttgart, pp. 201.

Volume 61(1):77-83, 2017
Acta Biologica Szegediensis
http://www2.sci.u-szeged.hu/ABS

ARTICLE

Discrimination of grape varieties by Start Codon Targeted genotyping using partially degenerate primers

Krisztina Miró, Tibor Nagy, Edit Korom, Ferenc Marincs*

Agricultural Biotechnology Institute, National Agricultural Research and Innovation Center, Gödöllő, Hungary

ABSTRACT DNA fingerprinting of crop species should be technically simple and easy-to-perform, reproducible, and should provide sufficient amount of information. PCR-based methods can meet one or more of these criteria, but they often employ multiple discrete primers or require to test large number of arbitrary primers to provide enough information, which make these methods technically complicated. Our aim was to develop a simple, reproducible, PCR-based method for grape genotyping, which overcomes these limitations. We tested twelve, partly degenerate primers to genotype 14 Hungarian and international grape varieties and found one primer producing 17 polymorphic bands after data normalization, which was sufficient to separate the varieties. The discriminating power of this primer, in term of the number of polymorphic bands, PIC and Rp values, was the same or better than the SCoT primers with definite sequences described in previous studies. The phylogenetic tree obtained using sequences amplified with this primer was reliably consistent with the publicly available information about the genetic origin of some of the tested varieties. We developed a simple and accurate method to genotype grapevine, which provided sufficient amount of data to discriminate 14 varieties.

Acta Biol Szeged 61(1):77-83 (2017)

KEY WORDS

degenerate primer
genotype
grapevine cultivar
PCR
SCoT marker

Introduction

PCR-based DNA fingerprinting techniques are popular in plant biology for genotyping, species/variety separation and phylogenetic studies, because they are relatively easy to perform. These methods can be broadly categorized into three groups (Poczai et al. 2013). Conserved DNA-, gene family-, transposon-, resistance gene- and RNA-based fingerprinting techniques require prior knowledge of the target gene sequences for primer design. RAPD, ISSR and AFLP fingerprinting methods use arbitrary primers and therefore no knowledge about the amplified sequences is needed. Targeted fingerprinting methods, such as SRAP (Sequence-Related Amplified Polymorphism) and SCoT (Start Codon Targeted) are between the arbitrary and other targeted techniques, since they require no or limited sequence information but still target genomic regions more or less specifically.

Of the targeted fingerprinting methods, SRAP genotyping employs 16-18 bp long forward and reverse primer pairs. The forward and reverse primers have constant, but different sequence, and their 3' triplet can be varied, which provide a certain level of amplification specificity. The SRAP molecular marker system was developed for *Brassica* (Li and Quiros 2001) and has been used in turf grass (Budak et al. 2004), bean (Alghamdi et al. 2012) and in a number of other crop species (Aneja et al. 2012). SCoT genotyping (Collard and Mackill 2009) is based on the amplification of genomic DNA using a single primer, which targets the conserved region around the start codon of highly (for example LEA, seed storage, mitochondrial, ribosomal, proline-rich and glycine-rich proteins, histones, globulins, calmodulins, just to name a few) and lowly (for example regulatory, signal transduction and cell wall proteins) expressed plant genes (Sawant et al. 1999). SCoT has been used to fingerprint rice (Collard and Mackill 2009), mango (Luo et al. 2010), potato (Gorji et al. 2011), peanut (Xiong et al. 2011), and ramie (Satya et al. 2015).

In grape (*Vitis vinifera*), which is a major crop worldwide with numerous international and very large number of local varieties, RAPD has been quite widely used for variety identification, polymorphism and diversity studies (Kocsis et al. 2005; Karataş and Ağaoğlu 2008; Salayeva et al. 2010; Butiuc-Keul et al. 2011; Zhao et al. 2011). SRAP and SCot genotypings were employed less frequently to study the relationship of cultivated grape varieties and/or wild grape species (Guo et al. 2012a; Liu et al. 2012).

Submitted November 16, 2016; Accepted January 31, 2017
*Corresponding author. E-mail: marincs.ferenc@abc.naik.hu

Ideally, a PCR-based genotypic method should produce a reasonable number of polymorphic bands, as only those have a diagnostic value. Moreover, this goal should be achieved using as few as possible primers or primer combinations. In methods such as RAPD, which use arbitrary primers, or in targeted fingerprinting, such as SRAP and SCoT, the design of primers is easy, since it can be done *in silico*. However, the problem with these methods is the large number of possible primer variations and consequently a large-scale testing of them is a major concern. For example, in RAPD random hexamers are used as primers and there are 4,096 variations of such oligonucleotides. In SRAP, the number of the 3' triplet variations for one primer can be 64, and because SRAP primers are used in pairs, 4,096 (64 x 64) combinations are possible. This number increases further by varying the core region of the primers. Even in SCoT genotyping, in which the number of possible primers is far less than in RAPD and SRAP, several dozens of primers have been tested (Collard and Mackill 2009).

In this study, we describe a simple and efficient SCoT genotyping of grapevine, in which we tested only twelve partially degenerate primers, and showed that a single primer was able to discriminate 14 cultivated international and local varieties being important for the Hungarian wine industry.

Materials and Methods

Young leaf samples of 14 Hungarian and international wine grape varieties (11 local 'Olaszrizling' ['Italian Riesling'] clones plus 'Furmint', 'Hárslevelű', 'Leányka', 'Ezerjó', 'Szürkebarát' ['Pinot Gris'], 'Rajnai Rizling' ['Rheine Riesling'], 'Chardonnay', 'Kékfrankos', 'Kadarka', 'Portugieser', 'Merlot', 'Pinot Noir' and 'Cabernet Savignon') were obtained from the vineyards of the Research Institute for Viticulture and Enology, National Agricultural Research and Innovation Center, Badacsony, Hungary.

DNA was isolated using the DNeasy Plant Mini Kit (Qiagen, Hilden, Germany) according to the instructions of the manufacturer, followed by an additional purification step using the Zymo OneStep PCR Inhibitor Removal Kit (Zymo Research, Irvine, CA, USA). DNA samples were quantified using a NanoDrop spectrophotometer (Thermo Fisher Scientific, Wilmington, DE, USA) and then diluted to 10 ng/µl for PCR.

PCR was performed in a 20 µl reaction volume comprising 40 ng DNA, 1 µM primer, 200 µM of each dNTPs, 1× final concentration of DreamTaq Green Buffer and 1.25 U DreamTaq Green DNA Polymerase (Thermo Fisher Scientific, Wilmington, DE, USA). The following PCR conditions were used: 1 cycle for 3 min at 94 ºC; 35 cycles of 94 ºC, 1 min, 50 ºC, 1 min, 72 ºC, 1 min; 1 cycle for 10 min at 72 ºC. PCR products were separated on 1% (w/v) agarose gel in 1× TBE buffer and the gels were photographed under UV illumination. Primer sequences (Table 1) were designed from the consensus sequences around the ATG start codon of highly and lowly expressed plant genes (Sawant et al. 1999), and were custom synthesized by Integrated DNA Technologies (Leuven, Belgium).

Gel images were analyzed by the freeware GelAnalyzer (www.gelanalyzer.com) using the "Valley-to-valley" option for background subtraction. Since diffuse bands can have a large total peak area, the peak height of the bands above the background was determined instead of the value of the total peak area. Peak height values in each sample were Z-score normalized in Excel, by which process the mean value and the standard deviation of the normalized intensities became 0 and 1, making the samples comparable. After normalization, the bands in each varieties with Z-score larger than the standard deviation of the normalized intensities (*i.e.* 1) were retained and allocated a value of 1, while the bands that were not present in a particular variety or had a Z-score smaller than 1 were dismissed and allocated the value of 0. The bands, which had only zero values in all varieties, were considered monomorphic, and the bands having both 1 and 0 values across varieties were considered as polymorphic. By this way, seventeen polymorphic bands were identified and the binary matrix obtained from their 0 and 1 values was used to perform cluster analysis of the samples using the R programming environment. The Euclidean distances between grape varieties were calculated using the "dist" function. Distance values were used to visualize the linkage-based clustering by the "hclust" function. Primer's Resolving power (Rp) and the Polymorphic Information Content (PIC) was calculated according to Gorji et al. (2011).

Results

The aim of this study was to design a simplified SCoT genotyping method by reducing the number of potential primers, which should be tested in order to receive polymorphic bands. To do this, six sequences were extracted from each of the conserved nucleotide sequence around the start codon of genes expressed at high or low levels, respectively (Sawant et al. 1999). Each sequence carries the ATG start codon at different position and the surrounding sequences, in which some nucleotides are degenerate (Sawant et al. 1999). Thus, in contrast to definite primers used by others for SCoT genotyping, we used partly degenerate primers in our study (Table 1).

Using single primers, PCRs were performed and the products were analyzed by agarose gel-electrophoresis. No products were detected with primers LE3, LE4 and LE5. For all other primers, the total number of bands for any primer

Table 1. Primers used in this study.

Primer [a]	Sequence (5′-3′) [b]
HE1	AATGGCTNCCT/ACNAC/TA/CCC
HE2	CAATGGCTNCCT/ACNAC/TA/CC
HE3	ACAATGGCTNCCT/ACNAC/TA/C
HE4	AACAATGGCTNCCT/ACNAC/T
HE5	A/CAACAATGGCTNCCT/ACNA
HE6	TA/CAACAATGGCTNCCT/ACN
LE1	NATGGNGNNGNNANANCC
LE2	ANATGGNGNNGNNANANC
LE3	G/AANATGGNGNNGNNANAN
LE4	NG/AANATGGNGNNGNNANA
LE5	NNG/AANATGGNGNNGNNAN
LE6	NNNG/AANATGGNGNNGNNA

[a] HE and LE, primers from around the start codon sequence of highly and lowly expressed plant genes (Sawant et al. 1999); [b] The ATG start codon is underlined.

ranged from twelve (primer LE2) to 44 (primer HE3). With the exception of primer LE2, for which all bands were monomorphic, polymorphic bands outnumbered monomorphic ones (Table 2), although the polymorphic/monomorphic ratio varied substantially from 1.4 to 5.0 (Fig. 1). Band intensities were normalized as described in the Materials and Methods section to make samples comparable. Elimination of the bands whose normalized intensity was below the set threshold reduced the total number of bands in each sample (Table 2). Only polymorphic bands remained after normalization for primer HE6 (Table 2), but the obtained seven bands did not discriminate the 14 varieties (data not shown). Other primers did not discriminate the varieties either, due to the low number of polymorphic bands. For primer HE3, for which 44 bands were detected in the genotyping (Fig. 1), 17 polymorphic bands remained after the thresholding (Table 2 and Supplementary Table 1). This polymorphism obtained by primer HE3 was sufficient to completely discriminate the varieties, but did not discriminate between the 'Olaszrizling' ('Italian Riesling') clones. The intra-varieties discrimination power of primer HE3 is reflected by its high PIC and Rp values of 0.997 and 5.86, respectively.

Cluster analysis of the 14 varieties using the binary matrix generated from polymorphic bands obtained with primer HE3 revealed three major clusters (Fig. 3). In the top cluster, three well-separated clades were observed, containing 'Chardonnay', a mixture of both white and red varieties and 'Merlot', respectively. The middle cluster contains all of the 'Olaszrizling' ('Italian Riesling') clones and two Hungarian white grape varieties, 'Hárslevelű' and 'Leányka', and an international red variety, 'Portugieser'. In the bottom cluster, two clades were observed, containing white ('Pinot Gris' and 'Rheine Riesling') and red ('Kadarka' and 'Pinot Noir') varieties, respectively.

Table 2. Numbers of bands obtained in grapes using degenerate SCoT primers.

Primer	Number of bands					
	Before normalization			After normalization		
	Total	Mono-morphic	Poly-morphic	Total	Mono-morphic	Polymor-phic
HE1	17	4	13	2	1	1
HE2	22	9	13	4	3	1
HE3	44	7	37	17	0	17
HE4	30	8	22	6	1	5
HE5	42	7	35	6	1	5
HE6	25	7	18	7	0	7
LE1	17	5	12	1	1	0
LE2	12	12	0	3	3	0
LE3	0	n.a.	n.a.	n.a.	n.a.	n.a.
LE4	0	n.a.	n.a.	n.a.	n.a.	n.a.
LE5	0	n.a.	n.a.	n.a.	n.a.	n.a.
LE6	26	6	20	4	1	3
Total	235	65	170	50	11	39

[a] n.a. = not applicable

Discussion

In this study, we described the Start Codon Targeted (SCoT) genotyping of 14 Hungarian and international grape varieties. We tested only twelve degenerate primers, which represent a significant reduction compared to other studies. In potato, Gorji et al. (2011) used 12 SCoT primers in 15 combination, although the theoretical number of combination for twelve primers is 144. In both rice and Chinese grape varieties, 36 primers were tested (Collard and Mackill 2009; Guo et al. 2012b), while in mango, peanut and ramie, 33, 18, and 20

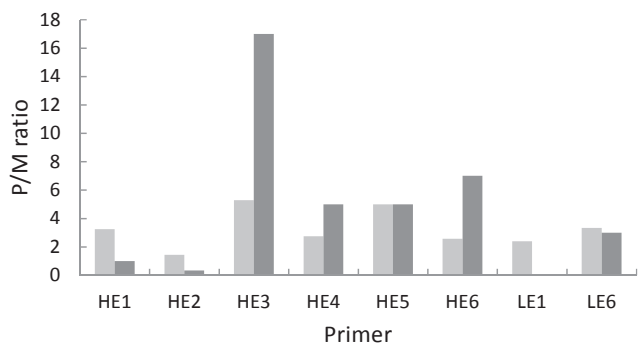

Figure 1. Ratios of the polymorphic/monomorphic (P/M) bands. ■: before normalization; ■: after normalization. For both before and after normalization, for primers with no polymorphic bands, no ratio is shown and for primers with no monomorphic bands, the number of polymorphic bands is shown (Table 2).

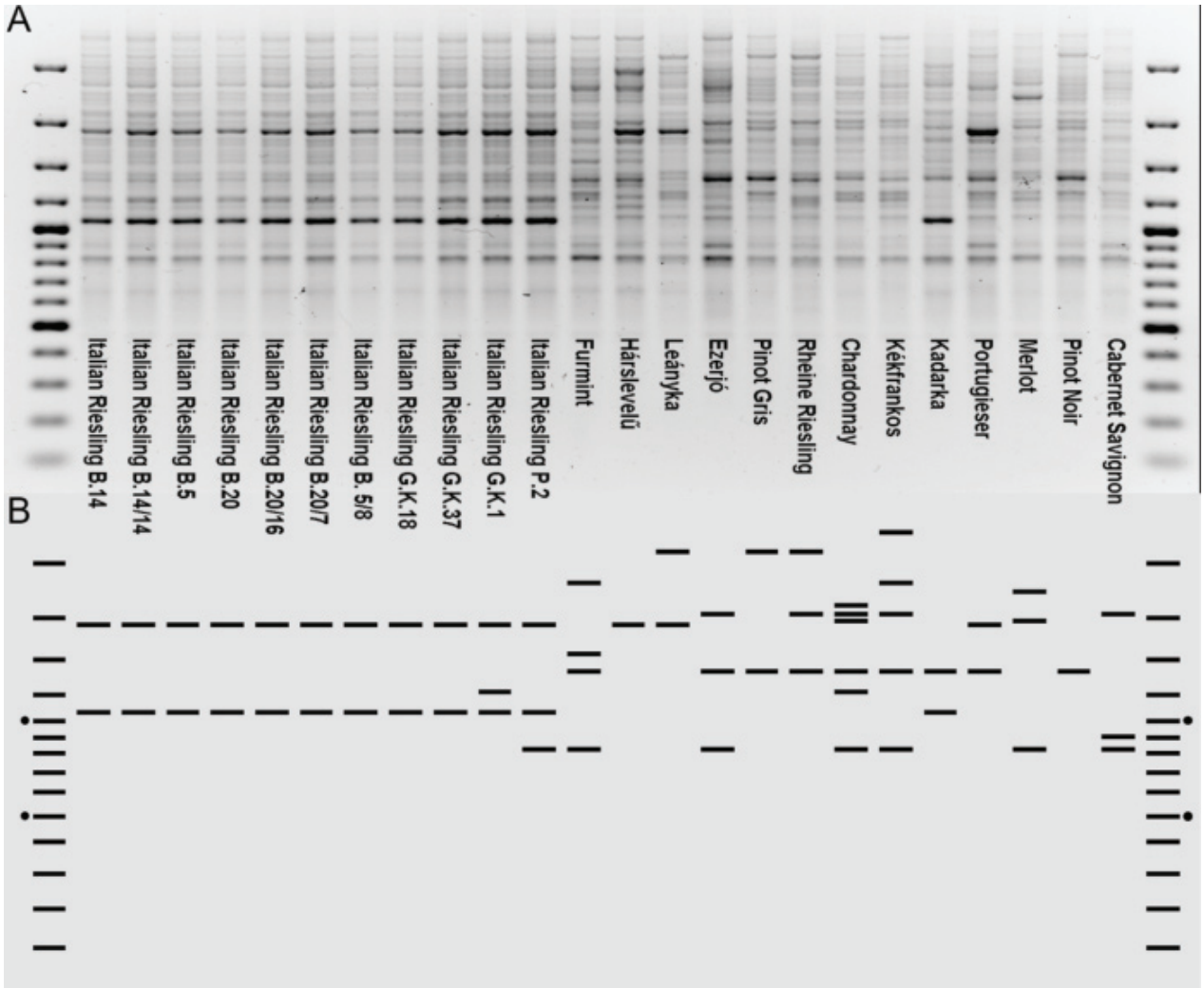

Figure 2. The genotyping profile of grape varieties obtained by the SCoT primer HE3. Panel A: image of the agarose gel electrophoretic separation of the PCR products. Panel B: simulated electrophoretic image of the polymorphic bands after normalisation and thresholding (Supplementary Table 1). The molecular marker is a 100 bp Plus DNA ladder. In Panel B, dots label the 500 and 1000 bp bands with stronger appearance in Panel A.

primers were evaluated, respectively (Luo et al. 2010; Xiong et al. 2011; Satya et al. 2015). In theory, the number of primers with definite sequence can be very high in SCoT genotyping, due to the degenerate nucleotides in the consensus sequence (Sawant et al. 1999). For example, if the degenerate primer HE3 used in this study were converted into definite-sequence primers, 160 primer sequences would be obtained. Therefore, by using degenerate primers, the same number of samples can be tested with less effort than by definite primers, or more samples can be tested, increasing the cost-effectiveness of the method.

Our study with the degenerate primers produced reliable results, compared to that of others with definite primers (Table 3) although, the 72% ratio of the polymorphic bands obtained in this study was only the fourth highest amongst compared studies. The number of polymorphic bands per degenerate primer was much higher than those achieved using definite primers (Table 3). Since three primers did not produce any band in our study, we achieved 235 bands in total by using only nine primers. Of these, 170 were polymorphic, and even after a strict normalization we obtained 39 polymorphic bands in total (Table 2). Here we would like to emphasize the importance of the normalization step in our method, because this can make data interpretation more objective. In contrast to the non-normalized data, where the mean value and the standard deviation vary from sample to sample, the applied Z-score normalization resulted in the same mean value and standard deviation, respectively, of the normalized band in-

Table 3. Comparison of the performance of SCoT genotyping studies.

Number of primers	Number of total bands[a]	Number of polymorphic bands	Polymorphic ratio (%)[b]	Average number of polymorphic bands per primer	Reference
13	n.g.	50	n.a.	3.8	Collard and Mackill (2009)
33	273	208	76	6.3	Luo et al. (2010)
15	130	26	20	1.7	Gorji et al. (2011)
18	157	60	38	3.3	Xiong et al. (2011)
17	131	122	93	7.2	Guo et al. (2012b)
20	136	119	87	5.9	Satya et al. (2015)
9	235	170	72	18.9	This study

[a] n.g. = not given; [b] n.a. = not applicable; in the "Number of primers" column, the boldface and underlined number indicates degenerate primers, normal lettering indicates definite primers.

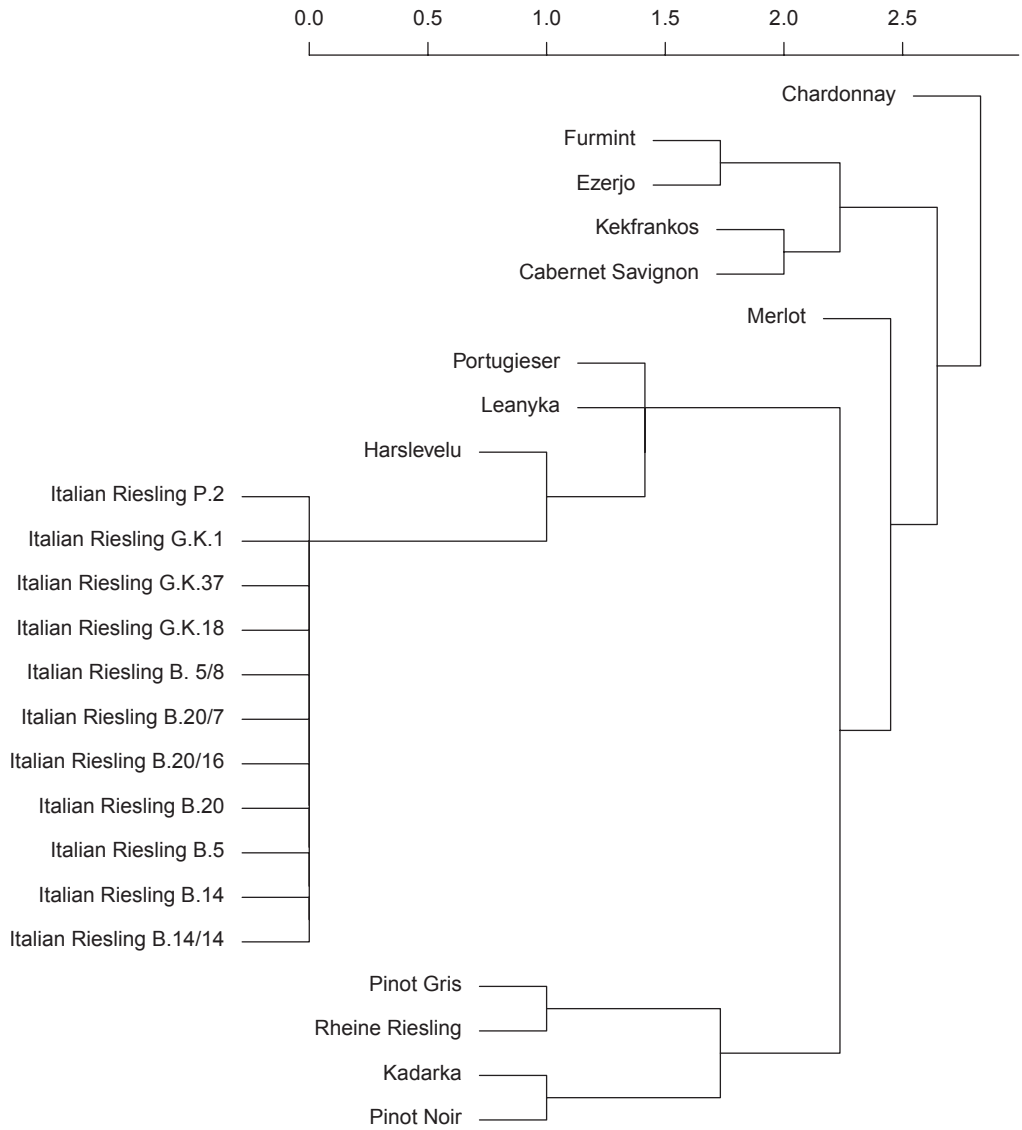

Figure 3. Cluster analysis of 14 grape varieties based on SCoT fingerprinting with primer HE3. Scale indicates Euclidean distance between the varieties.

tensities across varieties (see Materials and Methods). This makes data more comparable and by setting a threshold, under which normalized band intensity values were excluded from the analysis, the visual examination for the absence and the presence of bands can also be avoided. After normalization of data, one primer, HE3, produced 17 polymorphic bands (Supplementary Table 1) and a unique band pattern for each variety (Fig. 2). Thus it had a strong discrimination power reflected by its high PIC and Rp values of 0.997 and 5.86, respectively. For comparison, the highest PIC and Rp values reported by Gorji et al. (2011) and Satya et al. (2015) for a SCoT primer were 0.324 and 3.31, and 0.93 and 5.0, respectively. Although, a PIC value of 1.65 was reported in peanut, the highest number of polymorphic bands was only seven (Xiong et al. 2011). The best PIC value reported for a SCoT primer in grape was 0.91 (Guo et al. 2012b). From these comparisons we can conclude that the degenerate primer HE3 performed the same or even better than definite SCoT primers of other studies.

We wanted to know whether the phylogenetic tree produced by the 17 polymorphic markers is reliable, so we mined the literature to find any data, which might be consistent with the relationships between varieties in the tree. 'Cabernet Franc' was reported as one of the parents for both 'Merlot' and 'Cabernet Sauvignon' (Boursiquot et al. 2009) and this relationship was indicated by their position in the same cluster (Fig. 3). In the 'Pinot' family, the white 'Pinot Gris' variety is a mutant of the black variety 'Pinot Noir' (Yakushiji et al. 2006; Vezzulli et al. 2012), and these varieties were positioned in the same cluster (Fig. 3). 'Portugieser' might be related genetically to almost 100 red and white grape varieties (Regner et al. 1999). Although the Hungarian varieties, 'Hárslevelű' and 'Leányka', being in the same clade as Portugieser (Fig. 3), are not known as putative relatives of 'Portugieser' (Regner et al. 1999), a relationship between them is possible since white grapes have arisen from red varieties by mutations in MYB transcription factors regulating berry color (Walker et al. 2007). The exact genetic origin of the 'Riesling' and the Hungarian varieties included in this study is not known. It was reported, based on a RAPD study, that the Hungarian 'Ezerjó' and 'Hárslevelű' varieties are related (Kocsis et al. 2005), which, however, was not confirmed by our study. Guo et al. (2012b) analysed a number of Chinese and several international grape varieties using definite SCoT primers. Their analysis indicated that two varieties, 'Merlot' and 'Cabernet Sauvignon' are in closely related but separated clusters. Our above-described results are consistent with this and both analyses reflect to the written parentage of the two varieties (Boursiquot et al. 2009).

By employing degenerate primers, we were able to achieve a technically simple and easy to perform SCoT genotyping method, which discriminated 14 grape varieties and may be useful for genetic studies in grapes.

Acknowledgments

This work was supported by the Hungarian Ministry of Agriculture. The authors thank Dr. Gizella Jahnke for the leaf samples.

References

Alghamdi SS, Al-Faifi SA, Migdadi HM, Khan MA, EL-Harty EH, Ammar MH (2012) Molecular diversity assessment using sequence related amplified polymorphism (SRAP) markers in *Vicia faba* L. Int J Mol Sci 13:16457-16471.

Aneja B, Yadav NR, Chawla V, Yadav RC (2012) Sequence-related amplified polymorphism (SRAP) molecular marker system and its applications in crop improvement. Mol Breed 30:1635-1648.

Boursiquot JM, Lacombe T, Laucou V, Julliard S, Perrin F-X, Lanier N, Legrand D, Meredith C, This P (2009) Parentage of merlot and related winegrape cultivars of southwestern France: Discovery of the missing link. Aust J Grape Wine Res 15:144-155.

Budak H, Shearman RC, Gaussoin RE, Dweikat I (2004) Application of sequence-related amplified polymorphism markers for characterization of turfgrass species. HortScience 39:955-958.

Butiuc-Keul AL, Crăciunaş C, Coste A, Farago M (2010) Discrimination and genetic polymorphism in several cultivar of grapevine by RAPD markers. Rom Biotech Lett 15(Suppl):110-115.

Collard BCY, Mackill DJ (2009) Start Codon Targeted (SCoT) polymorphism: a simple, novel DNA marker technique for generating gene-targeted markers in plants. Plant Mol Biol Report 27:86-93.

Gorji AM, Poczai P, Polgar Z, Taller J (2011) Efficiency of arbitrarily amplified dominant markers (SCOT, ISSR and RAPD) for diagnostic fingerprinting in tetraploid potato. Am J Potato Res 88:226-237.

Guo D, Zhang J, Liu C, Zhang G, Li M, Zhang Q (2012a) Genetic variability and relationships between and within grape cultivated varieties and wild species based on SRAP markers. Tree Genet Genomes 8:789-800.

Guo DL, Zhang JY, Liu CH (2012b) Genetic diversity in some grape varieties revealed by SCoT analyses. Mol Biol Rep 39:5307-5313.

Karataş H, Ağaoğlu YS (2010) RAPD analysis of selected local Turkish grape cultivars (*Vitis vinifera*). Genet Mol Res 9:1980-1986.

Kocsis M, Járomi L, Putnoky P, Kozma P, Borhidi A (2005) Genetic diversity among twelve grape cultivars indigenous to the Carpathian Basin revealed by RAPD markers.

Vitis 44:87-91.

Li G, Quiros CF (2011) Sequence-related amplified polymorphism (SRAP), a new marker system based on a simple PCR reaction: its application to mapping and gene tagging in *Brassica*. Theor Appl Genet 103:455-461.

Liu C, Fan X, Jiang J, Guo D, Sun H, Zhang Y, Feng J (2012) Genetic diversity of Chinese wild grape species by SSR and SRAP markers. Biotechnol Biotec Eq 26:2899-2903.

Luo C, He XH, Chen H, Ou SJ, Gao MP (2010) Analysis of diversity and relationships among mango cultivars using Start Codon Targeted (SCoT) markers. Biochem Syst Ecol 38:1176-1184.

Poczai P, Varga I, Laos M, Cseh A, Bell N, Valkonen JPT, Hyvönen J (2013) Advances in plant gene-targeted and functional markers: a review. Plant Methods 9:6.

Regner F, Eiras-Dias JE, Stadlbauer A, Blahous D (1999) Blauer Portugieser, the dissemination of a grapevine. Cienc Tec Vitivinic 14:37-44.

Salayeva S, Akhundova E, Mammadov A (2010) Evaluation of DNA polymorphism among cultivated and wild grapevine accessions from Azerbaijan. Czech J Genet Plant Breed 46:75-84.

Satya P, Karan M, Jana S, Mitra S, Sharma A, Karmakar PG, Ray DP (2015) Start codon targeted (SCoT) polymorphism reveals genetic diversity in wild and domesticated populations of ramie (*Boehmeria nivea* L. Gaudich.), a premium textile fiber producing species. Meta Gene 3:62-70.

Sawant SV, Singh PK, Gupta SK, Madnala R, Tuli R (1999) Conserved nucleotide sequences in highly expressed genes in plants. J Genet 78:123-131.

Vezzulli S, Leonardelli L, Malossini U, Stefanini M, Velasco R, Moser C (2012) Pinot blanc and Pinot gris arose as independent somatic mutations of Pinot noir. J Exp Bot 63:6359-6369.

Walker AR, Lee E, Bogs J, McDavid DAJ, Thomas MR, Robinson SP (2007) White grapes arose through the mutation of two similar and adjacent regulatory genes. Plant J 49:772-785.

Xiong F, Zhong R, Han Z, Jiang J, He L, Zhuang W, Tang R (2011) Start codon targeted polymorphism for evaluation of functional genetic variation and relationships in cultivated peanut (*Arachis hypogaea* L.) genotypes. Mol Biol Rep 38:3487-3494.

Yakushiji H, Kobayashi S, Goto-Yamamoto N, Jeong ST, Sueta T, Mitani N, Azuma A (2006) A skin color mutation of grapevine, from black-skinned Pinot Noir to white-skinned Pinot Blanc, is caused by deletion of the functional VvmybA1 allele. Biosci Biotechnol Biochem 70:1506-1508.

Zhao MZ, Zhang YP, Wu WM, Wang C, Qian YM, Yang G, Fang JG (2011) A new strategy for complete identification of 69 grapevine cultivars using random amplified polymorphic DNA (RAPD) markers. Afr J Plant Sci 5:273-280.

Miró et al. (2017) Discrimination of grape varieties by Start Codon Targeted genotyping using partially degenerate primers.

Supplementary table

HE3 Bands

		Italian Riesling B.14		Italian Riesling B.14/14		Italian Riesling B.5		Italian Riesling B.20		Italian Riesling B.20/16		Italian Riesling B.20/7		Italian Riesling B. 5/8		Italian Riesling G.K.18		Italian Riesling G.K.37		Italian Riesling G.K.1		Italian Riesling P.2		Furmint		Hárslevelű		Leányka		Ezerjó		Pinot Gris		Rheine Riesling		Chardonnay		Kékfrankos		Kadarka		Portugieser		Merlot		Pinot Noir		Cabernet Savignon	
Band No.	Band Rf	Band peak height	Z-score	Band peak height	Z-score	Band peak height	Z-score	Band peak height	Z-score	Band peak height	Z-score	Band peak height	Z-score	Band peak height	Z-score	Band peak height	Z-score	Band peak height	Z-score	Band peak height	Z-score	Band peak height	Z-score	Band peak height	Z-score	Band peak height	Z-score	Band peak height	Z-score	Band peak height	Z-score	Band peak height	Z-score	Band peak height	Z-score	Band peak height	Z-score	Band peak height	Z-score	Band peak height	Z-score	Band peak height	Z-score	Band peak height	Z-score	Band peak height	Z-score
1	0,247	1	-0,568	1	-0,651	3	-0,545	2	-0,564	2	-0,602	1	-0,693	2	-0,557	3	-0,555																									3	-0,724					2	-0,890
2	0,252																	2	-0,696	1	-0,757	3	-0,722																	5	-0,862					5	-0,647	6	-0,557	10	-0,314	4	-0,695
3	0,258	11	-0,250	16	-0,200	10	-0,337	11	-0,250	15	-0,229	18	-0,165	14	-0,153	13	-0,233	19	-0,150	22	-0,078	27	0,074	33	0,535	40	0,331			43	0,552	15	-0,297					28	1,312												
4	0,266																									5	-1,038			2	-1,001			2	-0,747	1	-1,243												
5	0,274	4	-0,472	4	-0,561	4	-0,515	3	-0,529	4	-0,544	7	-0,507	3	-0,523	4	-0,523	6	-0,567	5	-0,628	7	-0,590	8	-0,672	6	-0,999			8	-0,774	6	-0,685	5	-0,589	6	-0,767	10	-0,340	2	-0,645	7	-0,569	6	-0,557	2	-0,682	4	-0,695
6	0,279																																							2	-0,645								
7	0,286	14	-0,154	18	-0,140	15	-0,188	15	-0,110	22	-0,029	23	-0,009	19	0,015	20	-0,007	25	0,043	24	-0,013	28	0,107	17	-0,238	21	-0,412	50	1,064	2	-1,001	53	1,337	71	2,906	22	0,753	15	0,119	3	-0,611	19	-0,106			37	0,926		
8	0,294	3	-0,504	6	-0,501	4	-0,515	3	-0,529	3	-0,573	5	-0,569	3	-0,523	3	-0,555	2	-0,696	3	-0,692	2	-0,755									3	-0,814			8	-0,577	2	-1,074					5	-0,647			3	-0,636		
9	0,302	15	-0,123	14	-0,260	14	-0,217	12	-0,215	17	-0,172	16	-0,227	16	-0,086	15	-0,168	16	-0,246	18	-0,207	20	-0,158	16	-0,286			12	-0,238	14	-0,547	11	-0,469	23	0,365	4	-0,958	5	-0,799	23	0,075	2	-0,763			8	-0,406	2	-0,890	
10	0,309	5	-0,441	5	-0,531	5	-0,486	6	-0,424	8	-0,430	9	-0,444	6	-0,422	5	-0,491									55	0,917	22	0,104							22	0,312			8	-0,524	11	-0,337	10	-0,454	1	-0,793			18	0,671	
11	0,313																	8	-0,503	10	-0,466	10	-0,490	11	-0,527													2	-1,074										
12	0,318																													1	-1,039	11	-0,469	12	-0,218	12	-0,197					4	-0,652	6	-0,498	2	-0,890	
13	0,329	24	0,164	35	0,371	30	0,259	26	0,274	37	0,401	38	0,457	27	0,284	34	0,444	36	0,396	40	0,504	38	0,439			41	0,370	14	-0,170	35	0,249	14	-0,340	8	-0,430	20	0,563	29	1,404	24	0,109			31	0,625	12	-0,222	7	-0,402	
14	0,334																							44	1,065							8	-0,599									37	0,590			7	-0,452	16	0,476	
15	0,342	10	-0,282	15	-0,230	12	-0,277	9	-0,319	13	-0,287	11	-0,382	11	-0,254	15	-0,168	14	-0,310	16	-0,272	16	-0,291	5	-0,817	6	-0,999	3	-0,547	12	-0,623	12	-0,426	13	-0,165	16	0,183	11	-0,248	9	-0,405	3	-0,724			10	-0,314	5	-0,597	
16	0,350	7	-0,377	11	-0,350	8	-0,396	9	-0,319	10	-0,373	11	-0,382	9	-0,322	12	-0,265	10	-0,439	12	-0,401	13	-0,391	16	-0,286	19	-0,490	13	-0,204	23	-0,206	23	0,047	12	-0,218	12	-0,197	11	-0,248	17	-0,131	13	-0,338	96	3,697	15	-0,085	11	-0,012	
17	0,358	3	-0,504	2	-0,621	3	-0,545	2	-0,564	1	-0,630	1	-0,693	3	-0,523	3	-0,555	2	-0,696	2	-0,725	2	-0,755	1	-1,010			11	-0,273					3	-0,694	7	-0,672	9	-0,432					7	-0,510	2	-0,682	3	-0,792	
18	0,372	17	-0,059	28	0,160	23	0,051	22	0,134	29	0,172	26	0,084	27	0,284	26	0,186	28	0,139	31	0,213	34	0,306	18	-0,189	4	-1,077	13	-0,204	2	-1,001	28	0,262	4	-0,642	26	1,134	6	-0,707	20	-0,028	12	-0,376	9	-0,415	19	0,099	7	-0,402	
19	0,382																											10	-0,307									29	1,404	3	-0,611			15	-0,132			25	1,354	
20	0,384	10	-0,282	14	-0,260	13	-0,247	9	-0,319	12	-0,315	14	-0,289	6	-0,422	11	-0,297	13	-0,342	16	-0,272	13	-0,391	17	-0,238	46	0,565			64	1,348	28	0,262	57	2,165	32	1,704									26	0,421		
21	0,391																																					17	0,303					42	1,145				
22	0,394																							19	-0,141					15	-0,509	42	0,864	10	-0,324	25	1,039			38	0,589					35	0,834	5	-0,597	
23	0,400	96	2,454	127	3,134	116	2,822	97	2,752	134	3,181	130	3,318	105	2,909	108	2,829	126	3,285	125	3,253	118	3,092			118	3,380	148	4,423							2	-0,747							107	3,294						
24	0,410	11	-0,250	17	-0,170	15	-0,188	10	-0,284	11	-0,344	18	-0,165	11	-0,254	11	-0,297	18	-0,182	17	-0,240	21	-0,125	35	0,631	47	0,604	15	-0,136	45	0,628	20	-0,082	8	-0,430	17	0,278	17	0,303	31	0,349	31	0,358	16	-0,084	14	-0,130	13	0,183	
25	0,415																											2	-0,581					4	-0,642	7	-0,672	8	-0,524					3	-0,699				
26	0,419	3	-0,504	7	-0,471	5	-0,486	8	-0,354	8	-0,430	7	-0,507	6	-0,422	6	-0,458	7	-0,535	8	-0,531	6	-0,623																										
27	0,426															3	-0,555							13	-0,431			9	-0,341			12	-0,426			15	0,088	3	-0,983	9	-0,405	17	-0,183	5	-0,604	9	-0,360	6	-0,500	
28	0,429	0	-0,600	2	-0,621	2	-0,575	2	-0,564	2	-0,602	1	-0,693	1	-0,591			3	-0,663	1	-0,757	0	-0,822			23	-0,334			24	-0,168			12	-0,218														
29	0,436	3	-0,504	6	-0,501	3	-0,545	4	-0,494	8	-0,430	6	-0,538	2	-0,557	3	-0,555	6	-0,567	6	-0,595	5	-0,656																					4	-0,652				
30	0,439																											3	-0,547			4	-0,771	6	-0,536	4	-0,958	4	-0,891			3	-0,724	9	-0,415	3	-0,636		
31	0,444	12	-0,218	10	-0,381	11	-0,307	9	-0,319	10	-0,373	12	-0,351	9	-0,322	8	-0,394	11	-0,407	12	-0,401	13	-0,391	46	1,162	26	-0,217	3	-0,547											14	-0,234							8	-0,304	
32	0,455																							3	-0,913															9	-0,405								
33	0,460																											17	-0,067							7	-0,672	8	-0,524			3	-0,724	12	-0,273				
34	0,464	9	-0,313	11	-0,350	10	-0,337	8	-0,354	10	-0,373	11	-0,382	6	-0,422	8	-0,394	12	-0,375	14	-0,337	14	-0,357			6	-0,999							10	-0,324													10	-0,109	
35	0,471	18	-0,027	21	-0,050	22	0,021	18	-0,005	19	-0,115	22	-0,040	15	-0,120	18	-0,072	23	-0,021	23	-0,046	23	-0,059	60	1,837	51	0,761	19	0,001	95	2,523	109	3,746	66	2,641	44	2,844	44	2,781	51	1,034	72	1,942	14	-0,179	107	4,142	10	-0,109	
36	0,481	1	-0,568	1	-0,651	3	-0,545	1	-0,599	2	-0,602	2	-0,662	3	-0,523	1	-0,620	2	-0,696	0	-0,789	5	-0,656	9	-0,624	14	-0,686	8	-0,376	8	-0,774			3	-0,694	3	-1,053									4	-0,590		
37	0,491																							25	0,148			13	-0,204			43	0,907			16	0,183	22	0,762			27	0,203	27	0,436	38	0,972	17	0,574	
38	0,501	35	0,514	46	0,701	41	0,587	36	0,623	48	0,716	47	0,737	32	0,452	37	0,541	53	0,942	58	1,086	54	0,969	15	-0,334	36	0,174	8	-0,376	10	-0,698	5	-0,728	11	-0,271	25	1,039	16	0,211	4	-0,576	1	-0,801	29	0,530	3	-0,636	7	-0,402	
39	0,513	8	-0,345	12	-0,320	11	-0,307	7	-0,389	10	-0,373	11	-0,382	4	-0,490	7	-0,426	21	-0,086	13	-0,369	14	-0,357	21	-0,045	36	0,174	8	-0,376	29	0,022	7	-0,642			5	-0,862	9	-0,432	6	-0,508	8	-0,531	4	-0,652	4	-0,590	8	-0,304	
40	0,528																							14	-0,382	34	0,096	23	0,139	36	0,287	15	-0,297	18	0,100	13	-0,102	19	0,486			26	0,165	16	-0,084	13	-0,176	9	-0,207	
41	0,534	145	4,012	134	3,345	146	3,716	127	3,800	140	3,353	122	3,069	128	3,682	135	3,699	117	2,996	112	2,832	114	2,959	3	-0,913																136	3,948								
42	0,560																							4	-0,865									6	-0,536			6	-0,707	4	-0,576								
43	0,571	8	-0,345	6	-0,501	7	-0,426	8	-0,354	9	-0,401	12	-0,351	7	-0,389	7	-0,426	11	-0,407	15	-0,304	11	-0,457	22	0,004	13	-0,725	10	-0,307	52	0,893	9	-0,556	15	-0,059	3	-1,053	0	-1,258	4	-0,576	42	0,783	7	-0,510	9	-0,360	42	3,013	
44	0,591	36	0,545	43	0,611	39	0,528	26	0,274	37	0,401	48	0,768	26	0,250	30	0,315	48	0,781	55	0,989	58	1,102	95	3,526	47	0,604	21	0,070	77	1,840	26	0,176	16	-0,006	25	1,039	32	1,679	38	0,589	47	0,976	46	1,334	25	0,375	37	2,525	
	Sum	509	0	612	0	575	0	490	0	621	0	629	0	501	0	546	0	639	0	659	0	669	0	570	0	694	0	455	0	597	0	504	0	419	0	380	0	370	0	458	0	500	0	409	0	421	0	278	0
	Mean	18,85	0	22,67	0	21,3	0	18,15	0	23	0	23,3	0	18,56	0	20,22	0	23,67	0	24,41	0	24,78	0	21,92	0	31,55	0	18,96	0	28,43	0	21,91	0	16,12	0	14,07	0	13,7	0	20,82	0	21,74	0	17,78	0	16,84	0	11,12	0
	SD	31,44	1	33,29	1	33,56	1	28,65	1	34,9	1	32,16	1	29,72	1	31,03	1	31,15	1	30,93	1	30,15	1	20,72	1	25,58	1	29,18	1	26,39	1	23,25	1	18,89	1	10,52	1	10,89	1	29,18	1	25,88	1	21,16	1	21,77	1	10,25	1

Threshold bands

	Italian Riesling B.14		Italian Riesling B.14/14		Italian Riesling B.5		Italian Riesling B.20		Italian Riesling B.2016		Italian Riesling B.2017		Italian Riesling B. 5/8		Italian Riesling G.K.18		Italian Riesling G.K.37		Italian Riesling G.K.1		Italian Riesling P.2		Furmint		Hárslevelű		Leányka		Ezerjó		Pinot Gris		Rheine Riesling		Chardonnay		Kékfrankos		Kadarka		Portugieser		Merlot		Pinot Noir		Cabernet Savignon	
Band No.	Band Rf	Band peak height	Z-score	Band peak height	Z-score	Band peak height	Z-score	Band peak height	Z-score	Band peak height	Z-score	Band peak height	Z-score	Band peak height	Z-score	Band peak height	Z-score	Band peak height	Z-score	Band peak height	Z-score	Band peak height	Z-score	Band peak height	Z-score	Band peak height	Z-score	Band peak height	Z-score	Band peak height	Z-score	Band peak height	Z-score	Band peak height	Z-score	Band peak height	Z-score	Band peak height	Z-score	Band peak height	Z-score	Band peak height	Z-score	Band peak height	Z-score	Band peak height	Z-score
1	0,247	1	-0,568	1	-0,651	3	-0,545	2	-0,564	2	-0,602	1	-0,693	2	-0,557	3	-0,555																															3	-0,724					2	-0,890
2	0,252																	2	-0,696	1	-0,757	3	-0,722																					5	-0,647	6	-0,557	10	-0,314	4	-0,695
3	0,258	11	-0,250	16	-0,200	10	-0,337	11	-0,250	15	-0,229	18	-0,165	14	-0,153	13	-0,233	19	-0,150	22	-0,078	27	0,074	33	0,535	40	0,331			43	0,552	15	-0,297					28	1,312												
4	0,266																									5	-1,038			2	-1,001					2	-0,747	1	-1,243											
5	0,274	4	-0,472	4	-0,561	4	-0,515	3	-0,529	4	-0,544	7	-0,507	3	-0,523	4	-0,523	6	-0,567	5	-0,628	7	-0,590	8	-0,672	6	-0,999			8	-0,774	6	-0,685	5	-0,589	6	-0,767	10	-0,340	2	-0,645	7	-0,569	6	-0,557	2	-0,682	4	-0,695
6	0,279																																							2	-0,645										
7	0,286	14	-0,154	18	-0,140	15	-0,188	15	-0,110	22	-0,029	23	-0,009	19	0,015	20	-0,007	25	0,043	24	-0,013	28	0,107	17	-0,238	21	-0,412	50	1,064	2	-1,001	53	1,337	71	2,906	22	0,753	15	0,119	3	-0,611	19	-0,106			37	0,926		
8	0,294	3	-0,504	6	-0,501	4	-0,515	3	-0,529	3	-0,573	5	-0,569	3	-0,523	3	-0,555	2	-0,696	3	-0,692	2	-0,755								3	-0,814					8	-0,577	2	-1,074			5	-0,647			3	-0,636		
9	0,302	15	-0,123	14	-0,260	14	-0,217	12	-0,215	17	-0,172	16	-0,227	16	-0,086	15	-0,168	16	-0,246	18	-0,207	20	-0,158	16	-0,286			12	-0,238	14	-0,547	11	-0,469	23	0,365	4	-0,958	5	-0,799	23	0,075	2	-0,763			8	-0,406	2	-0,890
10	0,309	5	-0,441	5	-0,531	5	-0,486	6	-0,424	8	-0,430	9	-0,444	6	-0,422	5	-0,491									55	0,917	22	0,104							22	0,312			8	-0,524	11	-0,337	10	-0,454	1	-0,793			18	0,671
11	0,313																	8	-0,503	10	-0,466	10	-0,490	11	-0,527													2	-1,074										
12	0,318																													1	-1,039	11	-0,469	12	-0,218	12	-0,197							4	-0,652	6	-0,498	2	-0,890
13	0,329	24	0,164	35	0,371	30	0,259	26	0,274	37	0,401	38	0,457	27	0,284	34	0,444	36	0,396	40	0,504	38	0,439			41	0,370	14	-0,170	35	0,249	14	-0,340	8	-0,430	20	0,563	29	1,404	24	0,109			31	0,625	12	-0,222	7	-0,402
14	0,334																							44	1,065									8	-0,599					37	0,590			7	-0,452	16	0,476
15	0,342	10	-0,282	15	-0,230	12	-0,277	9	-0,319	13	-0,287	11	-0,382	11	-0,254	15	-0,168	14	-0,310	16	-0,272	16	-0,291	5	-0,817	6	-0,999	3	-0,547	12	-0,623	12	-0,426	13	-0,165	16	0,183	11	-0,248	9	-0,405	3	-0,724			10	-0,314	5	-0,597
16	0,350	7	-0,377	11	-0,350	8	-0,396	9	-0,319	10	-0,373	11	-0,382	9	-0,322	12	-0,265	10	-0,439	12	-0,401	13	-0,391	16	-0,286	19	-0,490	13	-0,204	23	-0,206	23	0,047	12	-0,218	12	-0,197	11	-0,248	17	-0,131	13	-0,338	96	3,697	15	-0,085	11	-0,012
17	0,358	3	-0,504	2	-0,621	3	-0,545	2	-0,564	1	-0,630	1	-0,693	3	-0,523	3	-0,555	2	-0,696	2	-0,725	2	-0,755	1	-1,010			11	-0,273							3	-0,694	7	-0,672	9	-0,432							7	-0,510	2	-0,682	3	-0,792
18	0,372	17	-0,059	28	0,160	23	0,051	22	0,134	29	0,172	26	0,084	27	0,284	26	0,186	28	0,139	31	0,213	34	0,306	18	-0,189	4	-1,077	13	-0,204	2	-1,001	28	0,262	4	-0,642	26	1,134	6	-0,707	20	-0,028	12	-0,376	9	-0,415	19	0,099	7	-0,402
19	0,382																											10	-0,307									29	1,404	3	-0,611			15	-0,132			25	1,354
20	0,384	10	-0,282	14	-0,260	13	-0,247	9	-0,319	12	-0,315	14	-0,289	6	-0,422	11	-0,297	13	-0,342	16	-0,272	13	-0,391	17	-0,238	46	0,565			64	1,348	28	0,262	57	2,165	32	1,704									26	0,421		
21	0,391																																					17	0,303							42	1,145		
22	0,394																							19	-0,141					15	-0,509	42	0,864	10	-0,324	25	1,039			38	0,589					35	0,834	5	-0,597
23	0,400	96	2,454	127	3,134	116	2,822	97	2,752	134	3,181	130	3,318	105	2,909	108	2,829	126	3,285	125	3,253	118	3,092			118	3,380	148	4,423							2	-0,747							107	3,294						
24	0,410	11	-0,250	17	-0,170	15	-0,188	10	-0,284	11	-0,344	18	-0,165	11	-0,254	11	-0,297	18	-0,182	17	-0,240	21	-0,125	35	0,631	47	0,604	15	-0,136	45	0,628	20	-0,082	8	-0,430	17	0,278	17	0,303	31	0,349	31	0,358	16	-0,084	14	-0,130	13	0,183
25	0,415																											2	-0,581							4	-0,642	7	-0,672	8	-0,524					3	-0,699				
26	0,419	3	-0,504	7	-0,471	5	-0,486	8	-0,354	8	-0,430	7	-0,507	6	-0,422	6	-0,458	7	-0,535	8	-0,531	6	-0,623																										
27	0,426															3	-0,555							13	-0,431			9	-0,341			12	-0,426					15	0,088	3	-0,983	9	-0,405	17	-0,183	5	-0,604	9	-0,360	6	-0,500
28	0,429	0	-0,600	2	-0,621	2	-0,575	2	-0,564	2	-0,602	1	-0,693	1	-0,591			3	-0,663	1	-0,757	0	-0,822			23	-0,334			24	-0,168			12	-0,218														
29	0,436	3	-0,504	6	-0,501	3	-0,545	4	-0,494	8	-0,430	6	-0,538	2	-0,557	3	-0,555	6	-0,567	6	-0,595	5	-0,656																					4	-0,652						
30	0,439																											3	-0,547			4	-0,771	6	-0,536	4	-0,958	4	-0,891			3	-0,724	9	-0,415	3	-0,636		
31	0,444	12	-0,218	10	-0,381	11	-0,307	9	-0,319	10	-0,373	12	-0,351	9	-0,322	8	-0,394	11	-0,407	12	-0,401	13	-0,391	46	1,162	26	-0,217	3	-0,547											14	-0,234							8	-0,304
32	0,455																							3	-0,913															9	-0,405								
33	0,460																											17	-0,067									7	-0,672	8	-0,524			3	-0,724	12	-0,273		
34	0,464	9	-0,313	11	-0,350	10	-0,337	8	-0,354	10	-0,373	11	-0,382	6	-0,422	8	-0,394	12	-0,375	14	-0,337	14	-0,357			6	-0,999							10	-0,324													10	-0,109
35	0,471	18	-0,027	21	-0,050	22	0,021	18	-0,005	19	-0,115	22	-0,040	15	-0,120	18	-0,072	23	-0,021	23	-0,046	23	-0,059	60	1,837	51	0,761	19	0,001	95	2,523	109	3,746	66	2,641	44	2,844	44	2,781	51	1,034	72	1,942	14	-0,179	107	4,142	10	-0,109
36	0,481	1	-0,568	1	-0,651	3	-0,545	1	-0,599	2	-0,602	2	-0,662	3	-0,523	1	-0,620	2	-0,696	0	-0,789	5	-0,656	9	-0,624	14	-0,686	8	-0,376	8	-0,774					3	-0,694	3	-1,053									4	-0,590		
37	0,491																							25	0,148			13	-0,204			43	0,907			16	0,183	22	0,762			27	0,203	27	0,436	38	0,972	17	0,574		
38	0,501	35	0,514	46	0,701	41	0,587	36	0,623	48	0,716	47	0,737	32	0,452	37	0,541	53	0,942	58	1,086	54	0,969	15	-0,334	36	0,174	8	-0,376	10	-0,698	5	-0,728	11	-0,271	25	1,039	16	0,211	4	-0,576	1	-0,801	29	0,530	3	-0,636	7	-0,402
39	0,513	8	-0,345	12	-0,320	11	-0,307	7	-0,389	10	-0,373	11	-0,382	4	-0,490	7	-0,426	21	-0,086	13	-0,369	14	-0,357	21	-0,045	36	0,174	8	-0,376	29	0,022	7	-0,642					5	-0,862	9	-0,432	6	-0,508	8	-0,531	4	-0,652	4	-0,590	8	-0,304	
40	0,528																							14	-0,382	34	0,096	23	0,139	36	0,287	15	-0,297	18	0,100	13	-0,102	19	0,486			26	0,165	16	-0,084	13	-0,176	9	-0,207		
41	0,534	145	4,012	134	3,345	146	3,716	127	3,800	140	3,353	122	3,069	128	3,682	135	3,699	117	2,996	112	2,832	114	2,959	3	-0,913															136	3,948										
42	0,560																							4	-0,865									6	-0,536			6	-0,707	4	-0,576								
43	0,571	8	-0,345	6	-0,501	7	-0,426	8	-0,354	9	-0,401	12	-0,351	7	-0,389	7	-0,426	11	-0,407	15	-0,304	11	-0,457	22	0,004	13	-0,725	10	-0,307	52	0,893	9	-0,556	15	-0,059	3	-1,053	0	-1,258	4	-0,576	42	0,783	7	-0,510	9	-0,360	42	3,013
44	0,591	36	0,545	43	0,611	39	0,528	26	0,274	37	0,401	48	0,768	26	0,250	30	0,315	48	0,781	55	0,989	58	1,102	95	3,526	47	0,604	21	0,070	77	1,840	26	0,176	16	-0,006	25	1,039	32	1,679	38	0,589	47	0,976	46	1,334	25	0,375	37	2,525

Selected bands

		Italian Riesling B.14		Italian Riesling B.14/14		Italian Riesling B.5		Italian Riesling B.20		Italian Riesling B.20/16		Italian Riesling B.20/7		Italian Riesling B. 5/8		Italian Riesling G.K.18		Italian Riesling G.K.37		Italian Riesling G.K.1		Italian Riesling P.2		Furmint		Hárslevelű		Leányka		Ezerjó		Pinot Gris		Rheine Riesling		Chardonnay		Kékfrankos		Kadarka		Portugieser		Merlot		Pinot Noir		Cabernet Savignon	
Band No.	Band Rf	Band peak height	Z-score	Band peak height	Z-score	Band peak height	Z-score	Band peak height	Z-score	Band peak height	Z-score	Band peak height	Z-score	Band peak height	Z-score	Band peak height	Z-score	Band peak height	Z-score	Band peak height	Z-score	Band peak height	Z-score	Band peak height	Z-score	Band peak height	Z-score	Band peak height	Z-score	Band peak height	Z-score	Band peak height	Z-score	Band peak height	Z-score	Band peak height	Z-score	Band peak height	Z-score	Band peak height	Z-score	Band peak height	Z-score	Band peak height	Z-score
3	0,258	11	-0,250	16	-0,200	10	-0,337	11	-0,250	15	-0,229	18	-0,165	14	-0,153	13	-0,233	19	-0,150	22	-0,078	27	0,074	33	0,535	40	0,331			43	0,552	15	-0,297					28	1,312								
7	0,286	14	-0,154	18	-0,140	15	-0,188	15	-0,110	22	-0,029	23	-0,009	19	0,015	20	-0,007	25	0,043	24	-0,013	28	0,107	17	-0,238	21	-0,412	50	1,064	2	-1,001	53	1,337	71	2,906	22	0,753	15	0,119	3	-0,611	19	-0,106			37	0,926		
13	0,329	24	0,164	35	0,371	30	0,259	26	0,274	37	0,401	38	0,457	27	0,284	34	0,444	36	0,396	40	0,504	38	0,439			41	0,370	14	-0,170	35	0,249	14	-0,340	8	-0,430	20	0,563	29	1,404	24	0,109			31	0,625	12	-0,222	7	-0,402
14	0,334																							44	1,065							8	-0,599							37	0,590			7	-0,452	16	0,476
16	0,350	7	-0,377	11	-0,350	8	-0,396	9	-0,319	10	-0,373	11	-0,382	9	-0,322	12	-0,265	10	-0,439	12	-0,401	13	-0,391	16	-0,286	19	-0,490	13	-0,204	23	-0,206	23	0,047	12	-0,218	12	-0,197	11	-0,248	17	-0,131	13	-0,338	96	3,697	15	-0,085	11	-0,012
18	0,372	17	-0,059	28	0,160	23	0,051	22	0,134	29	0,172	26	0,084	27	0,284	26	0,186	28	0,139	31	0,213	34	0,306	18	-0,189	4	-1,077	13	-0,204	2	-1,001	28	0,262	4	-0,642	26	1,134	6	-0,707	20	-0,028	12	-0,376	9	-0,415	19	0,099	7	-0,402
19	0,382																											10	-0,307									29	1,404	3	-0,611			15	-0,132			25	1,354
20	0,384	10	-0,282	14	-0,260	13	-0,247	9	-0,319	12	-0,315	14	-0,289	6	-0,422	11	-0,297	13	-0,342	16	-0,272	13	-0,391	17	-0,238	46	0,565			64	1,348	28	0,262	57	2,165	32	1,704									26	0,421		
21	0,391																																					17	0,303					42	1,145				
22	0,394																							19	-0,141					15	-0,509	42	0,864	10	-0,324	25	1,039			38	0,589					35	0,834	5	-0,597
23	0,400	96	2,454	127	3,134	116	2,822	97	2,752	134	3,181	130	3,318	105	2,909	108	2,829	126	3,285	125	3,253	118	3,092			118	3,380	148	4,423					2	-0,747							107	3,294						
31	0,444	12	-0,218	10	-0,381	11	-0,307	9	-0,319	10	-0,373	12	-0,351	9	-0,322	8	-0,394	11	-0,407	12	-0,401	13	-0,391	46	1,162	26	-0,217	3	-0,547											14	-0,234							8	-0,304
35	0,471	18	-0,027	21	-0,050	22	0,021	18	-0,005	19	-0,115	22	-0,040	15	-0,120	18	-0,072	23	-0,021	23	-0,046	23	-0,059	60	1,837	51	0,761	19	0,001	95	2,523	109	3,746	66	2,641	44	2,844	44	2,781	51	1,034	72	1,942	14	-0,179	107	4,142	10	-0,109
38	0,501	35	0,514	46	0,701	41	0,587	36	0,623	48	0,716	47	0,737	32	0,452	37	0,541	53	0,942	58	1,086	54	0,969	15	-0,334	36	0,174	8	-0,376	10	-0,698	5	-0,728	11	-0,271	25	1,039	16	0,211	4	-0,576	1	-0,801	29	0,530	3	-0,636	7	-0,402
41	0,534	145	4,012	134	3,345	146	3,716	127	3,800	140	3,353	122	3,069	128	3,682	135	3,699	117	2,996	112	2,832	114	2,959	3	-0,913															136	3,948								
43	0,571	8	-0,345	6	-0,501	7	-0,426	8	-0,354	9	-0,401	12	-0,351	7	-0,389	7	-0,426	11	-0,407	15	-0,304	11	-0,457	22	0,004	13	-0,725	10	-0,307	52	0,893	9	-0,556	15	-0,059	3	-1,053	0	-1,258	4	-0,576	42	0,783	7	-0,510	9	-0,360	42	3,013
44	0,591	36	0,545	43	0,611	39	0,528	26	0,274	37	0,401	48	0,768	26	0,250	30	0,315	48	0,781	55	0,989	58	1,102	95	3,526	47	0,604	21	0,070	77	1,840	26	0,176	16	-0,006	25	1,039	32	1,679	38	0,589	47	0,976	46	1,334	25	0,375	37	2,525

Matrix

Italian Riesling B.14	Italian Riesling B.14/14	Italian Riesling B.5	Italian Riesling B.20	Italian Riesling B.20/16	Italian Riesling B.20/7	Italian Riesling B. 5/8	Italian Riesling G.K.18	Italian Riesling G.K.37	Italian Riesling G.K.1	Italian Riesling P.2	Furmint	Hárslevelű	Leányka	Ezerjó	Pinot Gris	Rheine Riesling	Chardonnay	Kékfrankos	Kadarka	Portugieser	Merlot	Pinot Noir	Cabernet Savignon
0	0	0	0	0	0	0	0	0	0	0	0	0	0	0	0	0	0	1	0	0	0	0	0
0	0	0	0	0	0	0	0	0	0	0	0	0	1	0	1	1	0	0	0	0	0	0	0
0	0	0	0	0	0	0	0	0	0	0	0	0	0	0	0	0	0	1	0	0	0	0	0
0	0	0	0	0	0	0	0	0	0	0	1	0	0	0	0	0	0	0	0	0	0	0	0
0	0	0	0	0	0	0	0	0	0	0	0	0	0	0	0	0	0	0	0	0	1	0	0
0	0	0	0	0	0	0	0	0	0	0	0	0	0	0	0	0	1	0	0	0	0	0	0
0	0	0	0	0	0	0	0	0	0	0	0	0	0	0	0	0	0	1	0	0	0	0	1
0	0	0	0	0	0	0	0	0	0	0	0	0	0	1	0	1	1	0	0	0	0	0	0
0	0	0	0	0	0	0	0	0	0	0	0	0	0	0	0	0	0	0	0	0	1	0	0
0	0	0	0	0	0	0	0	0	0	0	0	0	0	0	0	0	1	0	0	0	0	0	0
1	1	1	1	1	1	1	1	1	1	1	0	1	1	0	0	0	0	0	0	1	0	0	0
0	0	0	0	0	0	0	0	0	0	0	1	0	0	0	0	0	0	0	0	0	0	0	0
0	0	0	0	0	0	0	0	0	0	0	1	0	0	1	1	1	1	1	1	1	0	1	0
0	0	0	0	0	0	0	0	0	1	0	0	0	0	0	0	0	1	0	0	0	0	0	0
1	1	1	1	1	1	1	1	1	1	1	0	0	0	0	0	0	0	0	1	0	0	0	0
0	0	0	0	0	0	0	0	0	0	0	0	0	0	0	0	0	0	0	0	0	0	0	1
0	0	0	0	0	0	0	0	0	0	1	1	0	0	1	0	0	1	1	0	0	1	0	1

Volume 61(1):85-93, 2017
Acta Biologica Szegediensis
http://www2.sci.u-szeged.hu/ABS

ARTICLE

Micromorphology and leaf ecological anatomy of *Bassia* halophyte species (Amaranthaceae) from Iran

Somayeh Safiallah[1], Seyed Mohammad Mahdi Hamdi[2]*, Marius-Nicusor Grigore[3], Sara Jalili[1]

[1]Department of Biology, Garmsar Branch, Islamic Azad University, Garmsar, Iran
[2]Department of Biology, Central Tehran Branch, Islamic Azad University, Tehran, Iran
[3]Department of Biology, Alexandru Ioan Cuza University, Iaşi, Romania

ABSTRACT *Bassia* belongs to the family Chenopodiaceae, which is widely distributed in the world, especially in Irano-Turanian Region. According to the morphological similarities among the species of the genus, ecological implications of structural features were studied. In fact, understanding these relationships is of great importance in natural classification. We have studied the relationships of *Bassia* species using morphological, anatomical, and micro-morphological methods. The current results indicated that phenotypic plasticity and repetitive patterns were probably due to ecological adaptations, especially in decreasing the leaf surface by changing the inner structure. All species have a Kranz anatomy structure (Kochioid subtype), related to C_4 photosynthesis. The changes in cell size increasing the cell membrane thickness, the density of two-vascular systems, the increase of palisade to water storage parenchyma ratio and photosynthetic system. The leaf surface is covered with long highly dense hairs and microechinate ornamentation. Though the adaptation caused some morphological similarities, the variation was seen in other descriptive characteristics such as morphological and anatomical features especially in two synonym species of *B. turkestanica* and *B. pilosa*. Information about the similarity species is provided.

Acta Biol Szeged 61(1):85-93 (2017)

KEY WORDS

Amaranthaceae
classification
Kranz anatomy
phenotypic plasticity
structure

Introduction

Amaranthaceae is one of the biggest Caryophyllales family (Cuenoud et al. 2002), which is comprises 110 genera with 1700 species. They are predominantly found in arid to semi-arid, saline (Grigore 2012; Grigore et al. 2014), disturbed, and agricultural habitats of temperate and subtropical regions. Only a few genera present in the tropics, *e.g., Chenopodium*, *Halosarcia*, and *Suaeda*, but most species of the family are annuals or subshrubs. Herbaceous perennials, shrubs, small trees, and lianas are restricted to only a few genera (Kadereit et al. 2003). However, this family is very problematic from a taxonomical point of view and lots of attempts were recorded in order, to clarify its position within Caryophyllales, and especially the phylogenetic relationships between Amaranthaceae and Chenopodiaceae (Kadereit et al. 2003). Angiosperm Phylogeny Group II (2003) and APG III (2009) do not recognize Chenopodiaceae as a separate family from Amaranthaceae, instead only the latter is being maintained.

Submitted November 30, 2016; Accepted March 27, 2017
*Corresponding author. E-mail: m.hamdi@iauctb.ac.ir

Amaranthaceae and Chenopodiaceae constitute the most diverse lineage (180 genera and 2500 species) of the Caryophyllales (Kadereit et al. 2003) and have been regarded for a long time as two closely related families (Brown 1810; Bentham and Hooker 1880; Baillon 1887; Volkens 1893; Ulbrich 1934; Aellen 1965-1968; Behnke 1976; Thorne 1976; Carolin 1975). Some authors refer Chenopodiaceae in their work as "*sensu stricto*", while others Amaranthaceae, but also including species that traditionally have been previously described and regarded as Chenopods. Other authors refer to Amaranthaceae/Chenopodiaceae-Achatocarpaceae clade belonging to the core Caryophyllales (Cuenoud et al. 2002), and in this way a part of the Centrospermae as traditionally circumscribed (Cronquist and Thorne 1994).

Hedge et al. (1997) described 44 genera in the maintained Chenopodiaceae from Flora Iranica. Chenopodiaceae species are very well-represented in the Flora Iranica area with more than one third of the global total of genera present (Hedge et al. 1997). Ecologically and economically, this family is very important; in very inhospitable environments such as deserts, semi deserts or salt marshes (maritime and inland). This species are often dominants in plant communities and are an important source of forage for grazing livestock (Hedge et al. 1997).

Bassia in Flora of Iran was separated from genera of *Londesia*, *Bassia*, *Panderia*, and *Kochia* (Assadi et al. 2001; Akhani and Khoshravesh 2013). In addition to taxonomical comparisons between *Kochia*, *Bassia*, and *Chenolea*, they were separated based on anatomical and micromorphological differences (Turki et al. 2006). In a new classification based on phylogenic analyses and morphological studies, these two genera were introduced as one genus called *Bassia* based on the numerous similarities (Kadereit and Freitag 2011).

Hedge et al. (1997) described 5 species of *Bassia*, and separated this genus from *Kochia,* where 4 species are described in Flora Iranica, despite other authors reduced *Kochia* to synonymy under *Bassia* (Scott 1978). Nevertheless, they are closely related, being distinguished almost solely by the presence of wings on the fruiting perianth segments of *Kochia*, and spines or hooks in *Bassia.*

Many halophytes of the world belong to this above-mentioned lineage (Akhani et al. 1997). *Kochia* and *Bassia* of the family are so similar in small flowers, hairy leaves and wing perianth. *Kochia* has wing perianth during the maturity, while *Bassia* has spiny perianth (Chu and Sanderson 2008). *Panderia pilosa* with small urceolate (ornamentation) perianth and pilose hairs distribute in the Central Asia (Haber and Semaan 2007).

Moquin-Tandon (1849) recognized *Panderia* and *Kochia* genera, while Ulbrich (1934) added *Bassia* genus to the two mentioned genera; Scott (1978) maintained only *Panderia* and *Bassia* (including *Kochia*), Kühn et al. (1993) recognized *Panderia, Bassia* (including *Kochia*), while Kadereit and Freitag (2011) refer only to *Bassia* (including *Kochia* and *Panderia*).

The aim of this study is to discuss the ecological significance of micromorphology and anatomy of investigating species in relation to habitats, where since they have been collected.

Materials and Methods

Data and collection of plant material

Fresh plant material has been sampled from natural saline habitats of Iran. Majority of Iran is covered by Irano-Turanian Flora. We collected five taxa of the genus *Bassia* (Chenopodiaceae/Amaranthaceae) from Tehran, Garmsar, and Semnan areas of Iran based on the main source Flora of Iran, published by Research Institute of Flores and Rangland (Assadi et al. 2001; Hatami and Khosravi 2013). The species growth and development soil and the surface are usually dry and majority of these provinces visible to consist of essential element Na, Cl, K, Mg, in solonchak clay, loam and silt in Loes Zohary (1973).

Table 1. Collection data of *Bassia* with voucher number and province information studied. Investigated taxa, with their localities and correspondent voucher number.

Taxa	Locality	Voucher number (IAUGH)
Bassia scorparia (L.) A.J. Scott (= *Kochia scoparia* (L.) Schrad.) Freitag & G. Kadereit s.l. (2011) (= *Kochia scoparia*)	Tehran: Tehran-Karaj exp. Way, Vard Abad, Safiallah 1320 m	5893
Bassia stellaris (Moq.) Freitag & G. Kadereit s.l. (2011) (= K*ochia stellaris*)	Garmsar: km 7 from Garmsar to Varamin, Safiullah, 1000 m	5894
Bassia prostrata (L.) A.J. Scott (= *Kochia prostrata* (L.) Schrad.) Freitag & G. Kadereit s.l. (2011) (= K*ochia prostrata*)	Tehran, Firoozkouh Road, 13th km to Pol-e-Sefid, Safiullah, 1000 m	5895
Bassia pilosa (Fisch. & C.A. Mey.) Freitag & G. Kadereit s.l. (2011) (= *Panderia pilosa* Fisch. & C.A. Mey., including *P. turkestanica* Iljin)	Tehran: northern east of Firoozkouh to Pol-e- Sefid, Safiullah, 2000 m	5896
Bassia turkestanica (Fisch. & C.A. Mey.) Freitag & G. Kadereit s.l. (2011) (= *Panderia pilosa* Fisch. & C.A. Mey., including *P. turkestanica* Iljin)	Semnan: 32 km from western part of Semnan, next to Lasjerd, Safiullah 1400 m	5897

Bassia scoparia, B. pilosa, B. turkestanica, B. stellaris, and *B. prostrata* were studied after being collected and taxonomically identified (Table 1). The specimens were deposited in the herbarium of the Islamic Azad University, Garmsar Branch (IAUGH). Examples of soil profiles from species have been collected are depicted in Figure 1.

Micromorphology

For scanning electron microscope (SEM) analysis, leaves were prepared as follows: the leaf surfaces were mounted on stubs and attached with sticky tabs. They were covered with gold. SEM analysis was used to study the morphological characteristics of the hairs on the leaf surface and observed using a standard described method (Akhani and Khoshravesh 2013).

Then photos were taken using electron microscope Model Philips-XL30 and specialized terminology used to recognize the structure morphologically Payne (1978).

Anatomy

For light microscopy (LM) study, small sections of leaves

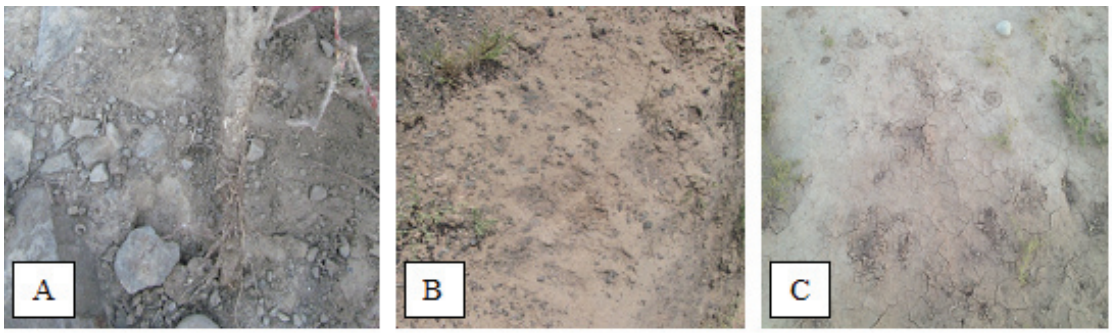

Figure 1. Soil samples from natural habitats of Iran. A: Tehran, Firoozkouh. B: Semnan, Lasjerd. C: Garmsar.

were used. Cross sections were collected from fresh leaves and were fixed in ethanol and glycerol (Purvis et al. 1966). Sections were cut by free hand. After sectioning and staining (Peterson et al. 1986), the samples permanent slides were studied by Olympus-BH2 light microscope. Both qualitative and quantitative methods were used in this investigation.

Results

Morphology and taxonomical features

Morphological observations in *Bassia* indicated traits such as simple, alternate and hairy leaves with parallel veined, 5-correlated perianth, spike inflorescence, pantadrous (5 stamen), curvate embryo and ovate seed. These traits are plesiomorphic ones, that show the near similarities and the relatives. The perianth ornamentation and wing, spiny or appendix perianth are apomorphic traits that are not important in the taxonomy of the species. With these characteristics of species morphology, the evolution could be followed by the weather changes and environment adaptation. In these species, the adaptation occurred with decreasing the leaf surface with much hair, while in some species, simple and long hairs were seen. *B. pilosa* is a decumbent-procumbent/prosrate plant with urceolate perianth and ornamentation. The main difference in comparison with *B. turkestanica* and the biggest differences among *B. scoparia, B. prostrata* and *B. stellaris* were found in quantitative characteristics, while in qualitative, *B. prostrata* was same with *B. pilosa* in decumbent vegetative form, but was different with other ones as a perennial plant (Table 2). The species were in red, purple, yellow, orange and green.

Light microscopy and modification of anatomical structure

The comparison of important anatomical characters of species reveals, that some structural changes of leaves were histologically decreased, while in some species increasing the cell size, cell wall thickness, vascular bundle dense area (phloem and xylem) and higher palisade parenchyma density compared with water storage parenchyma were observed. The palisade parenchyma cells were long and vertical or radiant to the vascular bundles. The development of mesophyll, that can be involved in increased photosynthetic activities is accompanied by reduced leaf area. Large bundle sheath (BS) cells are quite visible. These Kranz cells form bundle sheaths related to C_4 photosynthesis.

Usually, in all investigated species, the water storage tissue occupies the central part of the lamina, and its periphery, vascular bundles are located; the biggest bundles generally protrude toward the centre of the lamina.

B. prostrata was observed with more decrement in leaf surface, higher diameter of palisade parenchyma, while *B. turkestanica* was found to have an increase in leaf surface and less a decrease in the diameter of palisade parenchyma cells. *B. stellaris* is distinct with a very big irregular water storage parenchyma. In addition, numerous calcium oxalate crystals were noticed (Fig. 2A), more abundant in the palisade tissue cells and fewer in the water storage parenchyma. In studying the number of *Bassia* species, we recognized smaller size in leaf surface, more palisade cells in *B. pilosa*, the calcium oxalate crystals are fewer, but larger (Fig. 2E), especially located towards water parenchyma at the border to vascular bundles. In *B. turkestanica* (Fig. 2C), the calcium oxalate crystals seem to have a very precise localization, at the border of palisade and water storage tissues, thus having the occurrence of a regulate position.

The ratio between the length of palisade cells and development of water storage tissue, seem to be a very important trait in C_4 plants (Table 2).

Based on survey C_4 leaf anatomy, two subtypes of C_4 kochioid anatomy were recognized in the studied species as followed: 1.) *B. prostrata* subtype 2.) *B. scorparia* subtype include *B. pilosa*, *B. scoparia*, *B. turkestanica*, and *Bassia stellaris.*

Table 2. Comparison characters (morphological, anatomical and SEM of hair) in species of *Bassia*.

	B. scoparia	*B. prostrata*	*B. stellaris*	*B. pilosa*	*B. turkestanica*
Leaf phyllotaxis	Alternate	Alternate	Alternate	Alternate	Alternate
Leaf shape	Linear or lanceolate/ Acut apex	Linear or lanceolate/ Acut apex	Linear or lanceolate/ Acut apex	Linear or lanceolate/ obtuse apex	Linear or elliplic/ Acut or obtuse apex
Leaf length	50 ± 60	4 ± 30	4 ± 12	5 ± 6	3 ± 8
Leaf width	8 ± 10	1 ± 1.5	1 ± 1.5	1 ± 2.5	1 ± 3
Perianth ornamentation	-	-	-	+	-
Presence of hypodermis	-	+	-	-	-
Water storage parenchyma length (µm)	14.43 ± 5.99	14.95 ± 10.34	43.12 ± 12.99	30.61 ± 7.24	27.17 ± 4.56
Palisade parenchyma length (µm)	14.50 ± 6.11	23.57 ± 19.52	19.94 ± 7.08	17.62 ± 10.58	8.72 ± 8.34
Number of vascular bundles	12	18	17	8	22
Number of palisade cells	130	290	292	137	107
Number of water storage cells	55	37	35	50	57
Size of leaf surface (µm)	347/02	153/53	143/41	155/34	216/66
Hair ornamentation	Microechinate	Microechinate	Microechinate	-/seldom	Microechinate
Hair surface	Striate/ sulcate	Striate/sulcate	Striate/sulcate	Striate/sulcate	Striate/sulcate

SEM and leaf hairs morphology

Each studied species has hair possesses of similar shape, ornamentation and agglomeration. Most likely, the hair coverings keep a warm and dry microclimate of leaves, taking in considerations the ecological characteristics, where these species vegetate. In such conditions, hair increment (increase) is one of the morphological structural adaptations. The observed trichomes have high density and size in all species, and they have long hair, because of the ecological condition. Species investigated in the present study; simple, sulcate, striated hairs with small and microechinate/aculate ornamentation. The hair apex was sharp in the head (acute), but prominent at the end and on the base cuneate (Fig. 3F).

SEM micrographs of *Bassia* hair were compared and it showed that the hair in *B. pilosa* differs from other species and is non-ornamentation. Diagnostic character microechinate was found in *B. scoparia*, *B. turkestanica*, *Bassia stellaris* and *B. prostrata* (Fig. 3).

Discussion

Different organs showed relationships and structure correlations in many ways.

Morphological, micromorphological and anatomical features are important characteristics, that can be involved in taxonomical diagnosis, as well as in explaining ecological conditions, where halophytic species vegetate. *Bassia* genus in Flora of Iran has been divided into genera, including *Panderia*, *Kochia*, *Bassia*, and *Londesia* described by Assadi et al. (2001). According to Turki et al. (2006), *Kochia* and *Bassia* species were separated based on their morphology, anatomy and micromorphology. Based on morphological observations of the species, numerous similarities can be noticed, because of ecological and environmental conditions show a convergent evolution. Another important finding (Kadereit and Freitag 2011), that morphological studies showed a relationship and a convergence with phylogenetic analysis and suggested that there is a natural classification to distinct intra species and hence, *Panderia* and *Kochia* genera could be reclassified into genus as *Bassia*.

Adaptations made in morphology and anatomy due to facultative conditions among the species and the ecology. These include hairy cover on the perianth, leaf, and stem, yellow color of the leaves of some species, tiny flowers and photosynthetic system.

Grigore et al. (2012, 2014) described anatomical adaptive features in many halophyte species, including Chenopodiaceae, and the clarity of the adaptive structures in leaves, stems, and roots. Leaf anatomy in the studied species had C_4 kochioid photosynthetic system and dense mesophyll, which was due to dry and warm ecological conditions. They found that not all *Bassia* species have a C_4 photosynthetic pathway, despite similar ecological conditions; thus, *Bassia hyssopifolia* has the C_4 kochioid subtype, while *B. sedoides* and *B. hirsuta* were found to be C_3 species, based on the leaf anatomy. For all investigated species, *B. prostrata* presents a hypodermis, like other C_4 halophyte species (Grigore et al. 2014).

The presence of water storage parenchyma is very impor-

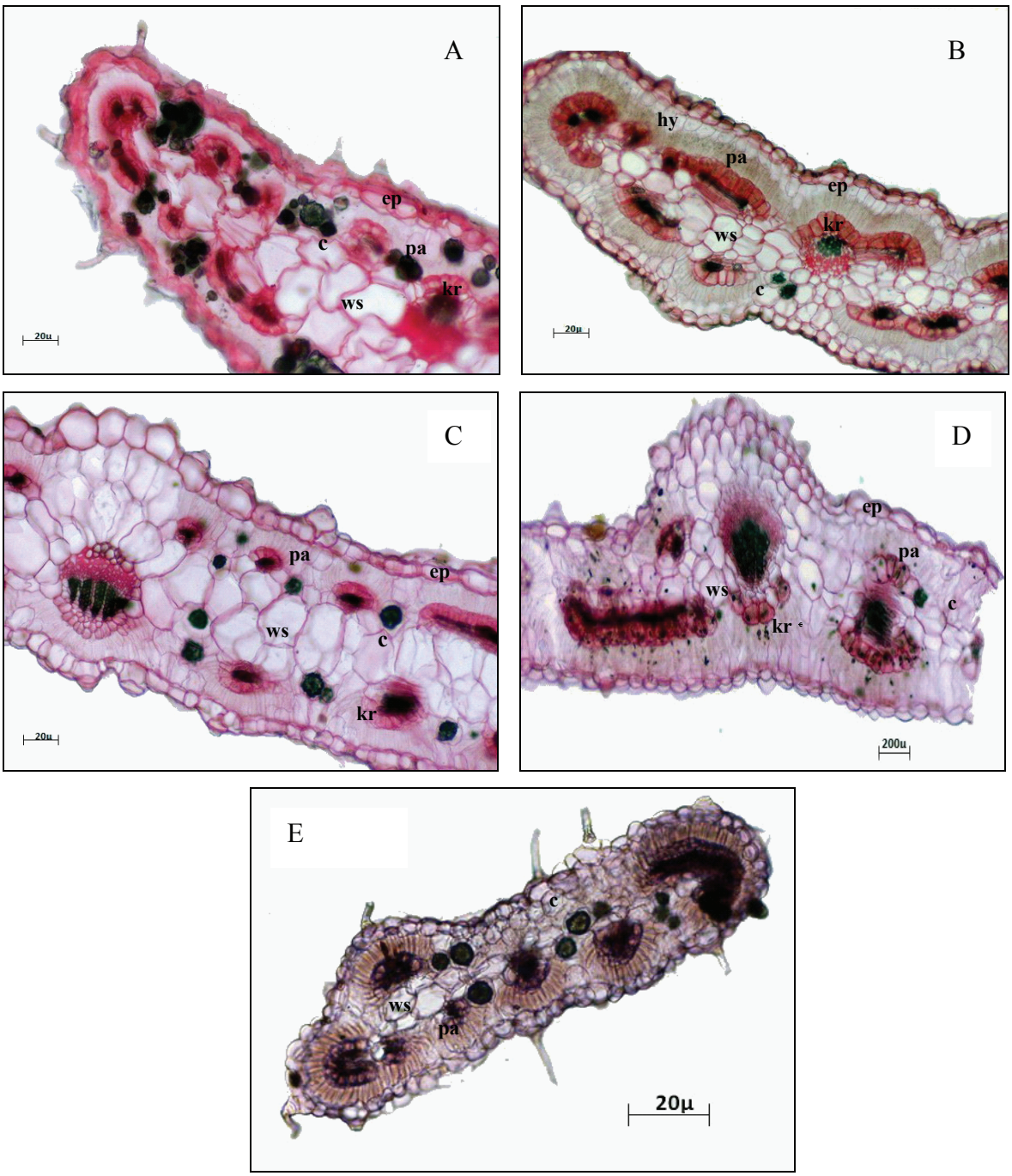

Figure 2. Cross sections of C_4 leaf in *Bassia stellaris* (A), *B. prostrata* (B), *B. turkestanica* (C), *B. scoparia* (D), and *B. pilosa* (E). c: crystal; ep: epidermis; kr: Kranz cells; hy: hypodermis; ws: water storage cell; pa: palisade cell.

tant in the direction of different metabolic processes related to C_4 photosynthesis; in addition, water deposit in the lamina of such species is explained by the ecological conditions, where these species grow, in environments dominated by dry and saline conditions. Bundle sheath cells surround the vascular bundles of the kochioid type of Kranz anatomy. In some individuals of *B. stellaris,* big water storage parenchyma was seen irregularly. According to observations, which made by (Payankov et al. 2010; Muhadit et al. 2007; Kaderedit et al. 2003) studies in phylogenetic and anatomical aspects, these

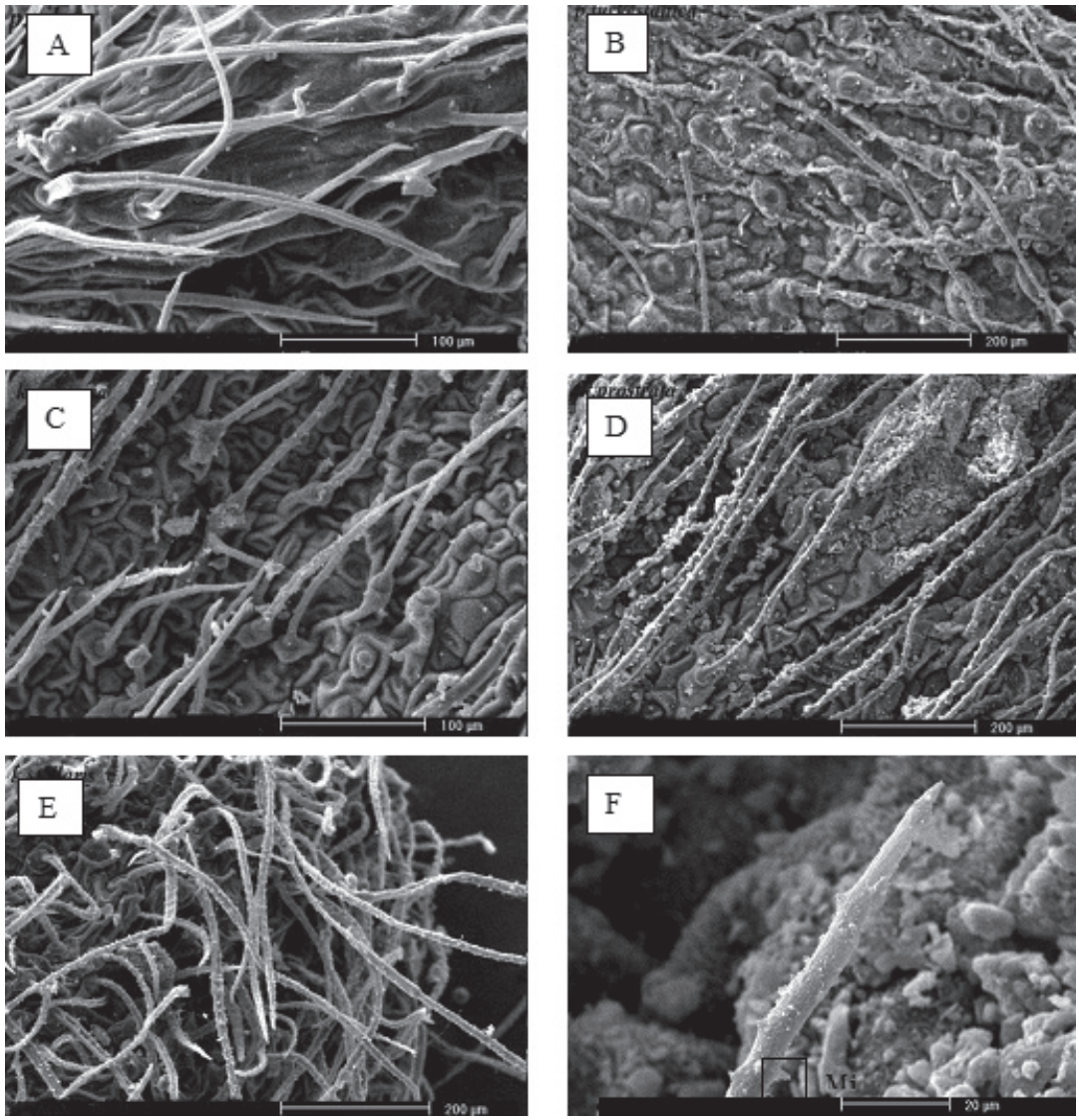

Figure 3. SEM micrographs of leaf hairs of *B. pilosa* (A), *B. turkestanica* (B), *B. scoparia* (C), *B. prostrata* (D), and *B. stellaris* (E). Microechinate (F).

similarities are due to convergence relationships. However, these adaptations could be different in some species. Freitag and Kadereit (2014) described two different types of Kranz anatomy kochioid and Atriplicoid in *Bassia* species. The Kranz cells form arcs along the xylem of peripheral bundles (Carolin et al. 1975; Jacobs 2001).

All investigated *Bassia* species have a C_4 photosynthetic pathway, based on the diagnosis of foliar anatomy. In the result of the study, C_3-C_4 does not quickly convert to C_4 in a single step. The tropism of palisade parenchyma around the bundle sheath is the most important development cause of the bundle sheath (Harold and Hatters Ley 1989). The result of this study indicated different types of the species based on C_4 kochioid photosynthetic system that the types are described based on the order. So, C_3 plesiomorphic conserved and C_4 apomorphic in this genus.

Based on the observed structure, it indicates that the most significant difference is between *B. turkestanica* and *B. pilosa*. Even some differences in perianth ornamentation were seen in the morphology of the vegetative form.

Grigore et al. (2014) have reported the presence of these crystals of calcium oxalate in many halophytic Chenopodiaceae. They assumed that beyond the possibility of being a common feature of the Chenopodiaceae family, the organic acids and the druses of calcium oxalate could be correlated with the metabolism of halophytes (Grigore et al. 2014). It

is known that the uptake of cations by plants is balanced partly by the absorption of inorganic anions and partly by the internal synthesis of organic anions (Waisel 1972). When the nitrates and the sulphates are assimilated or when the cations are absorbed excessively, a balancing with the help of organic anions in the growth processes is needed. In the case of many species of halophytes, the balance is made with the contribution of organic acids. Such organic acids can be excessively produced especially in the case of *Atriplex* species. The plants with such a metabolism can contain significant druses of calcium oxalate deposits. Hence, there are data suggesting that the oxalate synthesis is connected to the ionic balance. The druses of calcium oxalate can be considered as an effort to maintain the ionic balance (Franceschi and Horner 1980). The chemical leaf analyses of many halophytes species have shown that oxalic acid was present in notable quantities, appropriate to a high level of calcium oxalate (Osmond 1967).

For instance, the calcium oxalate in *Atriplex halimus* is the predominant compound of the total organic acid content. The content of this acid diminished only, when it was cultivated in weak ionic solutions (Mozafar et al. 1970). The same principle is applicable to other species, when the hydric potential of the tissues is low (Zolhevitch and Koretskaya 1959).

Osmond (1963) states that calcium oxalate was present in foliar cells as an antagonist for sodium and potassium.

The ecology of C_4 halophytic species is well-documented and supported (Ehleringer et al. 1997; Sage and Monson 1999; Tipple and Pagani 2007; Sage 2004). C_4 species form a particularly high proportion of the herbaceous flora of saline environments, even in cool temperate regions (Long and Mason 1983). Apparently, the inherently higher water use efficiency of C_4 species would have two theoretical advantages in saline environments (Long 1999). First, saline soils have a soil water potential of around 2.5 MPa; to extract water, the halophytes must generate a lower water potential, even though this exceeds limits that can apparently be tolerated by many mesophytic vascular plants. Transpiration must be minimal, and the higher water use efficiency of C_4 species would confer the advantage of maximizing carbon gain per unit of water lost. On the other side, plant mineral content is inversely correlated to water use efficiency as an assumed result of increased passive uptake with increased transpiration. For a halophyte, increased transpiration increases the energy needed to exclude Na^+ and Cl^- (Long and Mason 1983).

It has been suggested that halophytes are a special case among xerophytes (Wiessner 1899; Henslow 1895; Schimper 1903; Kearney 1904; Warming 1909; Clements 1920; McDougall 1941; Grigore and Toma 2010). This implies the occurrence of some mechanisms serving to protect the water reserves of the plant in periods of drought or high potential evapotranspiration when soil water potential fall. A cost of xeromorphy increased resistance to the diffusion of CO_2 to the mesophyll, because of the low leaf intercellular pressure, necessary to saturate C_4 photosynthesis, this cost is minimized in C_4 species.

Despite the fact, that C_4 species represent only about 8000 of the estimated 250000 to 300000 land plant species (Sage et al. 1999), they are major components of biomass that cover more than 35% of the Earth's land surface area. These species are dominant in tropical and subtropical grassland and savanna, warm temperate grassland and savanna, arid steppe, beach dunes, salt marshes, salt desert, hot deserts and semi deserts.

C_4 also represents an important ecological strategy in certain desert shrubs, most notably species of *Atriplex*, particularly in saline soils (Keeley and Rundel 2003). In these species, the key adaptation is the ability to maintain growth under high summer temperatures and drought conditions at a time when C_3 species are dormant. The maximal rates of photosynthesis in these desert C_4 species are generally no higher than that of concurring C_3 species, but the water use efficiency is far greater. In addition, C_4 plants have higher nitrogen use efficiency.

Some studies certify the close relationship between C_4 photosynthesis and extreme habitats such as deserts and salinized areas. Thus, Wang (2007) identified among species vegetating in the deserts of China that, 36.5% of the Chenopodiaceae species were found with C_4 photosynthesis, which was about 48% of the total C_4 species. These taxa were predominantly members of the genera *Anabasis, Atriplex, Kochia, Salsola,* and *Suaeda*.

Qualitative and quantitative differences in morphological and anatomical studies are also due to microevolution differences that are affected by ecologic and soil conditions. Akhani and Khoshravesh (2013) suggested that the hairy surfaces of the fruit of two species of *Bassia* are together with spinulose ornamentation. Our results indicated microechinate or spinulose ornamentation on the leaf surface. Having ornamentation such as microechinate on the hairy surface of the fruit and leave of the species. Morphological, anatomical and micromorphological observations indicated differences in the vegetative form, the ornamentation on the perianth surface and hair and photosynthesis subtype of C_4.

Conclusions

High morphological similarities exist among the species of Chenopodiaceae that are obvious in *Bassia* mixed genus. In addition to the phenotypic levels, they were also seen in anatomical and micromorphological structure levels. Qualitative and quantitative differences among *B. stellaris, B. scoparia* and *B. prostrata* are few, but significant differences were seen in anatomical, micromorphological and morphological as-

pects of the synonym species, *B. pilosa* and *B. turkestanicum*. Based on this, the two above mentioned species should be revised in the future. For better understanding of classification, also need phylogeny and cytogenetic study.

Acknowledgments

The authors thanks to Dr. Zahra Oraghi Ardebili, and Dr. Somayeh Kheiri for their help and support.

References

Aellen P (1965-1968) Chenopodiaceae. In Conert HJ, Hamann U, Schultze-Motel W, Wagenitz G, eds., Hegi G - Illustrierte Flora von Mitteleuropa. Parey, Berlin/ Hamburg, 533-747.

Akhani H, Trimborn P, Ziegler H (1997) Photosynthetic pathways in Chenopodiaceae from Africa, Asia and Europe with their ecological, phytogeographical and taxonomical importance. Plant Syst Evol 206(1-4):187-221.

Akhani H, Khoshravesh R (2013) The relationship and different C_4 Kranz anatomy of *Bassia eriantha* and *Bassia eriphora*, two often confused Irano-Turanian and Saharo-Sindian species. Phytotaxa 93(1):1-24.

APG II (2003) An update of the Angiosperm Phylogeny Group classification for the orders and families of flowering plants. APG II Bot J Linn Soc 141:399-436.

APG III (2009) An update of the Angiosperm Phylogeny Group classification for the orders and families of flowering plants. APG II Bot J Linn Soc 161:105-121.

Assadi M, Massoumi AA, Khatamsaz M (2001) Flora of Iran. Research Institute of Forests and Rangelands, Tehran 508.

Baillon HE (1887) Histoire des Plantes. Vol 5, Librairie Hachette, Paris.

Behnke HD (1976) Ultrastructure of sieve-element plastids in Caryophyllales (Centrospermae): evidence for the delimitation and classification of the order. Plant Syst Evol 126:31-54.

Bentham G, Hooker JD (1880) Genera Plantarum. Vol 3. Lovell Reeve, London.

Brown R (1810) Prodromus Florae Novae Hollandiae. Vol 1, Johnson, London.

Carolin RC, Jacobs SWL, Vesk M (1975) Leaf structure in Chenopodiaceae. Bot Jahrb Syst 95:226-255.

Chu G-L, Sanderson SC (2008) The genus *Kochia* (Chenopodiaceae) in North America. Madroño 55(4):251-256.

Clements FE (1920) Plant Indicators: The Relation of Plant Communities to Process and Practice. Carnegie Institution of Washington.

Cronquist A, Thorne RF (1994) Nomenclatural and taxonomic history. In Behnke HD, Mabry TJ, eds., Caryophyllales: Evolution and Systematics. Springer, Berlin, 5-25.

Cuénoud P, Savolainen V, Powell M, Grayer RJ, Chase MW (2002) Molecular phylogenetics of the Caryophyllales based on combined analyses of 18S rDNA and *rbcL*, *atpB* and *matK* sequences. Am J Bot 89:132-144.

Ehleringer JR, Cerling TE, Helliker BR (1997) C_4 photosynthesis, atmospheric CO_2 and climate. Oecologia 112:285-299.

Franceschi VR, Horner HT (1980) Calcium oxalate crystals in plants. Bot Rev 46(4):361-427.

Freitag H, Kadereit G (2014) C_3 and C_4 leaf anatomy types in Camphorosmeae (Camphorosmoideae, Chenopodiaceae). Plant Syst Evol 300:665-687.

Grigore MN, Toma C (2010) Halofitele. Aspecte de Anatomie Ecologica. Editura Universitatii Alexandru Ioan Cuza, Iasi.

Grigore MN (2012) Romanian Salt Tolerant Plants. Taxonomy and Ecology Edit. Tehnopress, Iasi.

Grigore MN, Toma C, Zamfirache MM, Boscaiu M, Olteanu Z, Cojocaru D (2012) Ecological anatomy in halophytes with C_4 photosynthesis: discussing adaptative features in endangered ecosystems. Carpat J Earth Environ Sci 7(2):13-21.

Grigore MN, Ivanescu L, Toma C (2014) Halophytes. An integrative anatomical study. Springer, Cham, Heidelberg, New York, Dordrecht, London.

Haber RM, Semaan MT (2007) A new record from Lebanon: *Panderia pilosa* Fish. & C. A. Mey (Chenopodiaceae). Turk J Bot 31:157-158.

Harold BR, Hattersley WP (1989) Leaf anatomy of C_3-C_4 species as related to evolution of C_4 photosynthesis. Plant Physiol 91:1543-1550.

Hatami E, Khosravi, AR (2013) Mapping of geographic distribution of C_3 and C_4 species of the family Chenopodiaceae in Iran. Iran J Bot 19(2):263-276.

Hedge IC, Akhani H, Freitag H, Kothe-Heinrich G, Podlech DR, Uotila P (1997) Chenopodiaceae. In Rechniger KH, ed., Flora Iranica. Vol. 172. Akademische Druck-und Verlagsanstalt, Graz, Austria.

Henslow G (1895) The Origin of Plant Structures by Self-Adaptation to the Environment. London, Kegan Paul, Trench, Trübner.

Jacobs SWL (2001) Review of leaf anatomy and ultrastructure in the Chenopodiaceae (Caryophyllales). J Torrey Bot Soc 128:236-253.

Kadereit G, Borsch T, Weising K, Freitag H (2003) Phylogeny of Amaranthaceae and Chenopodiaceae and the evolution of C_4 photosynthesis. Int J Plant Sci 164(6):959-986.

Kadereit G, Freitag H (2011) Molecular phylogeny of Camphorosmeae (Camphorosmoideae, Chenopodiaceae): Implications for biogeography, evolution of C_4 photosynthesis and taxonomy. Taxon 60(1):51-78.

Kearney TH (1904) Are plants of sea and dunes true halophytes? Bot Gaz 37:424-436.

Keelley JE, Rundel OW (2003) Evolution of CAM and C_4 carbon-concentrating mechanisms. Int J Plant Sci 164:(3 Suppl)55-77.

Kühn U, Bittrich V, Carolin R, Freitag H, Hedge IC, Uotila P, Wilson PG (1993) Chenopodiaceae. In Kubitzki K, ed., Families and Genera of Vascular Plants. Vol 2. Springer, Berlin, 253-281.

Long SP, Mason CF (1983) Saltmarsh Ecology. Blackie, Glasgow.

Long SP (1999) Environmental responses. In Sage RF, Monson RK, eds., C_4 Plant Biology. Academic Press, San Diego, London, Boston, New York, Sydney, Tokyo, Toronto, 215-249.

McDougall WB (1941) Plant Ecology (3rd ed). Lea & Febiger, Philadelphia.

Moquin-Tandon A (1849) Amaranthaceae. In de Candolle AP, ed., Prodromus Systematis Naturalis Regni Vegetabilis. Vol 13. Masson, Paris, 231-241.

Mozafar A, Goodin JR, Oertli JJ (1970) Na and K interaction in increasing the salt tolerance of *Atriplex halimus* L. Yield characteristics and osmotic potential. Agron J 62:478-481.

Muhaidat R, Sage FR, Dengler GN (2007) Diversity of Kranz anatomy and biochemistry in C_4 eudicots. Am J Bot 94(3):362-381.

Osmond CB (1963) Oxalates and ionic equilibria in Australian saltbushes (*Atriplex*). Nature 198:503-504.

Osmond CB (1967) Acid metabolism in *Atriplex*. I. Regulation of oxalate synthesis by the apparent excess cation absorption in leaf tissue. Aust J Biol Sci 20:575-587.

Payne W (1978) A glossary of plant-hair terminology. Brittonia 30:239-255.

Peterson L, Carol A, Lewise H (1986) Teaching plant anatomy theory creative laboratory exercise. NRC Research Press 154:63-119.

Purvis MJ, Collier DC, Walls D (1966) Laboratory Techniques in Botany. 2nd ed., Butterworths, London, 439.

Pyankov VI, Ziegler H, Akhani H, Deigele C, Luttge U (2010) European plants with C_4 photosynthesis: geographical and taxonomic distribution and relations to climate parameters. Bot J Linn Soc 163:280-305.

Sage FR, Monson RK (1999) C_4 Plant Biology. Academic Press, San Diego, London, Boston, New York, Sydney, Tokyo, Toronto.

Sage RF, Wedin DA, Li M (1999) The biogeography of C_4 photosynthesis: patterns and controlling factors. In Sage RF, Monson RK, eds., C_4 Plant Biology. Academic Press, San Diego, London, Boston, New York, Sydney, Tokyo, Toronto, 313-373.

Sage RF (2004) The evolution of C_4 photosynthesis. New Phytol 161:341-370.

Schimper AFW (1903) Plant Geography upon a Physiological Basis. Clarendon Press, Oxford. UK.

Scott AJ (1978) A revision of the Camphorosmoideae (Chenopodiaceae). Feddes Repert 89:101-119.

Tipple BJ, Pagani M (2007) The early origins of terrestrial C_4 photosynthesis. Annu Rev Earth Planet Sci 35:435-461.

Thorne RF (1976) A phylogenetic classification of the Angiospermae. Evol Biol 9:35-106.

Turki Z, El-Shayeb F, Sehata F (2006) Taxonomic studies in the Camphorosmeae (Chenopodiaceae) in Egypt. 1. Subtribe Kochiinae (*Bassia*, *Kochia* and *Chenolea*) Flora Med 16:275-249.

Ulbrich E (1934) Chenopodiaceae. In Engler A, Prantl K, eds., Die Natürlichen Pflanzenfamilien. Vol 16c. Engelmann, Leipzig, 379-584.

Volkens G (1893) Chenopodiaceae. In Engler A, Prantl K, eds., Die Natürlichen Pflanzenfamilien. Vol 1a. Engelmann, Leipzig, 36-91.

Zohari M (1973) Geobotanical Foundation of the Middle East. CRC Press, London, UK.

Zolkevitch VN, Koretskaya TF (1959) Metabolism of pumpin roots during drought. Fiziol. Rast 6:690-700.

Waisel Y (1972) Biology of halophytes. Academic Press, New York, London.

Wang RZ (2007) C_4 plants in the deserts of China: occurrence of C_4 photosynthesis and its morphological functional types. Photosynthetica 45(2):167-171.

Warming E (1909) Oecology of Plants. An introduction to the study of plant-communities. Clarendon Press, Oxford, UK.

Wiessner J (1899) Uber die Formen der Anpassung der Blatter an die Lichtstarke. Biol. Centralbl 19:1-14.

Volume 61(1):95-104, 2017
Acta Biologica Szegediensis
http://www2.sci.u-szeged.hu/ABS

ARTICLE

Pollen morphological diversity in the genus *Acer* L. (Sapindaceae) in Iran

Sedigheh Nikzat Siahkolaee[1]*, Masoud Sheidai[1], Mostafa Assadi[2], Zahra Noormohammadi[3]

[1]Faculty of Life Sciences & Biotechnology, Shahid Beheshti University, Tehran, Iran
[2]Research Institute of Forest and Rangelands, National Botanical Garden of Iran, Tehran, Iran
[3]Biology Department, Islamic Azad University, Sciences and Research Branch, Tehran, Iran

ABSTRACT Pollen grains of 19 specimens (representing 8 species, 6 subspecies, 3 sections) of the genus *Acer* L. distributed in Iran were investigated by scanning electron microscopy. Most of pollen grains were 3-zonocolpate, prolate. Based on exine sculpturing pattern, five types are distinguished: striate (frequent type), rugulate, reticulate, granular and smooth. Twenty-four pollen characters were examined by multivariate analysis. The result of multivariate analysis and exine sculpturing pattern indicated high diversity among different specimens even in specimens of a single species. Due to instability of pollen characters between and within studied specimens, they are not useful in delimitation of species, subspecies and sections. Only three species (*A. velutinum*, *A. negundo*, and *A. mazandaranicum*) were separated from other overlapping species. Pollen morphology does not confirm separation of subspecies and varieties in *A. monspessulanum* and *A. velutinum*.
Acta Biol Szeged 61(1):95-104 (2017)

KEY WORDS
Acer
plant systematic
pollen diversity
Sapindaceae

Introduction

The genus *Acer* L. belongs to Sapindaceae family and comprises 124-156 species (van Gelderen et al. 1994; de Jong 2004). This genus has 16 sections in recent classification (van Gelderen et al. 1994). The genus is easily recognized by opposite leaves and samaras fruit. However, other morphological characters are highly diversified. Due to morphological diversity, many varieties and forms were generated that makes the genus taxonomically very difficult (Delendick 1990; Park et al. 1993; Judd et al. 2002).

The *Acer* species does not produce large quantities of pollen (de Jong 1994). The pollens are generally tricolpate, isopolar and prolate to nearly spheroidal (de Jong 1994). Several studies have been conducted using light microscopy and SEM in order, to describe pollen grain features in the genus (Philbrick and Bogel 1981; Wodehouse 1935; Erdtman 1952; Praglowsk 1962; Helmish 1963; Biesboer 1975; Pozhidaev 1993; Gogichaishvili 1964; Loma et al. 2015). The results revealed high degree of diversity in pollen morphological characters even in populations of a single species (Philbrick and Bogle 1981). However, Loma et al. (2015) indicated the importance of pollen characters in identification and taxonomy of some *Acer* species in Himalayas. Four pollen types have been recognized in the genus *Acer* based on exine ornamentation including striate, rugulose, granular, and microreticulate (Biesboer 1975). Moreover, Pozhidaev (1995) indicated that pollen characteristics in *Aesculus* correspond to the sectional division. Also, natural polymorphism and deviation from typical forms have been observed in this genus (Dzyuba et al. 2006; Pozhidaev 1993). In Iran, the genus *Acer* comprises of 8 species: 6 species based on Flora Iranica (Murray 1969), one is newly recorded by Maroofi and Sharifi (2006), and another one is newly reported by Amini et al. (2008).

The genus consists of two main centers of distribution in Iran, namely Alborz (Northern Iran) and Zagros (Northwest to Southeast Iran). *A. velutinum* (with two varieties), *A. mazandaranicum*, *A. cappodocicum*, *A. hyrcanum*, *A.campestre*, *A. platanoides* and *A. monspessulanum* (with five subspecies) grow in both Alborz (*A. monspessulanum* subsp. *ibericum* & *turcomanicum*) and Zagros (*A. monspessulanum* subsp. *assyriacum*, *A. monspessulanum* subsp. *persicum*, *A. monspessulanum* subsp. *cinerascence*) (Murray 1969). *A. negundo* (sec. *negundo*) was introduced and cultivated as an ornamental tree.

The Iranian *Acer* species belong to section *Acer* (*A. velutinum*, *A. monspessulanum*, *A. hyrcanum)* and section *Platanoidea (A. cappadocicum*, *A. platanoides*, and *A. campestre)*. These sections are considered highly diverse, regard

Submitted January 29, 2017; Accepted May 17, 2017
*Corresponding author. E-mail: nikzat.sedighe@gmail.com

Table 1. *Acer* species and their localities.

Features	Locality*	Voucher number
A. hyrcanum	Gilan pr., Talesh	Pouramini 4028 (HSBU)
A. mazandaranicum	Gilan pr., Talesh	Pouramini 4029 (HSBU)
A. campestre	Gilan pr., Talesh	Pouramini 4022 (HSBU)
A. campestre	Mazandaran pr.	Assadi 78725 (TARI)
A. cappodocicum	Mazandaran pr.	Nikzat 4031 (HSBU)
A. cappodocicum	Gilan pr., Talesh	Poramini 4030 (HSBU)
A. platanoides	Gilan pr., Talesh	Pouramini 4024 (HSBU)
A. velutinum var. *velutinum*	Mazandaran pr.	Nikzat 4036 (HSBU)
A. velutinum var. *velutinum*	Gilan pr., Lahijan	Esfandani 4035 (HSBU)
A. velutinum var. *glabrescense*	Golstan pr., Gorgan	Nikzat 4034 (HSBU)
A. velutinum var. *glabrescens*	Mazandaran pr.	Nikzat 4033 (HSBU)
A. velutinum var. *velutinum*	Gilan pr., Siahkal	Nikzat 4032 (HSBU)
A. monspessulanum subsp. *turcomanicum*	North Khorasan pr., NE Shirvan	Joharchi 4025 (HSBU)
A. monspessulanum subsp. *persicum*	Kerman pr., Deh Bakri, Nayyer Mt.	Assadi 15940 (TARI)
A. monspessulanum subsp. *cinerascens*	Lorestan pr., Delfan	Masoumi 4027 (HSBU)
A. monspessulanum subsp. *cinerascens*	Kermanshah pr.	Masoumi 4026 (HSBU)
A. monspessulanum subsp. *cinerascens*	Isfahan pr., Semirom	Assadi 2044 (HSBU)
A. monspessulanum subsp. *ibericum*	Mazandaran pr., Siah Bisheh	Nikzat 4037(HSBU)
A. negundo	Tehran pr., Shahid Beheshti Univ.	Nikzat 4023 (HSBU)

* pr. = province; Mt. = Mountain

to molecular and morphological characteristics (Grimm and Denk 2013). Given to lack of our knowledge about pollen morphology of Iranian *Acer* species, we aim to: (I) describe pollen characters in Iranian *Acer* and (II) evaluate taxonomic importance of palynological data. We will compare our result with the data available from the earlier investigations in three sections; *Parviflora*, *Rubra* and *Macrantha* (Philbrick and Bogle 1981).

Materials and Methods

Pollen grains of 19 populations were studied by scanning electron microscope (SEM) in the following *Acer* species: *A. campestre* L., *A. velutinum* Boiss (var. *velutinum* & var. *glabrescense*), *A. cappadocicum* Gled, *A. hyrcanum* Fisch & C. A. Mey, *A. monspessulanum* (subsp. *cinerascence*, subsp *ibericum*, subsp. *turcomanicum*, subsp. *ibericum*, subsp. *persicum*), *A. platanoides* L., *A. mazandaranicum*, and *A. negundo* (cultivated species in Iran). The pollen samples were obtained mostly from fresh plant materials as well as from herbarium materials. Voucher specimens have been deposited in Shahid Beheshti University Herbarium (HSBU) and herbarium of Iran's Research Institute of Forests and Rangelands (TARI) (Table 1). Small quantities of pollen were attached to aluminum stubs with double-sided cellophane tape and coated with goal. The specimens were examined with a Phillips × L20 SEM. UTHSCSA Image Tool Version 3.0 was used to carry out required measurements. Statistical analysis including PCOA and PCA were performed using PAST software for plotting variation among populations and species (Hammer et al. 2001).

Ten to 30 fully developed pollen grains were randomly selected for analysis. Eleven quantitative and 13 qualitative palynological features were used for multivariate analysis including pattern of sculpturing (SC), type of branching in lira (BT), situation of lira after branching (SB), width ratio of lira & stria (WR), arrangement of lira to each other (AL), arrangement of lira to polar axis (ALP), shape of pit (SP), size of pit (SZP), distribution of pits (DP), regular of lira arrangement (RL), having resembling leaf venation (LV), width of mesocolpium (WM), width of lira (WL), length of colpus (LC), ratio of width in two ends of mesocolpium (RWE), number of lira in 25 μm^2 area (NL), polar axis length (P), equatorial axis length (E), ratio of polar axis to equatorial axis (P/E), number of branches in 25 μm^2 area (NB), number of pit in 25 μm^2 area (NP), ratio of colpus/P (RCP), shape of pollen (SP) (Table 2). Principal Components Analysis (PCA) was performed among the specimens to determine palynological features useful for separating the species. In order, to group the species, cluster analysis using UPGMA (Unweighted Paired Group with Arithmetic Average) methods and PCA ordination plot were performed using Euclidean and taxonomic distance among the species was calculated (Podani 2000). Exine sculpture elements were measured on the

Table 2. Details of examined characters of *Acer* specimens in this study.

Specimen	SC*	BT*	SB*	WR*	AL*	ALP*	SP	SZP	DP	WM	RL*	LV*LV*
A. hyrcanum	Type I-A	2	1	3	1	2	1	1	1	3	1	1
A. mazandaranicum	Type I-A	2	1	3	3	4	1	1	1	1	2	3
A. campestre	Type I-B-1	2	1	3	2	4	2	2	2	1	1	1
A. cappodocicum	Type I-B-2	1	2	2	3	2	2	3	3	3	2	1
A. cappodocicum	Type I-A	2	1	3	2	2	2	1	1	2	1	1
A. platanoides	Type I-B-1	1	1	3	3	4	1	2	2	4	2	1
A. velutinum var. *velutinum*	Type I-B-2	2	1	2	1	4	2	3	3	4	2	2
A. velutinum var. *velutinum*	Type I-B-2	2	1	1	2	1	3	2	3	3	1	3
A. velutinum var. *glabrescense*	Type I-B-3	1	2	2	3	3	3	2	3	4	2	2
A. velutinum var. *glabrescense*	Type I-B-2	2	2	2	1	1	3	3	3	4	1	3
A. velutinum var. *velutinum*	Type I-B-2	2	1	2	1	1	3	3	3	2	1	3
A. monspessulanum subsp. *turcomanicum*	Type I-B-3	1	1	2	3	4	3	3	3	2	2	1
A. monspessulanum subsp. persicum	Type I-B-1	2	1	3	2	4	3	2	2	4	2	1
A. monspessulanum subsp. *cinerascens*	Type I-B-2	1	2	2	3	2	1	3	3	4	2	2
A. monspessulanum subsp. *cinerascens*	Type I-B-2	1	1	1	2	4	3	2	3	1	2	2
A. monspessulanum subsp. *cinerascens*	Type I-B-2	2	2	1	2	2	1	2	2	2	1	1
A. monspessulanum. subsp. *ibericum*	Type II-B	1	1	3	3	4	1	2	2	1	2	2
A. negundo	Type II-A &III	1	1	3	3	4	1	1	1	1	2	2

Specimen	WMM*	WL	LC	RWE	NL	P	E	P/E*	NB	NP	RCP	SP
A. hyrcanum	13.77±1.7	1.9±0.2	34.08±1.56	0.94	12	41.12±2.17	21.61±1.58	1.9	3	0	0.83	1
A. mazandaranicum	15.43±1.25	1.58±.03	35.04±1.13	0.89	10	42.34±1.84	20.16±2.01	2.1	5	0	0.83	2
A. campestre	19.56±1.56	1.57±0.4	31.76±6.16	0.91	10	43.22±4.49	28.93±3.96	1.49	10	14	0.73	1
A. cappodocicum	18.34±1.61	1.29±0.24	46.52±.55	0.82	9	59.62±2.03	31.99±4	1.86	5	27	0.78	1
A. cappodocicum	35.79±1.73	1.34±0.04	42.4±2.89	0.82	12	50.78±3.56	35.79±2.24	1.41	3	0	0.83	1
A. platanoides	16.76±1.89	0.97±0.08	46.87±3.19	088	11	48.09±3.41	26.66±2.12	1.8	9	25	0.97	1
A. velutinum var. *velutinum*	19.41±1.45	1.21±0.22	45.83±2.94	0.76	12	53.67±3.81	29.66±1.01	1.8	2	39	0.85	1
A. velutinum var. *velutinum*	18.52±1.84	1.24±0.45	43.74±3.30	0.82	13	52.63±2.12	27.18±0.96	1.93	4	33	0.85	1
A. velutinum var. *glabrescense*	19.19±1.55	1.01±0.42	47.64±4.61	0.9	11	64±2.04	29.43±2.72	2.17	9	48	0.74	2
A. velutinum var. *glabrescense*	22.65±2.67	0.95±0.18	47.65±4.61	0.94	14	59.66±3.15	34.81±4.19	1.71	13	29	0.8	1
A. velutinum var. *velutinum*	18.96±1.68	1.32±0.14	48.41±2.48	0.85	11	60.43±1.92	30.65±1.47	1.97	5	43	0.8	1
A. monspessulanum subsp. *turcomanicum*	15.68±1.52	1.01±0.33	43.87±2.58	0.72	10	51.33±3.25	26.14±1.61	1.96	27	80	0.85	1
A. monspessulanum subsp. *persicum*	20.76±2.34	1.15±0.15	47.42±2.03	0.91	12	53.74±1.52	32.94±2.58	1.63	5	10	0.88	1
A. monspessulanum subsp. *cinerascens*	20.23±1.89	1.48±0.62	48.49±1.94	0.69	10	52.31±2.17	28.87±1.22	1.81	5	22	0.93	1
A. monspessulanum subsp. *cinerascens*	13.27±1.87	1.11±0.13	45.7±2.13	0.9	11	52.65±3.14	26.73±1.01	1.96	10	24	0.87	1
A. monspessulanum subsp. *cinerascens*	17.98±1.51	1.4±0.53	45.87±1.84	0.69	13	49.85±1.89	26.45±1.46	1.88	7	35	0.92	1
A. monspessulanum subsp. *ibericum*	9.41±2.19	1.21±0.39	35.91±2.29	0.94	12	43.06±1.58	18.19±1.65	2.36	13	27	0.83	2
A. negundo	13.43±1.16	1.22±0.45	31.07±1.96	0.84	11	38.88±1.62	23.67±1.52	1.64	25	0	0.8	1

SC: Pattern of sculpturing of pollen; BT: type of branching in lira (1: short and branched, 2: long and branched); SB: situation of lira after branching (1: close to each other, 2: far from each other); WR: width ratio of lira & stria (1: equal, 2: stria wider than lira, 3: lira wider than stria); AL: arrangement of lira to each other (1: parallel, 2: semi-parallel, 3: intersection); ALP: arrangement of lira to polar axis (1: parallel, 2: semi-parallel, 3: perpendicular, 4: variously arranged); SP: shape of pit (1: lack pit, 2: roundish, 3: roundish sometime elliptic); SZP: size of pit (1: lack pit, 2: similar diameter, 3: different diameter); DP: distribution of pits (1: lack pit, 2: sparse, 3: numerous); RL: regular of lira arrangement (1: regular, 2: irregular); LV: having resembling leaf venation (1: not having, 2: having in two pole, 3: having in one pole); WMM: width of mesocolpium (1: equal in throughout length, 2: narrow in one pole, 3: equal in two pole (pole acute) and wider in middle, 4: equal in two pole (pole wide) and wider in middle); WL: width of lira (μm); LC: length of colpus (μm); RWE: ratio of width in two ends of mesocolpium; NL: number of lira in 25 μm^2 area; P: polar axis length (μm); E: equatorial axis length (μm); P/E: ratio of polar axis to equatorial axis; NB: number of branches in 25 μm^2 area; NP: number of pit in 25 μm^2 area; RCP: ratio of colpus/P; SP: shape of pollen (1: prolate, 2: preprolate).

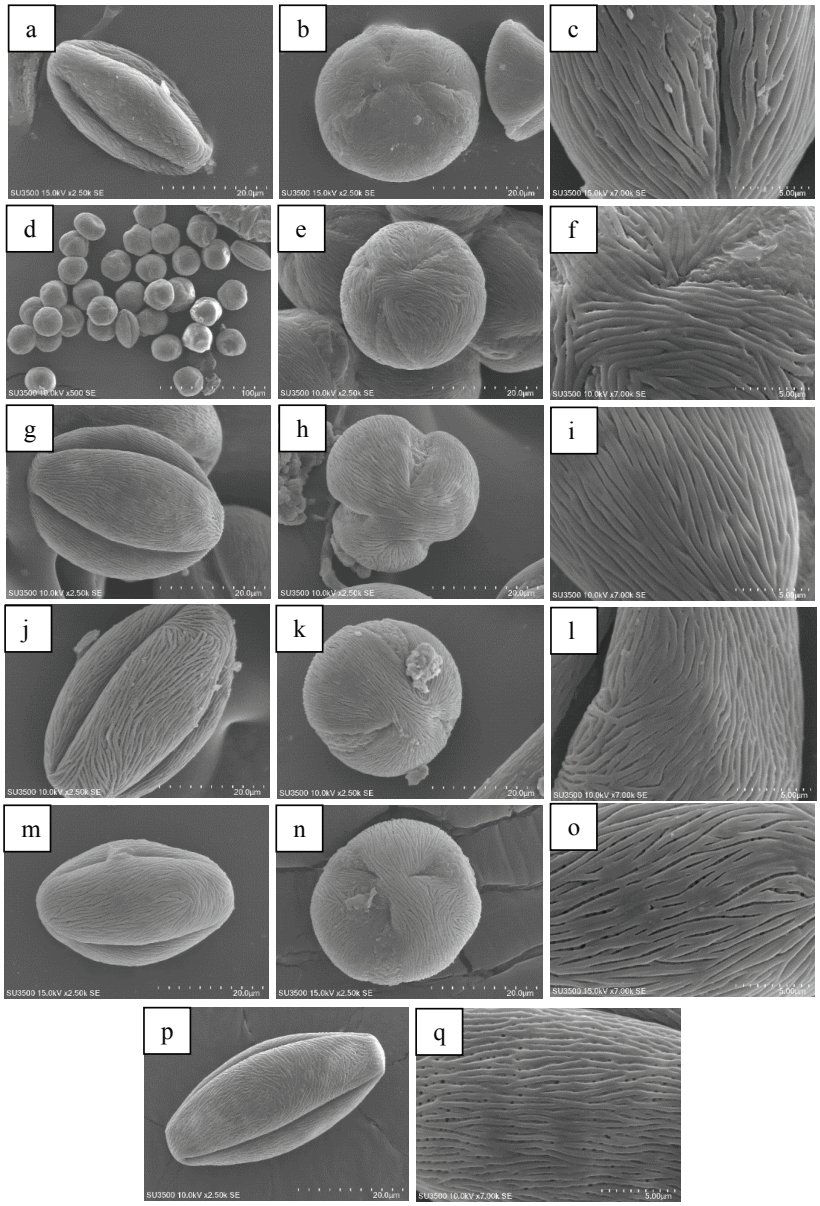

Figure 1. SEM micrographs of pollen grains in *Acer* sp. type I-A: (a-c) *A. hyrcanum*, (d-f) *A. mazandaranicum*, (g-i) *A. cappodocicum* (Talesh specimen). Type I-B-1: (j-l) *A. monspessulanum* subsp. *persicum*, (m-o) *A. campestre* (Talesh), (p,q) *A. platanoides*.

area of 25 μm^2. The terminology follows Hesse et al. (2009) and Erdtman (1952) that lira is a narrow ridge, which forms the murus in a striate pattern and stria is a groove between elongated sculpturing elements.

In addition to studied specimens, the pollen data of *A. spicatum* (sec. parviflora), *A. pensylvanicum* (sec. macrantha), *A. rubra* and *A. saccharinum* (sec. rubra) from other studies were used for sectional analyzes. The common features used for analyzing were shown by asterisks in Table 2.

Results

General pollen grain features

The pollen grain type ranged from prolate (Figs. 1a, j, m, p; 2a, d, g, j, m, p, s, v; 3a, g) to preprolate (Figs.1g; 3d, j) in equatorial view and spheroidal (Figs. 1b, e, h, k; 2b, x; 3b, e, h, n), oblate-spheroidal (Figs. 1n; 2y) to prolate-spheroidal

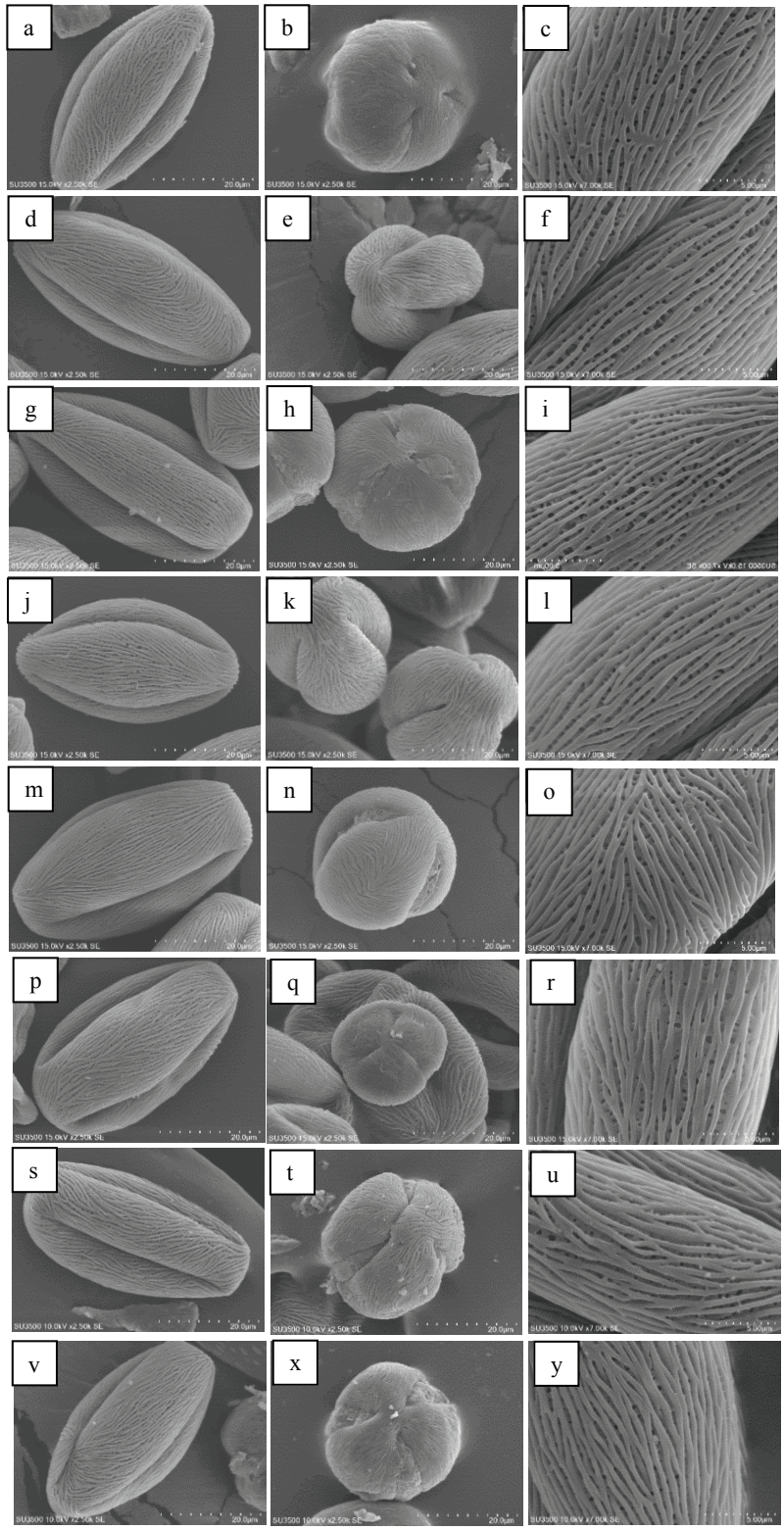

Figure 2. SEM micrographs of pollen grains in *Acer* sp. Type I-B-2: (a-c) *A. cappodocicum* (Toskacheshme specimen), (d-f) *A. velutinum* var. *velutinum* (Toskacheshmeh), (g-i) *A. velutinum* var. *velutinum* (Siahkal), (j-l) *A. velutinum* var.*velutinum* (Lahijan), (m-o) *A. velutinum* var. *glabrescens* (Shirgah), (p-r) *A. monspessulanum* subsp. *cinerascens* (Lorestan), (s-u) *A. monspessulanum* subsp. *cinerascens* (Kermanshah), (v-y) *A. monspessulanum* subsp. *cinerascens* (Esfahan).

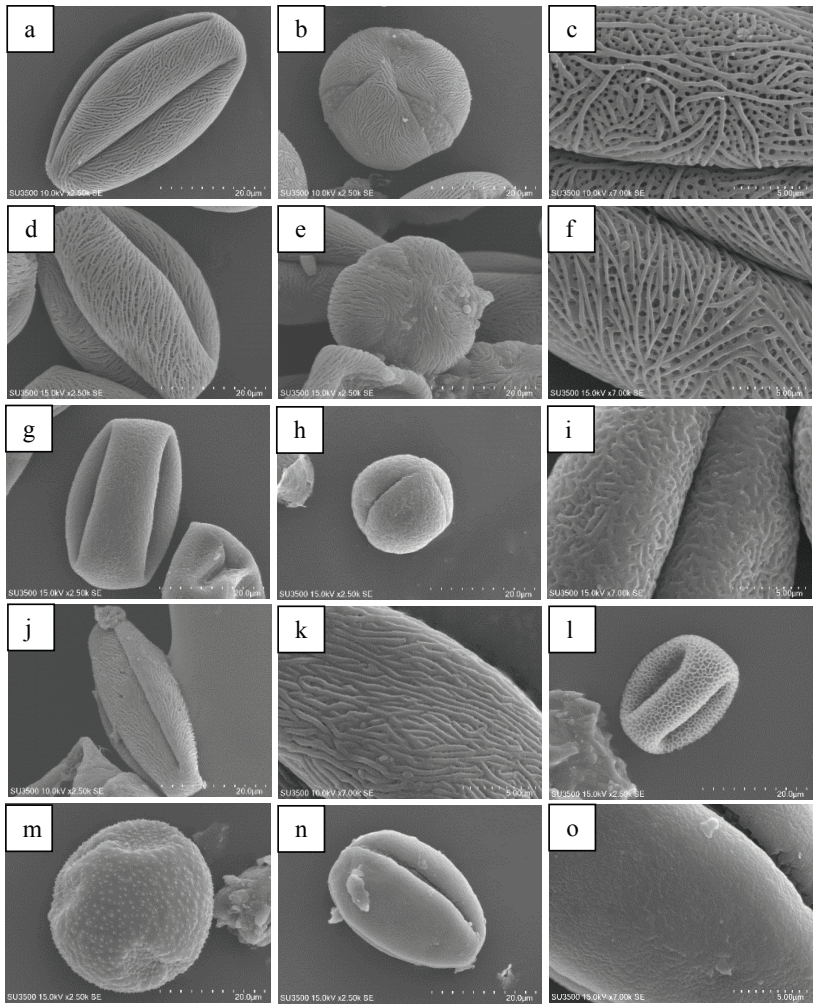

Figure 3. SEM micrographs of pollen grains in *Acer* sp. Type I-B-3: (a-c) *A. velutinum* var. *glabrescens* (Gorgan), (d-f) *A. monspessulanum* subsp. *turcomanicum*, type II-A: (g-i) *A. negundo*, type II-B: (j-l) *A. monspessulanum* subsp. *ibericum*, type III: (m) *A. negundo*, type IV: (n) *A. campestre* (Siahbishe), type V: (o) *A. campestre* (Siahbishe).

(Fig. 2t) in polar view. There were mainly zonocolpate (rarely 3-porate in *A. campestre*) (Fig. 3n) pollen grains with colpus extending the full length of the pollen grain. Mean length of the pollen grains varied from 38.88 µm (*A. negundo*) to 64 µm (*A. velutinum* var. *glabrescense*), while the width varied from 18.9 µm (*A. monspessulanum*. subsp. *ibericum*) to 35.79 µm (*A. cappodocicum*). The main colpus length varied from 31.07 (*A. negundo*) to 48.49 µm (*A. monspessulanum* subsp. *cinerascence*). According to the 8 analyzed species, the P/E ratio varied from 1.41 (*A. cappodocicum*) to 2.36 µm (*A. monspessulanum* subsp. *ibericum*). The main features of the investigated pollen grains are summarized in Table 2.

Three types were recognized based on mesocolpium width: (1) equal throughout the length (Figs. 1m; 2s; 3d, g) (2) narrow in one pole (Figs. 1g; 2g, 2v; 3d) and (3) wider in middle, while equal in two pole (poles acute or wide) (Figs. 1a, j, p; 2a, d, j, m, p; 3a, j).

Infrageneric variation

PCA analysis (Fig. 4) did not support the sectional classification of the studied species. The species of the sections *Acer* and *Platanoideae* were placed intermixed in the PCA plot.

PCOA analysis separated *A. velutinum* from the other studied species (Fig. 5), while *A. monspessulanum*, *A. hyrcanum*, and *A. mazandaranicum* overlapped. *A. hyrcanum*, *A. mazandaranicum*, *A. negundo*, *A. velutinum* and *A. monspessulanum* were separated from each other.

The PCA results, which represented the first three factors comprising about 66% of all the variation, showed that

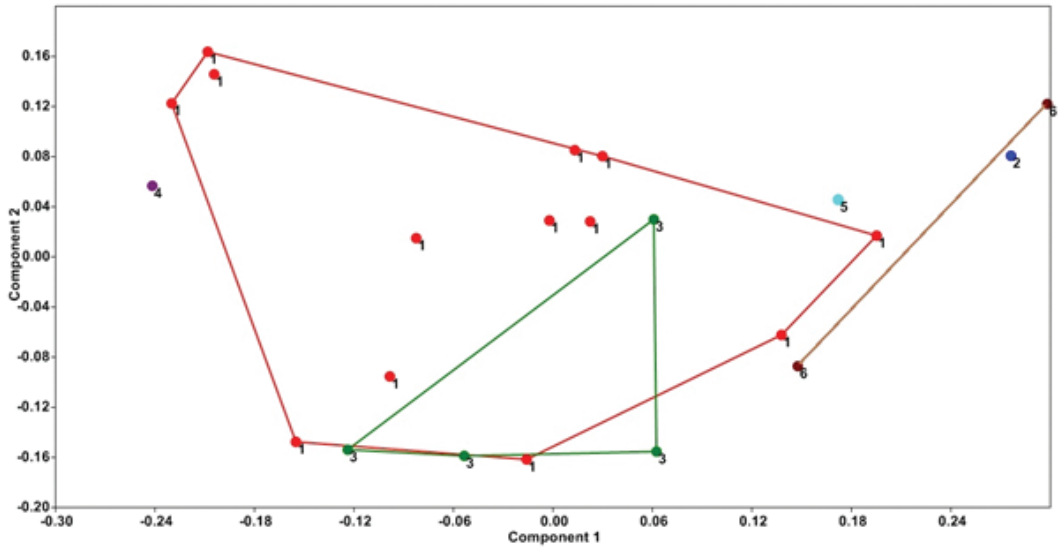

Figure 4. PCOA of *Acer* species studied based on palynological data. 1: sec. *Acer*; 2: sec. *Negundo*; 3: sec. *Platanoideae*; 4: sec. *Parviflora*; 5: sec. *Macrantha*; 6: sec. *Rubra*.

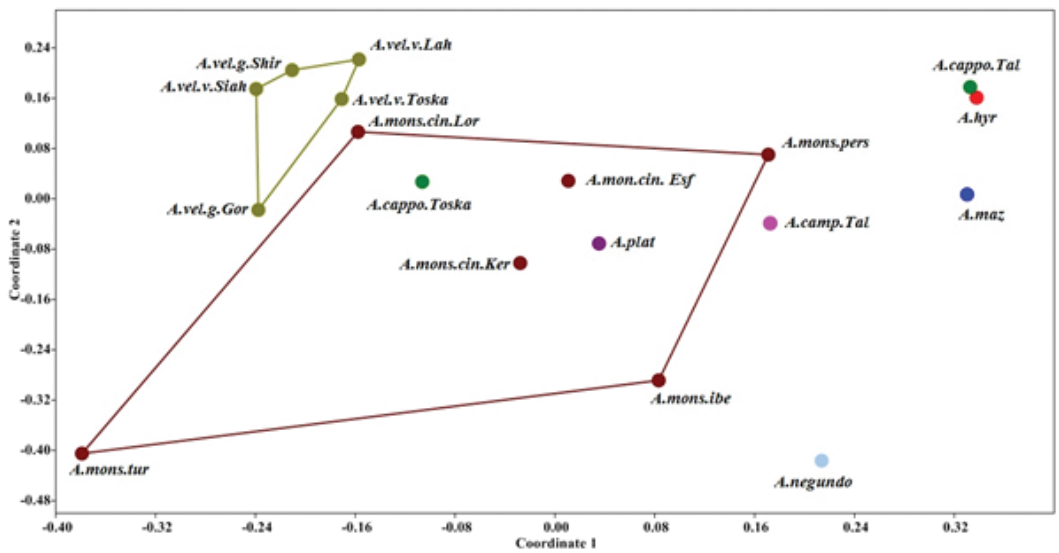

Figure 5. PCOA of palynological characters. Species abbreviations: A. hyr = *A. hyrcanum*, *A. maz* = *A. mazandaranicum*, *A. cappo.* Tal = *A. cappodocicum* (Talesh), A. cappo = *A. cappodocicum* (Toskacheshme), *A. camp*. Tal = *A. campestre* (Talesh), A. vel. v. Toska = *A. velutinum* var. *velutinum* (Toskacheshme), A. vel. v. Lah = *A. velutinum*. var. *velutinum* (Lahijan), *A. vel. v*. Siah = *A. velutinum*. var. *velutinum* (Siahkal), *A. vel. g*. Shir = *A. velutinum*. var. *glabrescence* (Shirgah), *A. vel. var. g.* Gor = *A. velutinum* var. *glabrescence* (Gorgan), *A. mons. Turc* = *A. monspessulanum* subsp. *turcomanicum*, *A. mons. Ibe* = *A.monspessulanum*. subsp. *ibericum*, *A. mons. cin*. Lor = *A. monspessulanum* subsp. *cinerascens* (Lorestan), *A. mons. cin*. Ker = *A. monspessulanum* subsp. *cinerascens* (Kermanshah), *A. mons. cin*. Esf = *A. monspessulanum* subsp. *cinerascens* (Esfahan), *A. mons. pers* = *A. monspessulanum* subsp. *persicum.*

features such as number of pit in 25 μm^2 area, shape, size, distribution of pit and sculpturing pattern, number of branching in 25 μm^2 area, and arrangement of lira to axis were the most variable pollen characteristics. UPGMA tree (Fig. 6) indicated that two varieties of *A. velutinum* overlapped together and pollen features were not useful in their delimitation. Distribution of two subspecies of *A. monspessulanum* (*persicum* and *cinerascens*) were close together and sometimes overlap each other. UPGMA tree based on pollen features, showed that these subspecies have close affinity together, and pollen characteristics are basically in accordance with their taxonomic similarities (Figs. 5, 7).

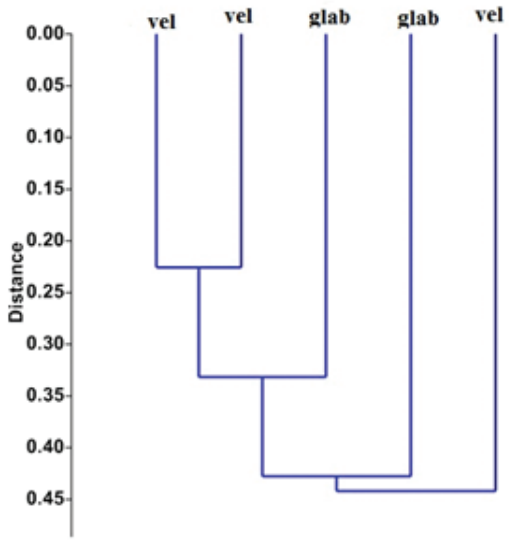

Figure 6. UPGMA tree of *A. velutinum* (vel) with two subspecies: *velutinum* (vel), and *glabrescens* (glab).

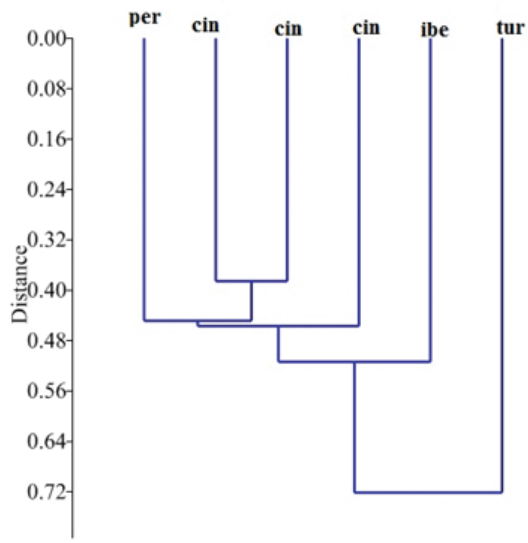

Figure 7. UPGMA tree of four *A. monspessulanum* subspecies: *turcomanicum* (tur), *ibericum* (ibe), *persicum* (per), and *cinerascence* (cin).

Exine sculpture type

On the basis, of differences in exine sculpturing pattern, the following five type are recognized: striate, rugulate, reticulate, granular, and smooth. Most of the specimens belong to striate pattern.

Type (I): striate

This type is recognized by distribution of lira throughout pollen surface. This type is subdivided according to the presence or absence of perforation between lira; type I-A with no perforation (Figs. 1c, f, i) and type I-B with striate perforation. Regarding to density and diameter of perforation, there are three different pattern in type I-B. Type I-B-1 with sparse perforation (Figs. 1l, o, q) and type I-B-2 with abundance and small to moderate perforation (Figs. 2c, f, i, o, r, u, y) and type I-B-3 with dense and large perforation (Figs. 3a, f, i).

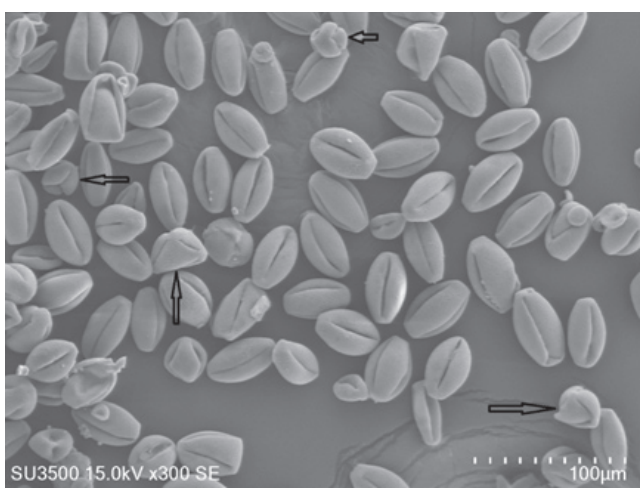

Figure 8. Deviated forms (shown by arrows) of typical form of pollen in *A. velutinum* var. *glabrescens* (Shirgah).

Type (II): rugulate

In this type, rugulate are irregularly arranged. This type is intermediate between striate and reticulate pattern. Based on intervals of rugulate, this type is subdivided to type II-A: rugulate with small intervals (*A. negundo*) (Fig. 3g) and type II-B: striate rugulate with large intervals (*A. monspessulanum* subsp. *ibericum*) (Fig. 3j).

Other exine sculpture types

The other patterns observed in this study are uncommon in genus *Acer*. Reticulate type (type III) was only observed in one specimen (*A. negundo*) (Fig. 3m) accompanied with low frequency of type II in the same individual. The granular type (type IV) was only observed in *A. campestre* (Fig. 3n). The smooth type (type V) was reported for the first time in genus *Acer* and co-occurred with type IV in *A. campestre* (Figs. 3o, p).

Irregularities observed

In *A. velutinum* var. *glabrescen*s (Shirgah) an irregular form of

pollen morphology was detected with low frequency (Fig. 6). This form is characterized by a 4-colpate (syncolpate) pollen with colpi arranged on the edges of a tetrahedron.

Discussion

Acer is a taxonomically diverse genus due to large variation in leaf shape, inflorescence structure and other morphological traits (Delendick 1990; Park et al. 1993). Our study indicated a similar variation in pollen morphological features even in different specimens of the same species. Pollen characters vary among studied material. However, delimitation of *Acer* species is difficult due to instability of these characters within the species. These results are in agreement with Oterdoom and de Jong (in maples of world book, van Gelderen et al. 1994), who suggested a limited application of pollen morphology for delimiting the sections in Aceraceae.

Philbrick and Bogle (1981) indicated inter- and intraspecific instability of important characters in *Acer* (*i.e.* apocolpium area index, P, E, P/E). Similar diversity of pollen morphological characters was reported by Lama et al. (2015) in Eastern Himalaya.

Hybridization provides a possible explanation for the extensive morphological variability in the genus *Acer* (Tirmenstein 1991). In this study, intermediate morphologies found in some specimens (*A. monspessulanum* subsp. *persicum*, *A. campestre* (Talesh), *A. platanoides*) may be due to the high occurrence of hybridization and gene flow inter- and intraspecies. It seems that exine sculpture is important in genus *Acer*, so that Biesboer (1975) distinguished four types among 40 taxa of *Acer*. Also, Clarke and Jones (1978) indicated that European maple belong to two Biesboer types. In this survey, most of taxa belong to Biesboer type I with high diversity regarding distribution, size, density, length and width of pits, distance and arrangement of stria.

According to our study, the common shape of pollen in Iranian distributed species was zonocolpate and prolate. Zonocolpate, subprolate to prolate pollens was reported in native New England species (Philbrick and Bogle 1981) and three colporate, prolate to nearly spheroidal forms were observed in eastern Himalaya species. Two subspecies of *A. monspessulanum* (*persicum* and *cinerascense*) show high similarity in morphological features so that sometimes distinguishing between them is controversial. These subspecies are distributed in Zagros Mountains and approximately distinct from two other subspecies (*trucomanicum* and *ibericum*), which are distributed in Alborz Mountain (Figs 7, 5). However, there is variability in most characters in subspecies of this species, especially in exine sculpture of pollen and there are no significant differences among the subspecies of *A. monspessulanum*.

In *A. velutinum*, the stability of characters related to perforation (size, distribution, shape) separates all specimens of this species from the other species.

High variation in features in two specimens of *A. cappodocicum* nested *A. cappodocicum* (Toskacheshme) among *A. monspessulanum* specimens. *A. hyrcanum* has morphological affinity to *A. monspessulanum*, but this survey indicated that these two species are located far from each other. The pollen type of *A. negundo* (cultivated species in Iran) was reported as regulate in previous studies (Philbrick and Bogle 1981; Kupriyanova and Aleshina 1972). The present study indicated that the reticulate type co-occurs with rugulate type.

The variability of pollen morphological characters is reported in other families such as *Malus* (Nazeri 2008), *Pyrus* (Zamani et al. 2010) and *Sorbus* (Bedworz and Maciejewska-Rutkowska 2005).

In many dicotyledon taxa, the deviated pollen forms can be found in the common forms (Pozhidaev 1993). These forms were reported in *Aesculus* (Pozhidaev 1995), *Acer tataricum* (Dzyuba 2006) and 31 species of 58 studied *Acer* species (Pozhidaev 1993). These uncommon forms vary in the number and arrangement of their typical aperture. We reported two deviated forms (4 colpate with different arrangement of colpus) for the first time in *A. velutinum* (Shirgah). The question of how and why these forms arise presents some difficulty. Pozhidaev (1995) proposed that the polarization in pollen cytoplasm conformation can induce the formation of deviated forms. Dzyuba et al. (2006) suggested that unfavorable ecological conditions increase frequency of these untypical forms.

Acknowledgements

The authors wish to thank Saeed Javadi Anaghizi in Central laboratory of the Shahid Beheshti University for providing SEM pictures.

References

Amini T, Zare H, Assadi M (2008) *Acer mazandaranicum* (Aceraceae), a new species from northern Iran. Iran J Bot 14(2):81-86.

Bednorz L, Maciejewska-Rutkowska I (2005) Pollen morphology of the Polish species of the genus *Sorbus* L. Acta Soc Bot Pol 74(4):315-322.

Biesboer DD (1975) Pollen morphology of the Aceraceae. J Grana 15(1-3):19-28.

Clarke GCS, Jones MR (1978) Aceracea. Rev Palaeobot Palynol 26:181-193.

de Jong PC (2004) World Maple Diversity. International Maple Symposium. Gloucestershire, England, Westonbirt Arboretum and Royal Agricultural College.

de Jong PC (1994) Taxonomy and reproductive biology of maples. In van Gelderen DM, de Jong PC, Oterdoom HJ, eds., Maples of the World. Timber Press, Portland, USA, 69-104.

Delendick TJ (1990) A survey of foliar flavonoids in the Aceraceae. Mem New York Bot Gard 54:1-129.

Dzyuba OF, Schurekova OV, Tokarev PL (2006) On the natural polymorphism of pollen grains of *Acer tataricum* L. Paleontol J 40(5):90-S594.

Erdtman G (1952) Pollen morphology and Plant Taxonomy. I. Angiosperms. Almsqvistand & Wiksell, Stockholm, Sweden.

Gogichaishviu LK (1964) The Morphology of the Maple Pollen for the Purpose of Pollen Analysis. United States Department of Agriculture and the National Science Foundation, Washington, USA.

Grimm GW, Denk T (2014) The Colchic region as refuge for relict tree lineages: cryptic speciation in field maples. Turk J Bot 38:1050-1066.

Hammer Ø, Harper DAT, Ryan PD (2001) Past: Paleontological statistical software package for education and data analysis. Palaeontol Electron 4(1):9.

Hesse M (1979) Ultrastruktur und Verteilung der Pollenkitt in der Insekten - und Windblutigen Gattung *Acer* (Aceraceae). Plant Syst Evol 131:277-289.

Hesse M, Halbritter H, Zetter R, Weber M, Buchner R, Frosch-Radivo A, Ulrich S (2009) Pollen Terminology - An Illustrated Handbook. Springer Wien, New York. 264 pp.

Helmich DE (1963) Pollen Morphology in the Maples *(Acer)*. Papers of the Michigan Academy of Science, Arts and Letters. Vol XLVIII.

Judd WS, Campbell CS, Kellogg EA, Donoghue MJ (2002) Plant Systematics: A Phylogenetic Approach, 2nd ed. Sinauer Associates, Sunderland, MA. 576 pp.

Kupriyanova LA, Aleshina LA (1972) Pollen and Spores of Plants of the European USSR (Nauka, Leningrad) Vol. 1 [in Russian].

Lama D, Moktan S, Das AP (2015) Diversity of pollen morphological characters in *Acer* Linnaeus (Sapindaceae) from Darjiling and Sikkim Himalayas. Biodiversity in Indian Tropical Ecosystem 153-165.

Maroofi H & Sharifi K (2006) *Acer tataricum* (Aceraceae), a new collection from W. of Iran. Iran J Bot 12(1):57-58.

Murray E (1969) Aceraceae in K. H. Rechinger Flora Iranica, no 61. Graz 11.

Nazeri JV (2008) Pollen morphology of the genus *Malus* (Rosaceae). Iran J Sci Technol 32:A2.

Park CW, Oh S, Shin H (1993) Reexamination of vascular plants in Ullung Island, Korea II: Taxonomic identity of *Acer takeshimense* Nakai (Aceraceae). Korean J. PI. Taxon (23):217-231.

Philbrick CT, Bogel AL (1981) The pollen morphology of the New England species of the genus *Acer* (Aceraceae). Rhodora 83(834):237-258.

Podani j (2000) Introduction to the Exploration of Multivariate Biological Data, English translation, Backhuys Publishers, Leiden 407 pp.

Pozhidaev A (1993) Polymorphism of Pollen in the Genus *Acer* (Aceraceae): Izomorphizm of Deviate Form of Angiosperm Pollen, Grana 32:79-85.

Pozhidaev A (1995) Pollen morphology of the genus *Aesculus* (Hippocastanaceae). Grana (34):10-20.

Praglowski J (1962) Notes on the pollen morphology of Swedish trees and shrubs. Grana Palyno 13(2):45-65.

Tirmenstein DA (1991) *Acer saccharum*. In Fire Effects Information System, [online]. U.S. Department of Agriculture, Forest Service, Rocky Mountain Research Station, Fire Sciences Laboratory (Producer).

van Gelderen DM, de Jong PC, Oterdoom HJ (1994) Maple of the World. Timber Press, Portland, Oregon, 458 pp.

Wodehouse RP (1935) Pollen Grains-Their Structure, Identification and Significance in Science and Medicine. Hafner Pub. Comp, New York, USA.

Zamani A, Attar F, Maroofi H (2010) Pollen morphology of the genus *Pyrus* (Rosaceae) in Iran. Acta Biol Szeged 54(1):51-56.

Volume 61(1):105-118, 2017
Acta Biologica Szegediensis
http://www2.sci.u-szeged.hu/ABS

DISSERTATION SUMMARIES

H2S confers colonoprotection against TNBS-induced colitis by HO-1 upregulation in rats

Amin Al-awar

Department of Physiology, Anatomy and Neuroscience, Faculty of Science and Informatics, University of Szeged, Szeged, Hungary

Ulcerative colitis (UC) is a chronic debilitating disease requiring patient hospitalization; however, despite rapidly developing new therapies there are unanswered questions regarding causes, course, treatments and outcomes. The standard approach to treatment is administration of intravenous steroids, but about 40% of patients fail to respond to this. The conventional UC therapy including aminosalicylates, corticosteroids, immune modulators, are associated with a limited response, loss of response, or specific side effects and ~ 25% of patients may undergo colectomy due to the failure of treatment. The advances in understanding the pathogenesis and drug response of UC led to multiple efforts to develop specific therapies, which could target unique elements mediating disease-related immunopathology.

Hydrogen sulfide (H_2S) is an endogenous mediator that contributes to many important physiological processes including vasodilation and vascular smooth muscle relaxation; in turn, preventing tissue damage and reducing inflammation. In the gastrointestinal tract, H_2S production is vital for the maintenance of mucosal integrity and for promoting the resolution of inflammation and healing of ulcers. Heme oxygenase (HO) enzymes, of which HO-1 is inducible to harmful stimuli, was found to regulate intestinal inflammation in experimental animal models. Thus, our aim was to investigate the protective effects of H_2S against 2,4,6-trinitrobenzenesulfonic acid (TNBS) - induced colitis in rats, and whether HO enzyme system is involved in the H_2S- induced colonic cytoprotection. Male Wistar rats were treated with TNBS to induce colitis, and H_2S donor (Lawesson's reagent) was prepared 2 times/day at different concentrations, and delivered per os (from day 1 to 3). Colon samples were collected after 72 hours of TNBS treatment, to measure the extent of inflammation, myeloperoxidase (MPO) level, HO activity, tumor necrosis factor-α (TNF-α) content, protein expression, CBS and CSE enzyme activities. In addition, separate experiments were conducted to test the inhibitory effect of HO, parallel to TNBS intracolonic (i.c.) administration and co-treatment with H_2S donor. Daily treatment (2 times/day) with H_2S donor could significantly decrease the extent of colonic inflammation compared to vehicle-treatment, and the most effective daily dose of H_2S donor against inflammation was 18.75 μM/kg/day. Per os administration of H_2S donor, reduced TNBS-provoked MPO activity and TNF-α level, while increased the colonic HO enzyme activity. In contrary, the protective effect of H_2S was abolished by the co-treatment with HO inhibitor. CBS and CSE enzyme activity decreased insignificantly in EtOH and TNBS treated groups, while significant increase was shown on the protein level. Our findings suggest that H_2S confers colonoprotection, probably by modulation of inflammatory parameters and HO enzyme activity.

Supervisor: Krisztina Kupai
E-mail: amin@expbio.bio.u-szeged.hu

In vitro somatic embryogenesis on *Arabidopsis* root explants

Dóra Bernula

Institute of Plant Biology, Biological Research Centre of the Hungarian Academy of Sciences, Szeged, Hungary

In higher plants, several developmental pathways can lead to embryo formation. Somatic embryogenesis (SE) can be induced from vegetative (sporophytic) plant cells *in vitro* by exposing explants to plant hormones (*e.g.,* auxins) and/or stress treatments. *Arabidopsis thaliana* is the most widely used model of plant developmental biology including *in vitro* plant regeneration. However, until now SE research in *Arabidopsis* was mostly limited to direct or indirect SE from immature/mature zygotic embryos due to the absence of an efficient and easy system using more differentiated tissues. Our aim was firstly to establish an efficient experimental system for studying SE *in vitro Arabidopsis* root cultures. In this system the emergence of the lateral root primordia was induced by auxin and the transdifferentiation of this primordia to shoot meristem could be induced on cytokinin-containing medium. We observed that if cytokinin-induced roots were transferred onto hormone-free medium at appropriate time points, somatic embryos appeared on the root surface instead of shoots. To characterize this system, molecular (gene expression measurement by RT-qPCR for the genes *ARABIDOPSIS THALIANA SEED GENE 1* (*ATS1), FUSCA 3 (FUS3), WUSCHEL (WUS) and LEAFY COTYLEDON 1 (LEC1)*) and cellular techniques (stereomicroscope, scanning electron microscope) were used. Furthermore, several embryogenesis marker lines and mutants (*lec1* and *fus3*) were created or collected for functional studies. Our results indicated that this *in vitro* root system can indeed be used for SE induction in a predictable way. In many

in vitro SE systems, the most common inducer is the auxin, however, in our system SE was induced by cytokinin. Therefore, we examined the effect of endogenous auxin transported from the shoot to the root on cytokinin-mediated SE formation on the roots of whole seedlings. We could show that blocking the auxin transport by the application of the auxin transport inhibitor TIBA (2,4,6-triiodobenzoic acid) or removing the shoot resulted more efficient cytokinin-induced embryo formation on induced *Arabidopsis* seedlings. Our results highlighted the importance of proper cytokinin/auxin balance for the parallel induction of shoot and root meristems during SE.

Supervisors: Attila Fehér, Katalin Gémes
E-mail: bernulad@gmail.com

Microbial degradation of hydrophobic organic compounds in polluted environments

Attila Bodor

Department of Biotechnology, Faculty of Science and Informatics, University of Szeged, Szeged, Hungary

Pollution of soils and waters by petroleum products or other oil-related compounds are still among the major environmental concerns due to accidental oil-spills or reckless human activity. These hydrophobic, organic compounds may represent serious risks to natural communities or human health. Several physicochemical and biological technologies are available in order, to remove these pollutants from the environment, but these methods still need further developments. Bacterial communities occur in aqueous and even in oil phases so isolation and examination of bacterial strains with the ability of hydrocarbon degradation from these oily environments can provide a promising tool for biological remediation and better understanding of the impact on structure and composition of microbial communities in oil-polluted niches. Aiming the bioremediation of a railway station area contaminated with engine oil containing long chain compounds, hydrocarbon-degrading bacterial strains were isolated from mazut, which is the bottom product of the atmospheric distillation process of crude oil. These new isolates were compared to other oil-degraders can be found in our departmental strain collection. Further small-scale biodegradation experiments were performed in the oil-contaminated soil to model and monitor a bioremediation process. Although, the optimal conditions of biodegradation are still barely revealed and need development, our results represent a targeted tool for bioconversion of petroleum products and on the other hand, brings us closer to our final goal, which is the complete bioremediation of an oil-polluted railway station area.

Supervisor: Katalin Perei
E-mail: bodor.attila@gmail.com

Salt stress-induced changes in ROS metabolism in wild type and ethylene receptor mutant *Never ripe* tomato: response of plants to exogenous ethylene precursor ACC

Péter Gábor Borbély

Department of Plant Biology, Faculty of Science and Informatics, University of Szeged, Szeged, Hungary

The synthesis of the gaseous plant hormone ethylene (ET) is readily activated when plant tissues are encountered with supra optimal salt concentrations. To reveal the effects of excess ET without stress, we investigated the most important physiological functions in wild type (WT) tomato (*Solanum lycopersicum* cv. Rio Fuego) exposed to immediate precursor of ethylene, 1-aminocyclopropane-1-carboxylic acid (ACC), in hydroponic culture. ACC is oxidised to ET by ACC oxidase that maintains elevated ethylene levels in treated plants. ACC applied at 0.01-100 µM concentrations caused significant changes in dry mass, ion accumulation and photosynthetic activity of plants during 7 days. In other words, ET generated from exogenous ACC may interfere with both ionic and osmotic components of salt stress. In order to reveal the physiological action of salt stress-induced ET, the effects of 100 mM, sublethal and 250 mM, lethal NaCl concentrations were investigated in WT and *Never ripe* (*Nr*) mutants of tomato (*S. lycopersicum* cv. Ailsa Craig). *Nr* mutants have a non-functional ET receptor; thus, they significantly lost the capacity to respond to ET in all tissues. The salt stress induced ET production both in WT and *Nr* plants. In contrast to WT plants, reduced K^+/Na^+ ratio was observed in *Nr* roots under sublethal salt stress, suggesting that the inhibition of ethylene signalling increased ionic stress in tomato exposed to high salinity. The nitro-oxidative stress was stronger in *Nr* roots, which

led to the programmed death of cells in root tips. In the leaves, $O_2^{\cdot-}$ accumulation was also significantly higher under sublethal salt stress in *Nr* mutants. Since $O_2^{\cdot-}$ production is mainly associated with the activity of photosystem I (PSI) in photosynthesizing tissues, PSI activities of *Nr* and WT leaves were determined. In *Nr* plants we found higher expression of FeSOD and Cu/ZnSOD localized to chloroplast and that of MnSOD localized to mitochondria, while the activity of the chloroplastic enzymes was also higher in the mutants. However, ET elevated artificially by 10 μM ACC (applied simultaneously with NaCl) caused significant changes in $O_2^{\cdot-}$ production in the leaves of WT plants and altered ROS, NO and $ONOO^-$ levels under salt stress.

Supervisor: Irma Tari
E-mail: borbely.peter01@gmail.com

How plants connect nutrient and energy status to growth regulatory mechanisms: regulatory links between energy sensor SnRK1 and growth regulatory E2F-RBR pathway

Márta Deli

Institute of Plant Biology, Biological Research Centre of the Hungarian Academy of Sciences, Szeged, Hungary

Coupling growth and cell proliferation with the available nutrient and energy supply is fundamental for cellular homeostasis, but in plants the mechanisms are little understood. Based on our data together with recent development in this field, RBR, the single retinoblastoma-related protein in *Arabidopsis* is in the focal point of many signalling events involving nutrients, energy and light for fine-tuning the rate of growth and proliferation. Similarly, to animal Rb proteins, the plant RBR is predominantly regulated on a post-translational level, mostly by phosphorylation. Previously we have shown that sucrose can stimulate RBR phosphorylation through a well-conserved cell cycle regulatory mechanism including cyclin-dependent kinases as the major players. Here we found that light can rapidly stimulate RBR phosphorylation, but only in the presence of functional chloroplasts. We suggest that the energy sensor SnRK1 could be involved in this regulation, but whether directly or indirectly is yet unknown. We demonstrated that SnRK1 is present in different protein complexes to regulate diverse processes in young developing seedlings. In nutrient limited conditions, we identified II class trehalose phosphate synthase (TPS) proteins as integral parts of the SnRK1 complex. In contrast to the stress-related SnRK1, RBR was found to associate with SnRK1 in non-stressed conditions. We suggest that RBR with SnRK1 could regulate normal developmental processes such as meristem maintenance. The RBR protein was sensitive to carbon and energy starvation and AKIN10 could regulate the protein abundance of RBR. Altogether our data indicates that RBR and SnRK1 are intimately connected in many effective ways.

Supervisor: Zoltán Magyar
E-mail: delimarti@hotmail.com

ELONGATED HYPOCOTYL 5 mediates light signaling to the plant circadian clock

Orsolya Katalin Dobos

Institute of Plant Biology, Biological Research Centre of the Hungarian Academy of Sciences, Szeged, Hungary

Circadian clocks are timing mechanisms providing daily rhythms for a wide range of molecular and physiological processes. Eukaryotic clocks are built on gene networks, where clock genes and the encoded clock proteins form interlocked regulatory loops capable of autonomous 24-h oscillations at the level of gene expression. Importantly, this primary oscillation is synchronized with the environmental light/dark cycles by light signals, which are perceived by wavelength-specific photoreceptors and eventually cause a change in the abundance or the activity of selected clock components. In plants, several clock genes are light-responsive offering entry points for synchronizing light stimuli. However, the final molecular steps of this process are poorly understood. ELONGATED HYPOCOTYL 5 (HY5), a bZIP transcription factor functions downstream of several photoreceptors and regulates the expression of more than a thousand responsive genes. Here we show that the function of the clock is impaired in hy5 mutants displaying short period rhythms in a blue light-dependent manner. We demonstrate that the phenotype arises from blue light-induced accumulation of HY5 in wild-type plants that is mediated by transcriptional and post-transcriptional mechanisms. We demonstrate that the blue light-induced change in HY5 levels modulates its binding to specific promoter elements of selected clock genes, activating or repressing their transcription. The HY5-dependent change in the expression level

of these genes is consistent with the period phenotype of hy5 mutants. Taken together, we identify HY5 as a component of the light-quality signaling pathway to the circadian oscillator in plants.

Supervisor: László Kozma-Bognár
E-mail: orsolya.dobos91@gmail.com

Characterization of regulatory genes controlling abiotic stress responses in higher plants

Dóra Faragó

Institute of Plant Biology, Biological Research Centre of the Hungarian Academy of Sciences, Szeged, Hungary

Extremophile plants are valuable sources of genes conferring tolerance traits, which can be explored to improve stress tolerance of crops. *Lepidium crassifolium* is a halophytic relative of the model plant *Arabidopsis thaliana*, and displays tolerance to salt, osmotic and oxidative stresses. During the identification of stress tolerance genes, the large-scale phenomics screen is inescapable process and requires an extremely high throughput. To identify stress tolerance genes from an extremophile plant, we have employed the modified Conditional cDNA Overexpression System and transferred a cDNA library from the halophyte *L. crassifolium* to the glycophyte *A. thaliana*. By screening for salt, osmotic and oxidative stress tolerance through *in vitro* growth assays and non-destructive chlorophyll fluorescence imaging, 20 *Arabidopsis* lines were identified with superior performance under restrictive conditions. Several cDNA inserts were cloned and confirmed to be responsible for the enhanced tolerance by analysing independent transgenic lines (Rigó et al. 2016). One of these insertion, rendered remarkable tolerance to paraquat and encoded a small protein (69 amino acid), with closest similarity to the predicted gene product of *AT3G52105* (92% identity), a gene with unknown function. For detailed characterization we introduced and overexpressed this ortholog gene in transgenic *Arabidopsis* plants. Our result showed this hypothetical protein resulted the same paraquat tolerance. To validate stress tolerance of the transgenic plants overexpressing the identified *Lepidium* gene growth tests were employed and rosette growth, changes of chlorophyll and anthocyanin contents were monitored by a Matlab-based image analysis software. The developed protocol permitted the non-destructive monitoring of growth and stress-related parameters of young *Arabidopsis* plants (Faragó et al. 2017).

Our future plan is to unfold those molecular differences and diversity between *Lepidium crassifolium* and *Arabidopsis thaliana* clones, which responsible for higher abiotic stress responses.

Supervisor: László Szabados
E-mail: faragod@brc.hu

Dissecting the main regulator of DNA damage tolerance

Orsolya Frittmann

Institute of Genetics, Biological Research Centre of the Hungarian Academy of Sciences, Szeged, Hungary

Cancer is one of the major causes of death in the present world. However, a growing body of evidence supports the idea that the roots of cancers lie in mutations in DNA, the genetic material of cells. DNA damage caused by extrinsic or intrinsic agents are usually removed from DNA and repaired by one of the several DNA repair systems of the cell preserving the genetic information. However, high exposure to DNA damaging agents can lead to the accumulation of unrepaired DNA damages that can block the replication machinery leading to cell death. To ensure survival, cells have evolved mechanisms that can sustain DNA replication on damaged DNA. These so-called damage tolerance or DNA damage bypass processes allow replication to continue on damaged DNA without removing the damaged bases. In human, increased error-prone bypass of DNA lesions causes increased mutagenesis and a rise in the incidence of cancers, whereas error-free replication of damaged DNA contributes to genetic stability. Our research focuses on Rad18, which is a key regulator of DNA damage tolerance (DDT) pathway. Based on yeast genetic experiments DDT can be divided into three different sub-pathways.

(I). The mutagenic translesion polymerase sub-pathway, which includes Polζ and Rev1.

(II). The error-free tolerance sub-pathway, which includes Polη.

(III). The error-free fork regression sub-pathway, which includes Rad5, Mms2-Ubc13.

The above mentioned sub-pathways cannot function without Rad18. In the cells Rad18 (E3 ubiquitin ligase) and Rad6 (E2 ubiquitin conjugase) form a complex, which ubiquitinates the proliferating cell nuclear antigen (PCNA) to initiate the above sub-pathways. The

Rad18 protein has 5 identified domains. These are the Ring-finger, the Zn-finger, and the SAP domains, and the ATP and Rad6 binding domains. The function of some of these domains in DDT is well-described, whereas not much is known about the others. Also, beyond these domains the other parts of Rad18 protein have not been characterized. Our goal is to investigate the exact function of the known domains and the uncharacterized regions of Rad18 using yeast as model organism, with the hope of better understanding the regulation of DNA damage tolerance.

Supervisor: Ildikó Unk
E-mail: forsolya@brc.hu

Identification of a new protein in the preservation of genome integrity

Lili Hegedűs

Institute of Genetics, Biological Research Centre of the Hungarian Academy of Sciences, Szeged, Hungary

DNA damage can occur as the result of several exogenous and endogenous factors. The lack of removal of these modifications may have serious consequences: replication may be blocked and the replication fork may break resulting in genomic rearrangements. The preservation of genome integrity is essential for cells therefore, several DNA repair pathways have evolved to remove the modified regions. Inappropriate operation of these processes may lead to the accumulation of mutations, which manifests in cancer predisposition, developmental disorders, and progeroid syndromes. Progeria is a rare genetic disorder with the early appearance of aging-related phenotypes. In Cocayne-, Bloom-, or Werner syndromes, non-functional DNA repair genes are the causative agents of the symptoms, but in several cases the mutated gene has not been described. Besides DNA repair genes, other factors have been identified as the origins of progeria. Mutations of the lamin genes may also lead to the acceleration of aging processes. The connection between DNA repair proteins and the nuclear lamina is poorly understood. Recently, several publications have examined the topic at the epigenetic level. It has been described that the Werner protein, together with the nuclear lamina, can form a complex with heterochromatinization proteins. In the absence or non-functional operation of these proteins, the heterochromatinization pattern of the cells may be altered, and thus genes that accelerate aging may be switched on. During our work, we have identified and characterized an unknown protein that can regulate these processes. It has both DNA repair and nuclear lamina-like phenotypes can influence the heterochromatinization state of the cell. It can also regulate the Werner protein. Based on our work, we suggest that its mutation may lead to a yet undescribed progeroid syndrome. This protein may be the missing link in our understanding of the processes that lead to aging.

Supervisor: Lajos Haracska
E-mail: lilidome@gmail.com

Functional characterization of nodule-specific cysteine-rich (NCR) peptides

Zsolt Csaba Horváth

Institute of Biochemistry, Biological Research Centre of the Hungarian Academy of Sciences, Szeged, Hungary

Medicago truncatula - like other legume plant in nitrogen starving conditions - forms symbiotic relationship with rhizobia leading to the formation of nodules, novel plant organs specialized for nitrogen fixation, where symbiotic form of bacteria called bacteroids reside.

The *dnf4* (Deficient in Nitrogen Fixation 4) mutant plants - generated with fast neutron irradiation - are incapable to complete the symbiotic development resulting in Fix^- nodules that stay small, poorly developed and white, and where bacteroid development is arrested. Due to this deficiency, the plants suffer from growth retardation and chlorotic discoloration of the leaves in growth medium not containing enough amount of exogenous nitrogen.

Wang et al. (2015) found that a deletion in the *dnf4* plant removed two neighbouring genes coding for very similar nodule specific cysteine rich peptides, NCR211 and NCR178 that share high amino acid sequence similarity. Interestingly, only the NCR211 gene can restore the symbiotic efficiency in the mutant. The *M. truncatula* genome contains >700 *NCR(-like)* genes of which, >600 genes are expressed exclusively in the (infected) nodule cells. The NCR peptides are characterized by conserved secretory signal peptides (Mergaert et al. 2003) targeting the peptides to the bacteroids through the peribacteroid membrane (Dürgő et al. 2015) and by 4-6 cysteines located in conserved positions. The mature peptides have very low sequence similarity that is mirrored in their isoelectric point ranging from 3.5 to 10.5. The mature NCR211 and NCR178 peptides are composed of 34 amino acids of which, 21 are identical.

There are multiple explanations, why the NCR178 peptide cannot replace the biological function of NCR211. One possibility is that, there is a significant, approximately ten-fold difference in the expression levels of the genes, thus, not enough *NCR178* is produced in the nodule cells. Another possibility is that, despite the high sequence conservation, the NCR178 cannot interact with those bacterial proteins that are interacting with and affected by NCR211. To investigate these possibilities, we have created shuffled genes by exchanging between the two genes different parts, such as the promoter, the promoter and the first exon or parts of the second exon of different length. Using these constructs in complementation experiments with *dnf4* plants, we concluded that the differences in the C-terminal half of the mature NCR178 render the peptide inactive during the symbiotic interaction.

In the future, we plan to further delimit the amino acids important for the activity and try to isolate the bacterial targets of the NCR211 peptide.

Supervisor: Attila Kereszt
E-mail: horvathzs1984@gmail.com

The role of a chloroperoxidase enzyme in the ochratoxin A biosynthetic pathway

Noémi Kiss

Department of Microbiology, Faculty of Science and Informatics, University of Szeged, Szeged, Hungary

Ochratoxin A (OTA) is a mycotoxin first characterized by van der Merwe and co-workers (1965) from a South African *Aspergillus ochraceus* isolate. Several other *Aspergillus* and some *Penicillium* species able to produce this secondary metabolite. This mycotoxin frequently contaminates various food and feed products, such as cereals, spices, nuts, coffee, rice, olives, grapes, wine and other beverages. OTA is a nephrotoxic, hepatotoxic, immunosuppressive, teratogenic and carcinogenic compound, classified as a possible human carcinogen (Group 2B) by the International Agency for Research on Cancer. Ochratoxin A is composed of a chlorinated polyketide dihydroisocoumarin ring linked via an amide bond to L-β-phenylalanine. Among Aspergilli, the biosynthetic pathway of OTA has not been elucidated completely yet. There are enzymatic reactions suggested to be responsible for the synthesis of OTA, but the order of reactions has not well-defined yet. In this pathway, a chloroperoxidase enzyme catalyses the addition of a chloride to the dihydroisocoumarin derivative. Harris and Mantle (2001) suggested that chlorination is the penultimate step in the synthesis. However, Gallo et al. (2012) disproved it and they established a new OTA biosynthesis pathway scheme. In this model, the attachment of phenylalanine and dihydroisocoumarin catalysed by a non-ribosomal peptide synthetase (NRPS) precedes the chlorination step in *A. carbonarius*.

In our work, we used *Aspergillus carbonarius* (SZMC 2020) to establish a chloroperoxidase knockout mutants. A plasmid was constructed based on the known genome sequence of *A. carbonarius* ITEM 5010 including a hygromycin B phosphotransferase from pCSN43 as dominant marker gene for selection. We isolated possible transformants, checked them with PCR and examined their toxin production. Further works are in progress to elucidate the exact role and the mechanism of action of this enzyme in the biosynthetic pathway of OTA.

Supervisors: Sándor Kocsubé, Csaba Vágvölgyi
E-mail: kissnoemi621@gmail.com

Molecular and functional markers of different neocortical interneuron types: combined electrophysiological, imaging and single-cell PCR analysis *in vitro* and *in vivo*

Balázs Kovács

Department of Physiology, Anatomy and Neuroscience, Faculty of Science and Informatics, University of Szeged, Szeged, Hungary

In the human neocortex, several pathways are still unknown, for instance the neuronal circuits, the cell functions and so on. For this reason, the focus of our study is the somatosensory cortex, more specifically, the molecular mechanisms underlying in the function of inhibitory cells like neurogliaform (NGF) and axo-axonic cells (AAC). These kinds of GABAerg inhibitory interneurons (NGF, AAC) located in the somatosensory cortex layer 1 and 2 in rats. Moreover, it is interesting to highlight the human brain single cell functions like in the cases of layer 2-3 pyramidal cells and layer 1 interneuron-, and rosehip cells. Our first aim was to collect NGF cell cytoplasms to

measure the difference in RNA level for molecular identity. For this experiment, low (0.5 mM) and high (10 mM) level glucose ACSF (Artificial Cerebro-Spinal Fluid) were used as well. The collected cytoplasms were used for cDNA-chip. Furthermore, we focused on the more efficient separation of AACs from the basket cells. For this reason, we use immune-cytological and PCR techniques to identify the AAC via Nav1.6 channel, which is an important element to separate both neuronal type. Finally, we are going to compare different human neuron cell types (pyramidal cells, interneurons, rosehip cells). However, in the case of NGF cells, we did not find any difference in the electrophysiological parameters, but we did find in the molecular level, which means several genes. These results may lead us to get better knowledge in some serious brain diseases. In the future, we perform *in vitro* single cell human experiments to collect pyramidal-, rosehip cells and any other layer 1 interneuron cytoplasm to analyse and separate them with NGS (Next Generation Sequencing) method, real-time PCR and pathway analysis.

Supervisor: Gábor Tamás
E-mail: rameiosmage@gmail.com

Genetic dissection of legume-rhizobia symbiosis via *Tnt1*-insertion mutagenesis in *Medicago truncatula*

Szilárd Kovács

Institute of Genetics, Biological Research Centre of the Hungarian Academy of Sciences, Szeged, Hungary

Legumes are special among flowering plants in their ability to establish symbiotic associations with nitrogen-fixing bacteria, collectively known as rhizobia. Revealing and understanding the functions of genes and proteins involved in the legume-rhizobia symbiosis have a great importance, not just in the basic, but also in the applied research. A very efficient way of identifying important genes in model plants is the forward and reverse genetic analyses of mutants. The use of tagged mutant collections has already proved to be successful in revealing plant genes that function in the nitrogen-fixing symbiosis. In this work, we have used the *Tnt1* insertion mutant collection of the model legume *M. truncatula* cv. Jemalong that was produced during the EU GLIP project in parallel to the one already existing at the Noble Foundation for ecotype R108 (http://bioinfo4.noble.org/mutant/). In the case of the GLIP collection, during the EU project only the construction of the mutant lines was financed. Consequently, only a limited number of mutants were characterized in this collection, despite the value of such characterized collections for the community. Now, we have done a large scale symbiotic screen using this mutant collection and those lines were selected, in which individuals with impaired symbiotic phenotype appeared. We focused on those mutants that indicated defects in different steps of the symbiotic process, thus 24 lines were chosen for back-cross and further genetic analyses. From these lines segregating populations were produced for 11 mutants. In the meantime, FST sequences belonging to these lines were also carefully analyzed to use candidate gene approach. Thorough phenotype characterization and genotype determination of the candidate genes resulted in the identification of the mutated gene responsible for the symbiotic phenotype in two different mutant lines. One of them is a novel gene, playing role in the early bacterial invasion of the nodule and the other is a new allele of the recently cloned NAD1. The characterization of these two genes and their protein products revealed their roles during the early symbiotic stages.

Supervisor: Gabriella Endre
E-mail: kovacssz@brc.hu

Phylogenetic analysis of *Propionibacterium acnes* by newly developed methods and the determination of antibiotic sensitivity and pathogenic potential of commensal vs. pathogenic strains

Márta Magyari

Institute of Biochemistry, Biological Research Centre of the Hungarian Academy of Sciences, Szeged, Hungary

The human skin is the first line of defense of our body. As such, it gets in contact with numerous microorganisms, both commensal and pathogenic. *Propionibacterium acnes* (*P. acnes*) is a Gram-positive, coryneform, non-spore forming, anaerobic, opportunistic bacteria that have been associated with the emergence of many diseases. It predominantly plays a role in the pathogenesis of acne vulgaris, a skin condition that has multifactorial origin and is characterized by chronic inflammation of the pilosebaceous follicles. In an attempt to better understand, the pathogenesis of acne vulgarism we have developed techniques - such as Touchdown Multiplex PCR and eMLST - which

can quickly, effectively and reliably identify and classify the different isolates of *P. acnes*. We have developed a workflow - follicle-specific sampling followed by Multiplex PCR and eMLST characterization of the cultivated strains - that efficiently classifies the given *P. acnes* strain into phylotypes. Moreover, by using eBURST analysis, we have subdivided the isolates derived from healthy and acneic skin into eST-s, which precisely reflects their pathogenic potential. In recent decades, treatment of acne occurred by widely used antibiotics, but their effects seem to fade, because their improper use leads to the formation of resistant strains. To determine if antibiotic resistance plays a role in the pathogenic potential, antibiotic sensitivity of the isolated *P. acnes* strains was determined and antibiotic resistant strains were typed accordingly. We have determined, that eST-s consisting of antibiotic resistant strains indeed has greater pathogenic potential. Finally, full genome sequences of isolated belonging to different eST-s highlighted numerous regions responsible for morphological differences, pathogenicity and antibiotic resistance.

Supervisor: István Nagy
E-mail: magyari.marta@gmail.com

Ubiquitin quantification in *Drosophila*

Ágota Nagy

Department of Genetics, Faculty of Science and Informatics, University of Szeged, Szeged, Hungary

Ubiquitination is a reversible posttranslational modification of proteins that plays critical roles in the regulation of many cellular functions. In my PhD project, I explore the mechanisms behind this process by focusing my research on the regulation of ubiquitin dependent protein degradation, the role of specific ubiquitinating and deubiquitinating enzymes, and on the balance between different ubiquitin pools. The ubiquitin pool in all eukaryotic cells is divided to distinct fractions that include free mono- and polyubiquitins as well as covalently linked mono- and polyubiquitin-protein conjugates. These ubiquitin forms thought to reach a dynamic intracellular equilibrium, in which the availability of free monoubiquitin appears to be essential for normal cell physiology. Precise measurement of the ubiquitin pool, and the ratio of free versus conjugated ubiquitin forms or their cycle dynamics an important step in the study of the ubiquitylation machinery and to better understand ubiquitin regulated intracellular processes. In this talk I present my results on ubiquitin quantification in different developmental stages and tissues of *Drosophila*.

To analyze ubiquitin pool dynamics, we adapted a simple and reliable Western blot based method to *Drosophila melanogaster*, which allowed us to quantify the different forms of ubiquitin. In this assay, endogenous DUBs present in the lysates process all conjugated ubiquitins to monoubiquitins therefore, the total ubiquitin content of cell lysates is determined in the form of monoubiquitins. The free monoubiquitin fraction in turn is determined from similar lysates supplemented with a strong DUB inhibitor. Appropriate samples of these lysates are Western blotted together with ubiquitin standards that permit the quantification of the different ubiquitin fractions by densitometric analysis. We determined the total, free monoubiquitin and conjugated ubiquitin concentrations in different developmental stages and in various tissues of *Drosophila melanogaster*. Our data demonstrate the highly dynamic nature of the ubiquitin equilibrium.

Supervisor: Péter Deák
E-mail: nagyagota.na@gmail.com

Measuring the activity of inhibitory neocortical cells with patch clamp technique *in vivo*

Gáspár Oláh

Department of Physiology, Anatomy and Neuroscience, Faculty of Science and Informatics, University of Szeged, Szeged, Hungary

To understand how the brain works it is essential to investigate it on cellular level. In the last few decades patch clamp technique was developed to measure physiological parameters of neurons. The use of this technique on brain slice preparations helps us to understand how neurons make local microcircuits, but we cannot get any information from long range connections due to the slicing, and it is impossible to associate physiological phenomenon with behavioral events. Our aim is to develop a pipeline, in which we can perform patch clamp recordings in anaesthetized mice, to investigate how inhibitory neocortical cells take part in brain state transitions. For visualize the inhibitory cells in the neocortex we use Ai9xvGATcre mouse line. In these animals GABAergic cells express red fluorescent protein (tdTomato)

so we can perform two-photon targeted whole cell patch clamp recordings from interneurons. It is crucial to fix the head of the animal during recording. This step is very stressful for mice, but it is possible to train them to concede it. We developed an automatic home cage for mice, in which they get water only in a head fixation frame. The frame detects the animal and the head fixation and water apply sequence run automatically. The time of the head fixation increases day by day. Within a week, the animals trained to head fixation and we can use them for *in vivo* recordings. A well-trained animal is able to rest under the two-photon microscope up to 4 hours, which contains sleeping periods. In this period, we are able to perform cellular electrophysiological measurements or two-photon Ca^{2+} imaging to investigate the function of inhibitory cells in brain state transitions. After the recording session, the animals are anesthetized and transcardially perfused with fixative solution and the brains are stored for further anatomical investigations.

Supervisors: Gábor Tamás
E-mail: olah.gaspar@gmail.com

Summation of metabotropic $GABA_B$ receptor mediated postsynaptic potentials in the supragranular layer of the neocortex

Attila Ozsvár

Department of Physiology, Anatomy and Neuroscience, Faculty of Science and Informatics, University of Szeged, Szeged, Hungary

In the mammal neocortex GABAerg interneurons forms diverse classes based on morphology and physiological properties. Among them the neurogliaform cell has the exclusive feature as capable to activate extrasynaptic $GABA_B$ receptors with a single action potential. The neurogliaforms cell forms uniquely dense axonal arborization, that contains presynaptic boutons very closely. However, the neurogliaform cell forms not only traditional synaptic connections. During synaptic transmission beside activating of the synaptic ionotropic $GABA_A$ receptor the released neurotransmitter reach the metabotropic extrasynaptic $GABA_B$ receptors through a molecular diffusion-based volume transmission of GABA neurotrasmitter. $GABA_B$ receptor activation is a key functional modulator in cortical microcircuits affecting basic properties like motor integration in the somatosensory cortex, sensory input control, interhemispheric inhibition, and initial changes in persistent cortical activity. Our aim was to characterize the quantal properties of the volume transmission, to have a better understanding what is the possible coverage of GABA release by a single action potential from neurogliaform cells in layer 1. Upon cooperative neurogliaform activation what is the possible effect on the postsynaptic cell, since spatial summation of ionotropic synaptic inputs is well-known, nevertheless to date there is no experimental analysis how neurons integrate metabotropic receptor mediated signals. We performed paired and triple whole cell patch clamp recordings on layer 2 pyramidal and layer 1 neurogliaform cells to measure neurogliaform cell induced postsynaptic potentials. We characterized the parameters of the neurogliaform synaptic transmission with Bayesian quantal analysis. With this approach, we were able to estimate the quantal parameters of the synaptic transmission: (1) probability of vesicular release, (2) number of functional release sites, (3) size of postsynaptic potentials mediated by single vesicle release. Our anatomical studies provided us to reconstruct neurogliaform cells axonal and bouton distribution in layer 1 and construct model of neurogliaform cell network. Using this model, we found that ~30% of the neurogliaform-cell outputs are overlapping. Therefore the co-activation of converging neurogliaform outputs summating on the dendrite region of the postsynaptic cell. With direct measurements of converging neurogliaform inputs we revealed linear summation of unitary $GABA_B$ mediated postsynaptic potentials.

Supervisor: Gábor Tamás, Gábor Molnár
E-mail: ozsat1990@gmail.com

Biotechnological route for hydrogenotrophic methanogenesis

Márk Szuhaj

Department of Biotechnology, Faculty of Science and Informatics, University of Szeged, Szeged, Hungary

Growing human population and activities increase the utilization of fossil energy resources, which in turn leads to the deterioration of the climate. Replacing the fossil fuels with renewable energy carriers is the promising solution. The rapidly increasing renewable capacities are wind and photovoltaics based electricity production, but these technologies operate inherently in fluctuating mode. Finding a solution to the problem of the storage of the surplus electricity generated by these renewables is indispensable. The excess power can be employed in

splitting water in an electrolyzer to H_2 and O_2. The technologies to store and transport the H_2 are not cost-effective and handling is complicated, therefore conversion H_2 to CH_4 is preferable. CH_4 can be transported and stored easily via the existing natural gas grid. The chemical methods to reduce CO_2 with H_2 are well-developed, but the same results can be reached in an environmentally friendly and economically feasible way with the help of biological systems. Hydrogenotrophic methanogens catalyze the conversion of H_2 and CO_2 to CH_4. These microbes are present in the biogas producing natural and man-made systems. An inexpensive source for hydrogenotrophic methanogens is the fermentation effluent of any industrial biogas plant.

Our aims were to determine the optimal conditions of a laboratory scale fermentation system, which operates well in the presence of H_2. The fermentation effluent from a mesophilic biogas plant was used directly as catalyst. The limiting factor in this system was the efficiency of gas/liquid mass transfer. Several operational conditions were tested and efficient CH_4 evolution was developed. The addition of stoichiometric combination of CO_2 and H_2 resulted stable and sustained CH_4 production. The proposed novel strategy suggests the utilization of the biogas effluent reservoir, which is part of most industrial-scale biogas facilities and stores the digested material until its utilization as organic fertilizer. The microbial community of the biogas effluent transforms green electricity-derived H_2 into bio CH_4, and thus acquire an entirely new function for the biogas plant. Based on our results, we also examined thermophilic biogas effluents in order, to achieve more effective methane production, although the thermophilic anaerobic microbial community may be more susceptible to instability.

Supervisor: Zoltán Bagi
E-mail: szuhaj@bio.u-szeged.hu

Pathogenicity of *Curvularia* species causing opportunistic phaeohyphomycoses

Eszter Judit Tóth

Department of Microbiology, Faculty of Science and Informatics, University of Szeged, Szeged, Hungary

Members of the genera *Curvularia* and *Bipolaris* are closely related melanin producing filamentous fungi. While *Bipolaris* species infect only plants and may cause serious agriculture damages, some *Curvularia* species has been recovered from opportunistic human infections. The human pathogenic species typically cause phaeohyphomycoses, *i.e.* mould infections caused by melanised fungi, which can manifest as invasive mycoses with frequent involvement of the central nervous system in immunocompromised patients or as local infections (*e.g.,* keratitis, sinusitis, and cutaneous lesions) in immunocompetent people. Although, their plant-fungal interactions have been intensively studied, there is only little information available about the human pathogenic feature of these fungi. During our study, interaction of human monocytes and neutrophil granulocytes with *Curvularia* and *Bipolaris* species were examined. *Curvularia* strains isolated from human infections were characterized also.

In case of monocytes, we analyzed the relative transcription level of certain activation related and cytokine or chemokine coding genes and measured the amount certain cytokines after interaction with the conidia and the hyphae of the fungi. Monocytes responded only to the hyphal form of *C. lunata*, while *C. spicifera* or *C. hawaiiensis* did not induced these immune cells. Role of the melanin in lack of recognizing the conidia by monocytes was examined by blocking the melanin biosynthesis during the production of the conidia. Responses of neutrophil granulocytes to *C. lunata*, *B. zeicola* and *Aspergillus fumigatus* were compared. Activation of neutrophils, production of hydrogen peroxide and superoxide anion was measured after co-incubation with un-opsonized or serum opsonized fungi. It was shown, that recognition of all investigated fungi is dependent of serum opsonisation. We analysed the appearance of a certain extracellular matrix on the surface of *C. lunata*. It seems, the production of this matrix is dependent on reduced oxygen tension and affect the interaction of the hyphae with the cellular components of the immune systems. In further studies, we would like to examine the interaction of other cell types of the innate immune system with *Curvularia* strains to identify the immune cell groups taking part in defence against these opportunistic human pathogenic fungi.

Supervisor: Tamás Papp
E-mail: scedobipo@gmail.com

Volume 61(1):105-118, 2017
Acta Biologica Szegediensis
http://www2.sci.u-szeged.hu/ABS

Traditional ecological knowledge of non-domestic animals in the Carpathian Basin

Viktor Ulicsni

Department of Ecology, Faculty of Science and Informatics, University of Szeged, Szeged, Hungary

Local people may possess rich knowledge of their environment that can be used for sustainable resource and nature conservation management. This widening of knowledge sources echoed in the policy arena of IPBES that declared the use of different knowledge systems. The understanding and use of traditional ecological knowledge (TEK) by academic researchers is, however, difficult due to different world views. Research on TK has mainly focused on boreal areas and the tropics, while the temperate continental areas were less examined. Previously, there has been no extensive data collection on TEK on wild animals in Central Europe, notably on the wild invertebrate fauna. We have documented such folk knowledge in seven regions in Hungary, Romania, Slovakia and Croatia using methods of social sciences such as semi-structured interviews, conducted picture sorts and participatory data collection. We documented ca. 412 wild folk taxa from which, 216 are invertebrates; discuss folk biological classification and nomenclature, morphologically, ecologically and culturally salient features, uses, economic impacts of these species and conservation. Besides the necessarily exploratory basic research, we analyzed sociocultural aspects of conservation management priority species and keystone species of ecosystems. We examined the development of new ecological knowledge and perceptions-knowledge-generation, hybrid knowledge in the case of the reintroduced Eurasian beaver and the sustainable elements in resource management of the European ground squirrel in Hungary. We also examined how well zoologists and a trait-based model can predict the level of knowledge among local people. We argue that if zoologists value, respect and seek for TEK and ethnobiologists help them locate target species for knowledge co-production, efficiency of cooperation between Western Science and traditional knowledge systems could be increased. This way traditional knowledge holders and their knowledge could participate more effectively in zoological and conservational knowledge co-production and thus contribute to a better understanding and conservation of biodiversity and ecosystem services.

Supervisors: Attila Gyula Torma, Zsolt Molnár
E-mail: ulicsni.viktor@t-online.hu

Role of carotenoids in the structure and function of cyanobacterial photosynthetic protein complexes

Sindhujaa Vajravel

Institute of Plant Biology, Biological Research Centre of the Hungarian Academy of Sciences, Szeged, Hungary

Carotenoids are critical for photoprotection, regulation of the membrane properties, but less information available about their structural roles. These pigments are classified into subgroups of xanthophylls and carotenes. The photosynthetic organisms contain especially high amount of carotenoids. On a global scale, the cyanobacteria represent an ecologically and biotechnologically important group of oxygenic photosynthetic organisms. In order to utilize their advantages, it is essential to understand the factors determining photosynthetic efficiency. Cyanobacterial photosynthesis is mediated by membrane embedded photosystem I (PSI) and photosystem II (PSII). The light harvesting efficiency is enhanced by the peripheral antennae complex, the phycobilisome (PBS). Our aim is to clarify the influence of carotenoids on the major photosynthetic protein complexes using *Synechocystis* sp. PCC 6803. Although, the PBS does not contain carotenoids, the absence or low level of β-carotene lead to the co-existence of unconnected peripheral rod units of PBS and assembled PBS with shorter rods. The presences of unconnected rods were independent from the presence of PSs or the level of reactive oxygen species. Enzymatic PBS proteolysis induced by nitrogen starvation in the carotenoid mutant cells revealed a retarded degradation of the unconnected rod units suggesting a distorted PBS metabolism. We also investigated the function of xanthophylls in the organization and structure of the trimeric PSI complex. We found echinenone and zeaxanthin molecules in the isolated PSI trimers and used various carotenoid biosynthesis mutants to study the specific role of these xanthophylls. Our spectroscopic results revealed specific structural changes of PSI complex in the absence of zeaxanthin and echinenone resulting in destabilization of the PSI trimer. Hence, these xanthophylls are important for the PSI trimer structure and they could be part of the complex or present in the vicinity of PSI. Currently, I am studying the possible correlation between xanthophylls and supramolecular organization of thylakoid membranes.

Supervisor: Zoltán Gombos
E-mail: vajravel.sindhujaa@brc.mta.hu

Volume 61(1):105-118, 2017
Acta Biologica Szegediensis
http://www2.sci.u-szeged.hu/ABS

Calorie restriction, high triglyceride diet and physical exercise in experimental menopause

Médea Veszelka

Department of Physiology, Anatomy and Neuroscience, Faculty of Science and Informatics, University of Szeged, Szeged, Hungary

Premenopausal women have a lower risk of developing cardiovascular disease (CVD) compared to age-matched men, however, this sex advantage for women gradually disappears after the onset of menopause, suggesting that sexual hormones have a strong influence on cardiometabolic and inflammatory parameters. It is widely accepted that physical exercise has become a non-pharmacological therapeutic option in the prevention and treatment of CVD. Furthermore, exercise-mediated cardioprotection has been linked to the induction of antioxidant defense mechanism and the reduction of metabolic risk factors. We hypothesize that 12-week voluntary exercise and calorie restriction (CR) are effective strategies to modify the cardiovascular, metabolic anti-inflammatory processes. Ovariectomized (OVX) and sham operated (SO) female Wistar rats were randomized to running (R) and non-running groups. The types of diet were standard chow (CTRL), high triglyceride diet (HT) and CR for 12 weeks. The levels of glucose, insulin, triglyceride (TG), leptin as well as the concentration of cardiac and aortic heme oxygenase (HO-1) enzymes, the concentrations of plasma interleukin-6 (IL-6) and tumor necrosis factor-α (TNF-α) in serum were detected by ELISA method. We measured the enzymatic activity of HO, myeloperoxidase (MPO) via spectrophotometric assay and detected the matrix metalloproteinases (MMP-2) activity by gelatin zymography. The HO activity and HO-1 concentration, the collagenase MMP-2 level, the metabolic and inflammatory were significantly decreased in the non-running groups, however, the 12-week physical exercise combined CR diet improve the parameters cased, by high triglyceride diet and "negative-effects" of estrogen depletion.

In this study, we revealed that moderate exercise training can attenuate the OVX induced heart fibrosis via MMP-2/HO/MPO regulation. This project supported by: ÚNKP-ÚNKP-16-4, (Pósa Anikó) and ÚNKP-ÚNKP-16-3 (Szabó Renáta) New National Excellence Program of the Ministry of Human Capacities and GINOP-2.3.2-15-2016-00062.

Supervisors: Csaba Varga, Anikó Pósa
E-mail: veszmed@gmail.com

CARD9 and Syk: dispensable for the control of systemic *Candida parapsilosis* infections?

Erik Zajta

Department of Microbiology, Faculty of Science and Informatics, University of Szeged, Szeged, Hungary

An important antimicrobial intracellular pathway initiated by C-type lectin receptors leads through Syk and CARD9. Several major fungal pathogens activate this route. *Candida parapsilosis* is a regular cause of candidemia and threatens especially neonates. Despite its clinical relevance, little is known about the immunological processes during *C. parapsilosis* infections. Our goal was to examine the role of CARD9 and Syk in *C. parapsilosis* infections.

We generated bone marrow chimeras with wild type, Syk- or CARD9-deficient hematopoietic systems. Mice were infected intravenously with *C. parapsilosis* or *C. albicans* and fungal burden was determined from organs and blood. Peritoneal macrophages and bone marrow derived macrophages were cultured and infected with *C. parapsilosis* or *C. albicans* and supernatants were analysed for cytokine content and LDH activity. Phagocytosis of *C. parapsilosis* by macrophages and fungal survival in co-cultures were assessed.

The absence of Syk or CARD9 in macrophages led to reduced IL-1β, TNFα and KC secretion upon *C. albicans* and *C. parapsilosis* infections. There was no difference in phagocytic activity between WT and CARD9-deficient BMDMs nor in their LDH release. Both Syk- and CARD9-deficient mice were highly susceptible to *C. albicans*. Notably however, Syk- and CARD9-deficient mice were only slightly more sensitive to *C. parapsilosis*.

Our data suggest that both Syk and CARD9 influence *C. parapsilosis* induced host responses *in vitro*. However, unlike in the case of *C. albicans*, these proteins are not key players in the immune-control of systemic *C. parapsilosis* infection.

This work was supported by the National Talent Programme (NTP-NFTÖ-16-0569).

Supervisor: Attila Gácser
E-mail: writetotono@gmail.com

Volume 61(1):105-118, 2017
Acta Biologica Szegediensis
http://www2.sci.u-szeged.hu/ABS

A novel reporter system for hairy root transformation and its application to study the function of NCR peptides

Senlei Zhang

Institute of Biochemistry, Biological Research Centre of the Hungarian Academy of Sciences, Szeged, Hungary

Hairy root transformation is widely used method in research of root nodule development and nitrogen fixation in legume plants. Biological reporters are normally used to distinguish transformed roots from adventitious roots, which can also develop from same site. However, those reporters can only be detected via specific methods: GFP with fluorescent microscopy, while GUS with specific staining, making them not convenient to handle. In this research, we are developing a new reporter system for hairy root transformation that visualize transformation events without any specific equipment or chemicals. The overexpression of the *MtLAP1* gene coding for a MYB-R2R3 family transcription factor facilitates anthocyanin accumulation in *Medicago*, *Trifolium* and tobacco cell vacuoles. Hairy roots expressing the constitutive *MtLAP1* gene showed very strong purple color as expected and complementation test with the *dnf7* mutant confirmed that nodules expressing this gene can conduct nitrogen fixation, while accumulate anthocyanin. As nodule-specific expressing genes, NCRs were proved quite essential for function of root nodule in IRLC plant, like *Medicago*. There are more than 700 members of NCRs in *Medicago* making it extremely difficult to discover their function for potential redundancy and function overlapping, however, the *dnf4* and *dnf7* mutants deficient in symbiotic nitrogen fixation were shown to be defective in the *NCR211* and *NCR169* genes, respectively. We use the reporter system described above to identify other essential *NCR* genes in *Medicago* with the help of the CRISPR-CAS gene knockout method.

Supervisor: Attila Kereszt
E-mail: senleizhang@126.com

DNA-dependent protease activity of human Spartan facilitates replication of DNA-protein crosslink-containing DNA

Eszter Zsigmond

Institute of Genetics, Biological Research Centre of the Hungarian Academy of Sciences, Szeged, Hungary

Our DNA is constantly exposed to different exogenous and endogenous factors that cause DNA damage which if left unrepaired, challenges the movement of the replication machinery. Stalling of the replication fork can lead to strand breaks and chromosomal rearrangements causing genome instability, early onset of aging and eventually cancer. To rescue the stalled replication fork, different DNA damage pathways have evolved. One of them is the DNA damage tolerance pathway, which is activated by the DNA damage-induced monoubiquitylation of the Proliferating Cell Nuclear Antigen (PCNA), the sliding camp of replicative polymerases. A regulatory function of human Spartan has been implicated in this pathway, but the exact function of the protein remained unclear. It is also known that mutations in SPARTAN are associated with early onset hepatocellular carcinoma and progeroid features.

The aim of our study was to reveal the role of human Spartan in facilitating replication of DNA-protein crosslink-containing DNA. We prove that purified Spartan has a DNA-dependent protease activity degrading certain proteins bound to DNA. In concert, Spartan is required for direct DPC removal *in vivo*; we also show that the protease Spartan facilitates repair of formaldehyde-induced DNA-protein crosslinks in later phases of replication using our DNA-Protein Crosslink-specific bromodeoxyuridine (BrdU) comet assay. Moreover, DNA fiber assay indicates that formaldehyde-induced replication stress dramatically decreases the speed of replication fork movement in Spartan-deficient cells, which accumulate in the G2/M cell cycle phase. Finally, epistasis analysis mapped these Spartan functions to the RAD6-RAD18 DNA damage tolerance pathway. Our results reveal that Spartan facilitates replication of DNA-protein crosslink-containing DNA enzymatically, as a protease, which may explain its role in preventing carcinogenesis and aging.

Supervisor: Lajos Haracska
E-mail: zsigmond.eszter@brc.mta.hu

Volume 61(1):105-118, 2017
Acta Biologica Szegediensis
http://www2.sci.u-szeged.hu/ABS

Investigation of the role of fungal prostaglandin like molecules in *Candida parapsilosis* host pathogen interaction

Tanmoy Chakraborty

Department of Microbiology, Faculty of Science and Informatics, University of Szeged, Szeged, Hungary

Candida parapsilosis is one of the opportunistic fungi, which cause systemic fungal infection in immunocompromised host. Although, *Candida albicans* is the most prevalent species in candidiasis, the occurrence of non-albicans *Candida* infection has increased significantly in recent decades. *C. parapsilosis*, one of the emerging non-albicans *Candida* species, is of special importance, because of its ability to cause infection primarily to immature infants, compared to adults. Although the virulence properties of *C. albicans* are extensively studied, very little knowledge is available for *C. parapsilosis*.

Prostaglandins are long chain fatty acid molecules that are involved in both pro- and anti-inflammatory response in humans. They also play important role in antifungal immunity with many other lipid mediators. Recently, it has been shown that pathogenic fungi like *C. albicans* and *Cryptococcus neoformans* can produce their own prostaglandin from exogenous arachidonic acid (AA) independent of the host prostaglandins. In *C. albicans*, two genes *OLE2* and *FET3* are involved in prostaglandin biosynthesis. Whereas, it has been shown from our lab that the *OLE2* homologue is not involved in prostaglandin biosynthesis in *C. parapsilosis,* so we are trying to find new genes or pathways involved in prostaglandin production in this pathogenic fungi. To investigate this, RNA sequencing was performed after growing *C. parapsilosis* in presence of exogenous AA and the sequence analysis shows several genes are up-regulated in which 14% are involved in lipid metabolism. We generated knock out (KO) mutants for 6 candidate genes and among them two KO mutants showed significant reduction in prostaglandin production. Further, to prove the role of fungal prostaglandin in inflammation we studied cytokine such as IL-1α, IL-1β, IL-8 and IL-10 production using human THP-1 cell lines. Our next aim is to check the mutants for host pathogen interaction studies by animal survival assay, phagocytosis and killing assay using different *in-vivo* and *in-vitro* model systems.

Supervisor: Attila Gácser
E-mail: tanmoy.microbiology@gmail.com

Instructions to Authors
(*Updated: January 2015*)

Submission of manuscripts

Submission of a manuscript to *Acta Biologica Szegediensis* automatically involves the assurance that it has not been published and will not be published elsewhere in the same form. Manuscripts should be written in English (consistent with either UK or US spelling). Since poorly-written material will not be considered for publication, authors are encouraged to have their manuscripts corrected for language and usage by a trusted expert. There are no explicit length limitations. However, a normal research article will occupy 4-8 printed pages; reviews might be considerably longer.

Manuscripts should be submitted to the Editor-in-Chief as an electronic attachment to **csaba@bio.u-szeged.hu**. All submitted manuscripts should be complete in themselves and firmly supported by properly detailed experimental data. Instructions to Authors is published in each issue and also available at **http://www2.sci.u-szeged.hu/ABS**. Correspondence relating to the status of the manuscripts, proofs, publication, reprints and advertising should be sent to **abs@bio.u-szeged.hu**.

Manuscript format

The following file formats are acceptable for the main manuscript document: Microsoft word (doc, docx) and Rich text format (rtf). All pages should be printed with full double spacing, 2.5 cm margins, and a nonjustified right margin. A standard 12 point typeface (e.g. Times New Roman, Helvetica or Courier) should be used throughout the manuscript, with symbol font for Greek letters. Footnotes are not permitted. Each page should be numbered at the bottom as follows:

Page 1. Title page: Complete title, first name, middle initial, last name of each author; affiliations of the authors; mailing and e-mail addresses and phone and fax numbers of the corresponding author and a running title of no more than 48 characters.

Page 2. Abstract: no more than 200 words, followed by 4-6 key words. The abstract should not contain any undefined abbreviations and references.

Beginning on page 3: Introduction, Materials and Methods, Results, Discussion, Acknowledgments, References, Tables, Figures. Each section should be begun on a new page.

Results should be clear and concise. Discussion should reveal the significance of the results, not repeat them. Combination of Results and Discussion can be acceptable. Avoid extensive citations and verbatim quotation of published literature in the Introduction and Discussion sections.

For reagents and instruments, the manufacturer's name should be given in parentheses. If microorganisms are used in the study, the collection or the strain number should be given; new isolates must be deposited in a publicly available culture collection. New nucleotide and amino acid sequences must be submitted in freely available databases (*i.e.* EMBL/GenBank) and the accession number should be provided. GenBank/EMBL accession number of the used amino acid or nucleic acid sequences also should be presented. Sources for all antibodies should be indicated. Customary abbreviations in common use need not be defined in the text (e.g. DNA, ATP or PCR). Other abbreviations should be defined at first mention and used consistently thereafter. Authors are required to use approved gene symbols and names; protein names should be in plain type. Quantitative results must be presented as graphs or tables and supported by appropriate experimental design and statistical tests. For studies that involve animals or human subjects, the institutional, national or international guidelines that were followed should be indicated. Species and genus names should be in italics (e.g. *Homo sapiens*).

Acknowledgments

This section can include sources of the financial support received for the work and recognition for colleagues who assisted in the study or the manuscript preparation or provided unpublished data.

References

Only work that has been published or is in the press may be referred to. Personal communications should be acknowledged in the text and accompanied by written permission. Posters, lectures cannot be cited. In the text, references should be cited by name and year, e.g. Bloom (1983) or (Schwarz-Sommer et al. 1990) or (Maxam and Gilbert 1977) or (Maxam and Gilbert 1977; Schwarz-Sommer et al. 1990) or (Maxam and Gilbert 1977; Sambrook et al. 1989, 2000). In the References, references should be listed alphabetically by first authors (including all coauthors) and chronologically for a given author (beginning with the most recent date of publication). Where the same author has more than one publication in a year, lower case letters should be used (e.g. 1999a, 1999b, etc.). Periods should not be used after authors' initials or abbreviated journal titles (e.g. Acta Biologica Szegediensis should be cited as Acta Biol Szeged). Inclusive page numbers should be used. Examples:

Journal article

Bloom FE (1983) The endorphins: a growing family of pharmacologically pertinent peptides. Annu Rev Pharmacol Toxicol 23:151-170.

Maxam AM, Gilbert WA (1977) A new method for sequencing DNA. Proc Natl Acad Sci USA 74:560-564.

Monod J, Changeux J-P, Jacob F (1963) Allosteric proteins and cellular control systems. J Mol Biol 6:306-329.

Schwarz-Sommer Z, Huijser P, Nacken W, Saedler H, Sommer H (1990) Genetic control of flower development by homeotic genes in *Antirrhinum majus*. Science 250:931-936.

Article by DOI

Weiss E (2012) Examining activity patterns and biological confounding factors: Differences between fibrocartilaginous and fibrous musculoskeletal stress markers. Int J Osteoarchaeol DOI: 10.1002/oa.2290.

Book

Sambrook J, Fritsch EF, Maniatis T (1989) Molecular cloning: a laboratory manual, 2nd ed. Cold Spring Harbor Laboratory Press, New York.

Book chapter

Coons AH (1978) Fluorescent antibody methods. In Danielli JF, ed., General Cytochemical Methods. Academic Press, New York, 399-422.

Online document

Benny GL (2009) Zygomycetes. Available: http://www.zygomycetes.org. Accessed 11 November 2010.

Dissertation

Velayos A (2000) Carotenogenesis en *Mucor circinelloides*. PhD Thesis. Universidad de Salamanca, Salamanca, Spain.

Units

Only SI units may be used (liter and molar are acceptable). The form g/ml is preferable instead of the form g ml-1.

Tables

Tables should be numbered consecutively with Arabic numerals. The first table in the text should be referred to as Table 1, and so on. A brief title should be included above the table. Each table should be double spaced, without vertical or horizontal lines, and on a separate sheet. Material in text should not be duplicated and methods should not be described.

Figure legends

Figures should be numbered consecutively with Arabic numerals. The first figure in the text should be referred to as Fig. 1, and

so on. The following information should be provided in the figure legend: Figure number (using as Figure 1), short title of figure and the detailed legend. Material in the legend should not be duplicated and methods should not be described. The size of scale bars should be indicated when appropriate.

Figures

All figures should be submitted in separate files. Preferred file formats are TIFF or EPS. In some cases, MSOffice files are also acceptable. Adequate resolution (at least 300 dpi, preferably 600 dpi) should be used in making the original image. Size the figures close to the dimensions of the journal pages. Do not use faint lines and pay attention to the sizes of fonts in your figures. Lines, texts and numbers should remain legible after setting the figures to their final size in the published version.

If figures are submitted with the main text, each of them should be presented in a separate page after the tables.

At the moment, color art is free of charge. However, color is permitted only if there is no other way to represent the scientific data. Necessity of color usage will be decided by the Editor. Color figures for only decorative purpose will be rejected or asked to modify to black and white or grayscale.